

# DISSERTATION

Understanding human mitotic protein complex organisation and  
phospho-regulation using a combined proteomics and chemical  
biology approach

angestrebter akademischer Grad

Doktor der Naturwissenschaften (Dr. rer.nat.)

Verfasser:	Björn Hegemann
Matrikel-Nummer:	0547126
Dissertationsgebiet:	A 091 490 (Molekulare Biologie)
Betreuer:	Dr. Jan-Michael Peters

Wien, am 02. Mai 2008



## Table of Contents

Table of Contents	1
Zusammenfassung	5
Abstract	7
1 Introduction	9
1.1 The cell cycle	9
1.2 Mechanisms of cell cycle control	11
1.3 Sister chromatid cohesion	13
1.4 Protein complexes in mitotic progression	14
1.4.1 How to detect protein complexes?	15
1.5 Mitotic protein kinases	17
1.5.1 How to find mitotic kinases substrates?	18
1.6 Aim of this study	20
2 Results	23
2.1 Manuscript in preparation: Systematic analysis of mitotic protein complexes using tandem affinity purification and mass spectrometry discovers 71 novel potential mitotic protein complexes	24
2.1.1 Abstract	24
2.1.2 Introduction	25
2.1.3 Results	27
2.1.3.1 Bait selection	27
2.1.3.2 Purification and LC-MS/MS analysis	28
2.1.3.3 Complex detection	29
2.1.3.4 Characterisation of novel complexes	33
2.1.3.5 Identification of ANAPC16 as a novel subunit of human APC/C	35
2.1.4 Discussion	38
2.1.5 Materials and methods	41
2.1.5.1 Cell culture and siRNA depletion	41
2.1.5.2 Protein extraction, purification and MS	41
2.1.5.3 Sucrose density gradients	43
2.1.5.4 Ubiquitination assay	43
2.1.5.5 Data processing and clustering analysis	43
2.1.5.6 Antibodies	44
2.1.5.7 Immunofluorescence microscopy	45
2.1.6 Figure legend	46
2.1.6.1 Figure 2.1-1	46
2.1.6.2 Figure 2.1-2	46
2.1.6.3 Figure 2.1-3	47
2.1.6.4 Figure 2.1-4	47
2.1.6.5 Supplemental table 2.1-1	49

## Table of Contents

2.1.6.6	Supplemental table 2.1-2 (See appendix 5.3)	49
2.1.6.7	Supplemental table 2.1-3 (See appendix 5.3)	49
2.1.6.8	Supplemental figure 2.1-1	49
2.1.7	Figures	50
2.2	Manuscript in preparation: A systematic approach to discover new PLK1 and AURKB substrates finds 17 novel PLK1 and 18 novel AURKB substrates on candidate proteins.	99
2.2.1	Abstract	56
2.2.2	Introduction	57
2.2.3	Results	60
2.2.3.1	Characterisation of the BI2536-related inhibitor BI4834	60
2.2.3.2	Bait selection, affinity purification and mass spectrometric analysis	61
2.2.3.3	Phospho-site analysis of LAP-tagged mouse Bub1b and endogenous WAPAL	62
2.2.3.4	Phosphorylation site analysis of 16 complex purifications	64
2.2.3.5	Identification and validation of WAPAL and Bub1b phosphorylation sites	66
2.2.3.6	MS data validation using phospho-specific antibodies	68
2.2.3.7	Potential novel PLK1 and AURKB substrates	71
2.2.3.8	Initial bioinformatic analysis of PLK1-dependent phosphorylation sites	72
2.2.4	Discussion	73
2.2.5	Materials and methods	76
2.2.5.1	Cell culture	76
2.2.5.2	Protein extraction and purification	77
2.2.5.3	MS and data analysis	77
2.2.5.4	Antibodies	80
2.2.5.5	<i>In vitro</i> kinase assay	81
2.2.5.6	Immunofluorescence microscopy	81
2.2.6	Figure Legend	83
2.2.6.1	Figure 2.2-1	83
2.2.6.2	Figure 2.2-2	83
2.2.6.3	Figure 2.2-3	84
2.2.6.4	Figure 2.2-4	84
2.2.6.5	Supplemental figure 2.2-1	85
2.2.6.6	Supplemental figure 2.2-2	85
2.2.6.7	Supplemental table 2.2-1	86
2.2.6.8	Supplemental table 2.2-2 (see appendix 5.5)	86
2.2.7	Figures	87
2.3	Generation and characterisation of cell lines stably expressing MYC-tagged versions of PDS5A and PDS5B	94

2.3.1	Cloning of PDS5A and PDS5B constructs into a MYC-Tet-On expression vector	94
2.3.2	Generation of stable doxycyclin-induceable HeLa cell lines expressing PDS5A-MYC and MYC-PDS5B	96
2.3.3	Characterisation of one stable PDS5A-MYC cell line (1136_21_8) and two stable MYC-PDS5B cell lines (1133_6_13/1133_6_22)	97
2.4	Contributions	103
3	Discussion	105
3.1	Protein interaction mapping	105
3.2	Phosphorylation site mapping	108
3.3	PDS5A and PDS5B cell lines	110
4	Materials and methods	112
4.1	Cell culture and siRNA depletion	112
4.2	Protein extract preparation and immunoprecipitation	112
4.3	Antibodies	112
4.4	Immunofluorescence microscopy	112
4.5	Cloning	113
5	Appendix	115
5.1	Plasmids generated for studying PDS5A and PDS5B	115
5.2	Sequence analysis of PDS5A and PDS5B	115
5.3	Interaction manuscript table S2 (all cleaned purifications)	116
5.4	Interaction manuscript table S3 (all annotated complexes)	145
5.5	Phosphorylation manuscript table S2 (all phospho-peptides)	161
6	Abbreviations	174
7	References	177
8	Acknowledgements	189
9	Curriculum Vitae	190



## Zusammenfassung

Während der mitotischen Phase des Zellzyklus verteilen Zellen ihre Chromosomen auf die zwei neu entstehenden Zellen. Dieser Prozess ist begleitet von immensen morphologischen Veränderungen wie zum Beispiel dem Abbau der Kernhülle, der Verdichtung der Chromosomen, dem Aufbau der mitotischen Spindel, der Chromosomenaufteilung und schließlich der Zytokinese. Die biochemischen Mechanismen, die diesen Prozessen zugrunde liegen und diese regulieren sind bisher erst wenig verstanden.

Einige Proteinkomplexe wurden als die wichtigsten Regulatoren der Mitose identifiziert. Die Aktivität der Cyclin-dependent Kinase 1 im Komplex mit Cyclin B 1 (CDK1/CCNB1) ist essentiell für den Eintritt in die Mitose und frühe mitotische Vorgänge, während der Anaphase-promoting Complex (APC/C) die Anaphase und das Ende der Mitose einleitet. Einige andere mitotische Proteinkomplexe wurden identifiziert, doch für die meisten Proteine, die wichtig für den Verlauf der Mitose sind, sind nur wenige oder gar keine Interaktionspartner bekannt. Um die biochemischen Mechanismen der Mitose besser zu verstehen, ist es nötig, ein umfassenderes Bild der Proteinkomplexe, die für die Regulation der Mitose wichtig sind, zu bekommen. Die kürzlich etablierte BAC TransgeneOmics pipeline ermöglichte die Herstellung einer großen Anzahl von menschlichen Zellen, die „localisation and affinity purification“ (LAP) getaggte Mausgene von ihrem endogenen Promoter exprimieren. Aus diesen Zellen konnten wir erfolgreich 175 mitotische Proteine aufreinigen und 787 spezifisch-interagierende Proteine mittels Massenspektrometrie identifizieren. Die weitere Analyse dieser Daten mit Hilfe bioinformatischer Methoden ergab 130 potentielle Proteinkomplexe, von denen bis dahin 71 unbekannt waren. Eine weitergehende Untersuchung einiger dieser Komplexe bestätigte einen neuen Komplex, der möglicherweise bei der Funktion des Zentrosoms eine Rolle spielt, sowie zwei neue Interaktionspartner des  $\gamma$ -tubulin ring complex ( $\gamma$ -TuRC) und eine neue APC/C Untereinheit. Unsere Ergebnisse sind der erste Schritt, um die Organisation der mitotischen Proteinkomplexe gründlicher zu verstehen. Weitergehende Untersuchungen dieser identifizierten Proteinkomplexe werden unser Verständnis der molekularen Basis der mitotischen Regulation weiter voranbringen.

Einige der wichtigsten Regulatoren, die den Eintritt und den Verlauf der Mitose kontrollieren sind mitotische Proteinkinasen. Die Phosphorylierung einer unbekannten Anzahl von Substraten wirkt wahrscheinlich wie ein Schalter, der die Aktivität, Stabilität und Lokalisierung dieser Substrate verändert. Dies löst die drastischen morphologischen Veränderungen aus, die nötig sind, damit Zellen zuverlässig durch die Mitose gehen und die mitotische Teilung vollziehen. CDK1/CCNB1 war das erste Mitglied der Familie der mitotischen Kinasen von der einige weitere identifiziert worden sind. Die Polo-like kinase 1 (PLK1) ist essentiell für die Mitose und ist an der Regulation vieler mitotischer Ereignisse beteiligt. Der Kontakt von PLK1 mit Substraten wird wahrscheinlich durch die Substratphosphorylierung von CDK1, aber vielleicht auch von PLK1 selbst kontrolliert. Aurora kinase B (AURKB) ist eine weitere essentielle mitotische Kinase, die, abgesehen von anderen

## Zusammenfassung

Funktionen, essentiell für den „spindle assembly checkpoint“ ist, indem sie inkorrekte Mikrotubuli-Kinetochore Verbindungen korrigiert. PLK1 und AURKB sind nur in der Mitose aktiv und ihre Lokalisierung ist streng reguliert. Das lässt vermuten, dass PLK1 und AURKB Substrate nur zu einer bestimmten Zeit und an einem bestimmten Ort phosphoryliert werden dürfen um ihre Funktion zu erfüllen. Versuche zum Detektieren von Kinase Substraten sind bisher allerdings meist *in vitro* durchgeführt worden, also in der Abwesenheit jeglicher zellulärer Kontrollmechanismen. Wir haben deshalb eine Zell-basierte Methode entwickelt, um neue PLK1 und AURKB Substrate zu finden. Mit Inhibitoren aus kleinen Molekülen gegen PLK1 und AURKB in Kombination mit LAP-Aufreinigung und Massenspektrometrie konnten wir Kinase-abhängige Phosphorylierungsstellen auf 16 potentiellen Substratkomplexen detektieren. Insgesamt haben wir 470 Phosphorylierungsstellen gefunden, von denen 41 PLK1- und 20 AURKB-abhängig waren. Wir haben einen Teil dieser Phosphorylierungsstellen mit Phospho-spezifischen Antikörpern validiert und 17 neue potentielle PLK1 Substrate sowie 18 neue potentielle AURKB Substrate gefunden.



## Abstract

During the mitotic phase of the cell cycle cells equally distribute their chromosomes into two daughter cells. This process is accompanied by immense morphological changes such as breakdown of the nuclear envelope, chromosome condensation, mitotic spindle assembly, chromosome segregation and finally cytokinesis. The underlying biochemical mechanisms regulating these processes are only beginning to be understood.

A number of protein complexes have been identified as the major mitotic regulators. The activity of cyclin-dependent kinase 1 bound to cyclin B (CDK1/CCNB1) is essential for entry into mitosis and early mitotic events while the activity of the anaphase-promoting complex (APC/C) initiates anaphase onset and mitotic exit. Some other mitotic protein complexes have been identified but for most proteins involved in mitotic progression only few or no binding partners are known. To better understand the biochemical mechanisms that govern mitosis, a more comprehensive picture of the protein complexes involved in mitotic regulation is necessary. The recently established BAC TransgeneOmics pipeline allowed the generation of a large set of human cells expressing localisation and affinity purification (LAP)-tagged mouse genes from their endogenous promoter. Using these cells we successfully purified 175 mitotic bait proteins and identified 787 specific interaction partners by mass spectrometry (MS). Further analysis of this dataset using computational methods predicted 130 protein complexes of which 71 were previously unknown. Some of those complexes and interacting partners were tested further to confirm one novel protein complex potentially involved in centrosome function, two novel interaction partners of the  $\gamma$ -tubulin ring complex ( $\gamma$ -TuRC) and one novel APC/C subunit. Our study provides the first step towards more comprehensively understanding mitotic protein complex organisation. Further studies of these identified protein complexes will advance our understanding of the molecular basis of mitotic regulation.

One of the key regulators that control entry and progression through mitosis are mitotic protein kinases. Phosphorylation of an unknown number of substrates is thought to act like a switch that changes activity, stability and localisation of these substrates. This triggers the drastic morphological changes that are necessary for cells to faithfully progress through and complete a mitotic division. CDK1/CCNB1 was the first member of the mitotic protein kinase family but several more have been identified. The Polo-like kinase 1 (PLK1) is essential for mitosis and has been implicated in the regulation of many events during mitosis. Targeting of PLK1 to its substrates is thought to be controlled by priming phosphorylation by CDK1 but might, for some substrates, also be regulated through PLK1's own activity. Aurora kinase B (AURKB) is another essential mitotic kinase which, apart from other functions, is essential for spindle assembly checkpoint function by correcting improper microtubule kinetochore attachments. The

## Abstract

activity of PLK1 and AURKB is limited to mitosis and their localisation is tightly regulated. This suggests that PLK1 and AURKB substrates must only be phosphorylated at a specific time and place to fulfil their function. Assays to detect kinase substrates have been, however, largely carried out *in vitro*, without any cellular regulatory systems in place. We have therefore set out to develop a cellular assay to find novel PLK1 and AURKB substrates. Using small molecule inhibitors against PLK1 and AURKB in combination with LAP purification and MS we could detect kinase-dependent phosphorylation sites on 16 candidate substrate complexes. In total we found 470 phosphorylation sites, 41 of which were PLK1-dependent and 20 of which were AURKB-dependent. We validated a subset of these sites with phospho-specific antibodies and detected 17 novel potential PLK1 substrates and 18 novel potential AURKB substrates.

## 1 Introduction

### 1.1 The cell cycle

The cell cycle is the ordered sequence of cell growth, DNA replication and cell division that leads to propagation of unicellular organisms and growth and differentiation of multicellular organisms. Cells progress from the first gap-phase (G1) into synthesis-phase (S) during which the genetic material is duplicated, through the second gap-phase (G2) into mitosis (M). Mitosis consists of six phases called pro-, prometa-, meta-, ana-, telophase and cytokinesis. Chromosomes are condensed and congress to the cell equator from pro- to metaphase. In anaphase chromosomes are then segregated to the two poles, decondense in telophase and the cells divide in cytokinesis.

The length of G1, S, G2 and M varies between organisms but also between developmental stages and cell types. During the gap-phases cells grow dependent on nutrient availability and, in multicellular organisms, dependent on extracellular signals. Cells can also exit the cell cycle from G1 into G0 to remain in a quiescent state if conditions are not suitable for division or if the cell terminally differentiates within a tissue. Early embryonic cell cycles, e.g. of the *D. melanogaster* and *X. laevis* embryo, are very short, consisting of only S- and M-phases. Unicellular organisms like *S. cerevisiae* and *S. pombe* run through cell cycles of a few h with only a G1- or a very short G1- and long G2-phase, respectively; while higher vertebrates have cell cycles of about 24 h. The order of S- and M-phase is the same in all organisms (Morgan, 2007).

S-phase must precede M-phase to ensure genome stability over cell generations. This irreversible sequence of events is determined by an autonomous biochemical oscillator. The oscillator consists of the cycling kinase activity of CDKs and high or low levels of proteolytic activity which are regulated by the ubiquitin ligase activity of the APC/C (Figure 1.1-1). CDK activity is turned on in late G1-phase, remains high during S-phase and until the anaphase of mitosis. During all this time, APC/C activity is low and only activated at the meta- to anaphase transition. This activation is mediated by CDK1 phosphorylation and leads to destruction of the CDK1 activating subunit Cyclin B1 (CCNB1) and decline of CDK activity. APC/C activity remains high in G1 which keeps CDK activity low. Thus, CDK and APC/C activity are interdependent. CDKs, APC/C and inhibitors and activators of CDKs not mentioned here form a bistable system. This bistable system oscillates between high states of either CDK or APC/C activity without any external input. Within this system each transition point (G1/S, G2/M and meta- to anaphase) behaves like a switch that generates an irreversible transition (Morgan, 2007).

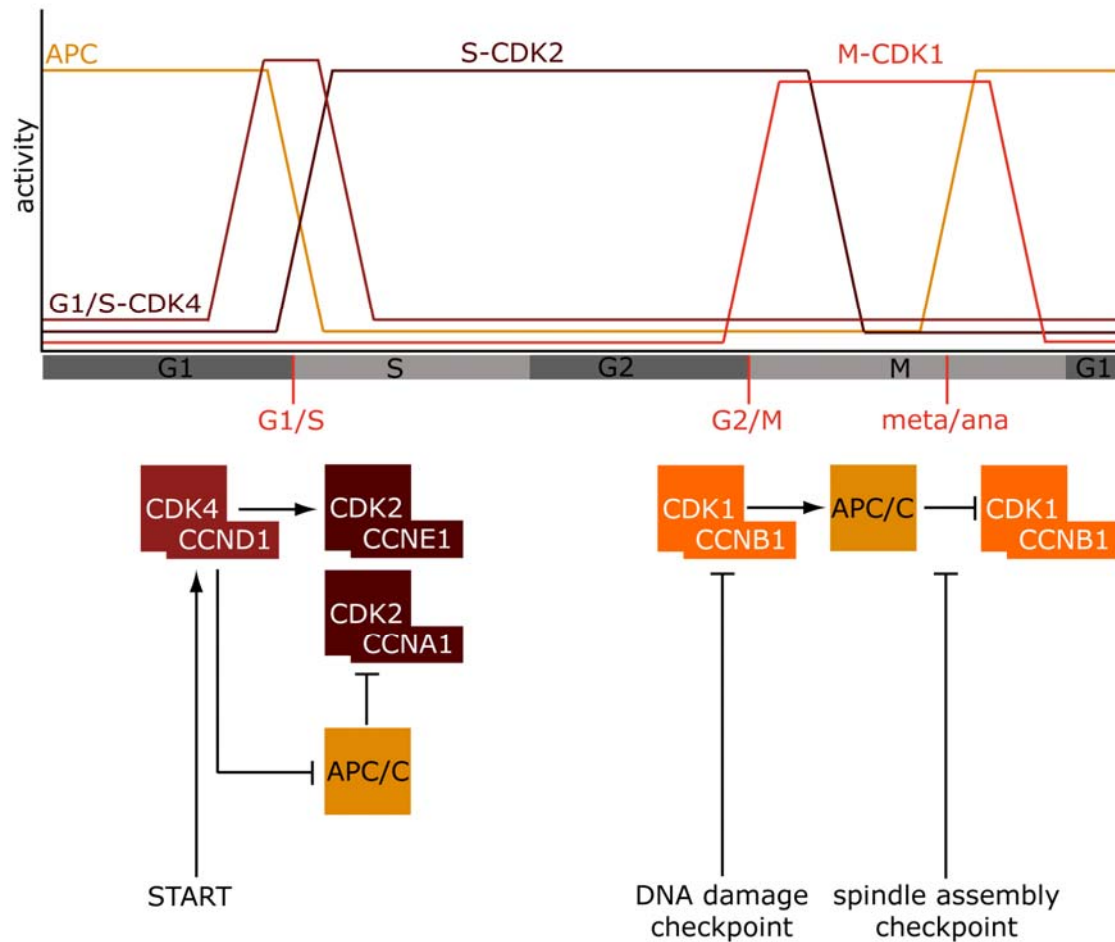


**Figure 1.1-1: The autonomous oscillator and its main components CDKs, cyclins (CCN) and APC/C together with the regulatory checkpoints.**

The graph shows the activity of the different cell cycle phase-specific cyclin-CDK complexes and the APC/C activity during the cell cycle. The scheme below shows the different CDK-cyclin complexes involved (CCND1: Cyclin D1, CCNE1: Cyclin E1, CCNA1: Cyclin A1, CCNB1: Cyclin B1) and the points where cell cycle checkpoints can modulate the phase transitions. Activating and inhibitory arrows do not necessarily indicate direct interactions. Additional CDK and APC/C inhibitors and activators are omitted for clarity.

The key property of a bistable switch is that after a certain level of input stimulation it switches to full activation and remains activated even if the input stimulus is removed. To achieve this irreversible transition using reversible biochemical reactions positive feedback loops are necessary. It is assumed that every of the key cell cycle transitions are regulated by bistable switches. The basic mechanisms for the G2/M transition are fairly well understood from studies in cycling *Xenopus laevis* egg extracts and are assumed to be similar in other organisms (Figure 1.1-2). CDK1 is kept inactive in G2-phase by inhibitory phosphorylations on T14 and Y15. The kinase Wee1 generates Y15 while Myt1 phosphorylates both T14 and Y15. The first step in CDK1 activation is binding to its activating subunit CCNB1 whose expression levels rise during G2. Further, CDK7 phosphorylates T160 once CCNB1 is bound and the phosphatases CDC25A, B and

C remove the inhibitory phosphorylations on T14 and Y15. Positive and double negative feedback loops turn this activation pathway into a bistable system. CDK1 phosphorylates CDC25A, B and C which prevents CDC25A degradation by SCF and enhances CDC25C phosphatase activity. In addition, CDK1 phosphorylation of MYT1 and WEE1 leads to their inactivation and in the case of WEE1 also to its degradation. CDK1 thus activates its own activator and inhibits its own inhibitor leading to rapid activation of CDK1. Additional positive feedback might be generated by PLK1 which can be activated by CDK1 and is assumed to further activate CDC25 and inhibit MYT1/WEE1 by phosphorylation (Morgan, 2007).

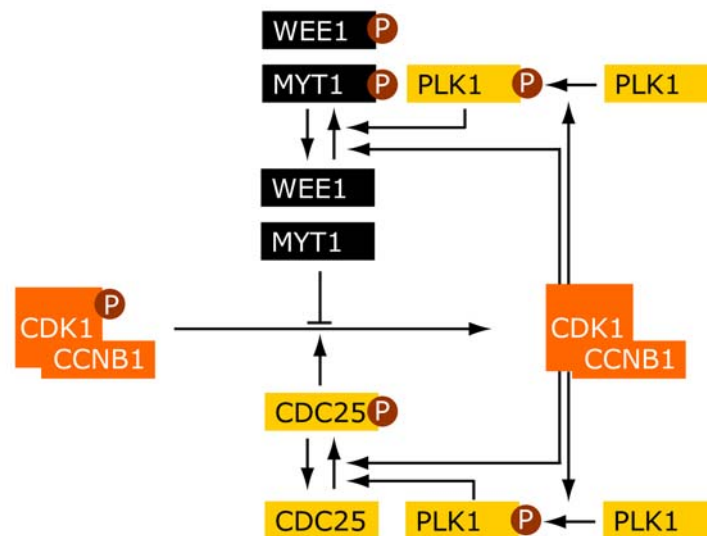


**Figure 1.1-2: Positive and double negative feedback loops at the G2/M transition.** Scheme showing the double negative feedback loop through WEE1, MYT1 and possibly PLK1 that leads to CDK1-CCNB1 activation as well as the positive feedback loop via CDC25 and possibly PLK1. CDC25 isoforms are omitted for clarity. Phosphates, indicated as P, do not reflect the actual number of phosphorylation sites on each protein, for CDK1 only the inhibitory phosphorylation is shown.

## 1.2 Mechanisms of cell cycle control

The transitions between cell cycle phases are controlled by so-called checkpoints at the G1/S, G2/M and at the metaphase to anaphase transition. The checkpoints ensure that cells contain all necessary metabolites to grow before entering into S-phase (G1/S checkpoint), that the genetic material has been copied and is intact before onset of mitosis (G2/M checkpoint) and that the genetic material can be equally segregated into the daughter cells before initiation of cell division (spindle assembly checkpoint (SAC)). The cell cycle is either halted at each checkpoint or it progresses to the next stage but it never reverses. This directionality is provided by the autonomous oscillator and its underlying switch like behaviour as described above (Morgan, 2007).

## 1 Introduction

Transition of the cell cycle from G0 into G1/S-phase depends on CDK4 activity in complex with D-type cyclins (CCND1 in Figure 1.1-1). CDK4 phosphorylates pRB family proteins which activate the expression of G1/S genes. Inhibition of the E- and A-type cyclins in complex with CDK2 is released by CDK4-mediated sequestration of their inhibitor CDKN1B (also known as p27 or Kip1). CDK4/D-type cyclin activity is largely regulated by mitogenic signals which can for example arise from nutrient-dependent intracellular signals or from extracellular signals in multicellular organisms. The G1/S transition is mediated by the E- and A-type cyclins (CCNE1 and CCNA1, respectively in Figure 1.1-1) in complex with CDK2. They induce the formation of the preinitiation complex on replication origins and the subsequent initiation of DNA synthesis by the replication machinery. As S-phase progresses and the replication forks have moved away from their replication origin, repeated firing of the origins has to be inhibited to avoid rereplication of DNA. Continued high activity of CDK2/CCNE1 in combination with geminin (GMNN) prevents formation of the prereplication complex (preRC). In late mitosis CDK activity is reduced and APC/C activity is high. APC/C targets geminin for destruction by the proteasome, enabling preRC formation, also called origin licensing, to set the stage for another round of DNA replication (Morgan, 2007).

The G2/M transition depends on the activation of CDK1/CCNB1 which drives many early mitotic processes like nuclear envelope breakdown, spindle assembly and chromosome condensation. To regulate the bistable switch at this transition described in 1.1 several of the described feedback loops for CDK1 activation are targeted. Signals inhibiting the G2/M transition are generated by the DNA damage response which is active upon stalled replication forks within S-phase or DNA damage within S- or G2-phase. The effector kinases of the DNA damage response, CHK1 and CHK2 (CHECK1 and CHECK2), phosphorylate the CDC25 phosphatases which leads to their increased degradation (A isoform), inactivation (B isoform) or inactivation and nuclear export (C isoform), altogether resulting in reduced activation of CDK1/CCNB1. A long term DNA-damage induced arrest is mediated by the activation of the p53 pathway which ultimately leads to expression of the CDK/CCNB1 inhibitor CDKN1A (p21) (Morgan, 2007).

Anaphase onset depends on the activation of the APC/C. APC/C mediated degradation of Securin (PTTG1) leads to cohesin cleavage by the protease separase (ESPL1) to allow sister chromatid separation. APC/C mediated CCNB1 degradation in anaphase initiates mitotic exit. APC/C is activated by phosphorylation of CDK1/CCNB1 and PLK1 in early mitosis but remains inhibited by the spindle assembly checkpoint (SAC) until sister chromatids are biooriented and spindle microtubules are properly attached to the kinetochores. The mitotic checkpoint complex (MCC) directly translates unattached kinetochores into APC/C inhibition. Once the SAC is silenced APC/C in conjunction with its coactivator CDC20 initiates cohesin cleavage and anaphase onset as well as initial

CCNB1 degradation. This leads to a reduction of CCNB1 activity allowing the second APC/C coactivator FZR1 to become dephosphorylated and active which leads to complete CCNB1 degradation and thus a drop in CDK1 activity (Morgan, 2007). Exit from mitosis requires many mitotic phosphoproteins to be dephosphorylated. In budding yeast this is accomplished by activation of the Cdc14 phosphatase. Whether mammalian cells also require increased phosphatase activity or whether CCNB1 degradation is sufficient, remains under discussion (Potapova et al., 2006; Skoufias et al., 2007).

### 1.3 Sister chromatid cohesion

The main role of the SAC is to ensure that sister chromatids become biooriented in metaphase and are equally segregated to opposite poles in anaphase. In addition to the APC/C, the cohesin complex plays a crucial role in this process. The cohesin complex holds replicated sister chromatids together from S-phase until the meta- to anaphase transition. The physical connection of sisters is thought to be required for their biorientation on the metaphase spindle. Cohesin is cleaved at anaphase onset to allow equal segregation of sister chromatids to daughter cells. In telophase cohesin is loaded back onto chromosomes by the Scc2-Scc4 complex (Watrin et al., 2006). Cohesion between sister chromatids is established in S-phase by a process requiring replication which is not fully understood. In yeast, members of the replication fork have been implicated in this process (Skibbens, 2005). During prophase, most of cohesin is removed from chromosome arms in mammals but not in yeast (Waizenegger et al., 2000). The remaining cohesin at the centromere is cleaved by the protease separase at the meta- to anaphase transition once all sister chromatids are bioriented and the spindle assembly checkpoint has been silenced.

The cohesin core complex consists of a heterodimer of SMC1A and SMC3 which connects to RAD21 to form a trimeric ring. RAD21 in addition interacts with STAG1 or STAG2, defining two cohesin isoforms (Strom and Sjogren, 2007). PDS5A and B, homologs of yeast Pds5p, bind cohesin throughout the cell cycle but their function is not well understood (Losada et al., 2005; Sumara et al., 2000). Yeast Pds5p is required for cohesion establishment in S-phase and maintenance in a prolonged G2 arrest (Hartman et al., 2000; Panizza et al., 2000). Human PDS5A and PDS5B are about 70% identical in their sequence and interact with cohesin exclusive of each other (Losada et al., 2005). Depletion of PDS5A or PDS5B by siRNA in HeLa cells leads to a very mild loss of cohesion phenotype in metaphase while depletion of both isoforms from *X. laevis* egg extracts lead to an increase of cohesin on mitotic chromosomes (Losada et al., 2005). The relatively weak phenotypes of PDS5A or B depletion might reflect a partial redundant function. However, another cohesin interactor and regulator called WAPAL preferentially interacts with PDS5A but not PDS5B (Kueng et al., 2006), suggesting a distinct role of PDS5A in association with WAPAL. Depletion of WAPAL by siRNA blocks

the removal of cohesin in prophase, placing it as a regulator of the so-called prophase pathway (Gandhi et al., 2006; Kueng et al., 2006). It has not been determined so far if the PDS5A-WAPAL interaction is required for WAPAL's function or whether the interaction is direct. Even though PDS5A and B are highly identical in their N-terminal part, their C-terminal shares little sequence similarity.

### 1.4 Protein complexes in mitotic progression

The APC/C and the cohesin complex are two protein complexes important for proper mitotic progression. That proteins can be organised into discrete protein complexes became clear with the discovery of macromolecular machines like the ribosome, the spliceosome or the proteasome (Alberts, 1998). Association of proteins into complexes enables grouping of sequential chemical reactions that would otherwise not happen at random in the protein-crowded intracellular space. Every molecular process studied so far involves a number of complexes that often form a physical and functional interaction network to carry out a specific function. Functional and structural characterisations of some of those complexes have shown that interactions within a complex are often mediated by protein domains and can be dynamically regulated, suggesting that protein complexes are not rigid structures but interchangeable and dynamic protein assemblies. This is exemplified in cell cycle complexes which are often composed of modules that bind via distinct domains in a cell cycle-dependent manner.

One good example of a cell cycle-dependent complex is the binary complex of the CDKs and their activating cyclin subunits. CDK/cyclin complexes exist in varying combinations in different phases of the cell cycle. Different cyclins bind to the same region in CDKs which results in a structural arrangement within CDK to allow activation. Specific cyclins can then direct the CDKs to distinct substrates, leading to phosphorylation of cell cycle-specific CDK substrates (Morgan, 2007, see also 1.1). Also the CDK antagonist within the cell cycle oscillator, the APC/C (see 1.1), interacts with varying coactivators and inhibitors. While the coactivator CDC20 enables the APC/C to ubiquitinate early mitotic substrates, the coactivator FZR1 targets the APC/C to late mitotic and G1-specific substrates (Peters, 2006).

Not only the composition of protein complexes can be cell cycle-dependent, they can also localise to different subcellular structures. Localisation can depend on different complex subunits. A recent very detailed structure function and localisation study has focussed on one such example: the chromosomal passenger complex or CPC. It consists of Aurora B kinase (AURKB), INCENP, Borealin (CDC8A) and Survivin (BIRC5) and is central to the regulation of the meta- to anaphase transition (Ruchaud et al., 2007). It localises to chromosomes in G2 and prophase, is then enriched at centromeres until



metaphase to finally travel via the anaphase central spindle to the midbody in cytokinesis. The enzymatic part of the complex, AURKB, is thought to function at the centromere from prophase to prometaphase and its activity is required to correct incorrect microtubule kinetochore attachments (Ruchaud et al., 2007). AURKB localisation and activity is dependent on INCENP (Sessa et al., 2005), which in turn binds to the remaining CPC members, where BIRC5 is the subunit targeting the whole complex to the centromere in pro- and prometaphase (Ruchaud et al., 2007). The mechanisms responsible for CPC localisation after metaphase are not well understood. A recent structural analysis followed by cell biological experiments suggests that a surface generated by INCENP and CDC8A is required for central spindle/midbody localisation and CPC cytokinesis function (Jeyaprakash et al., 2007). In this study, the interacting domains of BIRC5, CDC8A and INCENP have been crystallised to understand intra CPC binding as well as CPC movement throughout mitosis. This revealed that INCENP, Borealin and Survivin form a three-helical bundle with their interaction domains. Point mutations within these helices selectively disturb interactions within the complex and also the late mitotic localisation, implicating the helical bundle as the core of the chromosomal passenger complex. The core interactions ensure accurate localisation of the CPC and are directly coupled to AURKB localisation through INCENP, nicely illustrating how different members of a protein complex cooperate to build its function (Jeyaprakash et al., 2007). How the complex interacts with partners on the chromosome, the centromere, the central spindle and the midbody remains to be seen. A systematic analysis of mitotic protein-protein interactions might reveal such additional interaction partners and further advance our understanding of the CPC and other, albeit to date less characterised, mitotic protein complexes.

#### 1.4.1 How to detect protein complexes?

The basic building block of a protein complex consists of pair wise protein interactions. Thus, a protein complex could be viewed as a set of overlapping pair wise interactions between a number of proteins. To determine a protein complex from the bottom up, i.e. by first identifying pair wise interactions and then search for a set of overlapping pairs, the most commonly used assays are *in vitro* binding assays or yeast two hybrid assays (Y2H). Yeast two hybrid assays are amenable to very high throughput and have been used extensively to map pair wise interactions in whole genomes of various organisms from yeast to human (Parrish et al., 2006). An interaction is detected by fusing the cDNA of a bait to the DNA binding domain of a transcription factor and a library of prey proteins to the transactivation domain of the transcription factor. Positive hits transcribe the target gene, usually a selection marker, as a reporter of the interaction. The detected set of binary interactions can be used to draw an interaction graph and highly connected components might represent protein complexes (e.g. Wong et al., 2007). *In vivo* validation by immunopurification of the candidate is essential to confirm the

## 1 Introduction

interaction since a high false positive rate is common (Parrish et al., 2006). Since Y2H assays are limited to the number of available and expressible cDNA clones, they often miss *in vivo* interactions by not testing them. In addition, cooperative effects in complex formation are neglected, making it very difficult to systematically infer protein complexes from Y2H data.

To identify protein interactions *in vivo*, candidate proteins, either affinity-tagged or endogenous proteins, are analysed by affinity purification experiments. Purified complex members are separated by SDS-PAGE and detected by western blotting for candidate proteins or by silver staining followed by MS analysis. Importantly, co-immunopurifying proteins do not necessarily interact directly but might be connected through other components. Also, affinity purification coupled to MS (AP-MS) approaches do not just identify distinct protein complexes but also more transient and substoichiometric interactions. To confirm complex membership of a given protein, further biochemical characterisation is necessary. For example, cell extracts can be centrifuged through a density gradient to separate protein complexes by their S-value. Co-sedimentation of candidate complex members, detectable by western blotting or silver staining, confirms complex membership and allows an estimate of the complex size. Candidate complex members of which only a small fraction co-sediment with the complex can not be considered as complex members. They might represent substrates or regulators of the given protein complex but might also be members of complex isoforms that are present at a lower stoichiometry than the members of the main isoform. One example for different complex isoforms is the cohesin complex further described in 1.3. The core complex of SMC1, SMC3 and RAD21 associates mutually exclusive with either STAG1 or STAG2 resulting in either STAG1-cohesin or STAG2-cohesin (Losada et al., 2000; Sumara et al., 2000). These two isoforms in turn associate mutually exclusive with PDS5A or PDS5B resulting in four isoforms of cohesin (Losada et al., 2005). AP-MS can not necessarily differentiate complex isoforms like this. Proteins identified by AP-MS of a given bait represent a set of interacting proteins of which some might form a distinct protein complex.

To better define a protein complex by AP-MS, different potential complex members can be purified to test for their reciprocal interaction. The set of proteins that interacts reciprocally most likely represents the major isoform of the given complex. By using many baits in a systematic AP-MS analysis, protein complexes can thus be inferred from the overlaps between different bait purifications. This has been applied to the yeast *S. cerevisiae* where about 60% of the expressed proteome were identified in purification of about 2000 unique baits (Gavin et al., 2006; Krogan et al., 2006). A similar approach targeting disease related proteins in human cells identified 2235 proteins from purifications of 338 baits. Protein complexes were not inferred from the data set, presumably because of low overlap between the interacting proteins (Ewing et al.,

2007). To obtain a high confidence set of protein complexes it is essential to construct a dense, partially overlapping set of baits. This allows many complexes to be probed more than once, allowing confident complex identification. It is important to note, however, that the described high-throughput interaction studies solely rely on clustering methods to describe protein complexes. These computationally inferred clusters might overlap to some degree with the actual protein complex but might miss some complex members, isoforms or subcomplexes.

### 1.5 Mitotic protein kinases

Since the discovery that the key mitotic regulator Cdc2 is a kinase (Simanis and Nurse, 1986) a number of other mitotic kinases essential for mitotic progression have been identified and characterised. The key biochemical and morphological changes in mitosis are all dependent on kinase activity: mitotic entry, chromosome condensation, nuclear envelope breakdown, mitotic spindle assembly, spindle assembly checkpoint, APC/C activation and cytokinesis. How these changes are brought about by kinase activity is, however, not well understood. The key feature of protein phosphorylation is that it allows to transiently change the properties of the modified protein. A phosphorylation can lead to overall biochemical and structural changes or to creation or abolition of sequence-specific binding sites. A few kinase substrate relationships in mitosis have been well-characterised and include example where phosphorylation leads to the disintegration of subcellular structure, the generation of a degradation signal or the generation protein-protein interactions. These examples will be described in the following paragraphs.

One early mitotic event is nuclear envelope breakdown. It takes place in late prophase and results in the complete disintegration of the nuclear membrane and its underlying cytoskeletal support, the nuclear lamina. The nuclear lamina is a network of intermediate filaments constructed by the so-called lamins. The lamins were some of the first identified CDK1 substrates. Their phosphorylation causes the lamin network to disintegrate which is essential for nuclear envelope disassembly (Heald and McKeon, 1990; Peter et al., 1990; Ward and Kirschner, 1990). Phosphorylation inhibits the longitudinal association of B-type lamin *in vitro* and might thus cause a structural change of the entire lamin network that results in its disassembly (Peter et al., 1991). Similar mechanisms are the basis of the restructuring of the Golgi apparatus during mitosis. CDK1 and PLK1 mediate the disintegration of the Golgi stacks into vesicles which are localised around the spindle pole during mitosis and are consequently reassembled in telophase (Morgan, 2007).

Phosphorylation can generate or inhibit degradation signals. WEE1 kinase generates the inhibitory Y15 phosphorylation on CDK1 and needs to be inactivated to allow full CDK1

activation and mitotic entry. Its stability is negatively regulated by CDK1 and PLK1 phosphorylation sites which generate a so-called phospho-degron. This degron is recognised by SCF, an ubiquitin ligase, bound to  $\beta$ TrCP (SCF <sup>$\beta$ TrCP</sup>) which mediates ubiquitination and subsequent degradation (Asano et al., 2005; Watanabe et al., 2005; Watanabe et al., 2004). Conversely, phosphorylation can also inhibit degradation and thus stabilise proteins. This has been suggested for another component of the CDK1 regulatory system CDC25A which is stabilised upon CDK1 phosphorylation (Mailand et al., 2002). Since there are also a few APC/C substrates which have been shown to be protected from degradation through phosphorylation, this mechanism might be a more universal one to control protein stability in mitosis (Peters, 2006).

Phosphorylation can directly generate or abolish a protein binding site. This concept has been intensively studied in tyrosine phosphorylation cascades where SH2- and SH3-domain containing proteins specifically bind to phospho-tryosine residues (Koch et al., 1991). In mitotic regulation only few examples have so far been characterised. One is the polo box of PLK1 which binds phospho-serine or phospho-threonine residues (Elia et al., 2003b). The polo box is essential for correct localisation of PLK1 to many of its target sites (Hanisch et al., 2006). Conversely, CBX5 (also known as HP1alpha) binding to H3 has been shown to be negatively regulated by phosphorylation. It binds H3 in interphase via trimethylated lysine 9 and dissociates upon serine 10 phosphorylation by AURKB (Fischle et al., 2005; Hirota et al., 2005).

A few other kinase substrates relationships have been well studied and advanced our understanding of kinase function in mitosis. However, only few kinase substrates have been detected so far, mainly because efficient methods to identify kinase substrates have been lacking. To begin to understand the intricate steps of the various mitotic phospho-regulatory networks a systematic approach to kinase substrate detection needs to be established that allows finding kinase substrates in a cellular assay.

### 1.5.1 How to find mitotic kinases substrates?

Different methods have been used to identify mitotic kinase substrates and their respective phosphorylation sites. Early studies relied on comparing P<sup>32</sup>-labelled phosphopeptide maps from *in vitro* kinase assays using the candidate substrate and *in vivo* labelling of immunoprecipitated candidate substrate. Phosphorylation sites were identified by phospho-peptide mapping using 2D electrophoresis and Edman degradation (Morgan et al., 1989; Shenoy et al., 1989). The most commonly used method today relies on *in vitro* phosphorylation and radioactive labelling of recombinant candidate substrate, targeted mutation of potential phosphorylation sites and reanalysis in the kinase assay. The function of the detected phosphorylation sites can then be validated *in vivo* by using phospho-specific antibodies and the function tested by

expressing the phospho-mutants. By using the following different variations of this workflow most mitotic kinase substrates known to date have been detected (Figure 1.5-1).

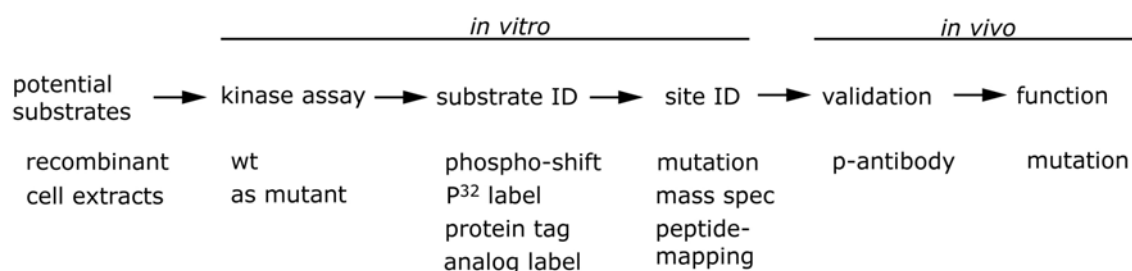


**Figure 1.5-1: Overview of different *in vitro* kinase assay variations commonly used to identify kinase substrates.**

The general workflow of kinase substrate detection is outlined using arrows, different variations for each step are given. Various combinations of these have been used, see text for examples (ID: identification, wt: wild type, as: analogue-sensitive, p-antibody: phospho-specific antibody).

A high throughput variation, which has often been applied, uses a  $\lambda$ -phage cDNA expression library and purified kinase to identify expressed clones that are P<sup>32</sup>-labelled (Fukunaga and Hunter, 1997). This allows screening for the entire genome but has the drawback of missing a number of candidates that are not properly expressed or are not encoded within the cDNA library. Cell extracts can be used to test phosphorylation of all possible substrates present in the cell. The major challenge is to then identify the phosphorylated endogenous proteins. To circumvent this problem an elegant assay using a library of yeast strains in which each strain contains one tagged protein has been combined with an analog- sensitive kinase (as-kinase) in an *in vitro* kinase assay (Ubersax et al., 2003). The as-kinases are generated by mutating the gate keeper residue of the kinase domain to allow a bulky ATP-analog to be used instead of ATP (Shah and Shokat, 2002; Witucki et al., 2002). Using a radiolabelled bulky analogue such as N<sup>6</sup>-(benzyl) ATP, only those proteins are labelled that are direct substrates of the as-kinase. To identify labelled substrates, candidate tagged substrates are purified via the generic tag and the incorporation of radiolabel is measured. While this method allows rather high throughput and establishes a kinase substrate connection under close to *in vivo* conditions, it still requires lengthy follow up mutational analysis to identify the relevant phosphorylation sites.

To directly identify the sites phosphorylated within kinase substrates without the need for mutational analysis, a conventional *in vitro* kinase assay with purified candidate substrates and recombinant kinases has been combined with MS based phospho-site mapping (Kraft et al., 2003). Comparison of the *in vitro* data with phosphorylation sites mapped on the same candidate substrates *in vivo* (APC/C subunits in this case) allowed

## 1 Introduction

partial validation of the substrates identified *in vitro*. A further improvement to the as-kinase method which allows *in vitro* phosphorylation in extracts and at the same time substrate and phosphorylation site identification was recently reported. The ATP analogue was modified to contain sulphur instead of oxygen in the  $\gamma$ -phosphate of the ATP ( $N^6$ -(benzyl) ATP- $\gamma$ -S). Proteins can be specifically labelled with the sulphur containing phosphate in an *in vitro* kinase assay using the as-kinase. Subsequently, proteins are digested and the thiophosphate peptides can be specifically enriched using iodoacetyl-agarose. Analysis of the thiophosphate peptides by MS then allows identification of the substrate and the phosphorylation site of the direct as-kinase target (Blethrow et al., 2008). A complementary approach allows to detect or enrich the thiophosphate using a monoclonal antibody (Allen et al., 2005).

Given the high importance of spatio- and temporal regulation of mitotic kinases the ideal assay would detect substrates in an *in vivo* setting. One possibility is to use specific kinase inhibitors that allow precise temporal control of a given kinase's activity in the cell and also permit large scale biochemical analysis. This approach has been taken using an as-Cdc5 allele and an as-kinase-specific inhibitor to identify potential substrates of Cdc5, the yeast PLK1 homolog (Snead et al., 2007).

The most challenging task in substrate identification still is the validation of the kinase substrate relationship *in vivo* and its subsequent functional characterisation. Current assays for substrate validation have used phospho-specific antibodies which can specifically detect the phosphorylated residue in fixed cells or in cell extracts and compared cells with or without the kinase activity present (e.g. Elowe et al., 2007). Even though this is the best validation that a given substrate is an *in vivo* substrate, this experiment has two drawbacks. First: it requires the complete elimination of kinase activity which is difficult to achieve. Second: it can not rule out that loss of the kinase activity has indirect effects which lead to the abrogation of the phosphorylation site. This problem can partially be addressed by using small molecule inhibitors since they can fully inactivate the kinase. Also, since inhibitors act immediately, they can be applied within a short time window, reducing the chance of indirect effects. Nevertheless the ideal method for detecting direct *in vivo* phosphorylation sites is not yet available.

### 1.6 Aim of this study

This study is divided into three parts. The first two parts are contained within the results section as manuscripts in preparation. An additional introduction to the questions posed in the manuscripts can be found in section 1.4 Protein complexes in mitotic progression

and in section 1.5 Mitotic protein kinases. An extended discussion of the results described within the manuscripts can be found in section 3.1 Protein interaction mapping and in section 3.2 Phosphorylation site mapping of the discussion.

The aim of the first two parts of this study was to more systematically understand the regulation of mitosis. While some general elements regulating entry and progression through mitosis have been identified, the molecular mechanisms underlying their function are not understood. Especially, the protein complex composition of many proteins known to be involved in mitosis is not or only partially understood. Further, many kinases that regulate various aspects of mitotic progression have been identified. Through which substrates these kinases exert their function is, however, poorly understood. As part of the EU-funded MitoCheck project we focussed on two aspects of mitotic regulation in human cells: the composition of mitotic protein complexes as well as the identification of mitotic phosphorylation sites on a subset of these complexes and the identification of substrates of the two mitotic kinases PLK1 and AURKB.

To understand the composition of mitotic protein complexes we wanted to establish a method allowing systematic analysis of a large set of protein complexes. To do this we wanted to adapt the tandem affinity purification protocol for localisation and affinity purification (LAP)-tagged proteins to purify LAP-tagged proteins expressed from bacterial artificial chromosomes (BACs). The tandem affinity purification would allow specific purification of LAP-tagged proteins and their interactions partners which could then be analysed with high sensitivity by MS (LAP-MS). At the same time, the generic purification protocol would allow analysis of a large number of diverse protein complexes, resulting in a more comprehensive set of protein interactions in mitosis. To analyse this large dataset of protein interactions, we wanted to set up a bioinformatic analysis pipeline that would allow detecting purified known and potential novel protein complexes within the dataset. Potential novel protein complexes could then be further analysed by follow up biochemical and functional characterisation.

To identify phosphorylation sites on mitotic protein complexes and to identify substrates of the two mitotic kinases PLK1 and AURKB we wanted to use a combination of LAP-MS and small molecule kinase inhibitors. Purified candidate protein complexes from cells in interphase, mitosis or mitosis in the presence of a kinase inhibitor specific for PLK1 or AURKB could be analysed by MS to identify the phosphorylation pattern specific for each cellular state. Phosphorylation sites present in mitotic cells and absent in mitotic cells treated with a kinase inhibitor would be identified as kinase-dependent phosphorylation sites, the corresponding protein would be identified as a potential kinase substrate. This method would allow identifying potential kinase substrates in a cellular assay. In addition, by using the LAP-MS method established in the first part of the study, we

## 1 Introduction

would be able to more systematically identify potential kinase substrates, thus creating a resource for further functional characterisation of PLK1 and AURKB substrates.

The third part of this study concerns the generation and development of stable cell lines that allow the functional analysis of the cohesin interactors PDS5A and PDS5B. The yeast homologue of human PDS5A and PDS5B, called Pds5p, has been implicated in the establishment of cohesion in S-phase and the maintenance of cohesion in G2 and M-phase. The role of PDS5A and PDS5B in human cohesion is not well understood. Since PDS5A and PDS5B bind the cohesin complex exclusive of each other and PDS5A but not PDS5B forms a subcomplex with the cohesin regulator WAPAL, it is conceivable that the function of PDS5A and PDS5B can be explained by their specific interaction partners. In a first step to understand the role of PDS5A and PDS5B I wanted to generate cell lines inducibly expressing MYC-tagged versions of PDS5A and PDS5B. These cell lines would allow studying the localisation and specific interaction partners of PDS5A and PDS5B.



## **2 Results**

The results part contains two manuscripts in preparation and additional results obtained to generate cell lines stably expressing MYC-tagged versions of PDS5A and PDS5B. The contributions to each of these parts are listed at the end of the results section (2.4).

**2.1 Manuscript in preparation: Systematic analysis of mitotic protein complexes using tandem affinity purification and mass spectrometry discovers 71 novel potential mitotic protein complexes**

James R.A. Hutchins<sup>1\*</sup>, Björn Hegemann<sup>1\*</sup>, Martina Sykora<sup>1</sup>, Jean-Karim Hériché<sup>2</sup>, Bettina A. Buschhorn<sup>1</sup>, Otto Hudecz<sup>1</sup>, Christoph Stingl<sup>1,4</sup>, Ina Poser<sup>3</sup>, Richard Durbin<sup>2</sup>, Anthony A. Hyman<sup>3</sup>, Karl Mechtler<sup>1</sup> and Jan-Michael Peters<sup>1</sup>

<sup>1</sup> Institute of Molecular Pathology, Dr. Bohr-Gasse 7, 1030 Vienna, Austria

<sup>2</sup> Wellcome Trust Sanger Institute, Hinxton CB10 1HH, England

<sup>3</sup> Max Planck Institute for Molecular Cell Biology and Genetics, Pfotenhauerstrasse 108, 01307 Dresden, Germany

<sup>4</sup> Present address: Erasmus Medical Center, Rotterdam, The Netherlands

\* These authors contributed equally to this work.

**2.1.1 Abstract**

Regulation of mitosis depends on a number of mitotic protein complexes. The activity of cyclin-dependent kinase 1 bound to CyclinB (CDK1/CCNB1) is essential for entry into mitosis and early mitotic events while the activity of the anaphase-promoting complex (APC/C) initiates anaphase onset and mitotic exit. A number of other mitotic protein complexes have been identified that are important for early mitotic events like spindle assembly, chromosome condensation, kinetochore structure and the spindle assembly checkpoint. It has become clear that in many cases complex formation is essential for protein function. However, for many proteins known to be involved in mitosis only few or no interaction partners are known. To better understand the function of mitotic proteins it is essential to identify their interaction partners and define the protein complexes in which they might function. Protein tandem affinity purification has proven to be a valuable tool to systematically identify protein interaction partners and to detect novel protein complexes in yeast. The recently established BAC TransgeneOmics pipeline allowed the generation of a large set of human cells expressing localisation and affinity purification (LAP)-tagged mouse genes from their endogenous promoter. Using these cells we successfully purified 175 baits and identified 787 specific interaction partners by mass spectrometry (MS). Computational analysis defined 130 potential protein complexes, 71 of which contained no known protein interactions. Comparison of our dataset to siRNA screens carried out to identify mitotic genes showed that 58 of the novel complexes contained one or more members required for mitosis. Further characterisation confirmed one novel protein complex potentially involved in centrosome function during mitosis. In addition we could confirm two novel interaction partners of the  $\gamma$ -tubulin ring complex ( $\gamma$ -TuRC) and one novel APC/C complex member. Our study provides the first step towards more comprehensively understanding mitotic protein

complex organisation. Further studies of these identified protein complexes will advance our understanding of the molecular basis of mitotic regulation.

### 2.1.2 Introduction

Entry into and progression through mitosis in eukaryotic cells requires the timely assembly and often activation of several mitosis-specific protein complexes. Some of these protein complexes, their localisation and their involvement in key mitotic processes have been characterised in some detail.

The master regulators of the cell cycle are the CDKs, which phosphorylate multiple target proteins controlling mitotic processes such as chromosome condensation, nuclear envelope breakdown and spindle assembly. The catalytic subunits of CDKs require heterodimerisation with a cyclin subunit for activation and are often also bound to a Cks protein (orthologue of *S.pombe* p13<sup>Suc1</sup>) and may be negatively regulated by being complexed by an inhibitory protein such as p21<sup>Cip1/Waf1</sup> or p27<sup>Kip1</sup> (Morgan, 1997).

Another mitotic protein kinase, Aurora B (AURKB), requires association with INCENP for catalytic activity, and with Survivin (BIRC5) and Borealin (CDCA8) to form a functional complex (Andrews et al., 2003; Vagnarelli and Earnshaw, 2001). Together, these proteins display a dynamic localisation (termed chromosomal passenger) behaviour during mitosis; the complex first associates with chromosomes in prophase, then moves onto the inner centromere in prometa- and metaphase, where its action is believed to promote sister chromatid biorientation by destabilising incorrect spindle-kinetochore attachments (Hauf et al., 2003; Tanaka et al., 2002). In anaphase the complex then undergoes a dramatic relocation, first to the central spindle, then in late mitosis to the midbody (Ruchaud et al., 2007).

One class of protein complex has vital roles in organising chromosomes during mitosis: the condensins and cohesins both contain a heterodimer of Smc-family proteins, with a linker in the form of a kleisin protein (Hirano, 2006; Nasmyth and Haering, 2005; Schleiffer et al., 2003), plus at least two additional regulatory proteins. The condensin complexes I and II associate with chromatin and act to maintain the duplicated chromosomes in a condensed state during mitosis (Hirano, 2005). Cohesin complexes in contrast are thought to form stable tripartite ring-like structures, which in association with other regulatory subunits topologically entrap sister chromatids to ensure that the latter are held together until specific cleavage of cohesin allows anaphase to begin (Nasmyth and Haering, 2005).

The APC/C is a multi-subunit E3 ubiquitin ligase, which when activated targets specific substrate proteins for degradation, thereby triggering anaphase onset and mitotic exit

(Peters, 2006). The activity of the APC/C is tightly regulated by the action of the spindle assembly checkpoint (SAC), whose effector, the mitotic checkpoint complex (MCC), inhibits the activity of the APC/C towards key substrates when one or more unattached kinetochores are present in the cell (Musacchio and Salmon, 2007).

On the centrosomes, the gamma-tubulin ring complex ( $\gamma$ -TuRC) serves as the point of initiation of microtubule polymerisation, which by contacting mitotic chromatids via their kinetochores ultimately leads to formation of the mitotic spindle (Wiese and Zheng, 2006). The kinetochores build the interphase between spindle microtubules and the centromeric regions on the mitotic chromosomes. While the inner kinetochore complexes remain associated with the centromere throughout the cell cycle, the outer kinetochore components are sequentially assembled in mitosis (Cheeseman and Desai, 2008). The complex composition at the kinetochore has been analysed to some detail and considerably advanced our understanding of kinetochore function (Cheeseman et al., 2006; Cheeseman et al., 2008; Cheeseman et al., 2004). These detailed studies by Cheeseman and colleagues have nicely shown that the understanding of complex composition forms the basis for understanding the regulatory mechanisms of a complex structure like the kinetochore.

A first step to understand the mechanisms underlying mitotic regulation is thus the identification of mitotic protein complexes. Although some protein complexes required for mitosis have been well characterised, the interaction partners for many mitotic proteins have not been identified. The identification of uncharacterised protein-protein interactions involved in mitosis in a thorough manner requires a systematic approach. The two principal techniques that are often employed to identify protein-protein interactions are yeast two-hybrid assays (Y2H), and affinity purification coupled to MS (AP-MS). Y2H has been employed in a large-scale survey of interactions in human cells (Stelzl et al., 2005) and has the advantage of great sensitivity, with even very transiently interacting proteins being identifiable. However, this technique can suffer from the drawbacks of generating a high rate of false positive hits, requiring extensive post-screening validation, and the limitation that only binary interactions can be detected (Parrish et al., 2006). AP-MS, by contrast, purifies a set of interacting proteins, irrespective of protein stoichiometry, that might be part of one or more protein complexes. The great sensitivity and accuracy of modern tandem MS means that the predominant co-purifying proteins can be identified with high confidence (Kocher and Superti-Furga, 2007; Steen and Mann, 2004). However, in contrast to Y2H AP-MS can not be used to identify binary interaction. Previous genome-wide proteomic studies have demonstrated the feasibility of AP-MS for the characterisation of protein complexes in yeast (Gavin et al., 2006; Krogan et al., 2006). Although AP-MS has been used to detect interaction partners of various disease-related proteins overexpressed in human

cells (Ewing et al., 2007), a study systematically identifying protein complexes in human is lacking.

In this study, we have used an AP-MS approach to isolate protein complexes from mitotic human cells, and to characterise their composition by MS. The affinity-tagged baits in our AP-MS experiments are proteins known to be required for mitosis, whose inclusion derives from several sources: from the biomedical literature relating to mitosis, from a previous screen to identify genes required for cell division (Kittler et al., 2007), from a proteomics screen to identify components of the centrosome (Andersen et al., 2003) and from a genome-wide RNAi screen to identify genes required for mitosis in human cells (Neumann et al., in preparation). By expressing LAP-tagged mitotic genes from bacterial artificial chromosomes (BACs) in cultured human cells (Cheeseman and Desai, 2005; Poser et al., 2008), followed by tandem affinity purification procedure from extracts of mitotic cells under native-like conditions, we were able to isolate protein complexes corresponding to 175 distinct mitotic baits. LAP-MS was used to identify mitotic bait and associated proteins from these preparations with a very high success rate. Several previously-known mitotic complexes were identified in their entirety and in some cases previously unreported interacting proteins could be identified. Bioinformatics clustering of our LAP-MS dataset allowed the mitotic protein-interaction network to be resolved into discrete potential protein complexes, whose existence in the cell could then be validated by biochemical and functional studies. This study represents the first step towards generating a comprehensive picture of the protein complexes within a human cell that are required for mitosis, and should serve as a basis for functional investigations to understand the mechanisms of mitotic regulation.

### **2.1.3 Results**

#### **2.1.3.1 Bait selection**

In order to set up an interaction screen that would enable us to systematically identify novel mitotic protein complexes, we first selected a number of baits that had previously been described as members of well characterised protein complexes. We defined 18 protein complexes consisting of 88 proteins which have been implicated in diverse functions essential for mitotic progression such as chromosome structure (Cohesin, SMC5/6), spindle organisation ( $\gamma$ -TuRC, Dynactin), kinetochore microtubule interaction (NDC80, MIS12) and the mitotic checkpoint (APC/C, mitotic checkpoint complex (MCC)) (Supplemental table 2.1-1 and references therein). Within the reference complex set we selected 39 baits. We further chose baits implicated to function in the areas described above but where clear information on complex membership was missing. In addition we selected baits that have been detected in a screen for centrosomal proteins (Andersen et al., 2003) or detected in screens for mitotic genes (Kittler et al., 2007; Neumann et al., in preparation). Annotation of these baits with Gene Ontology functional terms (Ashburner et al., 2000) showed that about half of the baits are associated with mitotic

## 2.1 Protein interaction mapping manuscript

or mitosis-related functions (Figure 2.1-2). In total 193 stable cell pools expressing mostly C-terminally tagged baits were generated following the transgeneomics pipeline as described in Poser et al. 2008. Importantly most of the analysed baits were mouse homologues of the human target genes. This facilitates the follow up analysis of each cell line by RNAi rescue experiments since the expression of the mouse gene will not be affected by the siRNA targeting the endogenous mouse gene for depletion. Throughout this manuscript, mouse proteins are named with their mouse genome informatics (MGI) symbol and human proteins are named with their human genome project genome nomenclature committee (HGNC) symbol, e.g. Bub1b (*Mus musculus*), BUB1B (*Homo sapiens*) which corresponds to the common human protein synonym BubR1. A list of all used gene names and their most common synonyms is given in the abbreviations section (6.).

### 2.1.3.2 Purification and LC-MS/MS analysis

To identify interaction partners of the selected baits, we grew cell pools of every bait to around 70% confluency, arrested the cells in nocodazole for 18 h and harvested about  $3.2 \times 10^8$  cells per pool. Cells were extracted to obtain a high speed extract supernatant of about 50 mg and tandem affinity purified using an adapted version of the LAP-protocol (Cheeseman and Desai, 2005) as outlined in Poser et al. 2008. The purified protein complexes were eluted with glycine, 20% of the eluate was separated by SDS-PAGE and visualised using silver staining. Of the remaining sample, 40% to 80%, depending on the intensity of the silver stained bands detected by SDS-PAGE, were digested in solution using trypsin, analysed by nano liquid chromatography coupled to fourier transform ion cyclotron (FT-ICR) or orbi trap (OT) MS (LC-MS/MS). Peptides were identified using the Mascot software to search a custom made version of the knowledge based management system (KBMS) database (187752 sequence entries, Applied Biosystems) containing all human sequence and all sequences of the mouse baits.

The SDS-PAGE silver stain result of a typical analysis of a set of ten different LAP-tagged baits is shown in Figure 2.1-1 B. While there are no bands visible for FGFR1OP (a human bait), 2810046L04Rik, Azi1 and Ogg1 (mouse); weak bands are visible for the purifications of Bach1 and Cep72 (not at the expected size) and strong bands are visible in the remaining purifications (in lanes Cep290, Cep55 and Cdc2 bands corresponding to the expected molecular weight are visible). Even though the amount of used starting material was similar, it is obvious that the amounts of purified complex varied strongly. It has been shown by Poser et al (2008) that the expression levels of transgenes in BAC-transfected cell pools is close to those of the endogenous gene so that differential expression of distinct genes is presumably due to endogenous regulation of expression levels.

In the illustrated set, the LC-MS/MS and Mascot analysis identified all ten bait proteins. Common contaminant proteins were removed (see below) to obtain a short list of identified proteins (72 for all ten baits). Each bait was identified with a sequence coverage between 2 and 89% (average 45%) and a Mascot score between 30 and 4863 (average 1448). A summary of the sequence coverage, Mascot score, molecular weight and number of identified copurifying proteins is shown in Figure 2.1-1 C. This result is representative of the whole dataset in which we could identify 175 of the 193 purified baits (success rate 91%). The reproducibility of our purification method was assessed by comparing 17 independent purifications of Cdc2-LAP which we used in every purification set as the positive control (Figure 2.1-1 D). In 17 purifications we always detected the bait, Cdc2. In 15 out of 17 cases we identified the main interaction partners expected for Cdc2 in prometaphase, CCNB1 and CCNB2. The two small substrate targeting subunits CKS1B and CKS2 were detected in 12 out of 17 cases, while the S/M-phase cyclin CCNA2 and its activator SKP2 were only detected 10 out of 17 times. This shows that most of the interaction partners can be reproducibly detected, even though, given a single purification, some might be missed.

As a first validation step of our mitotic protein complex mapping strategy we tested whether we could purify intact protein complexes. To assess this, we compared the interaction partners identified for the 39 baits of the reference complex set with the interaction partners expected from the literature. All but one reference complex was sampled at least once, more than half were sampled two or more times. Of the 88 reference complex members, 90% were detected at least once. We could retrieve all known complex members for 13 out of the 17 sampled reference complexes; all 17 complexes were at least partially retrieved. For two (5%) of 39 baits we only detected the bait itself, indicating that the largest fraction of baits interacted with most of their known complex members. By comparing expression levels of the baits on western blots and silver stained bands on SDS-PAGE gels it is likely that those baits which purify only a fraction of known complex members are either low abundant or interact with the endogenous complex members at substoichiometric levels (data not shown).

### **2.1.3.3 Complex detection**

To infer distinct protein complexes from the 175 unique bait purifications, we set up an analysis pipeline to map the peptides identified by Mascot onto Ensembl genes, to identify and remove contaminants and then to detect potential protein complexes by grouping copurifying proteins into distinct clusters using a computational approach. These clusters were then used to predict complex membership of each purified protein.

## 2.1 Protein interaction mapping manuscript

Peptides in the LC-MS/MS analysis of proteolytic digests were identified using the Mascot search algorithm which assigns a confidence score to each identified peptide. These peptides were then mapped to a minimal list of proteins annotated in the Ensembl database following the parsimony principle (described in Nesvizhskii and Aebersold, 2005). Only proteins identified by two or more peptides with a Mascot score of at least 30 were included. The identified proteins were related back to their corresponding genes, which were then used in the further analysis. For mouse genes the human orthologue was identified using Treefam (Li et al., 2006) and this human orthologue was used in the subsequent analysis.

It is essential to identify and remove copurifying contaminant hits from each purification prior to complex inference by clustering since these unspecific interaction partners are present in many purifications and would thus link many proteins into a large cluster. To define contaminants we first established a gene list of empirically determined contaminants by comparing a number of blank purifications (i.e. purifications from cell extracts not containing any tagged bait). This gene list comprised mostly cytoskeletal and ribosomal genes and was extended to include the entire gene family of an identified contaminant gene. In addition we removed prey that interacted with a large number of baits, assuming that unspecific interactors would co-purify with many baits. To determine how many bait-prey interactions would specify an unspecific interactor, we varied the number of bait-prey interactions allowed to be included into the dataset and tested the performance of the clustering algorithm (described below) on the dataset. Inclusion of prey interacting with ten or more baits increased the cluster size and connected known distinct complexes into larger clusters. We thus only included prey interacting with nine or less baits (5% of all baits). This is similar to how contaminants were removed in a large scale yeast interactome study (threshold of 3% Krogan et al., 2006) and in a human protein interactions screen (threshold of 5% Ewing et al., 2007). Thus, the proteins remaining in every bait purification after contaminant removal can be considered as specific interactors for two reasons: they were not identified in blank purifications and they only interact with few or none of the other baits in the dataset. After removing contaminants the 175 purifications contained 893 unique genes, involved in 1551 bait prey interactions. A comparison to human protein interactions recorded in different public databases (IntAct (Kerrien et al., 2007), HPRD (Peri et al., 2003), MINT (Chatr-aryamontri et al., 2007), MIPS (Mewes et al., 2002) and Reactome (Mewes et al., 2002)) showed that we recover 143 known bait - prey interactions and 591 prey-prey interactions (Figure 2.1-2 B).

To predict potential protein complexes we needed to detect copurifying proteins within the large purification data set. In previous AP-MS studies in yeast, different clustering algorithms have been used to group interacting proteins into clusters that were interpreted to represent protein complexes (Gavin et al., 2006; Krogan et al., 2006).



However, it was later pointed out that the clusters did not fully recover the organisation of several known complexes into isoforms and can thus not always be directly interpreted as protein complexes (Gingras et al., 2007). To assess how well a determined cluster corresponds to a protein complex, we first needed to define the characteristics of a protein complex. In general, a protein complex can be defined as an assembly of two or more proteins at similar stoichiometry which is biochemically stable and forms a structural and functional unit. In the framework of this study we can not determine functionality of complexes so we needed to have a complex definition based on AP-MS data. An AP-MS purification identifies a set of interacting proteins, irrespective of protein stoichiometry, that stably interact at the given purification conditions. If some of these interacting proteins form a complex, the purification of a second complex member should identify a similar set of proteins. Proteins that are present in both purifications most likely represent complex members. As a minimal definition of a protein complex we will thus consider a set of proteins copurifying with two independent baits. Computationally derived clusters that fulfil this definition will be called complexes; all other clusters will be named clusters or potential protein complexes.

To obtain clusters that best represent potential protein complexes, we wanted to use a method that does not depend on pre-set parameters. Specifically, we wanted to use a clustering method for complex inference that allows proteins to be members of more than one cluster and does not require predefining the cluster granularity, i.e. the number and size of clusters. Currently, Markov Clustering (MCL) seems to be the most robust clustering method for interaction graphs (Brohee and van Helden, 2006). However, MCL requires parameters that determine cluster granularity and MCL does not allow proteins to belong to multiple complexes. A spectral algorithm (Meila and Shi, 2001; Shi and Malik, 2000) is similar to MCL but allows determining of the number of clusters by the data-dependent eigengap heuristic. It further allows proteins to belong to more than one complex since the last step of the spectral clustering algorithm uses the fuzzy c-means algorithm (see materials and methods for details). We decided to use a combination of the spectral algorithm and the fuzzy c-means algorithm (SFCM) for data analysis since this best matched our requirements described above.

The main connected component as defined by the interaction graph constructed from the affinity purification data contained 787 genes. A set of 31 small connected components contained 106 genes (the largest small connected component contained 16 members, 17 connected components contained only one member). The small connected components were not subjected to clustering since, by definition, they do not interact with any other complex in the dataset. For these 31 components, the complexes were determined by the copurifying proteins of every bait. The main network was subjected to spectral fuzzy c-means clustering which produced 116 clusters. The complexes of the small connected components containing at least two members were added to the SFCM

## 2.1 Protein interaction mapping manuscript

clusters, to obtain 130 clusters that vary in size from 1 to 38 proteins. Of these 130 clusters 7 contain 21 to 38 members, 11 clusters contain 11 to 20 members, 111 clusters contain 2-10 members and one cluster contains only a single member (Figure 2.1-2 C, see appendix 5.4 for entire table including the small connected components).

In order to evaluate our computational approach, we tested how well the detected clusters corresponded to the reference complex set had we defined in the bait selection procedure (Supplemental table 2.1-1 and references therein). We detected 75% of the members of the reference complex set in the clusters. To determine whether the cluster size also corresponds to the size of the reference complexes, we calculated the accuracy, i.e. how many members of a cluster equal the reference complex members. The accuracy of our data in comparison to the reference complex set was 51%. This is in part due to the fact that some of the mitotic checkpoint and kinetochore complexes are highly interconnected and thus are grouped into larger clusters that contain two complexes as defined by the reference set. Additionally, some clusters contain potential novel members of the reference complexes (see 2.1.3.4) and thus also reduced the calculated accuracy.

To test to what extent we recovered novel interactions and novel complexes we used the matrix model to allow each cluster member to interact with all other cluster members and compared these binary interactions to the interactions recorded in public interactions databases as described above. In 130 clusters 368 interactions are known (107 are bait-prey interactions). A total of 58 clusters contain one or more known interaction, defining 71 clusters as potential novel complexes (Figure 2.1-2 B).

We wanted to know which of the potential novel complexes might play a role in mitosis. We compared the members of all clusters with data of various screens that have been performed recently to identify genes essential for mitosis (Goshima et al., 2007; Kittler et al., 2007; Rines et al., 2008; Sonnichsen et al., 2005). In addition we also annotated all clusters with the phenotypes detected in the genome wide siRNA screen carried out within the MitoCheck project. This screen combined siRNA knockdown with live cell imaging for all siRNA knockdowns and thus allowed a detailed description of the mitotic phenotypes (Neumann et al., in preparation). Application of this filter showed that 111 out of 130 clusters contained at least one member with a mitotic phenotype in one of the screens. Out of the 71 potential novel complexes, 58 showed at least one mitotic phenotype (Figure 2.1-2B and Supplemental table 2.1-3). The most striking example is a cluster containing the baits FAM29A and CEP27 (cluster 79, Supplemental table 2.1-3). It consists of six other members (NP\_219485.1, UCHL5IP, C14orf94, CCDC5, C4orf15 and KIAA0841) that all copurify with the baits in the original purifications. Out of these eight potential complex members, six have been detected as a hit in one or more of the genome wide screens for mitotic genes (Figure 2.1-3 D, Supplemental table

2.1-3). Only one member, CCDC5, has been previously described, where it was called HEI-C (Einarson et al., 2004). CCDC5 localises to centrosomes in interphase and to the mitotic spindle. Depletion of CCDC5 leads to mitotic spindle defects, prolonged metaphase arrest and apoptosis, consistent with the phenotype observed in the MitoCheck screen (Neumann et al., in preparation). To further elucidate and confirm the complex composition we tagged C14orf94, CCDC5 and C4orf15 for further purification experiments (see below).

Manual inspection of all clusters showed that, apart from the many potentially novel complexes, some well known complexes contained additional interaction partners that had not been previously described (Supplemental table 2.1-3). We will focus on a few interesting examples. The cluster containing the centralspindlin complex (cluster 93, Supplemental table 2.1-3), known to be composed of RACGAP1 and KIF23 and required for cytokinesis (D'Avino et al., 2005), contains a number of additional members: MICAL3, CD2AP, CCAR1 and TRAF3IP1. Interestingly, MICAL3 and CCAR1 also scored as a mitotic hit in the MitoCheck screen (Neumann et al., in preparation). Movies recorded from H2B-GFP-expressing HeLa cells after siRNA depletion of MICAL3 or CCAR1 show that loss of either protein leads to metaphase delay and multinucleated cells, suggesting that MICAL3 and CCAR are required during early mitosis or cytokinesis.

The  $\gamma$ -Tubulin ring complex ( $\gamma$ -TuRC) consists of the six subunits TUBG1 and TUBGCP2-6 (Raynaud-Messina and Merdes, 2007). Two clusters contain members of the  $\gamma$ -TuRC: 39 (TUBG1, TUBGCP4, 5 & 6) and 71 (TUBG1/2 and TUBGCP2 & 3). NEDD1, a known interactor of  $\gamma$ -TuRC (Luders et al., 2006), is located in cluster 39 while two previously unknown members are present either in cluster 39 (Q5VXS7\_HUMAN) or in cluster 71 (FAM128B). Both clusters are connected through the TUBG1 subunit (Figure 2.1-2 D). FAM128B and Q5VXS7\_HUMAN might, nonetheless, represent novel interactions partners of  $\gamma$ -TuRC. Most surprisingly was the finding that the APC/C, which has been affinity purified and analysed by MS in various organisms repeated times (Peters, 2006) also showed one previously unknown interaction partner, which is the gene product of c10orf104 (Figure 2.1-2 D).

To further test some of the predicted protein complexes, we tagged 29 genes within 17 predicted complexes. Analysis of this dataset is still ongoing, some preliminary results are summarised in the next section.

#### **2.1.3.4 Characterisation of novel complexes**

Of the 29 genes within the predicted complexes, we have so far analysed 14 by MS. Out of those 14 purifications, the bait was detected in 13 cases. Eight baits copurified at least one other interacting protein and four baits purified one or more of the members

## 2.1 Protein interaction mapping manuscript

of the predicted complex. In the following, five example are discussed which have so far only been analysed by SDS-PAGE and silver staining (the MS analysis has not yet been performed) and one example is discussed for which also the MS analysis has been carried out.

We first tested whether the two potential interactors of the  $\gamma$ -TuRC, FAM128B and Q5VXS7\_HUMAN, also copurify components of  $\gamma$ -TuRC. We prepared mitotic protein extracts from the three tagged cell pools used in the initial experiments (containing LAP-tagged TUBG1, TUBGCP2 and TUBGCP3) as well as mitotic protein extracts from TUBGCP6-LAP, FAM128B and Q5VXS7-LAP cell pools. We performed LAP purifications in parallel as described above and analysed 20% of the eluate by SDS-PAGE and silver staining (Figure 2.1-3 A). Bands were annotated based on the expected electrophoretic mobility of the  $\gamma$ -TuRC subunits as indicated in the table in Figure 2.1-3 A. The band pattern observed for TUBG1 and TUBGCP3 was identical to the one observed in the previous purification (data not shown), also for the TUBGCP2 we previously did not detect any bands. As expected, TUBGCP6 (also a  $\gamma$ -TuRC subunit) produced an identical band pattern. Importantly, the band pattern of FAM128B was identical to the  $\gamma$ -TuRC pattern apart from a band between 20 and 30 kDa which might correspond to the S-peptide-tagged form of FAM128B. The purification of Q5VXS7\_HUMAN-LAP resulted in weak bands at the sizes expected for TUBGCP5, 3, 2 and 4. MS analysis has not been carried out yet. The similarity of the band patterns for both predicted  $\gamma$ -TuRC interactors with the known  $\gamma$ -TuRC subunits however suggests, that FAM128B and Q5VXS7\_HUMAN are indeed novel members of the  $\gamma$ -TuRC. Analysis of TUBG1 purifications from interphase and mitosis indicate that both proteins are also present in the interphase form of the  $\gamma$ -TuRC (see phospho-mapping manuscript). Further functional analysis of these two novel members will help understand their role in  $\gamma$ -TuRC function.

Further we analysed the novel FAM29A complex. We prepared mitotic protein extracts of cell pools containing the LAP-tagged versions of the two founding members of the complex FAM29A and CEP27, as well as of cell pools containing LAP-tagged C4ORF15, C14ORF94 and CCDC5. Eluates of parallel LAP purifications were analysed by SDS-PAGE and silver staining (Figure 2.1-3 B). Bands were annotated based on the expected electrophoretic mobility of the potential FAM29A subunits as indicated in the table in Figure 2.1-3 B. The purification of FAM29A produced only a few weak bands which were, however, identical to the bands detected in the CEP27 purification. MS analysis of previous purifications of FAM29A and CEP27 showed that all eight potential FAM29A complex members copurified with both baits. While the C4ORF15 purification only yielded one band corresponding to its own size (slightly shifted due to the S-peptide-tag) the purification of C14ORF94 and CCDC5 yielded a number of bands identical with the CEP27 bands. The MS analysis of these purifications has not been carried out so far but the partially identical band patterns suggest that FAM29A, CEP27, C4ORF15,

C14ORF94 and CCDC5 are part of the same complex. Unique bands detected in the C14ORF94 purification might indicate the presence of additional interacting partners specific to C14ORF94. Further functional analysis of this complex will show if the whole complex is involved in mitotic spindle integrity as suggested by the study on CCDC5 (Einarson et al., 2004) or if it serves other functions.

#### 2.1.3.5 Identification of ANAPC16 as a novel subunit of human APC/C

One interesting finding of our complex analysis was the identification of a novel potential subunit of the APC/C. Previous work in yeast, *Xenopus* and human has identified the APC/C as the major regulator of the metaphase to anaphase transition (Peters, 2006). This 1.5 MDa complex, which consists of twelve subunits in human, is a ubiquitin ligase that ubiquitinates substrates to target them for proteasomal degradation. It was thus quite surprising for us to find a 11.7 kDa protein encoded by the c10orf104 gene as a potential additional subunit of the APC/C. This subunit was found in purifications with the mouse LAP-tagged subunits Anapc1, Anapc5, Cdc16, Anapc8 and Cdc26 (Figure 2.1-3 C) but also in purifications using an antibody against endogenous CDC27 (data not shown). To confirm this interaction we generated a cell pool expressing N-terminally tagged C10orf104. We used a variation of the LAP-tag called MitoTag which, in addition to the LAP-tag also contains a FLAG epitope. We purified C10orf104 from these cells using the standard LAP purification protocol as described above and analysed 20% of the eluate by SDS-PAGE and silver staining (data not shown) and 80% of the eluate by LC-MS/MS. We could detect the mouse bait C10orf104 as well as eight out of twelve APC/C subunits and three members of the mitotic checkpoint complex (Figure 2.1-3 C), confirming that LAP-tagged C10orf104 can interact with the APC/C.

To further characterise the interaction of endogenous C10orf104 with the APC we generated three polyclonal antibodies directed against three peptides located at the N-terminus (2185), the central region (2186) and the C-terminus of the protein (2184, Supplemental figure 2.1-1). We tested the antibodies by depleting C10orf104 from HeLa cells, preparing cell extracts 24, 48 and 72 h after transfection and probing them with the three different affinity purified antibodies. A specific antibody should recognise a band at about 12 kDa which should be reduced or absent in the C10orf104 depleted extracts. While the antibody raised against peptide 2185 did not recognise any specific bands, antibodies 2184 and 2186 did recognise a band at approximately 15 kDa in HeLa protein extracts that was absent (2186) or strongly reduced (2184) at 24, 48 and 72 h after siRNA transfection (Supplemental figure 2.1-1). We continued to use antibody 2184 (named C10orf104 hereafter) for detection of C10orf104 in western blots.

## 2.1 Protein interaction mapping manuscript

We also tested whether the 2186 antibody could immunoprecipitate C10orf104 and, more importantly whether it would also immunoprecipitate APC subunits. To do this we used 2186 antibody bound to Affiprep beads and CDC27 antibody (Gieffers et al., 1999) crosslinked to Affiprep beads and incubated them separately with HeLa extract from logarithmically growing cells. Precipitated proteins were eluted with glycine and analysed by SDS-PAGE followed by Western blotting with C10orf104 and APC2 antibodies. The 2186 antibody could immunopurify (IP) C10orf104 and APC2 in similar amounts as the CDC27 antibody (Figure 2.1-4 A), confirming our initial finding with six different LAP-tagged APC subunits that C10orf104 interacts with the APC (Figure 2.1-3 C). In a further immunoprecipitation experiment we wanted to test whether C10orf104 interacted with all APC/C subunits in different cell cycle stages. To do this we incubated 2186 antibody crosslinked to Affiprep bead as well as crosslinked CDC27 antibody with HeLa cell extracts from logarithmically growing cells, from cells arrested in S-phase by hydroxyurea and from cell extracts of cells arrested in prometaphase by nocodazole. Precipitated protein was glycine eluted and analysed by SDS-PAGE followed by silver staining. The resulting band pattern of the C10orf104 IP from all three cell cycle stages was indistinguishable from the CDC27 IPs (Figure 2.1-4 C); strongly suggesting that C10orf104 interacts with the whole APC/C complex.

To test whether C10orf104 is mainly present as an APC/C complex member we fractionated cell extract from logarithmically grown HeLa cells in a 10 to 30 % sucrose gradient and analysed the single fractions by SDS-PAGE and western blotting using antibodies against the APC/C subunits CDC16, APC10 and against C10orf104. Figure 2.1-4 B shows that the largest fraction of C10orf104 indeed co-sedimented with the APC/C while a minor fraction sedimented in fractions 6, 7 and 8. Since C10orf104 would have been expected not to enter the gradient due to its low molecular weight, this peak at fractions 6-8 suggests that C10orf104 either oligomerises, is a member of a smaller complex or partially dissociates from APC/C in the sucrose gradient.

The observation that C10orf104 interacts with APC/C was further confirmed in APC/C activity assays. We purified APC/C from interphase HeLa extracts using either the 2186 antibody directed against C10orf104 or the CDC27 antibody bound to beads. The purified complex was then incubated with all components of a ubiquitination assay to test if it can *in vitro* ubiquitinate a recombinant, <sup>125</sup>I – labelled CCNB1 (Cyclin B1) fragment. The reaction was stopped at different time points and analysed by SDS-PAGE and phosphorimaging (Figure 2.1-4 D) to show that APC/C purified via the C10orf104 protein is equally efficient in ubiquitination as the APC/C purified via the CDC27 antibody.

To analyse whether the expression of C10orf104 was regulated in a cell cycle-dependent manner we synchronised HeLa cells with a double thymidine block release and analysed

extracts prepared at different time points after S-phase release by SDS-PAGE and western blotting for C10orf104, CCNB1 and TUBA1B (Figure 2.1-4 E). As indicated by the TUBA1B signal the overall protein levels are similar between the different time points. The sharp drop of CCNB1 levels between 9 and 10.5 h after the S-phase release mark the metaphase- to anaphase-transition. The levels of C10orf104 seem to remain equally high throughout the cell cycle. A small reduction of its levels at the 15 and 16.5 h time point needs to be further analysed to determine whether they are due to small loading differences not discernible in the TUBA1B control or due to some degradation of C10orf104 prior to S-phase in G1.

We next wanted to test the function of C10orf104 as an APC/C subunit. If it was essential for APC/C's catalytic function we expected that depletion of C10orf104 would arrest cells at the meta- to anaphase transition or would abolish APC/C's activity in G1-phase. We first tested the former possibility by depleting C10orf104 by siRNA transfection for 48 h and testing whether cells accumulated in mitosis by counting the mitotic index of fixed cells and by analysing CCNB1 levels. Accumulation of cells in mitosis would lead to higher CCNB1 levels and an increased mitotic index. However, the contrary was the case. We observed a reduction of CCNB1 levels and a decrease of the mitotic index from 3.2% to 1.6% (Figure 2.1-1 F). To further investigate this observation in a synchronised cell population we depleted C10orf104 by RNAi and arrested cells in thymidine to block them in early S-phase. Six h after release from thymidine we added taxol to activate the spindle checkpoint and let cells accumulate in mitosis for three h. To confirm the C10orf104 depletion and G2/M cell cycle state we made cell extracts and analysed them by SDS-PAGE and western blotting using the indicated antibodies (Figure 2.1-4 G). CCNB1 levels were similar in control cells and cells treated with siRNA while the levels of C10orf10 were strongly reduced. Analysis of the cells before and after taxol treatment by immunofluorescence microscopy using CCNB1 and BUB1B antibodies showed that in control conditions about 90% of cells were in S- or G2-phase six h after thymidine release (Figure 2.1-4 H). These cells were positive for BUB1B and CCNB1 in the cytosol and the DAPI staining showed the chromatin to be in a decondensed state. After three h of taxol treatment 50% of control cells were in a prometaphase state with BUB1B staining the kinetochores, condensed chromatin and cytoplasmic staining of CCNB1. Cells depleted of C10orf104, however, did not accumulate in mitosis. Most cells retained cytosolic BUB1B and CCNB1 staining indicative of a G2 or S-phase state. There were no cells that passed metaphase which would have been CCNB1 negative. This indicates that cells lacking C10orf104 delay their progression through S and G2 or delay mitotic entry.

### 2.1.4 Discussion

To systematically map protein-protein interactions in mitosis we adapted the LAP-protocol (Cheeseman and Desai, 2005) into a fast, robust and clean tandem affinity purification procedure for bacterial artificial chromosome expressed transgenes (Poser et al., 2008). In combination with very sensitive FT or OT MS we were able to successfully identify 175 out of 193 (91%) purified baits, 718 additional unique proteins which involved in 1551 bait-prey interactions. Validation of 39 unique bait purifications by comparison to a reference complex set showed that 90% of expected complex members could be recovered and only 5% of the baits did not purify any of the expected complex members. Our approach thus enabled us to systematically identify mitotic protein complexes in HeLa cells with a high confidence.

The stringent tandem-affinity purification procedure strongly reduced the number of unspecific interactions usually detected when using antibodies against endogenous proteins. After removing common contaminants a typical purification resulted in a list containing tens of proteins instead of hundreds of proteins usually detected in single step antibody purifications. Nonetheless, in a few cases we were able to detect a number of rather transient or weak interactions like the APC/C substrate NEK2 or a number of Cdc2a substrates (ANAPC1, CDC25C).

A low number of unspecific interactors was key to allow for a clustering analysis of the purification data set. We used spectral fuzzy c-means (SFCM) clustering (Meila and Shi, 2001) which is based on the Normalised Cut algorithm (Shi and Malik, 2000) to obtain a largely unbiased analysis of the data set. Clustering was performed on 787 genes from the main connected component and resulted in 116 interaction clusters in addition to 14 complexes from small connected components. The large interaction graph of 787 genes reflects the overlapping set of protein interactions we analysed. The recent AP-MS studies in yeast covered over two thirds of the expressed genome and obtained a very densely connected set of interactions from most functional pathways (Gavin et al., 2006; Krogan et al., 2006). Since a whole genome analysis of protein-protein interactions in human is still far beyond the scope of currently available techniques, we focussed our analysis on a small subset of protein interactions, targeting proteins involved in cell cycle regulation. It was important to select baits from defined localisations within the cell to recover a dense protein interaction network with our data. Sparse complex coverage would have resulted in low overlap between copurifying protein so that complex inference would not have been possible.

It is important to note that, based on the definition of a protein complex as two baits and their overlap of copurifying proteins, the clusters obtained computationally do not always reflect true protein complexes. The overlap of cluster components (coverage) and cluster size (accuracy) with a set of well defined complexes can be used to assess



how well clusters reflect actual protein complexes. The clusters determined from our purification data have a coverage of 75% and an accuracy of 51%. In comparison to the coverage determined by Gavin et al. (78%) and the accuracy determined by Gavin et al. (78%) and Krogan et al. (72%) for their yeast interactome dataset, our coverage is similar but the accuracy is much lower. This is most likely due to the fact that both studies used clustering algorithms which have been trained (Krogan et al., 2006) or their parameters adjusted (Gavin et al., 2006) to best match a set of reference complexes. This introduced a bias towards the characteristics of the reference complexes and might not best reflect the original purification data. We avoided any bias in our data analysis by using SFCM clustering which does not require preset parameters to determine cluster number and cluster size. The comparison of our computationally defined clusters with our set of reference complexes indicate that most known complex members have been identified within the clusters but the cluster size is quite different from the expected complex size in the reference set.

This discrepancy can be explained in two ways. One reason could be that we detected a number of novel complex members, suggesting that the set of reference complexes is not very accurate. The other reason would be that the clustering procedure either fuses highly connected protein complexes into one cluster or splits one protein complex into two or more subclusters. While we could not yet test occurrence of the first explanation, we find several cases of the second in our data set. For example: a fusion of two complexes into one cluster was observed for the MIS12 and NDC80 complexes (reference complexes 11 and 12 in Supplemental table 2.1-1; cluster 67 in Supplemental table 2.1-3). Both complexes are highly connected at the outer kinetochore in mitosis (Cheeseman and Desai, 2008) and it is thus not surprising that purification of MIS12 and NDC80 finds mostly overlapping prey which confirms earlier findings (Cheeseman et al., 2004). Still, while the coverage for both complexes is 100%, the accuracy is 27% for the NDC80 complex and 45% for the MIS12 complex. Other examples for complex fusions into one cluster or splitting into several clusters exist, suggesting that this was a common phenomenon in our clustering procedure. In conclusion, the clusters serve as indicators for a potential complex but do not necessarily represent a protein complex.

Another common feature of protein complexes, their modularity, can not be easily assessed using a clustering approach. Many complexes are known to exist in isoforms with different subunit composition. This is exemplified in the complex regulation and targeting of the PP2A phosphatase where regulatory, catalytic and structural subunits combine mutually exclusive of each other to control PP2A's localisation and activity (Janssens et al., 2005). Gavin et al. attempted to resolve complex isoforms in their yeast interactome study by using iterative, slightly varied runs of their clustering procedure to define complex cores and modules. But as outlined in a recent review on

protein complex analysis by AP-MS, this approach did not allow detection of validated complex isoforms (Gingras et al., 2007). We also did not resolve this issue in our data analysis. The cohesin complex serves as one example. It is known to exist in four mutually exclusive isoforms in human (Losada et al., 2005; Sumara et al., 2000) but falls into one common cluster in our dataset (Supplemental table 2.1-3, Cluster 43). To determine mutually exclusive interactions or subcomplexes, many more baits per complex are required. Large scale analysis in addition would require that not just positive interactions are considered for complex inference but also the absence of interactions as outlined in (Collins et al., 2007).

To better assess the quality of the protein complex predictions made by the cluster analysis, we carried out a number of follow up experiments. We could show that two potential novel interaction partners of  $\gamma$ -TuRC (Q5VXS7\_HUMAN and FAM128B) are indeed complex members (Figure 2.1-3 A), that one potential novel interaction partner (C10orf104) of the previously well characterised APC/C (Peters, 2006) does indeed interact with APC/C subunits (Figure 2.1-3 C) and that the completely novel FAM29A complex, potentially involved in spindle organisation during mitosis (Einarson et al., 2004), does consist of at least five of the eight members predicted by our initial AP-MS and cluster analysis (Figure 2.1-3 B).

We further went on to investigate the biological significance of the interaction of C10orf104 with the APC/C. By purifying the endogenous protein via polyclonal antibodies, by density gradient centrifugation and ubiquitination activity assays we could clearly show that C10orf104 is a novel complex member of APC/C which we propose to name ANAPC16. We hypothesized that ANAPC16 could be required for APC/C activity at the meta- to anaphase transition similar to APC2, which, if knocked out, leads to a metaphase arrest in mouse hepatocytes (Wirth et al., 2004). Surprisingly, depletion of ANAPC16 did not lead to accumulation of cells in mitosis but rather delayed cells in S- or G2-phase. This was supported by the observation that CCNB1 levels and mitotic index were reduced after ANAPC16 depletion in asynchronously growing cells. Since S/G2 is the part of the cell cycle where APC/C is not active, this is a surprising finding. It is conceivable that instead of being necessary for APC/C activity, ANAPC16 could be involved in keeping APC/C inactive in S and G2. An APC/C lacking ANAPC16 could thus be, at least partially, active and delay the ordered progression of S, G2 and timely entry into mitosis by premature degradation of its mitotic substrates. Likewise, the origin licensing inhibitor geminin (GMNN), which is a target of APC/C bound to its coactivator FZR1 in late mitosis and early G1 could be prematurely degraded by APC/C- FZR1 that has not been inactivated at the G1/S transition. A similar role has recently been implicated for Emi1 (FBXO5), which is required for the stabilisation of GMNN and for the accumulation of CCNA1 and CCNB1 (Di Fiore and Pines, 2007). Further experiments as

to where exactly cells are delayed and how APC/C activity is changed when it is lacking ANAPC16 will help to understand the function of ANAPC16 as an APC/C subunit.

We have, for the first time, generated a comprehensive map of a subset of human mitotic protein complexes. The focus on proteins involved in mitosis defined 71 novel potential complexes and additional novel potential interactions partners for 58 other partially or well known protein complexes. This dataset, in combination with the results of a genome wide live cell imaging siRNA screen (Neumann et al., in preparation) and a comprehensive subcellular localisation screen carried out using the same cell pools as used in our study (Toyoda and Hyman, in preparation) will greatly enhance our understanding of human mitosis. More importantly, the accessibility of all data through a common website ([www.mitocheck.org](http://www.mitocheck.org)) will facilitate a large number of validation and follow up experiments within the cell cycle field that will lead to a more comprehensive understanding of the events leading to entry into and progression through mitosis.

## **2.1.5 Materials and methods**

### **2.1.5.1 Cell culture and siRNA depletion**

HeLa cells were grown on Nunc cell culture dishes in DMEM supplemented with 10% FCS, 0.2 mM L-glutamine, 100 U/ml penicillin, and 100 µg/ml streptomycin. For transfected cell lines the medium was supplemented with 500 µg/ml G418. Mitotic cells were arrested for 18 h using 100 ng/µl nocodazole, harvested by scraping, washed twice with PBS, frozen in liquid nitrogen and stored at -80°C until analysis. For a standard purification  $3 \times 10^8$  cells were grown on five 25x25 cm dishes. For cell cycle synchronisation cells were arrested at 50% confluency with 2 mM thymidine for 16 h. Cells were then released into fresh medium for eight h, then arrested a second time with 2 mM thymidine for 16 h and again released into fresh medium. Samples were collected at 1.5 h spaced time points for 18 h. To obtain S-phase arrested cells, 2 mM hydroxyurea was incubated with cells for 16 h prior to harvest. RNAi depletions were performed as previously described (Hirota et al., 2004) using a preannealed siRNA oligo targeting C10orf104 (Ambion): 5'-CGCUUAAACAGGUGAAACAtt-3' (database ID: 117, Ambion ID: 129750).

### **2.1.5.2 Protein extraction, purification and MS**

LAP-purification was carried out as described (Poser et al., 2008) using about 50 mg of high speed extract supernatant as input. Purified proteins were eluted from beads using 0.1 M glycine pH 2.0 and the eluate neutralised with 1/10 volume 1.5 M Tris pH 9.2. Of the eluate 20% was analysed by SDS-PAGE and silver staining, the remaining 80% of the eluate was subjected to in-solution digest using trypsin as described previously

## 2.1 Protein interaction mapping manuscript

(Kraft et al., 2003). Depending on protein abundance in the eluate, 50% or 100% of the sample were analysed by MS.

### MS analysis

Equipment - All nano HPLC separations were performed using UltiMate 3000 Nano-LC system (Dionex Benelux, Amsterdam, The Netherlands) equipped with a trap column (PepMap C18, 300 µm ID x 5mm length, 3 µm particle size, 100 Å pore size, Dionex Benelux) for sample desalting and concentration and an analytical column (PepMap C18, 75 µm ID x 150 mm length, 3 µm particle size, 100 Å pore size, Dionex Benelux) for the chromatographic separation. Loading buffer used contains 0.1% trifluoroacetic acid (Pierce). For chromatographic separation mobile phase A contains 5% acetonitrile (Merck, Darmstadt, Germany) and 0.1% formic acid (Merck) and mobile phase B 80% acetonitrile and 0.08% formic acid.

Mass spectrometric analyses were conducted either on a hybrid linear ion trap/Fourier transform ion cyclotron resonance (FTICR) mass spectrometer with a 7-Tesla superconducting magnet (LTQ-FT Ultra) or on a hybrid linear ion trap/Orbitrap mass spectrometer (both ThermoElectron, Bremen, Germany). The mass spectrometer was equipped with a nano-electrospray ionization source (Proxeon Biosystems, Odense, Denmark). Metal coated nano ESI needles were used (New Objective, Woburn, MA, USA).

LC separation - Samples were loaded onto the trap column at a flow rate of 20 µL/min loading buffer and were washed for ten minutes. Afterwards the sample was eluted from the trap column and separated on the separation column with a gradient from 0% to 35% mobile phase B in 85 minutes followed by 35% to 60% in 5 minutes at a flow rate of 300 nL/min.

MS detection - Eluting peptides were ionized with a spray voltage set to 1.5 kV. Fullscan (400-1800 Th.) was conducted in the ICR or OT cell yielding a survey scan with resolution of 100,000 and a typical mass accuracy < 2ppm (rms). CAD fragmentation and spectra acquisition were carried out in the linear ion trap using a multi stage activation (MSA) method. The target values of the automatic gain control (AGC) were set to 10,000 for CAD in the ion trap, and to 500,000 for FT-ICR fullscan spectra. In the applied MS method fragmentation was performed on the five most intense signals of the survey scan using MSA of the neutral loss of phosphoric acid. Singly charged ions were excluded for precursor selection and precursors of MS<sup>2</sup> spectra acquired in previous scans were excluded for further fragmentation for a period of 3 min whereas the exclusion mass tolerance was set to 5 ppm.

Database search - Acquired data (Xcalibur RAWfile) were converted into Mascot generic files using Mascot Daemon (Matrix Science, London, UK). For peptide identification a

database search against a custom database containing the human KBMS database (5.0.20050304, 187752 sequence entries, Applied Biosystems) and all relevant mouse bait sequences was carried out using Mascot (Matrix Science, London, UK; version 2.2.0). The following parameters were used for the database search: carboxymethylation (+58.0055 u) of cysteine was set as fixed and oxidation (+ 15.9949 u) of methionine as variable modification; enzymatic cleavage was specified for trypsin and mass tolerances of the parent ion and the fragments were set to 10 ppm and 0.80 Da, respectively. Proteins with two peptide hits, each having a Mascot score of 30 or higher, were kept as hits. Mascot results were exported into xml-files and converted to text files for further data processing.

#### **2.1.5.3 Sucrose density gradients**

Sucrose density gradients were prepared in ultra-clear centrifuge tubes (19 x 95 mm, Beckman) by mixing two sucrose solutions using a GradientMaster (Biocomp). Cell extracts supernatants were centrifuged at 42 000 rpm (TLA45 rotor) for 15 min in an Optima MAX ultracentrifuge (Beckman Coulter). Supernatant containing 2.5 mg protein was layered on a 10-30% sucrose gradient in TBS-Tween (0.01%). Gradients were centrifuged at 34 000 rpm for 18 h at 4°C in a Beckman SW40 rotor in a Beckman Optima MAX ultracentrifuge (Beckman Coulter). Gradients were fractionated into 400 µl aliquots using an ISCO fractionator at a flow rate of 1 ml/min.

#### **2.1.5.4 Ubiquitination assay**

Five µl of either C10orf104 or CDC27 immunopurified from interphase extracts on antibody beads was incubated in 7 – 10 µl XB buffer (20 mM Tris-HCl pH 7.5, 150 mM NaCl, 0.02% Tween 20) containing 10 µg ubiquitin, ATP regenerating system (7.5 mM creatine phosphate, 1 mM ATP, 1 mM MgCl<sub>2</sub>, 0.1 mM EGTA, 30 U/ml rabbit creatine phosphokinase type I (Sigma)), 0.25 µg His<sub>6</sub>-E1, 1 µg of E2 (His<sub>6</sub>-UbcH10 or a mixture of His<sub>6</sub>-UbcH10 and His<sub>6</sub>-Ubc4) and 0.2 µg purified FZR1 (as indicated). An iodinated fragment of human CCNB1 (amino acids 1-84, 3 µg) was used as a substrate. Reactions were incubated in a thermomixer (1400 rpm, 37°C) for the times indicated and the reaction was stopped by the addition of SDS-sample buffer. Samples were analyzed by SDS-PAGE and phosphorimaging.

#### **2.1.5.5 Data processing and clustering analysis**

Identification of interacting proteins - To map peptides to Ensembl proteins, we looked for proteins that perfectly match the peptides first in Ensembl then in Uniprot entries. Ensembl proteins corresponding to Uniprot matches were retrieved using Ensembl's mapping of Uniprot entries, then the peptide positions were identified by Smith-Waterman alignment. For each bait, interactors were determined using the parsimony

## 2.1 Protein interaction mapping manuscript

principle (Nesvizhskii and Aebersold, 2005). Proteins identified by only one peptide were discarded. In addition, proteins found in a list of common contaminants or recovered with more than 5% of the baits were considered contaminants and also discarded.

**Complex inference** - Complexes were defined as sets of densely connected proteins in the interaction graph. To identify them, we use the normalised cut spectral clustering algorithm (Meila and Shi, 2001; Shi and Malik, 2000). First, we formed a binary experiment matrix  $E$  by setting  $E_{i,j}$  to 1 if protein  $j$  is an interactor of bait  $i$  or 0 otherwise. From  $E$ , we derive the adjacency matrix  $A = E^T E$  and the corresponding normalised graph Laplacian  $L = I - D^{-1}A$  where  $D$  is the degree matrix of  $A$  and  $I$  is the identity matrix. A good approximation to the normalised cut is obtained by solving the eigenproblem  $Lz = \lambda Dz$  where the eigenvectors  $z$  are complex membership indicators. Complexes are identified by applying a clustering step to the proteins projected in the space defined by the eigenvectors  $z$  corresponding to the first  $k$  eigenvalues where  $k$  is the number of complexes determined from the data using the eigengap heuristic. To allow proteins to belong to multiple complexes, we perform the final clustering step using the fuzzy c-means algorithm. This algorithm associates each protein to all complexes through a membership value between 0 and 1 with values close to 1 indicating strong association. As  $m$  tends to infinity, memberships tend to  $1/k$  (ref ?). Thus this value represents a weak association and we assign proteins to complexes where they have membership  $>1/k$ . The fuzziness parameter  $m$  is determined by plotting the number of complexes per protein for different values of  $m$ . We observe a sharp transition between  $m=1$  where each protein belongs to one complex and  $m=1.1$  where each protein belongs to many complexes. We set  $m$  to a value in the lower part of the transition region to reflect our belief that proteins are unlikely to belong to many complexes. In this work,  $m= 1.04$ .

We run the fuzzy c-means algorithm at least 10 times and keep the complexes recovered in at least 70 % of the runs.

### 2.1.5.6 Antibodies

Antibodies against C10orf104 were raised in rabbits against three different synthetic peptides covering different regions of the protein sequence (supp fig2). Further antibodies used in immunopurification, western blotting and immunopurification were: rabbit  $\alpha$ -CDC27 (Gieffers et al., 1999), mouse  $\alpha$ -CCNB1 (GNS1, Santa Cruz Biotechnology), rabbit  $\alpha$ -BUB1B (gift from Gregor Kohlmaier), rabbit phospho-S10-H3 (05-499, Upstate), goat  $\alpha$ -GFP (Poser et al., 2008) and mouse  $\alpha$ -GFP (11814460001, Roche), rabbit  $\alpha$ -ANAPC10 (Herzog et al., in preparation), mouse  $\alpha$ -ANAPC2 (Gieffers et al., 1999).

#### **2.1.5.7 Immunofluorescence microscopy**

Cells were grown on 18 mm coverslips in 12 well plates and fixed with 4% PFA. Antibodies were used at a concentration of 2 µg/ml in 3% BSA and detected using Alexa 488 and Alexa 568 labeled secondary antibodies (Invitrogen). DNA was counterstained with Hoechst 33342 and slides were mounted using Vectashield Mounting Medium (H1000, Vector Laboratories). Image acquisition was performed as described (Waizenegger et al., 2000).

### 2.1.6 Figure legend

#### 2.1.6.1 Figure 2.1-1

Identification of bait and interacting proteins by LAP-MS

A) The scheme shows the analysis workflow from selecting candidate baits, tagging mouse homologs of candidate genes with a LAP-tag in BACs (Poser et al 2008), purifying proteins expressed from BACs in nocodazole (noc) arrested stable cell pools by tandem affinity purification, analysing the glycine eluted and in solution digested protein complexes by LC-MS/MS, followed by Mascot database searches and finally dataset wide contaminant removal followed by SFCM clustering to resolve the interactions data into discrete potential complexes.

B) Ten LAP-tagged proteins (FGFR1OP is a human gene, the remaining nine genes are mouse) were tandem affinity purified from nocodazole-arrested HeLa cells, glycine eluted and 20% of the eluate analysed by SDS-PAGE and silver staining. LAP-tagged Cdc2 (Cdc2) was used as a positive control and wild type HeLa cell extract (wt) was used as a negative control.

C) Of the protein complexes purified as described in B), 80% were digested in solution and analysed by LC-MS/MS followed by Mascot database searching. The percent sequence coverage (%SC), Mascot score (M-Sc) and molecular weight in kDa of the bait proteins are summarised. The number of proteins detected in the purifications after contaminant removal is shown in the last column (#prey).

D) Cdc2 was included with each set of LAP purifications performed so that Cdc2 was purified in 17 independent experiments. The reproducibility of co-purifying proteins (i.e. times and percentage found per 17 repeats) is indicated.

#### 2.1.6.2 Figure 2.1-2

Summary graphics of whole dataset

A) Ontology of bait proteins was annotated sequentially to a set of gene ontology (GO) biological process terms (Ashburner et al., 2000) in a non-redundant fashion (i.e. if a bait gene is associated with M-phase, it falls into this category and other GO terms for the same bait are disregarded).

B) The number of purified baits, detected bait-prey interactions and known interactions for the purification data (MS) as well as the number of total clusters with two or more members obtained, the number of clusters with known interactions, with no known interaction (novel potential complexes) and the number of novel potential complexes with at least one hit in one of the four siRNA screens

C) Complex size distribution

The number of interaction clusters with 1 member, 2-10 members, 11-20 members, 21-30 members and 31-38 members.



D) Examples of interaction clusters determined by sFCM clustering are shown in the spoke model representing bait-prey interactions present in the cluster. Baits are shaded in brown, prey are shaded in yellow, genes which show a mitotic phenotype in any of four genome wide screens are marked with an asterisk (Goshima et al., 2007; Kittler et al., 2007; Neumann et al., in preparation; Sonnichsen et al., 2005). The APC has been sampled with four different baits which all interact with a potential novel subunit C10orf104. The  $\gamma$ -TuRC has been sampled by three of its known components (TUBG1, TUBCP2 and TUBGCP3), one known interactor NEDD1 and is predicted to have two additional subunits (FAM128B and Q5VXS7\_HUMAN). Nevertheless, the  $\gamma$ -TuRC components fall into two different clusters, which are connected through TUBG1. The completely novel FAM29A complex has been predicted from the interactions of the LAP-tagged baits FAM29A and CEP27.

#### 2.1.6.3 Figure 2.1-3

Analysis of selected novel interactors and complexes

A) Mouse LAP-tagged versions of the known  $\gamma$ -TuRC members TUBG1, TUBGCP2, TUBGCP3 and TUBGCP6 were LAP purified and analysed by SDS-PAGE and silver staining alongside LAP purifications of two predicted novel  $\gamma$ -TuRC members FAM128B and Q5VXS7\_HUMAN. Bands were putatively annotated based on the expected protein size.

B) Mouse LAP-tagged versions of FAM29A and CEP27 that defined the novel FAM29A complex were LAP purified and analysed by SDS-PAGE and silver staining alongside LAP purifications of three predicted complex members C4ORF15, C14ORF94 and CCDC5. Bands were putatively annotated based on the expected protein size.

C) Comparison of the interaction partners of five mouse LAP-tagged APC/C subunits and the newly identified APC/C subunit C10orf104 shows a large overlap, suggesting that C10orf104 is indeed a new APC/C subunit. The number of unique peptides (Mascot score  $\geq 30$ ) for each interaction partner is shown. In addition to all APC/C subunits, also the members of the mitotic checkpoint complex (shaded in grey) and other APC/C-related proteins are shown.

#### 2.1.6.4 Figure 2.1-4

C10orf104 is an APC/C subunit that might be involved in S- and/or G2-phase progression.

A) Protein extracts from logarithmically growing HeLa cells were prepared and incubated with Affiprep beads bound to C10orf104 antibody or crosslinked to IgG or CDC27 antibody. Precipitated complexes were glycine eluted, separated by SDS PAGE and analysed by western blotting using the indicated antibodies.

## 2.1 Protein interaction mapping manuscript

B) Logarithmically growing HeLa cells were extracted and subjected to sucrose density gradient centrifugation through a 10% - 30% gradient. After centrifugation 28 fractions were collected and analysed by immunoblotting with the indicated antibodies. \* marks an unspecific band recognised by the APC10 antibody.

C) Protein extracts from logarithmically growing (L), hydroxyurea (HU) or nocodazole (N) arrested HeLa cells were prepared and incubated with Affiprep beads crosslinked to C10orf104 antibody or to CDC27 antibody. Precipitated complexes were glycine eluted, separated by SDS PAGE and visualised by silver staining. APC/C subunits were annotated according to their known electrophoretic mobility.

D) CDC27 or C10orf104 immunoprecipitates from logarithmically growing HeLa cells were incubated with E1 and E2 enzymes, recombinant FZR1, [<sup>125</sup>I]-labelled human CCNB1 fragment (amino acids 1 to 84) as substrate, ubiquitin and ATP for the times (in min) indicated and analysed by SDS-PAGE and phosphorimaging. CON indicates empty protein A beads and a condensin complex antibody (from left to right). \* marks a contaminating band present in the substrate preparation.

E) HeLa cells were synchronised by a double thymidine block, released into fresh medium and samples collected at indicated times after release. Cell pellets were lysed in SDS-sample buffer and by sonication, separated on SDS-PAGE and probed with the indicated antibodies.

F) C10orf104 depletion by siRNA leads to a decrease in CCNB1 levels.

Cells were transfected with c10orf104 siRNA for four h and afterwards split onto coverslips and tissue culture plates. Cells on coverslips were PFA-fixed and stained with DAPI and H3S10ph to count the mitotic index 48 h after transfection. Remaining cells were harvested 48 h after transfection, extracted, separated by SDS-PAGE and transferred to a membrane and probed with the indicated antibodies.

G+H) Cells were transfected with C10orf104 siRNA for twelve h, afterwards split onto coverslips and tissue culture plates, treated with 2 mM thymidine for 24 h, then released into fresh medium and six h later (TP1) treated with 10 µM taxol (T) or 100 ng/ml nocodazole (N) for three h (TP2). For immunoblot analysis (G) cells were harvested at time point 2, extracted, separated by SDS-PAGE, transferred to a membrane and probed with the indicated antibodies. For immunofluorescence microscopy cells were fixed at TP1 and TP2. Fixed cells were stained with BUB1B antibody, CCNB1 antibody and DAPI. More than 200 cells were counted at each time point and scored as either being in interphase (BUB1B/CCNB1 negative nuclei), prophase (CCNB1 positive nuclei before nuclear envelope breakdown) or prometa- and metaphase cells (BUB1B positive kinetochores and condensed chromosome morphology).

#### **2.1.6.5 Supplemental table 2.1-1**

Table summarising the reference complex set giving the number of known complex members (SU), the number of baits selected for each complex (baits) and the number of baits retrieving either all members of the reference complex (full com.) or only a fraction of the complex (part. com.). The latest research paper or review describing each complex is given in the last column.

#### **2.1.6.6 Supplemental table 2.1-2 (See appendix 5.3)**

Table summarising all 175 unique bait purifications plus all Cdc2 purifications after contaminant removal annotated with sequence coverage and the sum of the Mascot score for all identified peptides. Since the table is very long, it can be found in the appendix (5.3).

#### **2.1.6.7 Supplemental table 2.1-3 (See appendix 5.4)**

Table summarising all identified clusters, annotated with complex number, baits within these clusters, known interactions of the bait within the cluster, total known interactions within the cluster, probability of observing the given number of interactions with each cluster at random, summary of mitotic screen hits per cluster, screen hits (fly: Goshima et al., 2007; human esiRNA: Kittler et al., 2007; human siRNA: Neumann et al., in preparation; worm: Sonnichsen et al., 2005). Since the table is very long, it can be found in the appendix (5.4).

#### **2.1.6.8 Supplemental figure 2.1-1**

Characterisation of three polyclonal antibodies raised against C10orf104/ANAPC16

A: C10orf104 protein sequence with peptides used for antibody generation underlined and labelled with the peptide and antibody number in superscript.

B: Generation of rabbit polyclonal antibodies against C10orf104

Cells were transfected with siRNA against C10orf104 (siRNA) or water (CON) and protein extracts prepared at 24h, 48h or 72h after transfection. Extracts were separated by SDS-PAGE, transferred to a membrane and probed with the indicated antibodies.

2.1.7 Figures

Figure 2.1-1

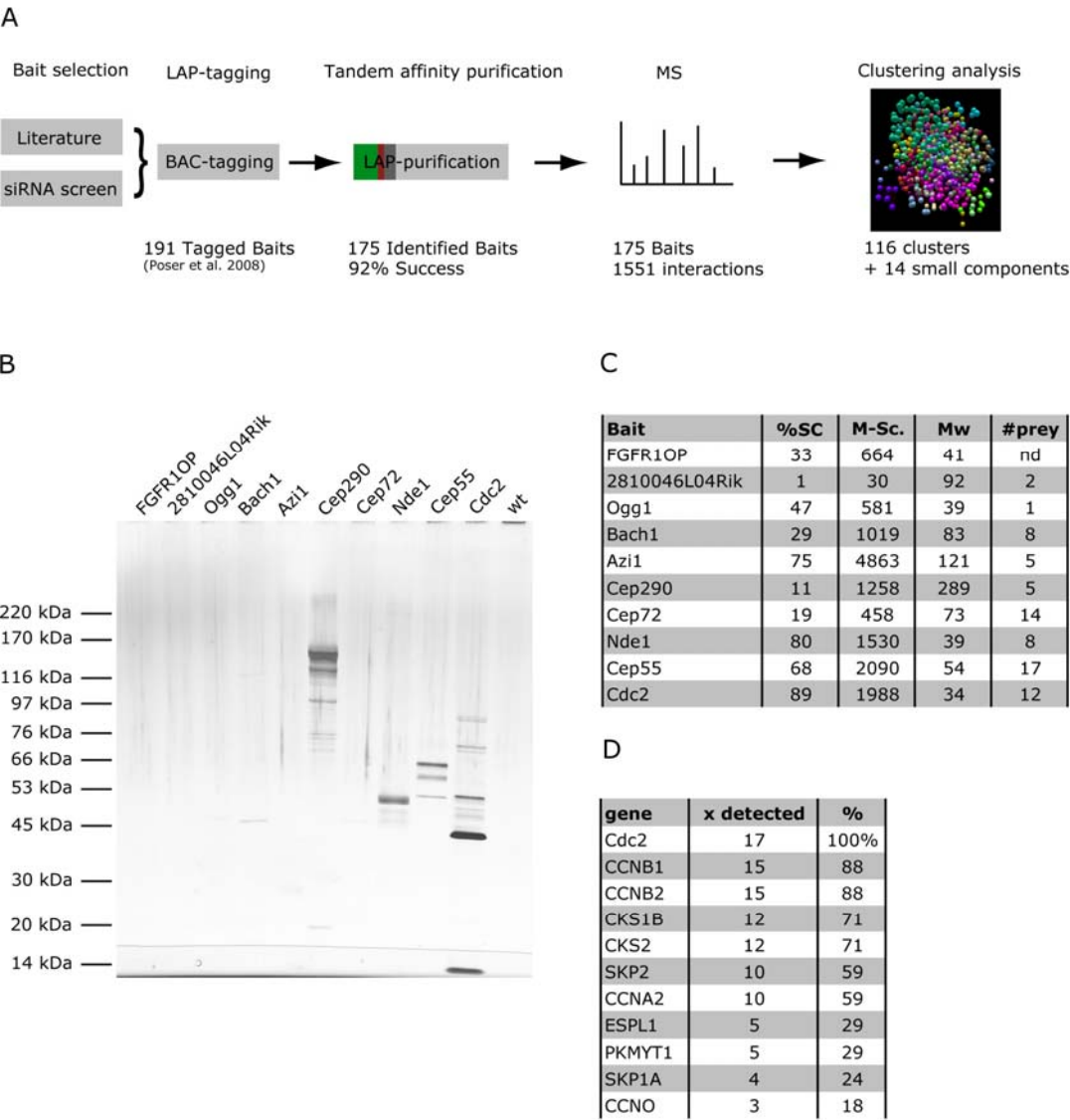
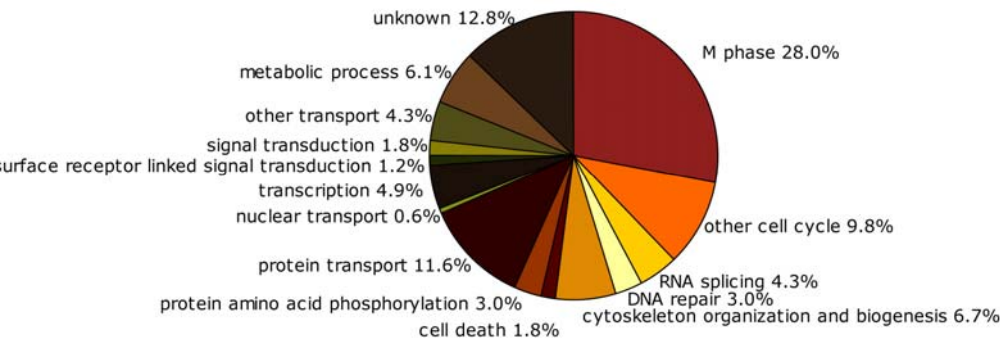
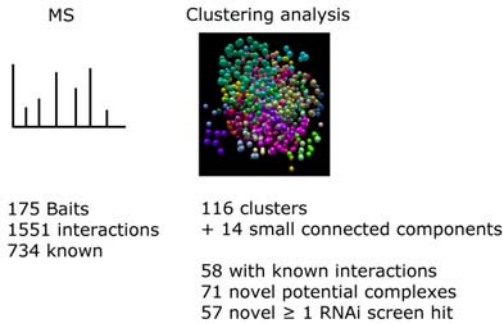


Figure 2.1-2

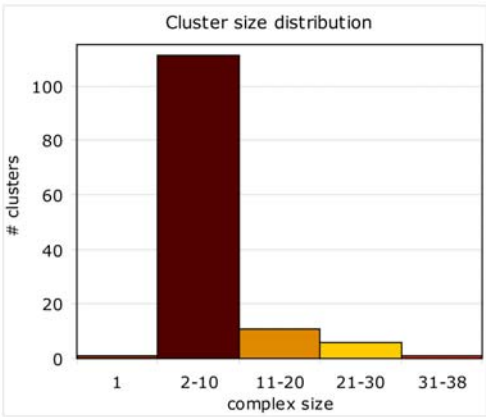
A



B



C



D

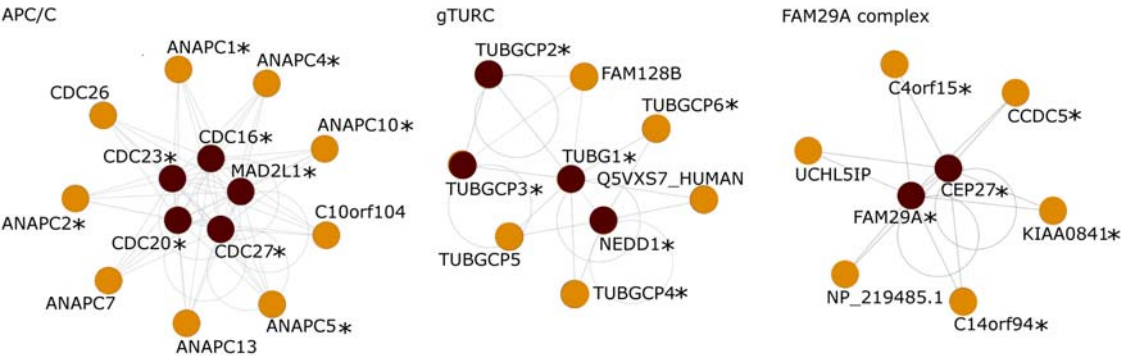
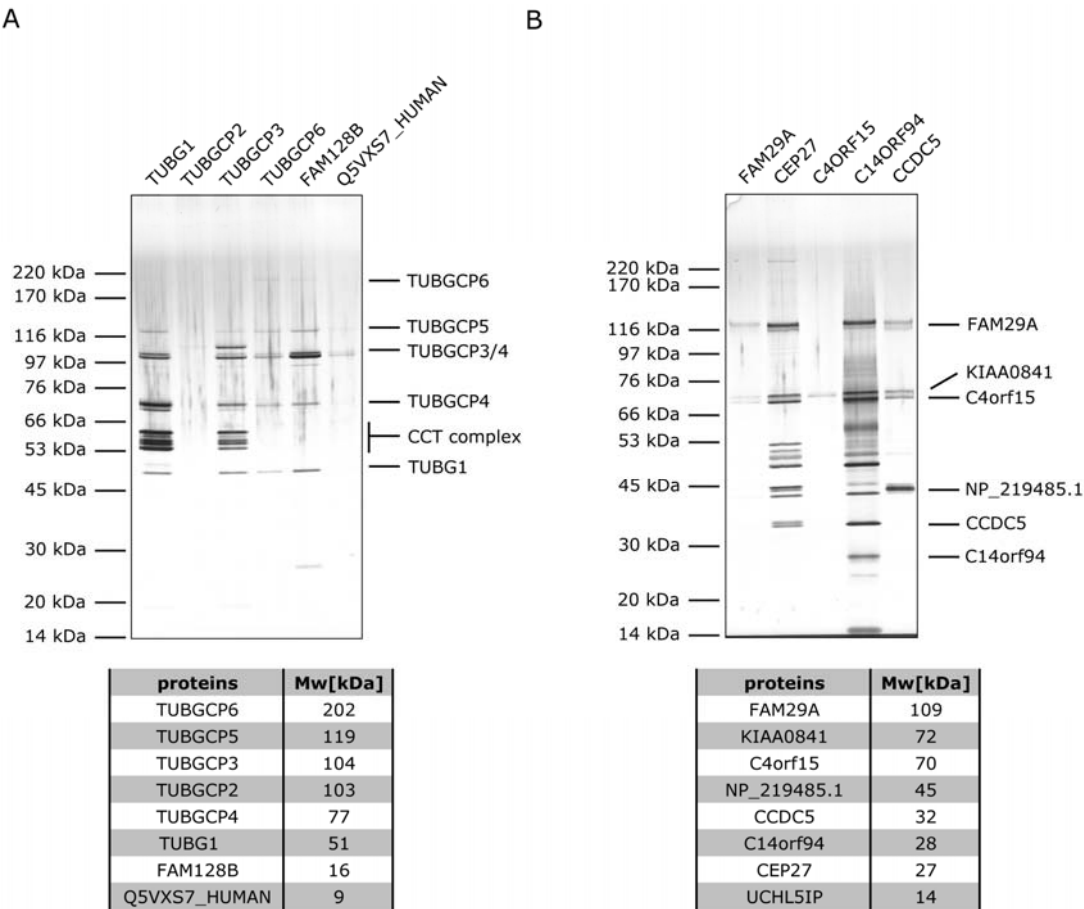


Figure 2.1-3

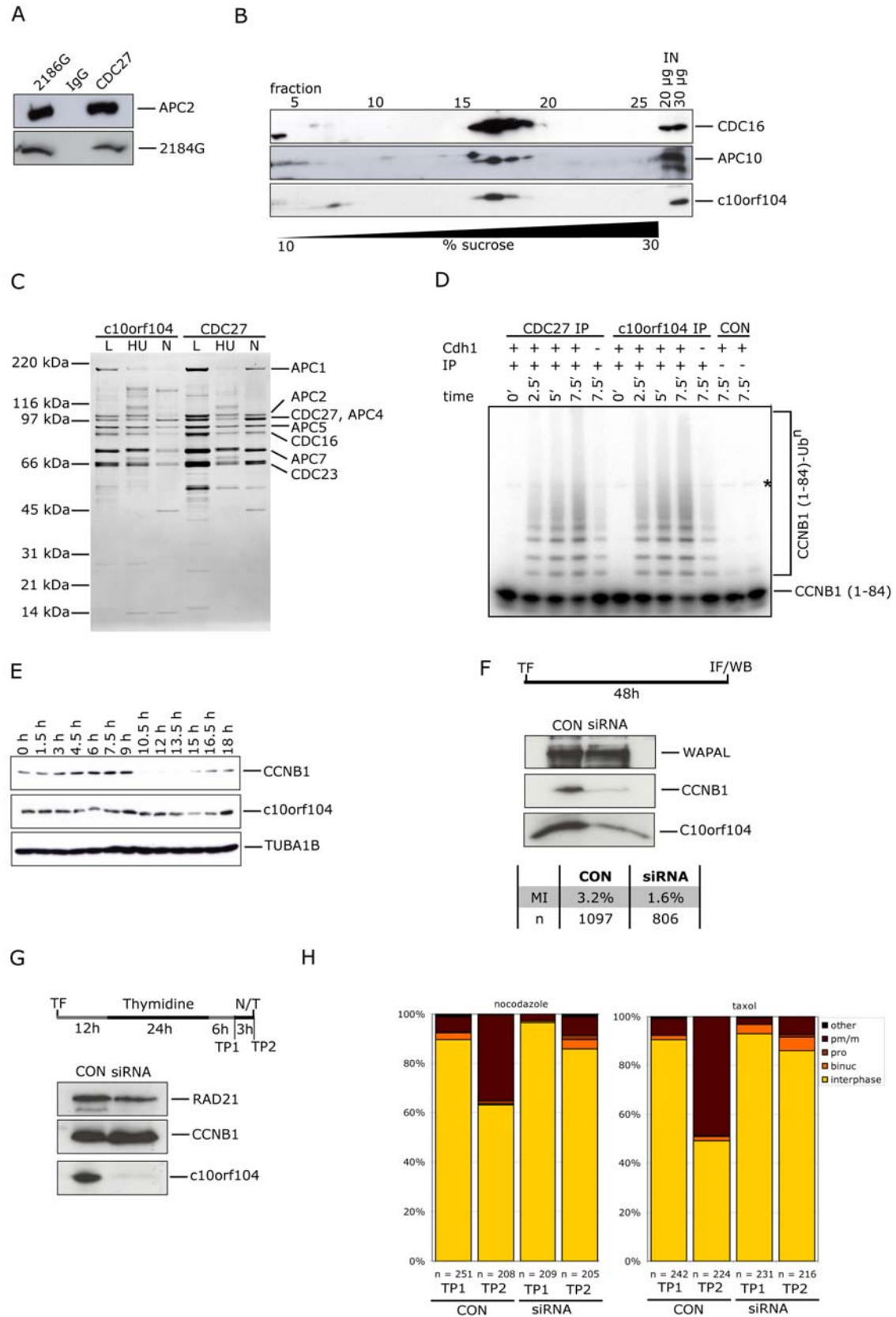


**C**

Unique peptides detected in reciprocal APC-LAP purifications and C10orf104-LAP purification

proteins	sp	Mw[kDa]	Anapc1	Anapc5	Cdc16	Anapc8	Cdc26	Anapc13	C10orf104
Bait	mm	216	37	38	11	4	10	5	2
ANAPC1	hs	216	31	48	70	50	56	19	7
ANAPC2	hs	94	21	7	30	25	27	3	-
CDC27	hs	93	23	12	36	25	29	14	8
ANAPC4	hs	92	18	13	33	24	27	9	1
ANAPC5	hs	85	22	-	32	26	26	8	4
CDC16	hs	72	20	12	26	25	24	10	6
ANAPC7	hs	67	23	19	31	26	26	11	10
ANAPC8	hs	68	-	13	39	37	36	28	-
ANAPC10	hs	21	7	3	9	8	8	2	1
ANAPC11	hs	10	-	-	2	2	2	-	-
ANAPC13	hs	9	2	-	5	5	4	-	-
CDC26	hs	10	7	6	8	8	5	5	1
CDC20	hs	55	-	13	17	17	14	3	5
BUB1B	hs	120	30	23	54	48	43	4	2
BUB3	hs	37	8	6	12	9	9	-	1
MAD2L1	hs	23	4	3	5	5	5	-	-
CDH1	hs	56	-	-	2	3	9	-	-
FBXO5	hs	50	2	1	4	-	6	-	-
NEK2	hs	52	-	-	10	2	12	-	-
C10orf104	hs	12	3	2	6	4	5	2	-

**Figure 2.1-4**



## 2.1: Protein interaction mapping manuscript

**Supplemental table 2.1-1**

#	Complex	SU	baits	full com.	part. com.	Ref.
1	Cohesin	8	4	3	0	Ström L and Sjögren C 2007
2	APC	12	8	3	4	Peters JM 2006
3	MCC	4	3	2	1	Musacchio A and Salmon ED 2007
4	Dynactin complex	9	4	3	1	Schroer TA 2004
5	Nup107-160 complex	9	2	2	0	Schwartz TU 2005
6	Scc2/4 complex	2	2	0	2	Watrin E et al. 2006
7	RZZ complex	3	1	1	0	Karess R 2005
8	Centralspindlin complex	2	2	2	0	D'Avino PP et al. 2005
9	Smc5/6	6	1	1	0	Ström L and Sjögren C 2007
10	g-TURC complex	6	3	2	1	Raynaud-Messina et al. 2007
11	Mis12 complex	5	1	1	0	Obuse C et al. 2004
12	Ndc80 complex	4	2	1	1	Ciferri C et al. 2007
13	Bub1-Bub3	2	1	1	0	Musacchio A and Salmon ED 2007
14	Separase-Securin	2	2	1	1	Waizenegger IC et al. 2000
15	Nup188 complex	5	1	0	1	Schwartz TU 2005
16	Nup214-Nup88 complex	3	1	0	1	Schwartz TU 2005
17	Ran-XPO1 complex	2	0	0	0	Hutten S and Kehlenbach RH 2007
18	CPC	4	1	0	1	Ruchaud et al. 2007



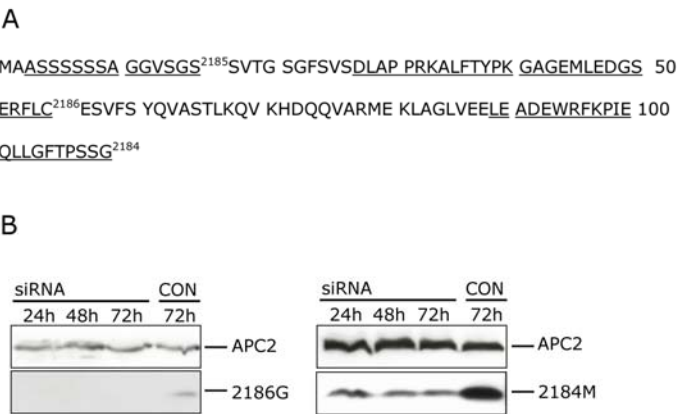
Supplemental table 2.1-2

See Appendix 5.3.

Supplemental table 2.1-3

See Appendix 5.4.

Supplemental figure 2.1-1



**2.2 Manuscript in preparation: A systematic approach to discover new PLK1 and AURKB substrates finds 17 novel PLK1 and 18 novel AURKB substrates on 99 candidate proteins.**

Björn Hegemann<sup>1\*</sup>, James R.A. Hutchins<sup>1\*</sup>, Otto Hudecz<sup>1</sup>, Christoph Stingl<sup>1,3</sup>, Peter Lénart<sup>1,4</sup>, Martina Sykora<sup>1</sup>, Ina Poser<sup>2</sup>, Anthony A. Hyman<sup>2</sup>, Karl Mechtler<sup>1</sup> and Jan-Michael Peters<sup>1</sup>

<sup>1</sup>Institute of Molecular Pathology, Dr. Bohr-Gasse 7, 1030 Vienna, Austria

<sup>2</sup>Max Planck Institute for Molecular Cell Biology and Genetics, Pfotenhauerstrasse 108, 01307 Dresden, Germany

<sup>3</sup>Present address: Erasmus Medical Center, Rotterdam, The Netherlands

<sup>4</sup>Present address: European Molecular Biology Laboratory, Meyerhofstrasse 1, 69117 Heidelberg, Germany.

\*These authors contributed equally to this work.

**2.2.1 Abstract**

Entry and progression through mitosis depends on the activity of a number of mitotic protein kinases. The Polo-like kinase 1 (PLK1) is essential for mitosis and has been implicated in the regulation of mitotic entry, bipolar spindle formation and maintenance, mitotic checkpoint function as well as cytokinesis. Targeting of PLK1 to its substrates is thought to be controlled by priming phosphorylation by the cyclin-dependent kinase 1 (CDK1) but might for some substrates also be regulated through PLK1's own activity. Aurora kinase B (AURKB) is another essential mitotic kinase which, apart from other functions, is essential for spindle assembly checkpoint function by correcting improper microtubule kinetochore attachments. Its localisation is tightly regulated by the so-called chromosomal passenger complex which moves from chromosome arms in G2-phase to centromeres in early mitosis to then travel via the central spindle in anaphase to the midbody in cytokinesis. The key functions of both kinases are mediated through their kinase activity since inhibition using small molecule inhibitors phenocopies siRNA depletion. Identification of PLK1 and AURKB substrates is therefore essential to understand how PLK1 and AURKB function. The tight spatio-temporal regulation of PLK1 and AURKB during mitotic progression suggests that their substrates must only be phosphorylated at a specific time and place to fulfil their function. Assays to detect kinase substrates have been, however, largely carried out *in vitro*, without any cellular regulatory systems in place. We have therefore set out to develop a cellular assay to find novel PLK1 and AURKB substrates. Using small molecule inhibitors against PLK1 and AURKB in combination with tandem affinity purification and mass spectrometry (MS) we could detect kinase-dependent phosphorylation sites on 16 candidate substrate

complexes. In total we found 470 phosphorylation sites, 41 of which were PLK1-dependent and 20 of which were AURKB-dependent. We validated a subset of these sites with phospho-specific antibodies and detected 17 novel potential PLK1 substrates and 18 novel potential AURKB substrates.

### 2.2.2 Introduction

Entry into mitosis depends on the activity of CDK1, originally termed maturation promoting factor or later M-phase promoting factor (MPF). Early work revealed that activity of MPF in *Xenopus laevis* eggs and its effects at the G2/M transition are independent of protein synthesis (Wasserman and Masui, 1975), implying that MPF acts through post-translational mechanisms to allow mitotic entry. Later observations showed that MPF activity is accompanied by a burst of protein phosphorylation (Maller et al., 1977) which generates distinct phosphoproteins reoccurring with every mitotic phase (Karsenti et al., 1987). This set the stage for the realisation that Cdc2 in *S. pombe* and Cdc28 in *S. cerevisiae* are the same as MPF and that Cdc2 (later called CDK1) is a kinase (Simanis and Nurse, 1986) regulated by the cycling levels of cyclins (Felix et al., 1989; Labbe et al., 1989) and phosphorylation (Morla et al., 1989). Since then, efforts have been underway to understand the function of CDK1 by searching for its substrates (Morgan et al., 1989; Shenoy et al., 1989). This was mainly conducted by either *in vitro* kinase assays with candidate substrates or by predicting candidate substrates using the soon-emerged CDK1 consensus phosphorylation motif [ST]-P-X-[KR] (Peter et al., 1990), followed by testing these substrates *in vivo* using phosphorylation site mutants. In parallel it became clear that CDK1 is not the only kinase specifically activated in mitosis. A number of other other proteins have subsequently been identified as kinases essential for mitotic progression: NIMA (Osmani et al., 1991), Wee1 (Piwnicka-Worms et al., 1991), Polo (Llamazares et al., 1991), Aurora (Chan and Botstein, 1993; Francisco and Chan, 1994) and Myt1 (Mueller et al., 1995). These kinases were initially identified in various model organisms and later found to be conserved in most species. Loss of function experiments using genetic tools in yeasts and flies, antibody injection or depletion experiments in vertebrates as well as siRNA-mediated knockdowns have revealed the involvement of these mitotic kinases in many aspects of cell division. This led to the understanding that phosphorylation, along with proteasome-mediated proteolysis (Glutzer et al., 1991), is one of the main regulatory switches for cells entering and progressing through mitosis. However, how these kinases exert their effects has remained elusive; mainly because only few substrates have been identified to date.

Polo-like kinase 1 (PLK1) has been identified in *Drosophila* (where it is named polo) as a gene essential for mitosis and bipolar spindle formation (Llamazares et al., 1991). It has

## 2.2 Phosphorylation site mapping manuscript

further been detected and characterised as a protein specifically expressed in G2- and M-phase in human (Golsteyn et al., 1994), confirming a conserved function in mitosis. Further functional studies of PLK1 by antibody depletion or siRNA mediated knockdown have revealed that PLK1's function is intimately linked to its localisation. Early studies showed that PLK1 is required for centrosome maturation (Lane and Nigg, 1996) and is localised to the centrosome (Arnaud et al., 1998). This is consistent with PLK1's role in centrosome separation, mitotic spindle formation (Sumara et al., 2004; van Vugt et al., 2004) and maintenance (Lenart et al., 2007). Centrosomal localisation might also be required for PLK1's proposed role in mitotic entry where it phosphorylates CCNB1 (Jackman et al., 2003). More recent data suggest however, that PLK1 might rather be involved in timely prophase progression into prometaphase (Lenart et al., 2007) than in entry into mitosis. During prophase PLK1 enters the nucleus and is involved in the removal of the bulk of the cohesin complex from chromosome arms, the so-called prophase pathway (Hauf et al., 2005). PLK1 then localises to kinetochores until prometaphase where it contributes to spindle checkpoint protein accumulation (Ahonen et al., 2005; Kang et al., 2006; Wong and Fang, 2005). During cytokinesis PLK1 phosphorylation allows the interaction of the two central spindle proteins RACGAP1 and ECT2 to initiate cleavage furrow ingression (Burkard et al., 2007; Petronczki et al., 2007). PLK1 is inactivated by APC/C-FZR1-dependent proteolysis in late mitosis to allow proper mitotic exit (Lindon and Pines, 2004).

The main mechanism of targeting PLK1 to its substrates is thought to function through its phospho binding domain called the polo box domain, PBD (Elia et al., 2003a). The two polo boxes of PLK1 that comprise the PBD sandwich the target phosphopeptide and bind it with very high affinity (Elia et al., 2003a). By using the PBD in pull down assays combined with MS a large number of potential substrates has been detected (Lowery et al., 2007). Furthermore several studies have successfully used mutations of the PBD binding motif (S-[pSpT]-[PX]) to understand the role of PLK1 phosphorylation for the function of certain substrates (Baumann et al., 2007; Elowe et al., 2007; Neef et al., 2007). This binding motif fits the consensus sequence of CDK1 and it has been speculated that CDK1 could be the main priming kinase for PLK1 binding. On the other hand recent studies using small molecule inhibitors have shown that PLK1 activity alone regulates its localisation (Lenart et al., 2007; Santamaria et al., 2007) supporting the idea that PLK1 can also generate its own binding sites (Neef et al., 2007). In addition, it has been shown that the PBD is not required for PLK1 function at the centrosome (Hanisch et al., 2006), indicating that PLK1 localisation might in addition be regulated by a mechanism other than polo box binding.

The first member of the Aurora kinase family was identified as Ipl1 (increase in ploidy) in budding yeast (Chan and Botstein, 1993) and later identified in *Drosophila* as aurora (later named Aurora A) where the mutant fails to separate centrosomes and does not

form a bipolar spindle (Glover et al., 1995). Vertebrates contain three orthologs of Aurora: Aurora kinases A, B and C. Vertebrate Aurora kinase B (AURKB) was first identified in rat cells (Terada et al., 1998) and was later found to be an integral component of the chromosomal passenger complex, CPC (Adams et al., 2000), that localises to chromosome until prometaphase, moves to centromeres in metaphase only to later travel via the spindle midzone in anaphase to the midbody in telophase and cytokinesis. This well described localisation change is thought to govern the function of AURKB during mitosis. While initial observations indicated that AURKB only functions in cytokinesis (Terada et al., 1998), it was subsequently shown that it functions throughout mitosis with its earliest sign of activity appearing in late G2/early M where it phosphorylates serine 10 on Histone H3 (Crosio et al., 2002). During prophase AURKB promotes the binding of the condensin I complex, which is thought to regulate mitotic chromosome structure, to chromatin (Takemoto et al., 2007) by phosphorylation of some of its subunits. It is however not involved in chromosome condensation mediated by condensin II (Lipp et al., 2007). A further role of AURKB in chromosome structure is to promote cohesin removal in prophase via the prophase pathway (Losada et al., 2002). Whether this is facilitated through direct phosphorylation of cohesin subunits or indirectly by delocalisation of SGOL1 and subsequent protection of cohesin phosphorylation by PLK1 is not clear (Dai et al., 2006; Kitajima et al., 2005). In prometaphase AURKB concentrates at centromeres where it is essential for ensuring correct, amphitelic, attachment of microtubules to kinetochores. It is thought that INCENP and Survivin of the CPC sense the tension applied across the kinetochore by microtubules and keep AURKB active in the absence of tension (Cheeseman et al., 2006; DeLuca et al., 2006; Sandall et al., 2006). Phosphorylation of the kinetochore component NDC80 by AURKB decreases its affinity to microtubules, allowing syntelically attached microtubules to detach until fully bi-oriented kinetochores under tension are generated (Cheeseman et al., 2006). This inactivates AURKB at the kinetochore which leads to silencing of the mitotic spindle assembly checkpoint (Ditchfield et al., 2003; Hauf et al., 2003; Morrow et al., 2005) and allows anaphase onset. While it is clear that AURKB is essential for cytokinesis (Terada et al., 1998), the underlying mechanism is not yet fully understood. Possibly, phosphorylation of the centralspindlin complex (RACGAP1 and KIF23) by AURKB is the key function in the regulation of cytokinesis by AURKB (Guse et al., 2005).

It is known that AURKB is targeted to its substrates through interaction with and localisation by the chromosomal passenger complex proteins (Adams et al., 2000). At the same time, interaction with INCENP is also essential for AURKB activation (Bishop and Schumacher, 2002). A recent study has further shown that full activity, at least against some substrates, requires a priming phosphorylation and microtubules (Rosasco-Nitcher et al., 2008). This indicates that, similar to the situation observed for PLK1, the function of AURKB is not only dependent on phosphorylating the right

## 2.2 Phosphorylation site mapping manuscript

substrate but more importantly on phosphorylating the right substrates at the right place and the right time. This implies that in order to understand PLK1 and AURKB function through their substrates; substrates need to be identified at the sites of PLK1 and AURKB function in cells. However, substrate identification has to date largely relied on *in vitro* kinase assays because of the lack of tools to specifically identify kinase substrates in cells. An approach to study kinase function in cells has recently been demonstrated using analogue-sensitive kinases (as-kinases). As-kinases are engineered kinases that accept a bulky ATP analogue in their ATP binding pocket (Shah and Shokat, 2002; Witucki et al., 2002). This bulky ATP-analogue can be used to inhibit the as-kinase. Cell lines expressing an as-PLK1 in a background lacking wild type PLK1 have been employed in combination with a bulky ATP-analogue inhibitor to understand PLK1's function in cytokinesis (Burkard et al., 2007). To inhibit the endogenous kinase in wild type cell lines, specific small molecule inhibitors can be used. The availability of the small molecule inhibitor Hesperadin for AURKB (Hauf et al., 2003) and BI2536 for PLK1 (Lenart et al., 2007; Steegmaier et al., 2007) allows creating a loss of function situation for these kinases in large cell populations. In combination with a highly robust tandem affinity purification protocol (Poser et al., 2008) and high mass accuracy MS we have set up a method to detect kinase-dependent phosphorylation sites on candidate substrates. We have used this method to screen 16 candidate substrate complexes of PLK1 and AURKB for mitotic phosphorylation sites that are sensitive to kinase inhibitor treatment. This resulted in a collection of 470 phosphorylation sites on 99 unique proteins and the detection of 17 novel potential PLK1 substrates and 18 novel potential AURKB substrates, almost doubling the number of substrates previously known.

### 2.2.3 Results

Given that additional factors control the targeting and activity of PLK1 and AURKB to its substrates, we set up a cellular assay to detect their substrates. Using a combination of kinase inhibitors, candidate substrate affinity purification and phosphorylation site mapping by MS we wanted to identify phosphorylation sites that are sensitive to treatment with either the small molecule inhibitor Hesperadin (Hauf et al., 2003) or the PLK1 inhibitors BI2536 (Lenart et al., 2007; Steegmaier et al., 2007) or BI4834 (see below). These inhibitors have been thoroughly studied and it was shown that they recapitulate the phenotypes previously described for siRNA or antibody mediated depletion in various mammalian systems (Taylor and Peters, 2008).

#### 2.2.3.1 Characterisation of the BI2536-related inhibitor BI4834

To inhibit PLK1 we used a structural relative of the recently described BI2536 inhibitor (Lenart et al., 2007; Steegmaier et al., 2007). To fully test BI4834's effect on HeLa cells

we used a number of cellular assays already described in Lenart et al. (2007) to determine the concentration at which PLK1 is fully inhibited. Penetrance of the monopolar spindle phenotype was tested by treating HeLa cells, synchronised with a double thymidine arrest release, for three h with concentrations ranging from 10 to 2500 nM of BI4834 before fixation and staining with TUBA1B antibodies as well DAPI. Using 250 nM BI4834 was sufficient to obtain 90% of cells that arrested in mitosis with a monopolar spindle (Supplemental figure 2.2-1 B and C) which is identical to the strongest PLK1 RNAi phenotype in human cells (Sumara et al., 2004). Cells treated as described above were also stained with TUBG1 antibodies to test at which concentration BI4834 fully inhibits centrosome maturation. Full inhibition was reached at a concentration range of 250 nM and 500 nM (Supplemental figure 2.2-1 D). To confirm that BI4834 could also prevent dissociation of cohesin from chromosomes in early mitosis we treated cells stably expressing RAD21-9x MYC (Hauf et al., 2005) with 250 nM BI4834, prepared cytopins and stained with MYC antibodies to visualise cohesin. Cohesin was strongly enriched on chromosomes in prometaphase (Supplemental figure 2.2-1 F), confirming the results obtained using 100 nM of BI2536 (Lenart et al., 2007). We further tested whether BI4834 would also abolish the electrophoretic mobility shift of BUB1B seen after depletion of PLK1 (Elowe et al., 2007; Matsumura et al., 2007) or inhibition of PLK1 with BI2536 (Lenart et al., 2007). Cells synchronised using a double thymidine block were released into nocodazole only or into nocodazole containing either 100 nM of BI2536 or 250 nM of BI4834. Supplemental figure 2.2-1 G shows that 250 nM BI4834 inhibit the phosphorylation of BUB1B equally well as 100 nM BI2536. In conclusion, treatment of HeLa cells with 250 nM of BI4834 induces a phenotype indistinguishable from treatment with 100 nM BI2536 (Lenart et al., 2007). We thus decided to use 250 nM final concentration of BI4834 in our phosphorylation mapping experiments.

### **2.2.3.2 Bait selection, affinity purification and mass spectrometric analysis**

In order to detect PLK1- and AURKB-dependent sites in a cellular assay we first selected a number of candidate protein complexes that localise to subcellular mitotic structures where PLK1 and AURKB are known to act. We focussed on groups of baits that are components of the kinetochore, the mitotic checkpoint complex, chromosomes, the spindle or the centrosome (Figure 2.2-1 A).

The 16 baits and their interaction partners were either tandem affinity-purified using the LAP-tag (Poser et al., 2008) or immunoprecipitated using antibodies against the endogenous proteins (Figure 2.2-4 A for details) from cultured HeLa cells. Most LAP-tagged baits used were the mouse homologues of the candidate human genes. This is possible since most LAP-tagged mouse proteins expressed in HeLa cells tested so far localise and function as expected from the human homologue (Poser et al., 2008).

## 2.2 Phosphorylation site mapping manuscript

Throughout this manuscript, mouse proteins are named with their MGI symbol, human proteins are named with their HGNC symbol, i.e. Bub1b (*Mus musculus*) or BUB1B (*Homo sapiens*), which corresponds to the commonly used human synonym BubR1. A list of all used gene names and their most common synonyms is given in the abbreviations section (6.).

To identify mitosis-specific and inhibitor-sensitive phosphorylation sites proteins were purified from HeLa cells growing exponentially (L), arrested in mitosis using nocodazole (N) or nocodazole arrested cells treated for two h with either 250 nM of BI4834 (NB) or 100 nM Hesperadin in combination with 10 µM MG132 (NHM). Addition of MG132 was necessary to prevent cells from exiting mitosis due to a spindle assembly checkpoint override that results from AURKB inactivation (Ditchfield et al., 2003; Hauf et al., 2003). A 5% fraction of the purified protein complex was analysed by SDS-PAGE and silver staining while the remaining sample was digested in parallel in solution using either trypsin or chymotrypsin or subtilisin. The resulting peptide mixtures were analysed using a nanoHPLC-FT-ICR or nanoHPLC-OT-ICR mass spectrometer. Using Mascot in combination with the knowledge based management system (KBMS) database (187752 sequence entries, Applied Biosystems) supplemented with the mouse bait sequences, peptides were identified. Detected phospho-peptide spectra were manually validated and assigned a confidence score from 0 to 3 (0 being low confidence, 3 high – only phospho-peptides with score 1-3 were kept). Figure 2.2-1 B and C shows a typical purification result of one bait purification, mouse Bub1b, including sequence coverage of selected interaction partners and their total number of identified phosphorylation sites. Bands are labelled according to the molecular weight of most abundant proteins identified in in solution digests. Sequence coverage was calculated by combining detected peptides from all three proteolytic digests with a Mascot score of 20 and higher. The same purifications have been carried out for a total of 16 protein complexes (Figure 2.2-1 A). We will first describe the detailed analysis of a LAP purification of the mitotic checkpoint protein Bub1b from HeLa cells and the immunoprecipitation of the cohesin interactor WAPAL before we summarise the results obtained from the whole data set.

### 2.2.3.3 Phospho-site analysis of LAP-tagged mouse Bub1b and endogenous WAPAL

To validate that mouse Bub1b interacts with the complex partners expected for human BUB1B, we compared the proteins identified by Mascot with the literature. The database search of mitotic samples (N, NB, NHM) resulted in a sequence coverage of 74% to 80% for Bub1b and sequence coverage from 15% to 89% for the three other members of the mitotic checkpoint complex, BUB3, CDC20 and MAD2L1 (Sudakin et al., 2001) as well



as for most members of the APC/C (Peters, 2006), the recently described Bub1b interactor and outer kinetochore component CASC5 (Cheeseman et al., 2008; Kiyomitsu et al., 2007) as well as components of the kinetochore complexes MIS12 and NDC80 (Cheeseman et al., 2006) (

Supplemental table 2.2-2). Unexpectedly, the ubiquitin ligase UBR5 was also found to interact with mouse Bub1b, showing a sequence coverage of 16% to 30%. UBR5, also known as EDD, might be involved in regulating the DNA damage checkpoints at G1/S, intra S-phase and G2/M (Henderson et al., 2006; Munoz et al., 2007; Ohshima et al., 2007) but has not been reported to interact with mitotic checkpoint or kinetochore components. It also interacts with mouse Bub1 (

Supplemental table 2.2-2), but in the reciprocal purification of UBR5 we did not detect BUB1 or BUB1B, suggesting that UBR5 might be an unspecific interactor (data not shown).

To evaluate the approximate stoichiometry of the most abundant interaction partners we compared the staining intensity of the most prominent silver stained bands. It is apparent that the Bub1b – BUB3 interaction exists in interphase and mitosis while CDC20 and CASC5 binding to Bub1b is strongly reduced in interphase. This change in complex composition is also partially reflected in the relative sequence coverage difference between the four different cellular states for CDC20 and CASC5 but also for the APC/C subunits and BUB1. This is consistent with earlier findings that the BUB1B checkpoint complex only interacts with APC/C and the kinetochore in mitosis (Chan et al., 1999; Jablonski et al., 1998).

To confirm that the Bub1b complex composition changes between interphase and mitosis we tested whether changes in the levels of interacting proteins could be monitored by integrating the intensities of peptides in the MS1 chromatogram. A similar approach has been successfully taken to compare the complex composition of the transcription factor FoxO3A before and after serum starvation (Rinner et al., 2007). However, we did not perform mixing experiments as described by Rinner et al. to minimise variations between chromatographic runs. So in order to normalise the levels between different runs and to also control for the different absolute peptide amounts present in each of the four different purifications (L, N, NB and NHM) we quantified six unmodified peptides of Bub1b in each run and calculated their change relative to Bub1b levels in condition N. This showed that Bub1b levels exhibit a relative change of 0.9 to 1.6 fold in the tryptic digests with a relative standard deviation of 17% to 32% (Figure 2.2-2 A). Thus, the observed variations between peptides of Bub1b in a single MS run are rather large so that for a relative change of an interactor to be significant it should be at least three fold.

## 2.2 Phosphorylation site mapping manuscript

We went on to quantify six peptides each for UBR5, BUB3, CASC5, CDC20, CDC27 and BUB1 in each tryptic digest of purifications from L, N, NB and NHM. The extent of variation between peptides of a single protein were similar to that detected for Bub1b and are indicated with the error bars (Figure 2.2-2 B). To assess the change of each protein relative to Bub1b we normalised the change to the N value and to Bub1b level changes and plotted it (Figure 2.2-2 B). It is apparent that while level changes of UBR5 and BUB3 relative to Bub1b remain around one in all four samples, the levels of the other four interactors relative to Bub1b drop 4- to 5-fold in interphase (L) compared to all mitotic samples. Since this result is in line with the previous findings discussed earlier, this suggests that we can use quantitative information of detected peptides to monitor changes of interacting protein level relative to bait protein level.

To further confirm this finding we carried out the same procedure on data obtained for immunopurified APC/C (Gieffers et al., 1999). The levels of CDC27 in all four runs were quantified and normalised to the amount of peptides in condition N and then compared to the normalised levels of BUB1B (Figure 2.2-2 C). BUB1B levels relative to CDC27 are reduced threefold in interphase compared to the mitotic samples. This is just outside of the standard deviation and thus confirms the validity of this approach to assess relative complex composition changes. Importantly, using this method we could semi-quantitatively detect changes for interaction partners that were not visible on the silver stained gels and thus obtain comprehensive results for most of the identified interaction partners.

We will employ a software tool called Superhirn (Mueller et al., 2007) which allows for automatic comparison of peptide levels between different chromatographic runs on FT and OT-MS instruments. Using Superhirn we plan to carry out quantitative analysis on the whole dataset. Given the well connected bait-prey networks (see below) we expect to obtain a comprehensive dataset of cell-cycle-dependent and possibly kinase inhibitor-sensitive protein protein interactions.

### 2.2.3.4 Phosphorylation site analysis of 16 complex purifications

To determine the cell cycle-dependent phosphorylation pattern of each protein we followed a qualitative strategy. We compared the identified phosphorylation sites from samples L, N, NB and NHM and classified each site as either being present in log-phase cells only (I), in log and mitotic phase (I/M) or only in the mitotic phase (M). For a phospho-site to be classified as an interphase site a phospho-peptide had to be present in interphase and an unphosphorylated peptide corresponding to the region of the phosphorylation site had to be present in mitosis or vice versa for mitosis-specific

phospho-sites. To classify a phosphorylation site as sensitive to treatment with either BI4834 or Hesperadin a phospho-peptide had to be present in interphase and/or mitosis, absent in the inhibitor treated sample and an unphosphorylated peptide corresponding to the region of the phosphorylation site had to be present in the inhibitor treated sample. Where the phospho-peptide was absent from the BI4834-treated sample we classified this site as sensitive to BI4834 (BI-sensitive), and where the phospho-peptide was absent from the Hesperadin-treated sample we classified this site as sensitive to Hesperadin (Hes-sensitive). Sites could also be sensitive to both inhibitor treatments (BI+Hes-sensitive). Finally, phospho-peptides could also be present in either or both of the inhibitor treated samples while an unphosphorylated peptide corresponding to the region of the phosphorylation site was present in all other samples. In this case the phosphorylation site was classified as inhibitor induced (BI-, Hes- or BI+Hes-induced).

The purification of Bub1b yielded 46 identified phosphorylation sites in total. Purifications of other baits yielded from four up to 106 phosphorylation sites, depending mainly on the number of proteins per complex and protein size. In total we identified 470 phosphorylation sites on 115 proteins (Figure 2.2-4 A; 99 unique proteins, 16 proteins are present two to five times in different bait purifications). Of these 470 sites, 15 were present exclusively in interphase, 125 were present in interphase and mitosis and 187 were present only in mitosis. A total of 143 sites could not be clearly assigned to one of these categories (ca. 66% of 143) or were induced by one or both of the kinase inhibitors (ca. 33% of 143). Of the mitotic phosphorylation sites, 41 were sensitive to the PLK1 inhibitor, 20 sites were sensitive to Hesperadin and 24 were sensitive to both inhibitors.

Of the 327 sites that could be classified, almost 38% were present in interphase and mitosis (I/M). This was surprising as we assumed a much larger difference of total phosphorylation sites in interphase compared to mitosis. To determine whether this small difference represented the true distribution of phosphorylation between interphase and mitosis, we took a closer look at phosphorylation sites we mapped on the APC/C and compared them to sites identified and characterised with phospho-specific antibodies previously (Kraft et al., 2003). Of the five mitotic phosphorylation sites validated with phospho-specific antibodies by Kraft et al., we identified four as being present in interphase and mitosis on the basis of our MS data. This indicated that at least a fraction of the I/M sites could actually be sites highly phosphorylated in mitosis and only phosphorylated at a basal level in interphase. Alternatively, contamination of interphase cells with mitotic cells may have led to detection of the phospho-peptides in the interphase sample.

## 2.2 Phosphorylation site mapping manuscript

Since we identified more than twice as many phosphorylation sites on the APC/C than Kraft et al. (106 as compared to 51), we assumed that this discrepancy is due to higher sensitivity of the FT-ICR mass spectrometer we used. However, this finding indicates that the qualitative method we use for phospho-site classification might produce a number of false negative hits, i.e. we might miss sites that are cell-cycle-dependent or inhibitor-sensitive because their fold change is within the dynamic range of the FT-ICR MS machine we are using. This finding prompted us to evaluate whether we could also analyse our phosphorylation site data semi-quantitatively to detect variations of phosphorylation levels in our protein purifications.

### 2.2.3.5 Identification and validation of WAPAL and Bub1b phosphorylation sites

We first applied the semi-quantitative peptide analysis to the cohesin regulator and interactor WAPAL (Kueng et al., 2006). WAPAL was immunoprecipitated using a polyclonal rabbit antibody (Kueng et al., 2006) from L, N, NB and NHM cells and its phosphorylation sites mapped and classified. Semi-quantification was done by measuring the levels of six WAPAL peptides in all three proteolytic digests (Figure 2.2-2 E; trypsin (Try), chymotrypsin (ChT) and subtilisin (Sub)). Subsequently, all detected phospho-peptides for a single phosphorylation site in all three digests were also quantified and their level change, normalised to N and relative to WAPAL, was calculated. In total 19 phosphorylation sites were detected throughout the WAPAL protein. To quantitate and classify them we had to test which fold change would represent a biologically significant difference in phosphorylation level. Since there is usually only one distinct peptide detected for each phosphorylation site per digest, it is not possible to assess the standard deviation of the fold change as was done for the relative complex stoichiometry analysis above. So in order to determine which fold change in phospho-peptide levels would correspond to a significant and biologically informative phosphorylation change, we independently validated the results obtained by semi-quantitation on the peptide level with phospho-specific antibodies. For three phospho-peptides we could quantitate distinct peptides in each of the three digests. Figure 2.2-2 E shows the levels relative to WAPAL for the sites on S465, S528 and S1154 change from N to NHM between 1.25 and 0.5 fold (0.25 for the Sub digest of the S1154 peptide). The level change relative to WAPAL from N to L and N to NB was much more pronounced, between 0.2 and 0.05 fold, i.e. there was a 5 to 20 fold reduction of the quantified phospho-peptides. This change was largely consistent for three distinct peptides per phospho-site quantified in the three different proteolytic digests.

To test if these five- to twenty-fold changes were significant we generated three phospho-specific polyclonal peptide antibodies (pWAPAL\_S465, pWAPAL\_S528 and

pWAPAL\_S1154). These antibodies were tested on WAPAL immunoprecipitated from HeLa cell extracts of L, N, NB or NHM, separated on SDS-PAGE and transferred to a membrane for western blotting. All three of the tested antibodies confirmed the results obtained by MS and semi-quantitation (Figure 2.2-3 A and C, Supplemental figure 2.2-2 B and data not shown). This led us to conclude that relative changes of at least five fold are needed to confidently classify a phosphorylation site as absent in a given sample. Consequently we classified the 19 phosphorylation sites of WAPAL (Figure 2.2-2 E) and obtained six sites present in interphase and mitosis, ten sites present only in mitosis and three sites that could not be classified. Of the ten mitotic sites seven were BI-sensitive and one BI- and Hes-sensitive. In comparison to the qualitative analysis we performed on the WAPAL phosphorylation sites we could retrieve a more complete picture of the cell-cycle and kinase-dependent phosphorylation changes. Of the 19 total sites, two that had not been classified were now classified and three sites which had been classified as I/M were now classified as M (Figure 2.2-2 E, e.g. S465).

Using this semi-quantitative method we could now further investigate the phosphorylation sites identified on Bub1b. The levels of six Bub1b peptides were quantified in all three proteolytic digests and the phospho-peptide level change normalised to N was calculated relative to the Bub1B level changes. Based on these quantifications the phospho-sites for Bub1b were classified and summarised in a schematic representation of Bub1b (Supplemental figure 2.2-2 E). In total four sites were present in interphase and mitosis, seven were mitosis-specific, one of the mitotic sites was BI-sensitive and three sites could not be clearly classified. These three phosphorylation sites were reduced by approximately four fold compared to N only in L (S360) or in L and NHM (T601 and T613/S620/S621). Since this is close to the borderline for classifying these sites as absent in the given cellular states they were marked as unclassified. Despite this relatively large standard deviation between peptides, we could achieve a more comprehensive data set for the Bub1b phosphorylation sites. Three sites that had not been classified or were only present in a single state were now classified over all four states and three sites which had been classified as I/M were now classified as M.

In summary the semi-quantitative analysis of phosphorylation sites yielded a more complete set of data and abolished a number of previously false negative assignments (i.e. mitosis-specific sites had been classified as being present in interphase and mitosis). However, further testing of the label free quantification method is necessary to achieve more accurate classification of the phosphorylation sites. In particular automatic analysis using the SuperHirn software described above will allow more sophisticated statistical analysis to better define the confidence threshold. In addition, control experiments to estimate the run to run variation and dynamic range of the nano HPLC and FT-MS instruments will improve the data confidence.

### 2.2.3.6 MS data validation using phospho-specific antibodies

To better estimate the reliability of our data we generated a panel of phospho-specific polyclonal peptide antibodies against phosphorylation sites that were classified as either I/M, M, M and BI-sensitive as well as M and Hes-sensitive. The phospho-antibodies were then tested on either cell extracts from L, N, NB and NHM samples or on proteins that were immunoprecipitated from these samples. Figure 2.2-3 A shows results obtained with four of these antibodies. When tested on PDSBB immunoprecipitates the antibody pPDS5B\_S1388 recognised PDS5B in all four states, as was predicted from the MS results. This phosphorylation site has also been detected in two independent large scale phosphoproteomics studies, however, without any information regarding the cell cycle dependence (Beausoleil et al., 2004; Olsen et al., 2006). The pPDS5B\_S1417 antibodies gave similar results (Supplemental figure 2.2-2 A). An antibody recognising pS1237 on immunoprecipitated PDS5A confirmed that this phosphorylation site is only present on mitotic PDS5A and is not sensitive to the PLK1 inhibitor nor to Hesperadin.

We generated seven antibodies against phosphorylation sites classified as PLK1-inhibitor-sensitive sites (of a total of 41 sites) on the cohesin subunits RAD21, STAG2, WAPAL and PDS5A (Figure 2.2-3 C). Two sites on RAD21 were classified as present in I/M and BI-sensitive. These two sites (pS153 and pS175) were detected in previous phosphorylation site mapping experiments comparing S-phase and mitotic HeLa cells (Hauf et al., 2005). It was shown that pS175 was present in S-phase and mitosis while pS153 was only found in mitosis. The two phospho-antibodies we generated (pRAD21\_S175 and p RAD21\_S153) showed that these sites were present in mitosis, confirming earlier results by Hauf et al. and confirmed our MS data that both sites were BI-sensitive (Supplemental figure 2.2-2 B). The three WAPAL phospho-antibodies confirmed the results obtained by qualitative and quantitative MS-analysis as described earlier (Figure 2.2-3 A and C, Supplemental figure 2.2-2 B and data not shown). The phospho-PDS5A antibody directed against a mitotic and BI-sensitive site recognised immunoprecipitated PDS5A equally well in N, NB and NHM but not in interphase, contradicting our finding that this site was BI-sensitive but confirming its mitosis-specificity (Supplemental figure 2.2-2 B).

In total 20 sites were classified as Hesperadin-sensitive. We tested four of them by generating phospho-specific antibodies. The Hesperadin-sensitive site on INCENP (S446) and the site on NUP85 (T91) could be confirmed by phospho-specific antibodies (Figure 2.2-3 A and C and Supplemental figure 2.2-2 C), while the site on NCAPH T1388 or T1389 could only be confirmed as a mitotic site but not as Hes-sensitive.

To summarise, using phospho-antibodies we have tested four sites classified as I/M of which two were I/M and two were M. Of the nine tested M sites, nine were confirmed by antibodies to be mitosis-specific. We could further show that six out of the seven sites

classified as BI-sensitive were correct and two out of the three Hesperadin-sensitive sites could be confirmed by phospho-specific antibodies. These results suggest that our MS-based method is an approach which identifies cell cycle- or kinase-regulated phosphorylation sites with reasonable accuracy. It is important to note that some sites we classified as present in interphase and mitosis are actually mitosis specific (e.g. S465 on WAPAL, comparison to Kraft et al 2005). This indicates that we might miss sites whose levels change within the dynamic range of the FT-ICR-MS between states. The number of kinase inhibitor and mitosis-specific sites we find might therefore be an underestimate.

It was previously shown that nocodazole arrest is a valid method to identify phosphorylation sites that are also present in unperturbed mitosis (Kraft et al., 2003) and that have a functional significance in prometaphase phosphoregulation (Hauf et al., 2005). We nevertheless wanted to address whether the phosphorylation sites we identified from nocodazole arrested cells were only generated in cells arrested for a long time in prometaphase. We tested some of the generated phospho-antibodies on western blots prepared from cell extracts of cells synchronised without long nocodazole treatment. Using a double thymidine arrest we blocked cells in early S-phase and released them into fresh medium to allow progression into G2-phase. Cells were harvested four h after release (G2), ten h after release by mitotic shake off (SO) or were first treated with nocodazole seven h after release and harvested three h later (sN) or nocodazole treated cells were treated for the last two h of the three h mitotic arrest with either BI4834 (sNB) or Hesperadin and MG132 (sNHM). Cell extracts were prepared, separated by SDS-PAGE and analysed by western blotting using antibodies against Cyclin B (CCNB1), phosphorylated S10 on Histone H3 (H3S10ph), Histone H3 (H3) and the APC/C subunit CDC27 to control for the cell cycle stage (Figure 2.2-3 B). CCNB1 levels were similar in all conditions, indicating that cells were in G2/M. Serine 10 phosphorylation on Histone 3 was high in SO cells but much higher in sN and sNB, indicating that mitotic cells were enriched in SO but mitotic phosphorylation much higher in sN and sNB. Judging by the phosphorylation shift of CDC27 (Kraft et al., 2003; Peters et al., 1996) all cells in sN, sNB and sNHM were mitotic. Probing these extracts with the phospho-specific antibody pSTAG2-S1224 (Kueng et al., 2006) showed that this phosphorylation site was also present in cells isolated by mitotic shake off. A similar result was obtained using the antibody pRAD21\_S175 (Supplemental figure 2.2-2 D) and two other phospho-specific antibodies (pRAD21\_S153 and pWAPAL\_S465, data not shown). In agreement with earlier studies (Hauf et al., 2005; Kraft et al., 2003) these results indicate that the phosphorylation pattern detected in prolonged nocodazole arrests resembles the situation of cells in an unperturbed mitosis. We can not exclude, however, that the relative level of phosphorylation is much higher in prolonged nocodazole arrests.

## 2.2 Phosphorylation site mapping manuscript

Our analysis of phosphorylation sites that are sensitive to treatments with PLK1 or AURKB inhibitors might detect indirect phosphorylation changes on proteins that are substrates of a kinase downstream of PLK1 or AURKB. Since it is not possible to measure direct phosphorylation events in living cells we tested whether two of the detected BI-sensitive phosphorylation sites could also be generated directly by PLK1 in an *in vitro* kinase assay. We purified STAG2 or WAPAL by immunoprecipitation from interphase cells and incubated it with recombinant PLK1, ATP and PLK1 inhibitor as indicated (Figure 2.2-3 D). The phosphorylation site S1224 on STAG2 as well as the phosphorylation site S465 on WAPAL are phosphorylated by PLK1 directly, suggesting that these sites might be direct phosphorylation sites also *in vivo*.

We further tested whether the phospho-specific antibodies could recognise their epitopes in immunofluorescence microscopy (IF) of HeLa cells. To do this we treated HeLa cells grown on coverslips for 30 minutes with PLK1-inhibitor prior to fixation and stained them with the phospho-antibody and an antibody against the unphosphorylated protein. So far, only the STAG2\_pS1224 antibodies were of sufficient specificity to be useful for IF experiments. These antibodies stain chromatin associated STAG2 in early prophase and soluble cohesin in prometa- and metaphase while the signal is reduced in telophase and not present in cytokinesis, interphase and S-phase (Figure 2.2-3 E). The antibody also stains two structures specifically in mitosis which might represent the centrosomes. Since control staining with STAG2 antibodies did not stain these two structures, we assume that this signal of STAG2\_pS1224 antibodies results from a cross reaction. Most importantly, the signal is completely abolished after treating the cells for 30 minutes with the PLK1 inhibitor (Figure 2.2-3 E) or after 24 siRNA depletion of PLK1. This shows also in immunofluorescence that the phosphorylation site on S1224 of STAG2 is dependent on PLK1. Whether loss of this phosphorylation site is responsible for the cohesin enrichment on mitotic chromatin after PLK1 inhibition (Hauf et al., 2005) remains to be seen. Phospho-mutants of STAG2 suggested that all phosphorylation sites need to be mutated to cause a similar cohesin enrichment phenotype as is seen with PLK1 inhibition. However, mutants of only S1224 or S1224 together with the second BI-sensitive site on STAG2 (S1091) have not been tested.

In conclusion, we have shown that a large fraction of the phosphorylation sites we analysed by phospho-specific antibodies confirmed our MS results. In addition, the phosphorylation sites mapped in prolonged nocodazole arrest are not likely to be different from the phosphorylation sites generated during an unperturbed mitosis and at least two of the BI-sensitive sites can be directly generated by PLK1 *in vitro*. We are thus confident that our experimental approach finds true mitotic phosphorylation sites and true PLK1 and AURKB-dependent phosphorylation sites. This allows us to use our data to define novel potential substrates of PLK1 and AURKB which might help us to understand the essential roles of these two kinases in mitosis.



### 2.2.3.7 Potential novel PLK1 and AURKB substrates

We identified in total 39 BI-sensitive phosphorylation sites on 25 proteins, 23 Hesperadin-sensitive phosphorylation sites on 21 proteins and 26 sites that are sensitive to both inhibitors on a total of 13 proteins (Figure 2.2-4 B and C). We also find ten proteins that have both, PLK1 inhibitor-sensitive sites and Hesperadin-sensitive sites. Of the 25 potential PLK1 substrates, eight have been described previously, of the 21 potential AURKB substrates, four have been described previously.

Compared to the previously known PLK1 substrates that were included in our data set we also found ANAPC1 (Kraft et al., 2003), Bub1 (Qi et al., 2006), Bub1b (Elowe et al., 2007), CDC27 (Kraft et al., 2003), Kif23 (Liu et al., 2004), PLK1 (Kelm et al., 2002), RAD21 and STAG2 (Sumara et al., 2002) but not ANAPC4, ANAPC7 (Kraft et al., 2003) and CyclinB (Jackman et al., 2003; Toyoshima-Morimoto et al., 2001). Most of these known substrates, with the exception of BUB1B, have been found using *in vitro* kinase assays with recombinant kinases or mitotic extracts of HeLa cells or *Xenopus* eggs. In few cases the actual phosphorylation sites were mapped using amino acid substitution or MS.

We found that the cohesin subunit RAD21 is phosphorylated *in vivo* by PLK1 on four sites (S134/S138, S175, S153 and S545) and another cohesin subunit, STAG2, is phosphorylated on two sites (S1091, S1224). This is consistent with earlier findings that phosphorylation of RAD21 by PLK1 enhances its cleavage by separase (Hauf et al., 2005) and that STAG2 phosphorylation, presumably by PLK1, is required for the bulk of cohesin to dissociate from chromatin in early mitosis (Hauf et al., 2005). This latter effect, the so-called prophase pathway (Waizenegger et al., 2000), can only be partially inhibited by making STAG2 unphosphorylatable or by inhibiting PLK1 activity. A full block in this pathway is observed when the cohesin interaction partner WAPAL is depleted. We could now show that WAPAL is highly phosphorylated in mitosis, that seven out of its nine mitotic phosphorylation sites are sensitive to Plk-inhibitor treatment (Figure 2.2-2 E) and that at least one of these inhibitor-sensitive sites can be directly generated by PLK1 (Figure 2.2-3 D). This is the only protein we found where the majority of mitotic phosphorylation sites is dependent on PLK1. In the future it will be interesting to test if WAPAL phosphorylation by PLK1 has a role in the prophase pathway of cohesion dissociation from chromatin.

Of the known AURKB substrates we find AURKB (Yasui et al., 2004), INCENP (Honda et al., 2003), NCAPD2 (Lipp et al., 2007) but not NDC80 (Cheeseman et al., 2006; DeLuca et al., 2006). Interestingly, we find a Hesperadin-sensitive site on BUB1B in purification

## 2.2 Phosphorylation site mapping manuscript

of MAD2L1 since it has been speculated previously that BUB1B might be an AURKB substrate. Data from AURKB inhibition experiments using the small molecule inhibitor ZM447439 showed that BUB1B hyperphosphorylation is abolished when AURKB is inhibited already before mitosis (Ditchfield et al., 2003) but not when it is inhibited during mitosis (Morrow et al., 2005). We could now find that at least one site, T354, on human BUB1B is dependent on AURKB during mitosis. Experiments in yeast show that phosphorylation of the BUB1B homolog Mad3 by Ipl1p – the AURKB homolog – is required for the spindle checkpoint response to the lack of tension (King et al., 2007). We are planning to mutate the identified site in LAP-tagged BUB1B to test if this function is conserved in human.

In summary, we have detected 17 novel potential PLK1 and 18 novel potential AURKB substrates at the kinetochore, the chromosome, the centrosome and the mitotic spindle. Further investigation by mutational analysis will reveal the function of these potential substrates and might help advance our understanding of the role of PLK1 at these mitotic structures.

### 2.2.3.8 Initial bioinformatic analysis of PLK1-dependent phosphorylation sites

Our approach of mapping PLK1- and AURKB-dependent phosphorylation sites in cells lead to detection of potential physiological substrates of these kinases, two of which we could show to be direct substrates *in vitro*. The consensus sequence for PLK1 has been determined in an *in vitro* kinase assay using peptides as model substrates (Nakajima et al., 2003). Some, but not all of the identified PLK1 phosphorylation sites on its substrates match this proposed consensus [DE]-X-[ST]-Φ-X-[DE] (Φ = hydrophobic amino acid). Several of those sites have been determined *in vitro* (Supplemental table 2.2-1, (Barr et al., 2004)). Since our data represents the first systematic identification of potential PLK1 phosphorylation sites in cells, we wanted to test to what extent these sites correspond to the proposed consensus sequence.

Initial sequence analysis surrounding the PLK1 inhibitor-sensitive phosphorylation sites was done as follows: the occurrence of Glutamate (E) and Aspartate (D) at the position -3, -2 or -1 relative to the phosphorylation site was counted and compared to the expected occurrence at random (11%). At the +1 and +2 positions the occurrences of hydrophobic residues (Φ = I, L, V, M, F, C) was counted and compared to the expected occurrence at random (26%). The only enrichment detectable was that of D and E at the -2 position (3.8 fold enrichment) which is partially consistent with the consensus sequence [DE]-X-[ST]-Φ-X-[DE] (as determined by *in vitro* kinase assays (Nakajima et al., 2003). More detailed analysis might show whether this weak correlation is due to a more relaxed consensus sequence *in vivo*, i.e. conserved residues could be distributed

over several positions, or whether our data set contains phosphorylation sites that are not direct targets of PLK1. In addition it will also be interesting to test whether these proteins that carry PLK1 inhibitor-sensitive phosphorylation sites also contain a potential PBD binding site and, if yes, whether this is also phosphorylated.

#### 2.2.4 Discussion

The key mitotic roles of PLK1 and AURKB are reasonably well understood, but the search for their substrates and ultimately their substrate's function still lags behind. In an effort to develop a systematic assay for the detection of PLK1 and AURKB substrates, we established a protocol to purify candidate substrate complexes from HeLa cell and detected kinase-dependent phosphorylation sites by combining small molecule inhibitors of PLK1 (Lenart et al., 2007; Steegmaier et al., 2007) and AURKB (Hauf et al., 2003) and MS. We could show that this protocol successfully detects known PLK1 substrates like RAD21 (Hauf et al., 2005) and known AURKB substrates like INCENP (Honda et al., 2003). At the same time we could identify additional phosphorylation sites dependent on AURKB on INCENP and finally pinpoint the phosphorylation sites on RAD21 that are PLK1-dependent. In addition we could confirm two PLK1 substrates, the cohesin complex members STAG2 and WAPAL, and one novel AURKB substrate, NUP85, with phospho-specific antibodies. This finally led to the identification of 17 novel potential substrates each for PLK1 and AURKB, approximately doubling the number of substrates that are known for these two kinases. In addition we have identified the phosphorylation sites on each substrate that are dependent on PLK1 or AURKB, which has not been the case for most of previously identified substrates. In particular, only one *in vivo* PLK1 site had been previously established within the eight known PLK1 substrates we tested (BUB1B S676 (Elowe et al., 2007)). Considering the usual workflow of mutational analysis, *in vitro* kinase assays and finally generation of a phospho-specific antibody to show that a single phosphorylation site is kinase-dependent *in vivo*, our approach yields results faster and can be applied on a more systematic level. With the availability of a high throughput pipeline for BAC tagging (Poser et al, 2008) a large collection of candidate complexes is available for further analysis.

We could show that the analysis of phospho-mapping as well as interaction mapping data can be further improved by label-free semi-quantitative analysis of proteolytic peptides in the mass spectrometer. Semi-quantitative analysis of phospho-peptides reduced false negative identification of phosphorylation sites in the Bub1b and WAPAL phospho-site analysis and thus improved the detection of mitosis-specific and inhibitor-sensitive sites. In addition, analysis of the relative complex stoichiometry of Bub1b recapitulated the mitosis-specific formation of a mitotic checkpoint-kinetochore complex (Chan et al., 1999; Jablonski et al., 1998) including the recently identified CASC5. It is

## 2.2 Phosphorylation site mapping manuscript

thus conceivable that quantification of the entire cell cycle- and inhibitor-dependent data set would provide an informative data set about complex stoichiometry of the selected baits.

A number of the identified substrates could play important role in processes regulated by PLK1 and or AURKB on the different cellular structure that we probed: the kinetochore/mitotic checkpoint complex, the spindle/centrosome and the mitotic chromosome.

For example, it was initially shown that the mitosis-dependent phosphorylation shift of BUB1B is abolished when PLK1 or AURKB is inhibited or depleted before cells enter mitosis (Ditchfield et al., 2003; Matsumura et al., 2007) but not when PLK1 (unpublished results) or AURKB (Ditchfield et al., 2003) are inhibited during mitosis. Whether this was due to direct phosphorylation by either of the two kinases was not clear. It was later shown that mutation of the potential PBD binding motif of BUB1B inhibited the formation of proper kinetochore microtubule interactions and caused chromosome congression defects as well as a delay in prometaphase. Subsequent identification of a PLK1-dependent phosphorylation site on S676 showed that this site is selectively phosphorylated when kinetochores are attached but not under tension in prometaphase, indicating that PLK1 directly phosphorylates BUB1B and that this phosphorylation is necessary to mediate kinetochore microtubule interactions but not to fulfil its checkpoint function (Elowe et al., 2007). It was not shown whether S676 was the only PLK1 phosphorylation site on BUB1B or whether mutation of the PBD binding motif abolished the phosphorylation of BUB1B. We found a site adjacent to S676, S670, phosphorylated on BUB1B that copurified with CDC27 and Mad21. This site was mitosis-specific but not sensitive to inhibitor treatment. On Bub1b we do not find a peptide covering the sequence surrounding S676 but we find that T47 is sensitive to PLK1 inhibitor treatment, indicating that a number of sites on BUB1B might be phosphorylated by PLK1 *in vivo*.

How AURKB might be involved in BUB1B phosphorylation on the kinetochore is not fully understood. Inhibition of AURKB using Hesperadin or ZM447439 inhibits localisation of BUB1B to the kinetochore in prometaphase (Ditchfield et al., 2003; Hauf et al., 2003) and AURKB inhibition leads to immediate override of a taxol induced arrest or a three h delayed override of a nocodazole induced arrest (Hauf et al., 2003). A study in yeast showed that phosphorylation of Mad3p (the yeast homolog of BUB1B) is required for checkpoint activation in response to loss of tension at the kinetochores but not in response to loss of attachment (King et al., 2007). This is consistent with the immediate override of a taxol arrest which mimics a loss of tension situation compared to the delayed override of nocodazole arrested cells. We have identified T354 on BUB1B to be Hesperadin-sensitive and S733 to be sensitive to the PLK1-inhibitor and Hesperadin.

Phospho-mutants of these sites together with the PLK1-dependent sites could be used to delineate whether the phosphorylation of BUB1B by PLK1 and AURKB is interdependent. Based on the recent finding that for AURKB to efficiently phosphorylate its centromeric substrate MCAK, MCAK needs to first be phosphorylated by PLK1 (Rosasco-Nitcher et al., 2008), one could speculate that a similar temporal regulation of phosphorylation is also in place for BUB1B. This would explain why inhibition of PLK1 and AURKB abolished the BUB1B mitotic phosphoshift and why we detect a phosphorylation site which perfectly matches the AURKB consensus sequence (Cheeseman et al., 2002) that is sensitive to treatment with the PLK1 inhibitor and Hesperadin.

We have also detected three PLK1-dependent and six AURKB-dependent sites out of 49 total phosphorylation sites on the NUP107-NUP160 complex. A previous phosphorylation mapping study has identified twelve sites in total, seven of which we could also detect (Glavy et al., 2007). The NUP107-NUP160 subcomplex of the NPC localises to the kinetochore during mitosis (Belgareh et al., 2001) and has been proposed to be involved in bipolar spindle formation (Orjalo et al., 2006). Detailed evidence of its mitotic function, however, is lacking. It is conceivable that components of the NUP107-NUP160 complex need to be phosphorylated at the kinetochore to fulfil their functions.

Analysis of the centrosomal  $\gamma$ -tubulin ring complex ( $\gamma$ -TuRC), which is required for microtubule nucleation and mitotic spindle organisation, has detected three BI-sensitive sites, three Hes-sensitive sites and one site sensitive to both inhibitors out of the 20 total sites identified on the complex. It is particularly interesting to note that TUBG1 contains one phosphorylation site that is dependent on PLK1. For a long time it has been known that depletion of PLK1 leads to a block in centrosome maturation, i.e. the accumulation of TUBG1 on centrosomes in mitosis (Lane and Nigg, 1996; Lenart et al., 2007; Sumara et al., 2004). It is, however, not clear how this process is regulated on a molecular basis. Depletion of the p58 variant of CDK11 by RNAi blocks centrosome maturation but also leads to a loss of PLK1 and AURKA from the centrosome (Petretti et al., 2006). The ninein like protein Nlp localizes to centrosomes in interphase but is displaced from centrosomes by PLK1 phosphorylation at the onset of mitosis (Casenghi et al., 2005; Casenghi et al., 2003). A non-phosphorylatable mutant of Nlp remains at the centrosome in mitosis and prevents centrosome maturation. It was later shown that this failure in centrosomal dissociation is most likely due to the fact that PLK1 phosphorylation of Nlp leads either to a defect of Nlp transport to the centrosome by dynein-dynactin or to inhibition of Nlp binding to the centrosome (Casenghi et al., 2005). It is thus likely that additional activating events are necessary to recruit extra TUBG1 to the centrosome in mitosis. By generating an S131A mutant of TUBG1 we will test whether direct phosphorylation of TUBG1 is required for centrosome maturation.

## 2.2 Phosphorylation site mapping manuscript

Of the chromosomal proteins it was especially interesting to look at the cohesin complex members. We know from previous studies that phosphorylation of RAD21 by PLK1 is required for efficient cleavage by Separase and that phosphorylation of STAG2, presumably by PLK1 is required for cohesin's efficient removal from chromosome arms in prophase (Hauf et al., 2005), the so-called prophase pathway (Waizenegger et al., 2000). Even though the mitosis-specific phosphorylation sites of RAD21 and STAG2 have been identified (Hauf et al., 2001), it was not clear which of these are dependent on PLK1. We could identify four PLK1 sites on RAD21 and two sites on STAG2, two of the RAD21 sites and one STAG2 site were further validated using phospho-specific antibodies. In addition to the previous phosphorylation analysis we could now also identify phosphorylation sites on STAG1, PDS5A, PDS5B and WAPAL. The most striking result was that WAPAL, which is essential for the prophase pathway, is highly phosphorylated in mitosis and that seven out of the nine mitosis-specific phosphorylation sites are dependent on PLK1. One speculative explanation of this finding is that PLK1 indeed functions upstream of WAPAL in the prophase pathway and that WAPAL needs PLK1 phosphorylation to be fully active in prophase when it is involved in the removal of cohesin from chromatin. This would be the simplest explanation why PLK1 inhibition leads to a mild defect in the prophase pathway and why phosphorylation of STAG2 alone is not sufficient to remove it from chromatin in prophase (Kueng et al., 2006). Mutational analysis of the identified phosphorylation sites on WAPAL should be able to test this speculative hypothesis.

To conclude, the dataset we generated presents a basis for further research of the functions of PLK1 and AURKB at the centrosome, the centromere, the spindle and in chromosomal architecture. In addition, further application of this method to more candidate substrates in mitotic protein complexes will likely yield more detailed idea of which proteins are the key targets of PLK1 and AURKB and will ultimately lead to a better understanding of kinase substrate interactions in mitosis.

### 2.2.5 Materials and methods

#### 2.2.5.1 Cell culture

HeLa cells were grown on Nunc cell culture dishes in DMEM supplemented with 10% FCS, 0.2 mM L-glutamine, 100 U/ml penicillin, and 100 µg/ml streptomycin. For transfected cell lines the medium was supplemented with 500 µg/ml G418. Mitotic cells were arrested for a total of 18 h using 100 ng/µl nocodazole. Inhibition of PLK1 was achieved using either 250 nM of BI4834 or 100 nM of BI2536 (Lenart et al., 2007; Steegmaier et al., 2007) during the last two h of nocodazole arrest. AURKB was inhibited using 100 nM Hesperadin (Hauf et al., 2003) in combination with 10 µM MG132 during the last two h of nocodazole arrest. For BI4834 characterisation, RAD21-9x MYC cells (Hauf et al., 2005) were induced by 2 µg/ml doxycycline for three days.

### 2.2.5.2 Protein extraction and purification

Protein extracts for immunopurifications using antibodies against the endogenous proteins were prepared using IP-buffer (20 mM Tris-HCl, pH 7.5; 150 mM NaCl, 5 mM EDTA, 20 mM  $\beta$ -glycerophosphate, 10 mM NaF, 10% glycerol, 0.1% NP-40, 1  $\mu$ M okadaic acid, 0.2 mM NaVO<sub>4</sub>, 1 mM DTT and protease inhibitor mix (PIM: leupeptin, chymostatin and pepstatin at 10  $\mu$ g/ml). Extracts from cell treated with either BI2536, BI4834 or Hesperadin/MG132 also contained these components at the concentrations given.

Endogenous proteins were immunopurified using antibodies described in the antibody section. After immunoprecipitation using antibodies crosslinked with DMP (Harlow and Lane, 1988) to affiprep beads (Bio-Rad, USA), purified complexes were washed extensively in 100x bead volume of IP buffer for a total of 1 h at 4°C. For mass spectrometric analysis the last three washing steps were carried out in IP-buffer without detergent.

FLAG-purification was done from cells expressing either NCAPH-GFP-FLAG fusion or NCAPH2-GFP-FLAG fusion proteins (Hirota et al., 2004). Cells were extracted using IP-buffer B (50 mM HEPES-KOH, pH 7.5; 5 mM EDTA, 150 mM KCl, 10% glycerol, 1% Triton X-100, 20 mM beta-glycerophosphate, 10 mM NaF, 10 mM Na-pyrophosphate, 1  $\mu$ M okadaic acid, 0.1 mM PMSF, 1 mM Na<sub>3</sub>VO<sub>4</sub>, 1 mM DTT and PIM). After immunoprecipitation using FLAG-M2 beads (Sigma-Aldrich), beads were washed extensively in IP-buffer B (Triton was substituted by 0.5% NP-40), then three times with 50 mM HEPES-KOH, pH 7.5, 5 mM EDTA, 150 mM KCl, 10% glycerol and finally three times with 150 mM KCl.

LAP-purification was done as described (Poser et al., 2008). All buffers additionally contained 1  $\mu$ M okadaic acid and either BI2536, BI4834 or Hesperadin/MG132 when proteins were purified from inhibitor-treated cells. Purified proteins were eluted from beads using 0.2 M glycine pH 2.0 and the eluate neutralised with 1/10 volume 1.5 M Tris pH 9.2.

### 2.2.5.3 MS and data analysis

Elution and in-solution digest

Eluted and neutralised proteins were subjected to in-solution digest using trypsin, chymotrypsin, subtilisin or GluC as described previously (Kraft et al., 2003). Approximately equal amounts of digested peptide mixtures were analysed by MS.

## 2.2 Phosphorylation site mapping manuscript

### MS analysis

Equipment - All nano HPLC separations were performed using UltiMate 3000 Nano-LC system (Dionex Benelux, Amsterdam, The Netherlands) equipped with a trap column (PepMap C18, 300  $\mu$ m ID x 5mm length, 3  $\mu$ m particle size, 100 Å pore size, Dionex Benelux) for sample desalting and concentration and an analytical column (PepMap C18, 75  $\mu$ m ID x 150 mm length, 3  $\mu$ m particle size, 100 Å pore size, Dionex Benelux) for the chromatographic separation. Loading buffer used contains 0.1% trifluoroacetic acid (Pierce). For chromatographic separation mobile phase A contains 5% acetonitrile (Merck, Darmstadt, Germany) and 0.1% formic acid (Merck) and mobile phase B 80% acetonitrile and 0.08% formic acid.

Mass spectrometric analyses were conducted on a hybrid linear ion trap/Fourier transform ion cyclotron resonance (FTICR) mass spectrometer (LTQ-FT Ultra, ThermoElectron, Bremen, Germany) with a 7-Tesla superconducting magnet. The mass spectrometer was equipped with a nano-electrospray ionization source (Proxeon Biosystems, Odense, Denmark). Metal coated nano ESI needles were used (New Objective, Woburn, MA, USA).

LC separation - Samples were loaded onto the trap column at a flow rate of 20  $\mu$ L/min loading buffer and were washed for ten minutes. Afterwards the sample was eluted from the trap column and separated on the separation column with a gradient from 20% to 50% mobile phase B in 180 minutes at a flow rate of 300nL/min.

MS detection – Eluting peptides were ionized with a spray voltage set to 1.5 kV. Fullscan (400-1800 m/z) was conducted in the ICR cell yielding a survey scan with resolution of 100,000 and a typical mass accuracy < 2ppm. CAD fragmentation and spectra acquisition were carried out in the linear ion trap using a multi stage activation (MSA) method. The target values of the automatic gain control (AGC) were set to 10,000 for CAD in the ion trap, and to 500,000 for FT-ICR fullscan spectra. In the applied MS method fragmentation was performed on the five most intense signals of the survey scan using MSA of the neutral loss of phosphoric acid. Singly charged ions were excluded for precursor selection and precursors of MS<sup>2</sup> spectra acquired in previous scans were excluded for further fragmentation for a period of 3 min whereas the exclusion mass tolerance was set to 5 ppm.

Data base search – Acquired data (Xcalibur RAW-file) were converted into Mascot generic files using Mascot Daemon (Matrix Science, London, UK). For peptide identification a database search against a custom database containing the human KBMS database (5.0.20050304, 187752 sequence entries, Applied Biosystems) and all relevant mouse bait sequences was carried out using Mascot (Matrix Science, London, UK; version 2.2.0). The following parameters were used for the database search: carboxymethylation (+58.0055 u) of cysteine was set as fixed and oxidation (+ 15.9949



u) of methionine and phosphorylation (+79.966331 u) as variable modification; enzymatic cleavage was specified to either Trypsin, Chymotrypsin or no specificity (for Subtilisin digests). Mass tolerances of the parent ion and the fragments were set to 10 ppm and 0.80 Da, respectively. Unphosphorylated peptides with a Mascot score greater than 20 were kept and used to calculate the sequence coverage of detected proteins after combining all parallel digests (usually trypsin, chymotrypsin and subtilisin). Detected phospho-peptides with a Mascot score greater than 15 were manually validated and rated with a score between 0 (lowest) and 3 (highest). Phosphorylation sites within peptides were assigned to, if possible, unambiguous positions. Peptides scored 1-3 were kept for further analysis.

Phosphorylation sites from all four cell cycle conditions (interphase (L), mitosis (N), mitosis + PLK1 inhibition (NB), mitosis + AURKB inhibition (NHM)) were compared. For each cell cycle state the phosphorylation site could either be present (M), absent with an unmodified peptide covering the site (UM) or absent with no peptide covering the site (nd). We disregard the sites that are nd in one state or UM in all states, so that we are left with 15 possible combinations for a single site. The name of each combination is given in the table below. Most sites that were detected fall into the first six categories (Phosphorylated (M), unphosphorylated (UM) or no peptide (nd) present).

Category	Abbrev.	L	N	NB	NHM
interphase	I	M	UM	UM	UM
interphase and mitosis	I/M	M	M	M	M
mitosis	M	UM	M	M	M
PLK1 inhibitor-sensitive	BI-sens	UM	M	UM	M
Hesperadin-sensitive	Hes-sens	UM	M	M	UM
PLK1 inhibitor- & Hesperadin-sensitive	BI+Hes sens	UM	M	M	M
I/M, PLK1 inhibitor-sensitive	I/M, BI-sens	M	M	UM	M
I/M, Hesperadin-sensitive	I/M, Hes-sens	M	M	M	UM
I/M, PLK1 inhibitor- & Hesperadin-sensitive	I/M, BI+Hes sens	M	M	M	M
PLK1 inhibitor-induced	hes-ind	UM	UM	UM	M
Hesperadin-induced	bi-ind	UM	UM	M	UM
PLK1 inhibitor & Hesperadin-induced	BI+Hes-ind	UM	UM	M	M
I & PLK1 inhibitor-induced	I, BI-ind	M	UM	M	UM

## 2.2 Phosphorylation site mapping manuscript

I & Hesperadin-induced	I, Hes-ind	M	UM	UM	M
I & PLK1 inhibitor- & Hesperadin-induced	I/bi+hes-ind	M	UM	M	M

The following categories were assigned to sites where sequence information could not be detected in all four states:

Category	Abbrev.	I	N	NB	NHM
potentially mitosis	m?	nd	M	M	M
potentially in interphase and mitosis	I/M?	M	M	nd	nd
potentially in interphase	I?	M	nd	nd	nd
potentially Hesperadin-induced	hes-ind?	nd	nd	nd	M
potentially PLK1 inhibitor-induced	bi-ind?	nd	nd	M	nd
potentially PLK1 inhibitor- & Hesperadin-induced	BI+Hes-ind?	nd	nd	M	M
potentially I & PLK1 inhibitor-induced	I/BI-ind?	M	nd	M	nd

Peptide quantification: We integrated the intensities for each charge state of a given peptide manually using QualBrowser (Thermo Fisher Scientific). To determine the level changes of a protein, at least six unmodified peptides that did not contain methionine and no mis-cleavage sites were integrated. The intensity of each peptide was normalised to the nocodazole sample and the changes relative to nocodazole were averaged over all peptides of a single protein. The standard deviation of relative level changes was calculated and is indicated with the error bars in the graphs. To compare relative complex composition changes the relative level change of a given prey protein was normalised to the relative level changes of the bait. The standard deviation indicated is that of the different peptides of the prey protein. To assess relative changes of phospho-peptide the same method was used. Since only one peptide per digest was detected for a given phosphorylation site, no standard deviation could be computed.

### 2.2.5.4 Antibodies

Phospho-antibodies (listed Figure 2.2-3 C) were raised against 8mer to 13mer synthetic peptides in rabbits and affinity purified as described (Kraft et al., 2003). Further

antibodies used in immunopurification, western blotting and immunofluorescence were (antibodies are from rabbit if not stated otherwise):  $\alpha$ -CDC27 (Gieffers et al., 1999),  $\alpha$ -PDS5A (521, (Sumara et al., 2000)),  $\alpha$ -PDS5B (1531: QLKGLEDTKSPQFNRYFC and 2230: VSTVNVRRRSKRERR (Losada et al., 2005)),  $\alpha$ -STAG1 (444 (Sumara et al., 2000)),  $\alpha$ -STAG2 (446 (Sumara et al., 2000)),  $\alpha$ -WAPAL (986 and 987 (Kueng et al., 2006)),  $\alpha$ -NUP85 (Loiodice et al., 2004),  $\alpha$ -NCAPH (Yeong et al., 2003), mouse  $\alpha$ -phospho-S10-H3 (05-499, Upstate), goat  $\alpha$ -H3 (sc8654, Santa Cruz), mouse  $\alpha$ -CCNB1 (GNS1, Santa Cruz Biotechnology),  $\alpha$ -CDC25C (Cell Signaling),  $\alpha$ -BUB1B (gift from Gregor Kohlmaier),  $\alpha$ -INCENP (Hauf et al., 2005),  $\alpha$ -TUBG1 (T3559, Sigma), mouse  $\alpha$ -TUBA1B (clone B-5-1-2, Sigma),  $\alpha$ -phospho CDC16 (Kraft et al., 2003), human CREST (Cortex Biochem), mouse  $\alpha$ -MYC (4A6, 05-724, Upstate) and  $\alpha$ -SMC2 (Yeong et al., 2003).

Secondary antibodies used for western blotting were  $\alpha$ -mouse,  $\alpha$ -rabbit or  $\alpha$ -goat coupled to horse radish peroxidase (HRP); for immunofluorescence Alexa 488, Alexa 568 and Alexa 633 labeled secondary antibodies were used (Molecular Probes (Invitrogen)).

#### 2.2.5.5 *In vitro* kinase assay

WAPAL and STAG2 were immuno purified as described above. *In vitro* phosphorylation was performed as described (Kraft et al., 2003) using 10 mM ATP and recombinant 6xHis-tagged PLK1. Recombinant human PLK1 was expressed as a 6xHis-tagged fusion protein using a baculoviral expression system and purified by affinity chromatography using Ni-NTA (QIAGEN). Where indicated, reactions were supplemented with 1  $\mu$ M BI 2536.

#### 2.2.5.6 Immunofluorescence microscopy

Cells were grown on coverslips and fixed with 4% formaldehyde in PBS at RT or -20 °C methanol for 15 min. RAD21-9x MYC cells were cytopun (Shandon Brand), extracted with 0.5% Triton-X100 in PBS for 2 min and fixed with 4% formaldehyde in PBS (Hauf et al., 2005). After fixation samples were permeabilized with 0.5% Triton-X100 in PBS for 15 min and thereafter blocked with 10% FCS in PBS containing 0.01% Triton-X100. Coverslips were incubated for 1 h each at RT with primary and secondary antibodies (at 2  $\mu$ g/ml in 3% BSA in PBS containing 0.01% Triton-X100), DNA was counterstained with Hoechst 33342 coverslips and mounted with either ProLong Gold (Molecular Probes) or Vectashield Mounting Medium (H1000, Vector Laboratories) onto slides. Image acquisition was performed as described (Waizenegger et al., 2000) or (for BI4834 characterisation) images were taken on a Zeiss Axioplan 2 microscope using 100x Plan-Apochromat objective lens (Carl Zeiss, Jena) equipped with CoolSnapHQ CCD camera (Photometrics). For signal intensity quantification, images were acquired as raw

## 2.2 Phosphorylation site mapping manuscript

12-bit images taken at identical exposure times within each experiment. Images were processed in ImageJ (<http://rsb.info.nih.gov/ij/>). Images shown in the same panel have been scaled identically. For quantification of TUBG1 intensities a circular region with fixed diameter was measured on the centrosome and a same-sized region was also measured in the cytoplasm. After subtracting the background outside the cells ratio of these values was calculated and average and standard deviation of these measurements were plotted. For each measurement at least 20 centrosomes were quantified. Mitotic phenotypes were classified based on the TUBA1B and DAPI staining; for each measurement 100 cells were counted.

### 2.2.6 Figure Legend

#### 2.2.6.1 Figure 2.2-1

Summary of analysed baits and example of Bub1b purification from four cellular states.

A) The baits (either LAP-tagged mouse (mm) baits, a single LAP-tagged human bait (hs SMC6) or endogenous baits purified via polyclonal antibodies (hs)) are sorted according to their subcellular localisation.

B) LAP-tagged Bub1b was tandem purified and glycine eluted from log-phase cells (log), noc-arrested cells (N) and noc-arrested cells treated for two h with either BI4834 (NB) or Hesperadin and MG132 (NHM). 7% of the eluted complex was analysed by SDS-PAGE/silver staining and the remaining sample was digested in solution using, in parallel, trypsin, chymotrypsin and subtilisin. The combined sequence coverage and the number of detected phosphorylation sites per protein are shown in C).

#### 2.2.6.2 Figure 2.2-2

Relative quantification of Bub1b and WAPAL phosphorylation sites and determination of relative Bub1b complex stoichiometry.

X-axes in all plots in this figure represent fold change while all y-axes give the source of the measured peptide as log-cells (L), noc-arrested cells (N) and noc-arrested cells treated for two h with either BI4834 (NB) or a combination of Hesperadin and MG132 (NHM).

A) Six unmodified peptides of Bub1b were quantified by integrating ion intensities over all charge states observed between 400 and 1800 m/z in the MS1 chromatogram of three different digests (trypsin, chymotrypsin, subtilisin). Integrated areas were normalised to the nocodazole sample (N) and the average fold change calculated.

In B) fold changes for UBR5, BUB3, CASC5, CDC20, CDC27 and BUB1 over all four samples were derived from integrated intensities of six tryptic peptides. Values were normalised to N and their change relative to observed Bub1b level changes in the tryptic digest were plotted. Error bars indicate standard deviation calculated for each data point of each protein.

C) Fold changes for CDC27 and BUB1B in a CDC27 immunopurification were calculated as in A. The fold change for BUB1 relative to CDC27 levels was calculated as in B.

D) Based on the calculated fold changes for Bub1b given in A, relative phospho-peptide levels of each identified phosphorylation site in Bub1b were calculated for all digests (Supplemental figure 2.2-2 E for details). Phosphorylation sites were then categorised into sites present in interphase and mitosis (orange), sites present exclusively in mitosis (red) and sites that could not be clearly categorised (dark grey). See text for details on categorisation. \* denotes sites sensitive to BI4834, # denotes sites sensitive to

## 2.2 Phosphorylation site mapping manuscript

Hesperadin, protein domains are shaded in grey and labelled according to Interpro names.

E) Fold changes for WAPAL in WAPAL immunoprecipitations from L, N, NB and NHM were calculated as in A, relative phospho-peptide levels were determined and three examples are shown for phosphorylation sites S465, S528 and S1154. All sites were categorised and labelled as in D.

### 2.2.6.3 Figure 2.2-3

Phospho-specific antibodies generated against a subset of phosphorylation sites validate the MS results.

A) Phospho-specific polyclonal antibodies raised against different phosphopeptides listed in C) were tested on protein immunopurified using the indicated antibodies from extracts obtained from log-phase cells (L), noc-arrested cells (N) and noc-arrested cells treated for two h with either BI4834 (NB) or a combination of Hesperadin and MG132 (NHM). (B) The pSTAG2\_S1224 antibody was tested on protein extracts from cells synchronised with a double thymidine arrest release and harvested either four h after release (G2), ten h after release by mitotic shake off (SO), ten h after release with the last three h in nocodazole (N), with last three h nocodazole and last two h either BI4834 (NB) or Hesperadin/MG132 (NHM). The cell cycle stage was controlled using antibodies against CCNB1, H3S10ph, H3 and CDC27 as indicated. (C) Lists the phosphopeptides used to generate polyclonal rabbit phospho-specific antibodies against the listed proteins. # Refers to the antibody and antigenic peptide number. The phospho-site category as determined by mass spectrometry (MS) and subsequent western blotting (WB) is indicated. D) STAG2 and WAPAL immunopurified from interphase cells and subsequently incubated with recombinant Plk1, ATP and 1  $\mu$ M of BI2536 as indicated were separated by SDS-PAGE and transferred to a membrane for subsequent immunoblotting using two different phospho-specific antibodies (pSTAG2\_S1224 and pWAPAL\_S465). (E) Shows cells grown on coverslips and treated or not with 100 nM of BI2536 for 30 min prior to fixation and staining with the pSTAG2\_S1224 phospho-specific antibody (pSTAG2), STAG2 antibody, H3S10ph antibody and DAPI.

### 2.2.6.4 Figure 2.2-4

Summary of all analysed baits and prey, the number of detected phosphorylation sites and potential Plk1 and Aurora B kinase substrates:

A) Summary table of all analysed baits and prey, number of phospho-sites per cell cycle stage (I – interphase, I/M – interphase and mitosis, M – only present in mitosis) and number of hesperadin-sensitive (H-sens) and Plk1 inhibitor-sensitive (B-sens) sites.

List of detected potential novel Plk1 (B) and Aurora B kinase (C) substrates. The number of inhibitor-sensitive sites (BI-site and Hes-sites), total sites in mitosis and mitosis-specific sites is given.

#### 2.2.6.5 Supplemental figure 2.2-1

BI4834 is structurally and functionally related to BI2536

A) BI4834 is an ATP analogue, very similar in structure to BI2536 (Lenart et al., 2007; Steegmaier et al., 2007).

B) Addition of 250 nM BI4834 to cells released from a single (24h) thymidine arrest arrests cells in prometaphase with a monopolar spindle (DNA stained with DAPI (blue), Tubulin stained with  $\alpha$ -TUBA1B antibody (red)).

C) The same experiment as described in B) was performed with different concentrations of BI4834, the mitotic phases were scored and compared to treatment with 100 nM BI2536.

D) Cells were treated as in C, fixed and stained with TUBG1 antibody and the ratio of centrosomal to cytoplasmic TUBG1 was calculated. A representative image of cells treated with 250 nM BI4834 is shown.

E) Cells were treated as in B but fixed and stained with pAPC6 antibody (Kraft et al., 2003).

F) To test the effect of BI4834 on cohesin dissociation from chromosomes in early mitosis, cells stably expressing MYC-tagged cohesin were treated as in A, cytopspun onto slides, fixed and stained with CREST serum,  $\alpha$ -SMC2 and  $\alpha$ -MYC antibodies.

F) To monitor the effect of BI4834 and BI2536 on BUB1B phosphorylation, cells were treated as in A, harvested ten h after thymidin release, whole cell extracts were prepared and analysed by SDS-PAGE and western blotting with the indicated antibodies. Phosphorylated (P) and no-phosphorylated (NP) forms of BUB1B and CDC25C are marked.

#### 2.2.6.6 Supplemental figure 2.2-2

Phospho-specific antibodies against various interphase, mitosis-specific and inhibitor-sensitive phosphorylation sites. Quantification of all BUB1B phosphorylation sites.

Phospho-specific polyclonal antibodies raised against different phosphopeptides listed in Figure 2.2-3 were tested on immunopurified protein (IP) using the indicated antibodies or directly on extracts (XT) obtained from log-phase cells (L), hydroxyurea-arrested S-phase cells (HU), noc-arrested cells (N) and noc-arrested cells treated for two h with either BI4834 (NB) or a combination of Hesperadin and MG132 (NHM). Antibodies against sites determined by MS to be present in interphase and mitosis (A), to be mitosis-specific and sensitive to the PLK1 inhibitor (B) and to be mitosis-specific and sensitive to Hesperadin treatment (C) are shown. The pRAD21\_S175 antibody was

## 2.2 Phosphorylation site mapping manuscript

tested on protein extracts from cells synchronised with a double thymidine arrest release and harvested either four h after release (G2), ten h after release by mitotic shake off (SO), ten h after release with the last three h in nocodazole (N), with last three h nocodazole and last two h either BI4834 (NB) or Hesperadin/MG132 (NHM). The cell cycle stage was controlled using antibodies against CCNB1, H3S10ph, H3 and CDC27 as indicated.

D) Based on the calculated fold changes for Bub1b (Figure 2.2-2 A), relative phosphopeptide levels of each identified phosphorylation site in Bub1b were calculated for all digests in which the phosphorylation site was detected (trypsin (yellow), chymotrypsin (orange) and subtilisin (brown)).

### **2.2.6.7 Supplemental table 2.2-1**

List of detected potential known Plk1 (B) and Aurora B kinase (C) substrates. The number of inhibitor-sensitive sites (BI-site and Hes-sites, respectively) total sites in mitosis and mitosis-specific sites is given.

### **2.2.6.8 Supplemental table 2.2-2 (see appendix 5.5)**

All identified annotated phosphorylation sites and their classification. Since this table is very long it is in the appendix.



2.2.7 Figures

Figure 2.2-1

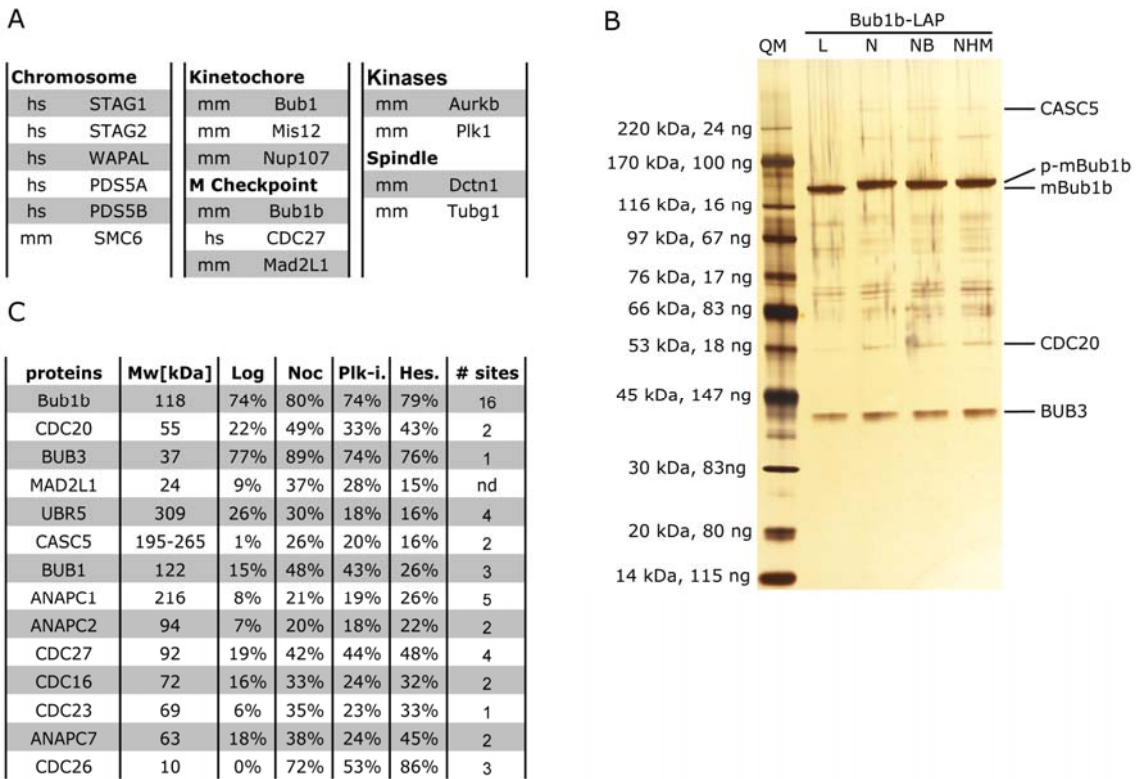


Figure 2.2-2

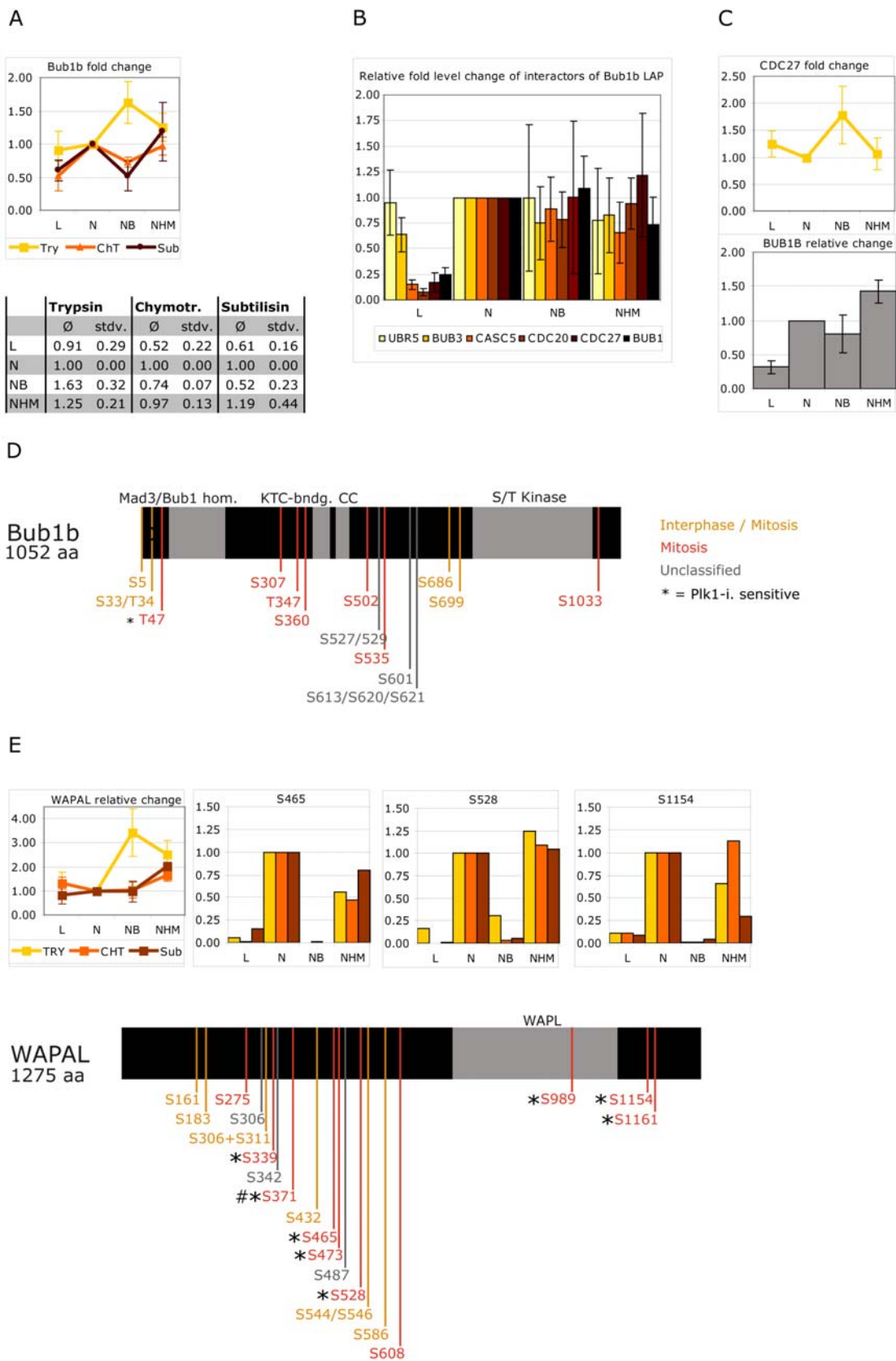
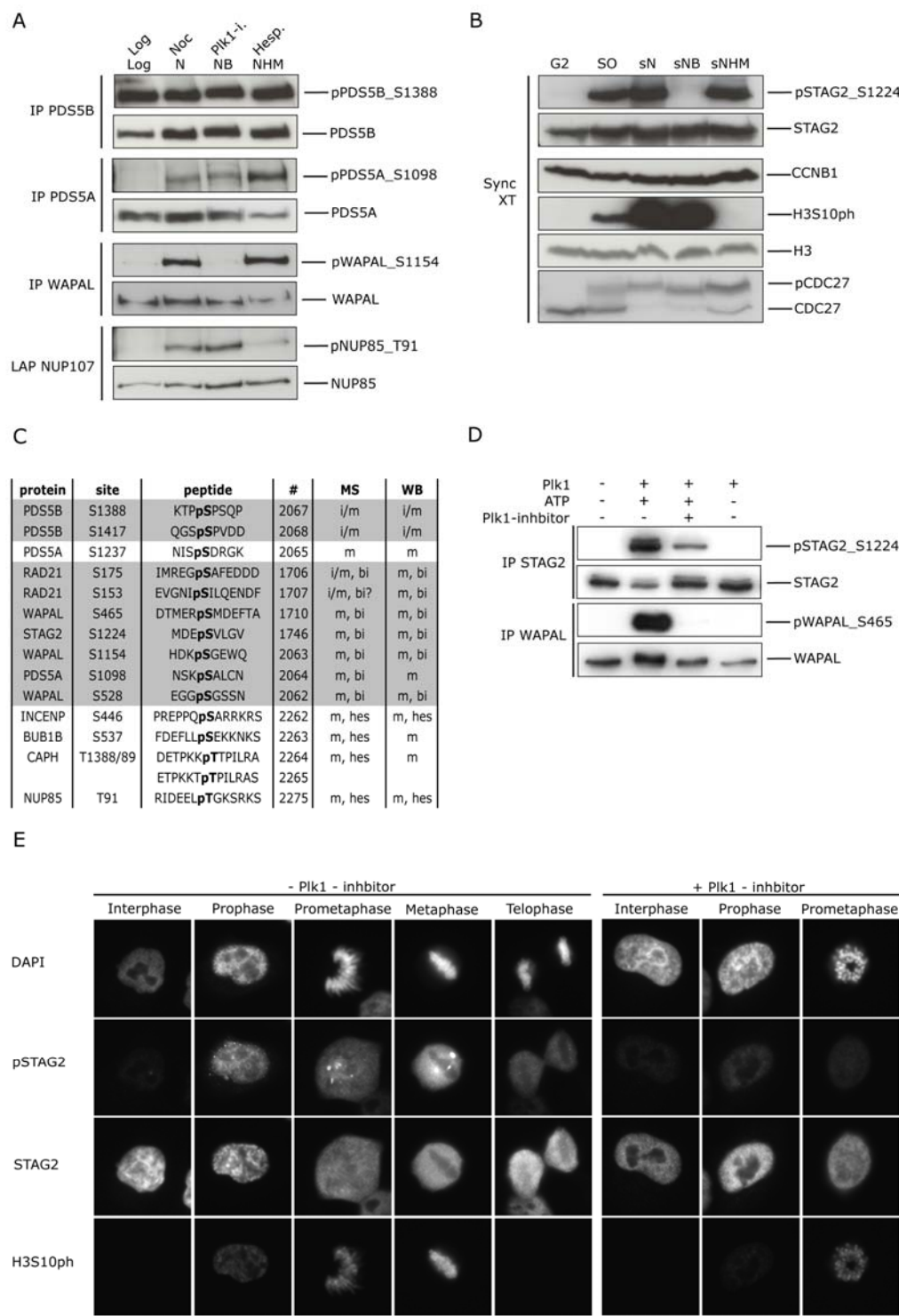


Figure 2.2-3



## 2.2 Phosphorylation site mapping manuscript

**Figure 2.2-4**

**A**

Data set summary

sp	bait	prey	total sites	I	I/M	M	H-sens	B-sens	H+B-sens
mm	Aurkb	5	48	1	4	27	3	4	10
mm	Bub1	9	37	0	9	20	1	5	4
mm	Bub1b	7	47	1	6	15	2	2	0
hs	CDC27	19	106	2	39	29	0	6	2
mm	Dctn1	3	4	0	3	0	0	0	0
mm	Mad2L1	5	28	1	7	12	3	4	1
mm	Mis12	14	36	7	12	0	1	0	0
mm	Nup107	8	49	1	9	28	5	3	5
hs	PDS5A	6	16	0	1	15	0	1	0
hs	PDS5B	5	13	0	11	3	0	0	0
mm	Plk1	4	6	0	1	1	0	1	0
mm	SMC6	6	19	1	8	4	2	1	1
hs	STAG1	4	4	0	0	3	0	0	0
hs	STAG2	7	21	0	0	15	0	4	0
mm	Tubg1	6	20	0	6	7	3	3	1
hs	WAPAL	7	16	1	9	8	0	7	0
<b>total</b>	<b>16</b>	<b>115</b>	<b>470</b>	<b>15</b>	<b>125</b>	<b>187</b>	<b>20</b>	<b>41</b>	<b>24</b>

**B**

Potential novel PLK1 substrates

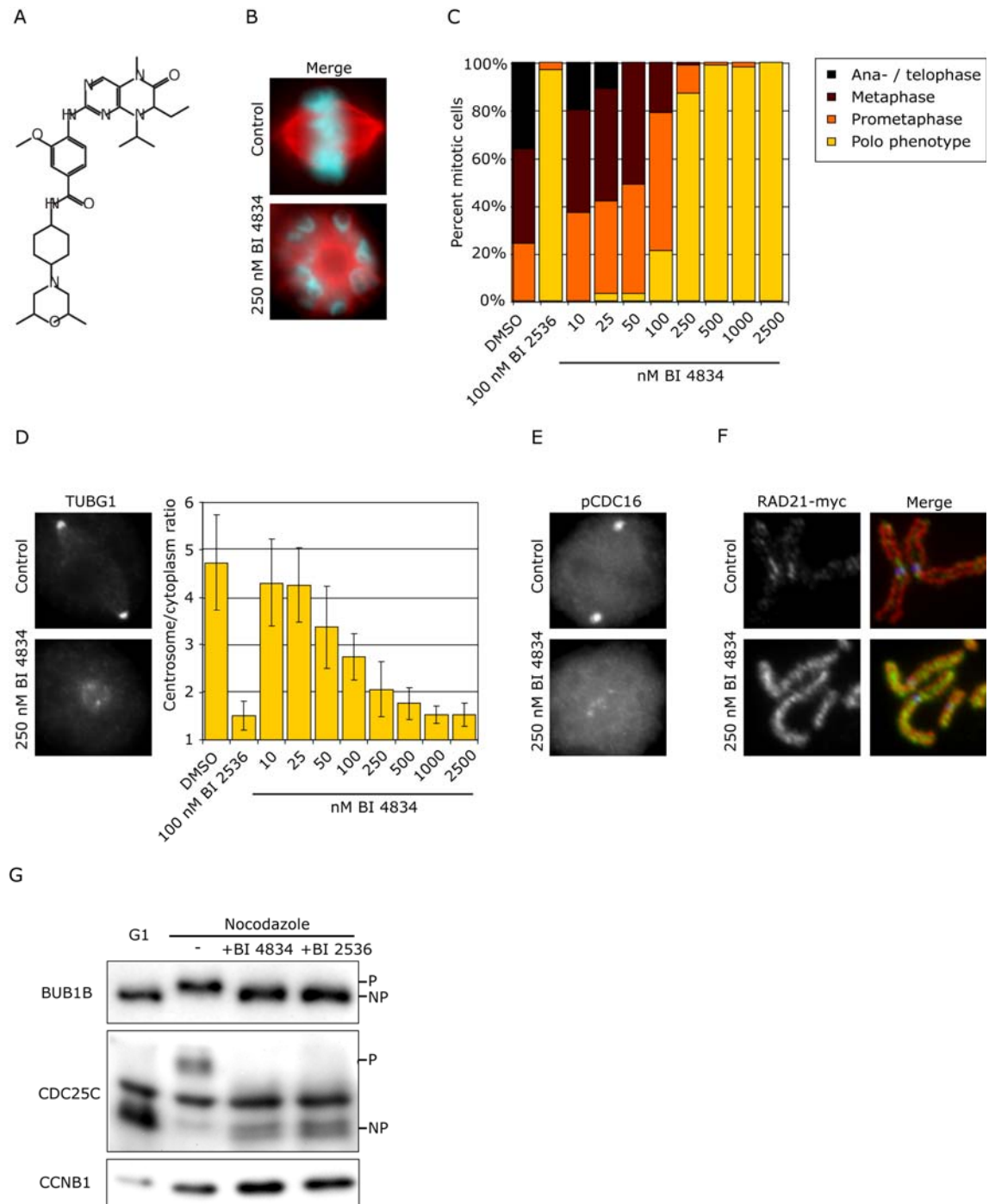
sp	prey	BI-sites	M sites	M-spec	Site(s)
hs	ANAPC5	1	5	4	S221
hs	ANAPC6	1	3	1	S112
mm	Bub3	2	3	3	S211, S325
hs	CDC26	1	7	2	S52/S3
hs	Cdc37	1	1	1	S377
hs	INCENP	3	35	19	S828, S831, T832
hs	MAD1L1	1	8	5	S490
mm	Mad2L1	2	3	2	S72, S148/S150
hs	MAD2L1BP	1	3	1	S78
hs	NSMCE4A	1	4	1	T58
hs	NUP85	1	2	2	S224
hs	NUP98	2	16	9	S949, T983
hs	PDS5B	1	16	4	T1301
hs	RACGAP1	1	1	1	S203
mm	Tubg1	1	3	1	S131
hs	TUBGCP6	1	7	4	S242, T963/T964
hs	WAPAL	7	19	9	S339, S465, T473, S528, S989, S1154, S1161

**C**

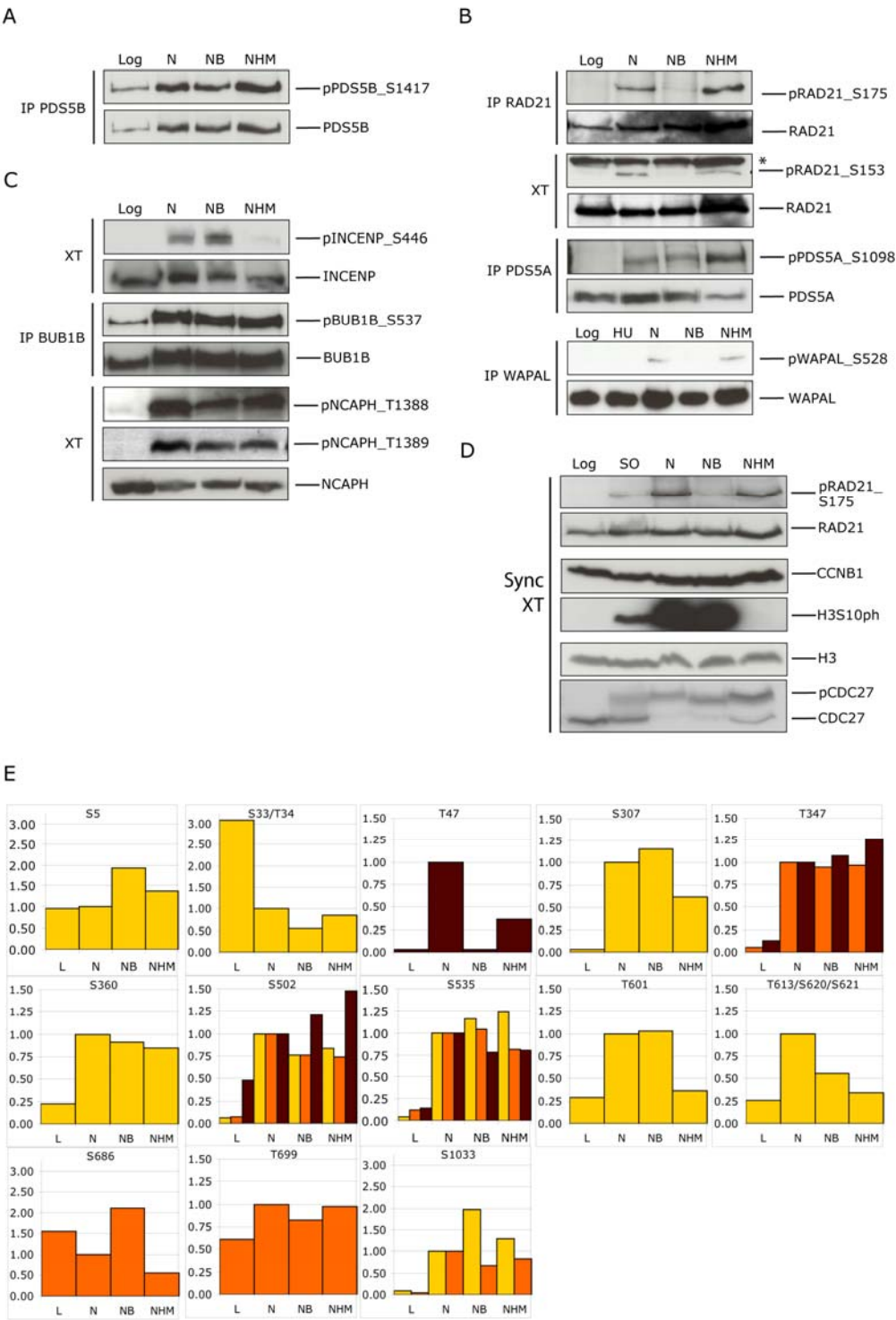
Potential novel AURKB substrates

sp	prey	Hes-sites	M sites	M-spec	Site(s)
hs	BUB1	1	14	8	T452
hs	BUB1B	1	11	4	T354
hs	CASC5	1	10	5	T487
hs	CDC26	1	7	2	S42, S52
hs	DSN1	1	10	0	T38/S39/S41
hs	MAD1L1	1	8	5	S547
mm	Nup107	2	14	10	S27, T91/S93/S94/Y96/S101
hs	NUP133	1	10	5	T63
hs	NUP85	1	2	2	T91
hs	NUP98	2	16	9	S1001, S1448
hs	PDS5A	1	10	9	S1305
hs	PDS5B	2	16	4	S1220, S1416/S1417
hs	RAD21	1	9	7	S46
hs	SMC5	2	5	2	S12, S979/S980
mm	Tubg1	1	3	1	S284
hs	TUBGCP5	1	2	1	S610/T611
hs	TUBGCP6	1	7	4	S655/S57
hs	UBR5	1	5	2	S110

Supplemental figure 2.2-1



Supplemental figure 2.2-2



Supplemental table 2.2-1

**A**

Known detected PLK1 substrates

sp	prey	BI-sites	M sites	M-spec	Site(s)	ID meth.	Site(s)	Ref.
hs	ANAPC1	1	26	6	S351	IVK, MS	S520, S547, S605	Kraft et al.
mm	Bub1	4	14	8	S188/92,S320,S399,S472	IVK	nd	Qi W and Yu H
mm	Bub1b	1	11	6	T47	MS / pAb	S676	Elowe et al.
hs	CDC27	1	22	15	T372	IVK, MS	T220, S427, S434, S435	Kraft et al.
mm	Kif23	1	1	1	S683/S685	IVK	S911/912 (by homology)	Liu et al.
mm	Plk1	1	2	1	T210/214,S331	IVK, MS	S335 (xPlk1)	Kelm et al.
hs	RAD21	4	9	7	S134/S138,S153,S175,S545	IVK	nd	Sumara et al.
hs	STAG2	2	8	7	S1091,S1219	IVK	nd	Sumara et al.

**B**

Known detected AURKB substrates

sp	prey	BI-sites	M sites	M-spec	Site(s)	ID meth.	Site(s)	Ref.
mm	AURKB	2	4	4	S232, T237	IVK	T237 (XI)	Yasui et al.
hs	INCENP	4	35	19	S72, S208, S213, S446	IVK, MS	T897, 898, S899	Honda et al.

Supplemental table 2.2-2

Since this table is very long it is in the appendix (5.5).

### 2.3 Generation and characterisation of cell lines stably expressing MYC-tagged versions of PDS5A and PDS5B

The cohesin complex interaction with PDS5 proteins is conserved from yeast to mammals. Studies in yeast have placed PDS5 in the cohesion establishment/maintenance pathway (Hartman et al., 2000; Panizza et al., 2000) but their function in yeast as well as in human, which have two orthologs designated PDS5A and PDS5B, is not well understood (Losada et al., 2005). A recent study identifying another cohesin interactor and regulator called WAPAL has shown that PDS5A but not PDS5B interacts with WAPAL (Gandhi et al., 2006; Kueng et al., 2006), indicating that PDS5A and B might have distinct roles within the cohesin complex. To further investigate this question I wanted to generate MYC-tagged version of PDS5A and PDS5B inducibly expressed in HeLa cells.

The vertebrate orthologs of yeast Pds5 (PDS5A, PDS5B) are very similar (Losada et al., 2005). The 1140 amino acid N-terminal domain is 72% identical in sequence and contains a number of HEAT repeats just like the yeast Pds5b (Losada et al., 2005; Panizza et al., 2000). To better define the number of these repeats and their position within the sequence we used profile based searches employing hidden Markov models (HMMs) (HMMER, Eddy, S., unpublished data). The REP and Pfam databases provide specific repeat definitions, which can be used for the identification of HEAT elements in a query sequence (Andrade et al., 2000).

The analysis showed that PDS5A contains 18 HEAT motifs within amino acids 69 to 756 followed by two Armadillo repeats (ARM) from amino acids 829 to 1033 and an unstructured C-terminus (Table 5.2-1). PDS5B also contains 18 HEAT repeats from amino acid 58 to 779, a charged C-terminal region from amino acids 1084 to 1447 including a potential DNA binding AT-hook domain (Table 5.2-2). HEAT and ARM repeats are a very common sequence motif present in many proteins and involved in mediating protein interactions (Andrade et al., 2001), suggesting that the role of PDS5A and PDS5B in the cohesin complex might be to mediate inter complex protein interactions.

#### 2.3.1 Cloning of PDS5A and PDS5B constructs into a MYC-Tet-On expression vector

To generate a cDNA of PDS5A and PDS5B that contains a MYC array on the N- or C-terminus, that is resistant to siRNA knockdown and whose expression is inducible with doxycyclin I pursued the following cloning strategy (Table 4.5-1: Primers used for amplification and Quickchange mutagenesis.). A sequence containing (from 5' – 3') start codon, kozak sequence, twelve repeats of the MYC-tag coding sequence followed by the coding sequence for a five glycine linker and the restriction site for *NarI* was cloned into



the pTRE2hyg vector (TetOn System, Clontech) via *Mlu*I and *Nhe*I resulting in plasmid 1132. A sequence containing (from 5' – 3') restriction sites for *Mlu*I, *Nar*I and *Not*I; the coding sequence for a five glycine linker, nine repeats of the MYC-tag coding sequence and a stop codon was cloned into the pTRE2hyg vector via *Mlu*I and *Sa*I resulting in plasmid 1131. The coding sequence for PDS5A was previously cloned into the pBluescript expression vector (plasmid 124, gift from E. Roitinger). Plasmid 124 was used to generate an siRNA resistant construct by introducing six silent point mutation within the target site of siRNA 32 (Figure 2.3-1) with the Quickchange system. The resulting plasmid 1137 was used to amplify PDS5A for cloning it into plasmid 1131 via *Nar*I and *Not*I resulting in plasmid 1136. The plasmid 124 coding sequence contained an insertion of two T after base 739 (as counted from start codon). The insertion was removed in plasmid 1136 using the Quickchange system (Stratagene). This plasmid thus contains the siRNA resistant sequence for expressing PDS5A with a C-terminal 9x MYC-tag in mammalian cells. The coding sequence of PDS5B is fully included in the KIAA0979 cDNA (Nagase et al., 1999) which was obtained from the Kazusa consortium and entered into the cDNA database as plasmid 1138. To generate an siRNA resistant cDNA six silent point mutations were introduced in the target sequence of siRNA 34 (Figure 2.3-1) using the Quickchange system. The resulting plasmid 1139 was used to amplify the siRNA resistant cDNA of KIAA0979 for cloning into plasmid 1132 via *Nar*I and *Not*I resulting in plasmid 1133. This plasmid thus contains the siRNA resistant sequence for expressing PDS5B with an N-terminal 12x MYC-tag in mammalian cells.

Following a similar strategy plasmids with N-terminally tagged 12x MYC PDS5A (#1135) and C-terminally tagged PDS5B 9x MYC (#1134) were also generated.

A



siRNA resistance    wt    554 - T G C A C A T G C T A G A T T T G A - 571  
                          mut    554 - T G C A T A T G T T G G A C C T A A - 571

B



siRNA resistance    wt    464 - C C C A G C T A T A C A G A A C C T - 482  
                          mut    464 - C G C A A T T G T A T C G A A C C T - 482

## 2.3 PDS5A/PDS5B cell lines

### Figure 2.3-1

Scheme of PDS5A-MYC and MYC-PDS5B fusion protein including their siRNA resistant sites on the corresponding cDNA sequence.

A) PDS5A contains 17 HEAT repeats, one HEAT or ARM repeat and two ARM repeats in the region from amino acid 69 to 1033. Some repeat boundaries could not be well defined (see supplement x for details). A 9x MYC array was fused with a linker to the C-terminus of PDS5A. At the target sequence of siRNA #32 (bp 554 – 571) six silent mutations were introduced to render the resulting mRNA siRNA resistant.

B) PDS5B contains 17 HEAT repeats and one HEAT or ARM repeat (amino acids 58 – 779) as well as a charged C-terminus (amino acids 1084 – 1447). A 12x MYC array was fused with a linker to the N-terminus of PDS5B. At the target sequence of siRNA #34 (bp 464 – 482) six silent mutations were introduced to render the resulting mRNA siRNA resistant.

### 2.3.2 Generation of stable doxycyclin-induceable HeLa cell lines expressing PDS5A-MYC and MYC-PDS5B

To obtain HeLa cell lines that stably express the inducible, MYC-tagged constructs of PDS5A and PDS5B generated in 2.3.1, I largely followed the protocol suggested by Clontech, the supplier of the TetOn system. The plasmids 1133, 1134, 1135 and 1136 were amplified in *E. Coli* and purified using the Maxi Prep kit (Qiagen). HeLa cells were grown to about 40% confluency on a 10 cm dish ( $4 \times 10^6$  cells) and transfected with 4 µg of DNA using the Lipofectamin PLUS reagent (Invitrogen). Two days after transfection cells were split 1:40 to 1:80 into selection medium containing 400 µg hygromycin/ml. Most of the cells died within one day after addition of selection medium, colonies started appearing eleven days after transfection. The colonies were picked two weeks after transfection when they were sufficiently dense and seeded onto a 12-well plate.

To screen the single colonies for expression level and localisation, cells were split either on to 8-well Labtek chambers for immunofluorescence or into another 12-well plate for western blot analysis. Expression was induced for two days using 1 µg/µl doxycycline and the hygromycin concentration was lowered to 100 µg/ml. Cells on Labtek chambers were PFA-fixed, stained for DNA, MYC and the cohesin subunit STAG2. Cells on 12-well plates were washed, trypsinised, resuspended in 4x SDS-PAGE buffer, sonicated and analysed by SDS-PAGE separation and western blotting using MYC and STAG2 antibodies. In total, 30 clonal cell lines were screened +/- doxycycline which yielded a number of cell lines with expression levels similar to the endogenous gene, little expression in the uninduced cells and with nuclear localisation during interphase but cytoplasmic, non-chromatin localisation during mitosis (see Table 2.3-1). No clones for C-terminally tagged PDS5B were obtained while there were some clones for N-terminally tagged PDS5B. The N-terminally tagged PDS5A clones localised correctly but were not as homogenous as the C-terminally tagged PDS5A clones. Since the

expression level variation within each cell line was still quite high, some clones were split again onto selection medium for another round of selection, colony picking and screening. This resulted in four N-terminal 12x MYC PDS5B clones and three C-terminal 9x MYC PDS5A clones. Clones 1133\_6\_13, 1133\_6\_22 for PDS5B and clone 1136\_21\_8 showed the most homogenous expression and their expression levels were similar to endogenous expression (data not shown). These clones were then further characterised.

**Table 2.3-1: PDS5A and PDS5B MYC-tagged cell lines**

<b>Cell clone</b> <i>1st selection</i>	<b>Gene</b>	<b>Tag</b>
1133_4	PDS5B	Nterm 12x MYC
1133_6	PDS5B	Nterm 12x MYC
1133_10	PDS5B	Nterm 12x MYC
1135_18	PDS5A	Nterm 12x MYC
1135_8	PDS5A	Nterm 12x MYC
1136_4	PDS5A	Cterm 9x MYC
1136_16	PDS5A	Cterm 9x MYC
1136_20	PDS5A	Cterm 9x MYC
1136_21	PDS5A	Cterm 9x MYC
<i>2nd selection</i>		
1133_4_14	PDS5B	Nterm 12x MYC
1133_6_10	PDS5B	Nterm 12x MYC
1133_6_13	PDS5B	Nterm 12x MYC
1133_6_19	PDS5B	Nterm 12x MYC
1133_6_22	PDS5B	Nterm 12x MYC
1136_21_8	PDS5A	Cterm 9x MYC
1136_21_9	PDS5A	Cterm 9x MYC
1136_16_12	PDS5A	Cterm 9x MYC

### **2.3.3 Characterisation of one stable PDS5A-MYC cell line (1136\_21\_8) and two stable MYC-PDS5B cell lines (1133\_6\_13/1133\_6\_22)**

Initial experiments using different doxycyclin concentrations (0.2 µg/ml – 2 µg/ml) for 48 or 72 h to induce PDS5A-MYC or MYC-PDS5B expression were carried out to determine the doxycyclin concentration that lead to a near to endogenous expression level. Using 1 µg/ml doxycyclin for 48 or 72 h gave the best results (data not shown) and was thus used in all subsequent experiments.

To test whether the generated tagged proteins are resistant to siRNA depletion the cell lines 1136\_21\_8, 1133\_6\_13 and 1133\_6\_22 were transfected or not with siRNA specific for either PDS5A or PDS5B and also treated or not with doxycyclin to induce exogenous protein expression. Two days after transfection and induction, cells were harvested, extracted, separated on SDS-PAGE and transferred to a membrane. Membranes were probed with PDS5B or PDS5A antibodies to compare expression and extent of depletion between wild type and PDS5B cell lines (Figure 2.3-2). Myc-PDS5B expression in the line 1133\_6\_13 is very similar to endogenous levels when doxycycline is

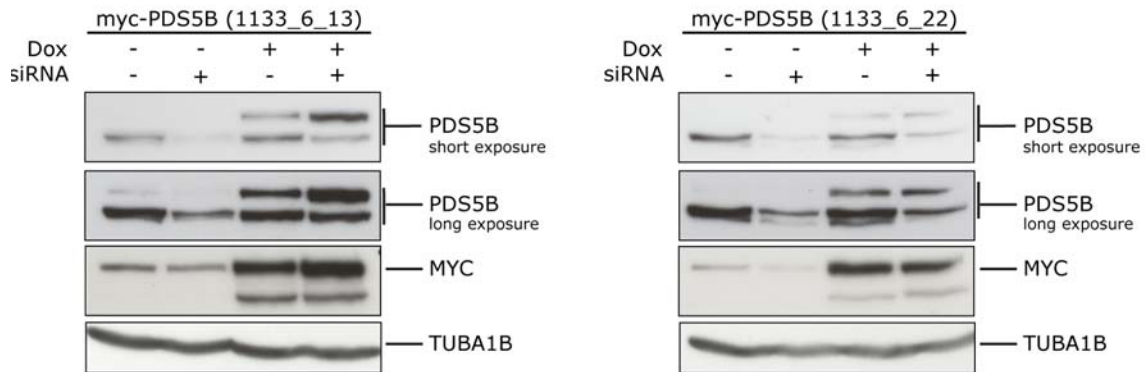
### 2.3 PDS5A/PDS5B cell lines

added but almost undetectable in untreated cells. Weak expression is detectable using the MYC antibody since the 12x MYC epitope strongly amplifies the signal. Importantly, the exogenous protein levels are not reduced upon siRNA transfection but rather slightly increased; indicating that the MYC-PDS5B construct is indeed resistant to the siRNA which reduces the endogenous protein levels to less than 50%. The MYC antibody detects a faster migrating band in the + doxycyclin sample which does not match the endogenous PDS5B band size and thus might be a truncated version of PDS5B that is being expressed.

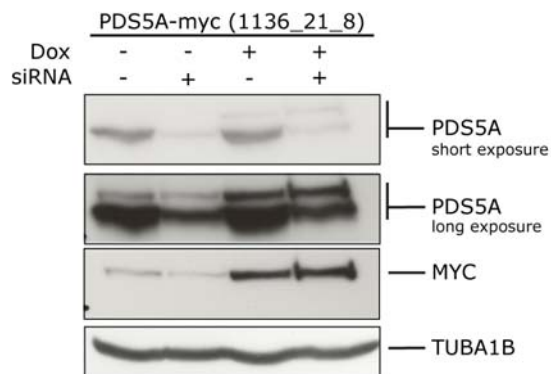
Myc-PDS5B expression in the 1133\_6\_22 line is less than half the level of wild type cells upon doxycyclin induction but not detectable in control cells. However, weak expression is detectable using the MYC antibody. The siRNA depletion of endogenous protein reduces endogenous protein levels to less than 50% but did not affect the levels of MYC-PDS5B. Similar to the 1133\_6\_13 cell line the MYC antibody detects a faster migrating band in the + doxycyclin sample which does not match the endogenous PDS5B band size. This might also be a truncated version of PDS5B that is being expressed.

The 1136\_21\_8 cell line expresses PDS5A-MYC at much lower levels than the endogenous protein upon doxycyclin addition. The background expression level in uninduced cells is only about 50% lower than the induced levels, indicating that the expression is quite leaky. Transfection of these cells with siRNA specific for PDS5A leads to a reduction of endogenous PDS5A levels while PDS5A-MYC levels do not change, confirming that the PDS5A-MYC construct is resistant to the PDS5A siRNA.

A



B

**Figure 2.3-2**

PDS5A-MYC and MYC-PDS5B fusion proteins are expressed at near endogenous levels after doxycyclin addition and are resistant to siRNA silencing.

A) Cell lines stably expressing MYC-PDS5B (1133\_6\_13 and 1133\_6\_22) were transfected with siRNA directed against endogenous PDS5B or water, 1 mg/ml doxycyclin was added or not and protein extracts were prepared 48 h later (-> check methods). Extract supernatants were separated by SDS-PAGE, transferred to membranes and probed with the indicated antibodies. Two different exposure times for the PDS5B signal are displayed.

B) A Cell line stably expressing PDS5A-MYC (1136\_21\_8) was transfected with siRNA directed against endogenous PDS5A or water, 1 mg/ml doxycyclin was added or not and protein extracts were prepared 48 h later. Extract supernatants were separated by SDS-PAGE, transferred to membranes and probed with the indicated antibodies. Two different exposure times for the PDS5A signal are displayed.

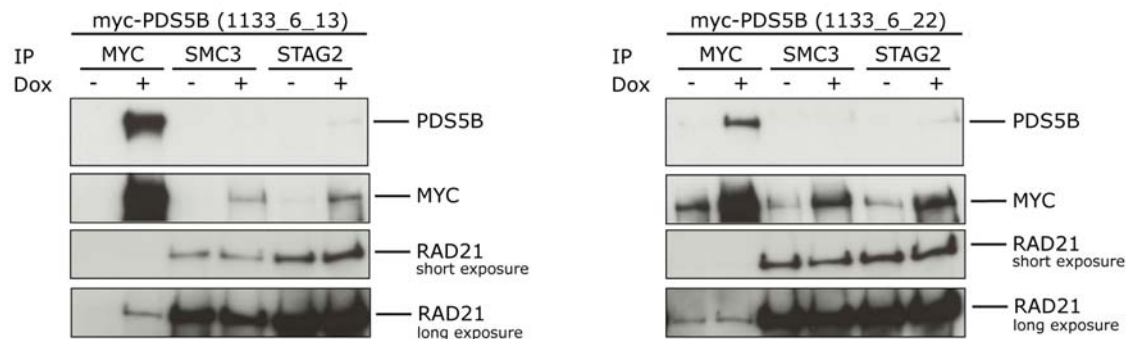
To test the functionality of PDS5A and PDS5B I analysed whether exogenous PDS5A and PDS5B can integrate into the cohesin complex. Myc-PDS5B cell lines and PDS5A-MYC cell lines were grown for 48 h in the presence of absence of doxycyclin, protein extracts prepared and incubated with antibodies crosslinked to Affiprep beads directed against either the MYC-tag (MYC) or the cohesin subunits SMC3 or STAG2. Immunoprecipitated proteins were eluted with glycine, separated by SDS-PAGE, transferred to membranes

### 2.3 PDS5A/PDS5B cell lines

and probed with antibodies against PDS5A or PDS5B, the MYC-tag or RAD21 (Figure 2.3-3). Myc-PDS5B can be immunoprecipitated from both cell lines (1133\_6\_13 and 1133\_6\_2) using the MYC-antibody and also copurifies RAD21. SMC3 and STAG2 can both co-IP small amounts of PDS5B that were only detectable using the MYC antibody and, as expected, RAD21. SMC3 and STAG2 can however not IP detectable amounts of endogenous PDS5B which is not consistent with earlier findings (Losada et al., 2005). It is possible that only a small amount of PDS5B interacts with cohesin that, in this case, can only be detected using the MYC antibody against the exogenous MYC-PDS5B. Further characterisation of the MYC-PDS5B cell lines and their complex integration using sucrose gradients might give a clearer answer which fraction of the tagged PDS5B integrates into the cohesin complex as compared to the endogenous PDS5B.

PDS5A-MYC can be immunoprecipitated from the 1136\_21\_8 cell line using the MYC-antibody and also copurifies RAD21 (Figure 2.3-3). SMC3 and STAG2 can both co-IP endogenous and exogenous PDS5A at roughly equal levels from doxycyclin induced cells while no PDS5A-MYC is coimmunoprecipitated from uninduced cells. This indicates that MYC-tagged PDS5A associates with the cohesin complex equally well as the endogenous protein.

A



B

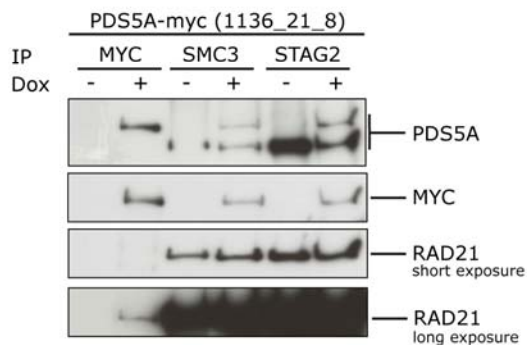


**Figure 2.3-3**

PDS5A-MYC and MYC-PDS5B fusion proteins interact with SMC3, STAG2 and RAD21 subunits of the cohesin complex.

A) Cell lines stably expressing MYC-PDS5B (1133\_6\_13 and 1133\_6\_22) were induced with 1 mg/ml doxycyclin or not and protein extracts were prepared 48 h later. Extracts were incubated with different antibodies (as indicated) crosslinked to Affiprep beads. Glycine eluates of the immunoprecipitate were separated by SDS-PAGE, transferred to a membrane and probed with the indicated antibodies. Two different exposure times for the RAD21 signal are displayed.

B) A Cell line stably expressing PDS5A-MYC (1136\_21\_8) was induced with 1 mg/ml doxycyclin or not and protein extracts were prepared 48 h later. Extracts were incubated with different antibodies (as indicated) crosslinked to Affiprep beads. Glycine eluates of the immunoprecipitate were separated by SDS-PAGE, transferred to a membrane and probed with the indicated antibodies. Two different exposure times for the RAD21 signal are displayed.

Finally I wanted to test the expression level variation as well as the localisation of PDS5A-MYC and MYC-PDS5B within cells. Expression of tagged PDS5A and PDS5B was induced for 48 h using 1 µg/ml doxycyclin and the cells fixed and stained with antibody against the MYC-tag and RAD21. All cell lines show a very similar staining pattern. Only nuclei are stained with very few high expressing cells showing some cytoplasmic staining. The expression level varies from cell to cell in induced cells with the highest expressing cells showing the most intense staining in the nuclear membrane or associated structures (Figure 2.3-4). In high expressing cells it is difficult to discern nucleoli while in medium and low expressing cells the nucleoli are not stained. The nuclear localisation of PDS5A-MYC is consistent with earlier findings (Losada et al., 2000; Sumara et al., 2000). PDS5B localisation has not been previously analysed by immunofluorescence microscopy. However, localisation of PDS5B to the nucleus is consistent with earlier findings that it is chromatin associated in biochemical fractionation experiments (Losada et al., 2005). Further experiments are needed to characterise the localisation of PDS5A and PDS5B during mitosis to answer the question whether these two cohesin interactors also localise to mitotic chromosome centromeres as has been described for RAD21 and STAG2 (Hauf et al., 2005).

### 2.3 PDS5A/PDS5B cell lines

A

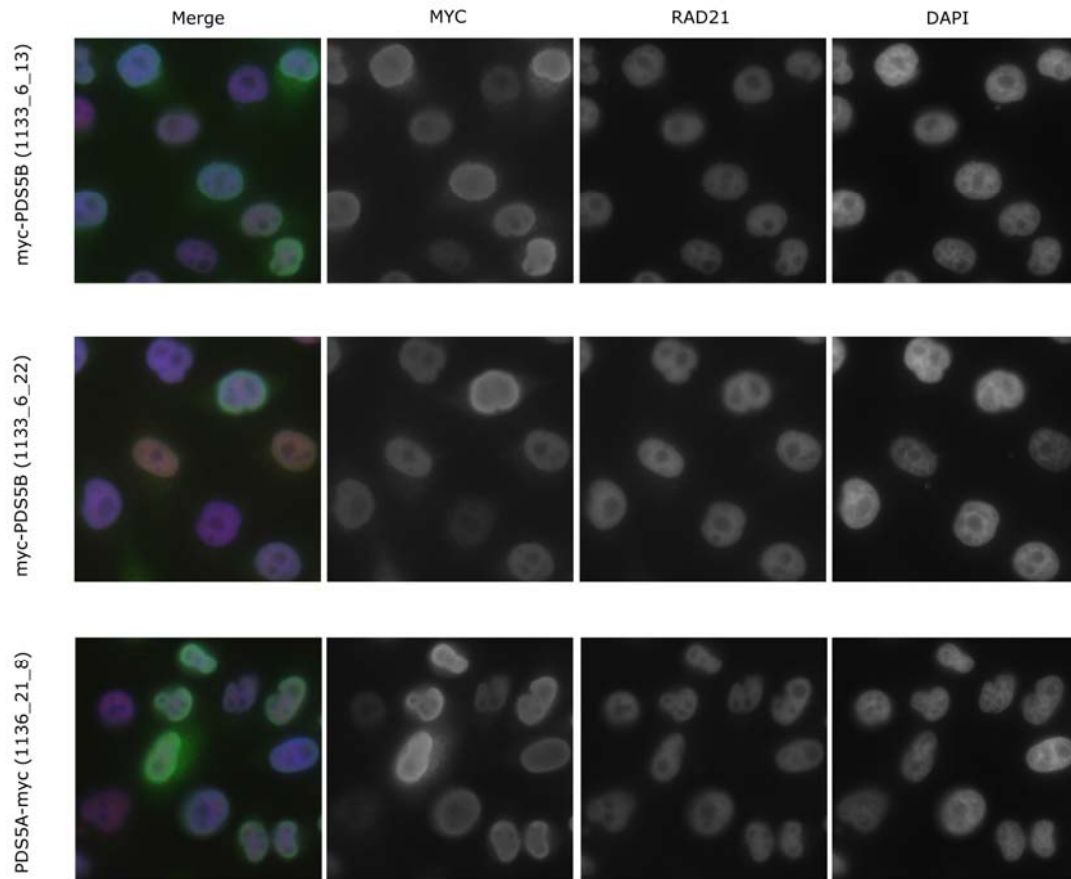


**Figure 2.3-4**

PDS5A-MYC and MYC-PDS5B fusion proteins localise to the nucleus and expression levels vary from cell to cell.

Cell lines stably expressing MYC-PDS5B (1133\_6\_13 and 1133\_6\_22) or PDS5A-MYC (1136\_21\_8) were grown on cover slips, induced with 1  $\mu$ g/ml doxycyclin and fixed with PFA 48 h later. Antibodies against the MYC-tag (MYC, green channel) and RAD21 (red channel) were used and DAPI was applied to visualise the DNA.



## 2.4 Contributions

2.1 Manuscript in preparation: Systematic analysis of mitotic protein complexes using tandem affinity purification and mass spectrometry discovers 71 novel potential mitotic protein complexes

The LAP method adaption was initiated by me and continued by Martina Sykora and James R.A. Hutchins. Generation of LAP-tagged cells lines was performed by Ina Poser and colleagues in the laboratory of Anthony Hyman (Max-Planck-Institute of Cell Biology and Genetics, Dresden, Germany). LAP purifications were mainly done by Martina Sykora and James R.A. Hutchins, some were performed by me. MS-analysis and database searching was done by Ines Steinmacher, Christoph Stingl and Otto Hudecz (IMP/IMBA Protein Chemistry Facility). Primary data analysis was performed by Martina Sykora, James R.A. Hutchins and me. The interaction data analysis pipeline was set up by Jean-Karim Hériché in the group of Richard Durbin (Wellcome Trust Sanger Institute, Hinxton CB10 1HH, England) in collaboration with James R.A. Hutchins and me. Data interpretation was done by Martina Sykora, James R.A. Hutchins and me. The validation experiments for the  $\gamma$ -TuRC and the FAM29A complex were performed by Martina Sykora, the validation of the C10orf104/ANAPC16 interaction by LAP-MS was performed by James R.A. Hutchins, the remaining C10orf104/ANAPC16 characterisation was done by Bettina A. Buschhorn and me. The manuscript was written by me (except the main part of the introduction which was written by James R.A. Hutchins) in discussions with Jean-Karim Hériché, James R.A. Hutchins and Jan-Michael Peters.

2.2 Manuscript in preparation: A systematic approach to discover new PLK1 and AURKB substrates finds 17 novel PLK1 and 18 novel AURKB substrates on 99 candidate proteins

The characterisation of BI4834 was done by Peter Lenart. LAP method adaption was as above. LAP and antibody purifications were mainly done by James R.A. Hutchins and me, Aurkb purification was done by Martina Sykora. Data evaluation and analysis was done by Otto Hudecz, James R.A. Hutchins and me. Peptide quantification was done by me. Phospho-peptide antibody generation was initiated by me, peptides were synthesized by Mathias Madalinski and Gabriela Krssakova (IMP/IMBA Protein Chemistry Facility), rabbit immunisation was done at Gramsch Laboratories, Schwabhausen, Germany, all further phospho-antibody experiments were done by me. The manuscript was written by me in discussions with James R.A. Hutchins and Jan-Michael Peters.

2.3 Generation and characterisation of cell lines stably expressing MYC-tagged version of PDS5A and PDS5B

## 2.4 Contributions

All experiments were performed by me. The bioinformatic analysis of PDS5A and PDS5B was performed by Maria Novatchkova.

### 3 Discussion

The discussion sections 3.1 and 3.2 are in addition to the discussion within the manuscripts included in section 2.1 and 2.2, respectively.

#### 3.1 Protein interaction mapping

We aimed to establish a method that would allow large scale analysis of human protein complex composition to systematically identify mitotic protein complexes. Further we wanted to use computational methods to analyse the data generated by this large scale analysis.

We adapted the LAP-protocol (Cheeseman and Desai, 2005) into a fast, robust and clean tandem affinity purification procedure. In combination with very sensitive FT or OT MS we were able to successfully identify 91% of purified baits and a large number of specific interacting proteins. Further computational analysis of the data set identified 75% of the members of a set of known complexes and predicted 70 novel complexes. Preliminary validation experiments confirmed one novel complex and three novel interaction partners of known complexes. The combination of LAP-MS purifications and computational analysis thus enabled us to systematically identify potential mitotic protein complexes.

The main difficulties in protein complex analysis by AP-MS are 1) to separate true from spurious interactions and 2) to define the actual protein complex by separating substoichiometric components, that might be substrates or members of lower abundant complex isoforms, from near stoichiometric complex components (see definition of protein complexes, section 2.1.3.3).

To address the first point it is essential to use a purification procedure that minimises unspecific interactions but conserves less stable interactions, i.e. increases the number of true positives and decreases the number of false negatives, respectively. The tandem affinity purification procedure, originally developed in yeast (Rigaut et al., 1999), has proven in many studies to be very successful in avoiding unspecific interactions. Even though some high abundant proteins still copurify in tandem procedures and some less stable interactions might be lost in tandem purifications in comparison to single step purifications, tandem affinity purification has become the method of choice for many large scale complex analysis projects (Gingras et al., 2007). Two approaches have been used to remove unspecific interactors from tandem affinity purifications. Proteins present above a certain percent threshold of all identified prey are removed based on the assumption that most proteins will only interact with a small number of other proteins (Krogan et al., 2006 and this study). Alternatively, the expected frequency of a protein in a dataset is calculated based on the number of prey it purifies when it is a

bait. Proteins present above their expected frequency are considered as contaminants (Gavin et al., 2006). The second method is only applicable to genome scale interaction studies since all potential contaminants need to be tagged to calculate their expected frequency.

The second point is much more difficult to address. The definition of a protein complex is rather arbitrary; we have chosen a simple definition which can be fulfilled by AP-MS data alone (see section 2.1.3.3). With an AP-MS approach as taken in this study, a set of interacting proteins can be defined. The relationship between these proteins, however, remains unknown. It is likely that some or all of the proteins identified by reciprocal AP-MS experiments form a very stable complex which represents a structural and functional unit. This is the case for the APC/C which we purified with a number of its subunits used as baits and which has been characterised structurally and functionally in some detail (Peters, 2006). However, some of the interacting proteins identified by AP-MS might also be substoichiometric interactors. This is exemplified by NEK2 which copurifies with the APC/C, but which has been identified as a substrate and not as a complex member of APC/C (Peters, 2006). At the same time we also find CDC20 and FZR1 (also known as Cdh1) in purifications of APC/C. However, CDC20 and FZR1 are APC/C coactivators that bind exclusive of each other to the complex. To resolve this problem and to separate stoichiometric interactors from substoichiometric interactors cell extracts can be analysed with density gradient centrifugation. All close to stoichiometric interactors should largely cosediment while substoichiometric interactors would only cosediment to a small fraction with the main peak.

This established method and the data set of potential mitotic protein interactions opens two perspectives: the further extension of the dataset and more detailed characterisation of detected protein complexes as outlined below.

The dataset generated within this study is focused on a relatively small number of proteins involved in mitosis. This concentrated approach was necessary to obtain a certain overlap between purified complexes that would allow the higher confidence prediction of novel complexes. Ultimately, to understand mitotic regulation, the aim should be to obtain a complete interaction map of all protein complexes involved in mitosis. To define a set of "mitotic protein complexes" the correlation of protein interaction data and functional data is necessary. As part of the MitoCheck project, the laboratory of Jan Ellenberg (EMBL, Heidelberg, Germany) has conducted a genome wide, live cell imaging based siRNA screen to identify genes required for mitosis (Neumann et al., in preparation). This screen has identified about 1200 genes by their specific mitotic phenotype. Ideally all of these hits should be analysed for their interaction partners. So far, only 67 of the ca. 1200 hits have been purified as baits and another 88 have been detected as prey. Since the analysis of the first 175 baits took

slightly less than two years, the analysis of the remaining screen hits (ca. 1100) might take quite a long time. It would thus be necessary to improve the throughput of the purification procedure considerably before extending the protein interaction mapping to the whole set of mitotic screen hits. As an alternative, a reiterative purification and tagging cycle might cover all siRNA screen hits with less than 1200 baits since it is likely that the 1200 screen hits are part of less than 1200 distinct protein complexes (in the current set 65% of siRNA screen hits hit predicted clusters and small connected components twice or more often).

More detailed characterisation of predicted novel complexes and protein interaction partners has already been initiated. Two new potential interaction partners of the  $\gamma$ -TuRC and five members of the predicted novel complex FAM29A were validated by reciprocal tagging and purification. The novel potential APCC/C subunit C10orf104/APC16 was validated by reciprocal LAP-purification as well as antibody purification of the endogenous protein. In addition, further biochemical characterisation confirmed ANAPC16 as an APC/C subunit and initial functional characterisation suggest ANAPC16 might be important for APC/C's function in S- or G2-phase.

Further validation and characterisation of other potential novel complexes and interaction partners can be carried out. Using the LAP-tagged cell lines, the localisation via the GFP moiety of the LAP-tag can be done in fixed cells or in live cells if the expression levels are high enough (Poser et al., 2008). The complex composition can be further analysed throughout the cell cycle by purifying candidate complexes from cells synchronised at different cell cycle stages. A cell cycle-dependent change of complex composition could be best analysed by using quantitative proteomic approaches as described in the phosphorylation mapping manuscript (section 2.2.3.5) or as outlined in a recent review (Bantscheff et al., 2007).

The use of mouse genes offers the possibility to perform RNAi mediated depletion of the endogenous gene while the transgene remains unaffected by the RNAi reagent (Kittler et al., 2005b). This offers a useful tool to test the functionality of each transgene and also allows testing the effect of mutations or deletions on the functionality. Especially those potential novel complexes that have one or more hits within the MitoCheck siRNA screen (Neumann et al., in preparation) can be tested by using the validated siRNA oligos used in the screen and following the detected phenotype.

A further potential application of the BAC transgene rescue would be to remove the endogenous protein corresponding to the transgene in a large cell population followed by purification of the bait. This would avoid potential competition of transgene and the endogenous copy for interaction partners and thus create a situation closely resembling a knock in situation. The main obstacle for this experiment is the large number of cells

that need to be transfected and the high amount of RNAi reagent. The costly siRNA oligos could be replaced by a self made endoribonuclease prepared so-called esiRNA pool (Kittler et al., 2005a; Yang et al., 2002). Whether efficient esiRNA transfection of large cell pools is possible remains to be seen.

#### **3.2 Phosphorylation site mapping**

We wanted to set up a method that would allow the identification of PLK1 and AURKB substrates in cells using small molecule inhibitors, protein purification and MS.

We detected 470 phosphorylation sites on 99 unique proteins purified with 16 different baits. Out of those 99 proteins, 25 were identified as potential PLK1 substrates (17 were novel) and 18 were identified as potential AURKB substrates (18 were novel). The main improvement of the method we established is that we can map kinase-dependent phosphorylation sites directly in a cellular assay which avoids artefacts that might be introduced in *in vitro* kinase assays commonly used to find kinase substrates. In addition we mainly used the robust tandem affinity purification of LAP-tagged proteins as described in section 2.1 which allows a systematic analysis of a large number of protein complexes involved in mitosis. The drawback is, however, that some of the identified PLK1 or AURKB-dependent phosphorylation sites might not be direct targets of PLK1 or AURKB but rather caused by kinases downstream of PLK1 and AURKB. In addition, we also find a number of phosphorylation sites that are induced by addition of the PLK1 inhibitor or Hesperadin. This might also point to indirect effects which might be caused by blocking inhibitory functions of PLK1 or AURKB.

A very short inhibitor treatment might minimise the extent of indirect effects on other phosphorylation sites. However, there also needs to be sufficient time after kinase inhibition for the phosphorylation sites generated by PLK1 or AURKB to be removed by phosphatases. Initial experiments in which we monitored the phosphorylation of Serine 10 on histone H3 (H3S10ph) at different timepoints after Hesperadin addition indicated that two h of inhibition are required to fully abolish phosphorylation on Serine 10 of histone H3. Whether this rather slow turnover observed for H3S10ph is true for many mitotic phosphorylation sites is not clear. Previous experiments using the BI2536 PLK1 inhibitor showed that addition of BI2536 to cells arrested in metaphase by the proteasome inhibitor MG132 converted from a bipolar spindle to a monopolar spindle within 60 to 120 minutes. This indicates that the activity of PLK1 is not just required for bipolar spindle formation but also for its maintenance. In addition, it indicates that to achieve a full PLK1 phenotype, i.e. monopolar spindles, it takes at least 60 minutes, suggesting that PLK1 phosphorylations presumably required for bipolar spindle maintenance are reversed rather slowly. Using the set of six phospho-specific antibodies detecting PLK1-dependent sites and two phospho-specific antibodies detecting AURKB

phosphorylation sites we can now test the turnover rate of a few phosphorylation sites in mitosis.

We used mainly a qualitative analysis to detect mitosis-specific and kinase- dependent phosphorylation sites. As pointed out in section 2.2.3.4-5, upon inhibitor treatment or in interphase some phosphorylation sites are not diminished to an extent that they are not detectable by MS anymore. Using a semi-quantitative approach we could show that a relative change of phosphorylation levels by 5- to 20-fold can be within the dynamic range of the mass spectrometer (e.g. phosphorylation of S465 on WAPAL, Figure 2.2-2 D) and is sufficient to identify a kinase-dependent phosphorylation site (compare Figure 2.2-3 D). This suggests that we might miss phosphorylation sites in our qualitative analysis since their relative change is within the dynamic range of the mass spectrometer. It will be therefore essential to extend the quantitative analysis performed on the Bub1b and WAPAL phosphorylation sites to all phospho-proteins we detected.

The quantitative analysis of unlabelled peptides in the mass spectrometer has become possible due to the high mass accuracy and sensitivity of the FT and OT mass spectrometers. Most quantitation of MS experiments, especially in large scale proteomics of whole cell extracts or similar complex samples, is often done using isotopic labels (Stable isotope labelling of amino acid in cell culture - SILAC) or isobaric labels (isobaric tag for relative and absolute quantitation - iTRAQ). This allows for several samples being mixed and compared in a single MS run (reviewed in (Bantscheff et al., 2007)). These approaches are more difficult to apply for protein complex purification because of a number of reasons. SILAC allows direct labelling of proteins in the growing cells by supplementing the growth medium with heavy isotope amino acids, usually arginine and lysine (Ong et al., 2002). The advantage of SILAC is that cells can be mixed prior to extract preparation which avoids all possible quantification artefacts due to variable sample preparation. However, SILAC only allows the direct comparison of up to three samples since proteins are labelled with either two of a heavy or one light amino acid by supplementing the cell culture medium. In addition, the high price of SILAC media would make experiment with large amounts of cells very expensive.

The iTRAQ label (Ross et al., 2004) is covalently bound to the proteolytic peptide at the amino-terminus of each peptide and allows comparison of up to eight different samples (Choe et al., 2007). However, the label is only detectable in the MS/MS chromatogram in the low mass range ( $m/z$  113-121) which is not detectable using a standard ion trap instrument with a typical mass range of 400 to 1800  $m/z$ . In addition, since the label is only added during the proteolytic digest of the sample differences in sample variation can not be avoided. Thus, using a label-free quantitation is the only method that allows for potentially unlimited amounts of samples to be compared and does not require the

use of other instrumentation. Differences in sample amounts due to variations during sample preparation as well as run to run variation need to be normalised and will lead to a relatively high standard deviation. The standard deviation can best be assessed by automated comparison and quantification of samples (Mueller et al., 2007). Automated comparison allows many more peptides to be compared and outliers to be identified by statistical methods to keep the standard deviation at a minimum.

#### **3.3 PDS5A and PDS5B cell lines**

To better understand the function of the cohesin interacting proteins PDS5A and PDS5B I wanted to generate cell lines inducibly expressing MYC-tagged PDS5A and PDS5B.

Using the Tet-ON doxycyclin inducible expression system I generated stable cell lines inducibly expressing N-terminally tagged MYC-PDS5A and C-terminally tagged PDS5B-MYC. The tagged exogenous proteins are resistant to siRNA mediated knockdown of the endogenous proteins, incorporate into the cohesin complex and localise to the nucleus just like cohesin. I decided to generate MYC-tagged inducible cDNA constructs instead of the LAP-tagged BAC versions for two reasons. First, we know from previous experiments that to visualise cohesin on centromeres in mitosis it is necessary to use at least an array of nine MYC tags (Waizenegger et al., 2000). This might thus also be the case for PDS5A and PDS5B. Second, stable expression of PDS5A has been tried in the lab previously and showed to be toxic to the cells, we thus needed an inducible system to avoid this problem.

The two PDS5 cell lines thus allow to further study the function of PDS5A and PDS5B in cohesion. In a first experiment one could test the interaction partners of PDS5A and PDS5B by MS and compare them to earlier results obtained with antibodies directed against the endogenous proteins (data not shown). Since both proteins contain the same tag, unspecific interaction partners should be more easily identified.

To further understand the interaction of WAPAL and PDS5A, deletion mutants of MYC-PDS5A could be constructed, inducibly expressed in HeLa cells and purified to identify the binding region of PDS5A to WAPAL. Based on the phosphorylation sites identified on PDS5A (5.5 Phosphorylation manuscript table S2 (all phospho-peptides)) phospho-mutants could also be constructed and the effect of phosphorylation on WAPAL binding could be tested. Once a mutant version of PDS5A has been identified that can not bind WAPAL anymore, the phenotype of this mutant can be tested by depleting the endogenous PDS5A in cell lines expressing the mutant PDS5A. To test whether PDS5A associates with centromeres in mitosis like described for RAD21 (Waizenegger et al., 2000), mitotic cells could be analysed by cytospin and MYC staining.



The role of PDS5B in cohesion is even less understood than that of PDS5A. Sequence analysis showed that the only region that distinguishes PDS5A and PDS5B from each other is the C-terminal unstructured region which is highly charged and contains a potential AT-hook in PDS5B. The AT-hook is a DNA binding domain present in many high mobility group proteins (HMG) that preferentially bind the minor groove of DNA and often interact with transcription factors (Reeves, 2001). Since the AT-hook in PDS5B is the only known DNA binding domain within the cohesin complex one can speculate that PDS5B is needed to connect the cohesin complex to DNA. However, siRNA depletion of PDS5B does not lead to displacement of cohesin from DNA (Losada et al., 2005). By comparing the chromatin association of PDS5B-MYC with a truncated version lacking the AT-hook and the charged C-terminus, it could be tested whether PDS5B binding to chromatin is dependent on this region. In a rescue experiment using wild type or a truncated version of PDS5B-MYC in parallel to siRNA-mediated depletion, the function of the PDS5B C-terminus in cohesion could be tested.

## 4 Materials and methods

### 4.1 Cell culture and siRNA depletion

HeLa cells were grown on Nunc cell culture dishes in DMEM medium supplemented with 10% FCS, 0.2 mM L-glutamine, 100 U/ml penicillin, and 100 µg/ml streptomycin. For TetOn cell lines the medium was supplemented with 100 µg/ml G418 and 200 or 400 µg/ml hygromycin for maintenance or selection, respectively. RNAi depletions were performed as previously described (Hirota et al., 2004) using a preannealed siRNA oligo (Ambion) targeting PDS5A (5'- UGCACAUGCUAGAUUUGAUtt-3' (database ID: 32) or PDS5B (5'-CCCAGCUAUACAGAACCUtt-3' (database ID: 34, Ambion ID: 203071)).

### 4.2 Protein extract preparation and immunoprecipitation

Protein extracts for immunopurifications were prepared using IP-buffer A (20 mM Tris-HCl, pH 7.5; 150 mM NaCl, 5 mM EDTA, 20 mM β-glycerophosphate, 10 mM NaF, 10% glycerol, 0.1% NP-40, 1 mM DTT and protease inhibitor mix (PIM: leupeptin, chymostatin and pepstatin at 10 µg/ml). Equal volumes of cell pellet and buffer were used to resuspend the pellet using a 27G needle and corresponding syringe. Crude cell extracts were centrifuged at 13 200 rpm in a table top centrifuge at 4°C for 15 minutes and the supernatant kept. The concentration was determined using the BRADFORD reagent (Bio-Rad).

Proteins were immunopurified using the following antibodies: α-SMC3 (725 (Sumara et al., 2002)) α-STAG2 (446 (Sumara et al., 2000)) and α-MYC 9E10 (Waizenegger et al., 2000). After immunoprecipitation using antibodies crosslinked with DMP to affiprep beads (BIORAD, USA), purified complexes were washed in TBS Tween (0.01%) and eluted with 200 mM glycine pH 2.0. Eluates were neutralised with 1/10 volume 1.5 M Tris pH 9.2 and analysed by SDS-PAGE and western blotting.

### 4.3 Antibodies

To detect proteins on western blots (WB) or in immunofluorescence microscopy (IF), the following antibodies were used: α-RAD21 (Upstate, 05-908), α-PDS5B (Bethyl Labs, BL2352), α-MYC 9E10 (Waizenegger et al., 2000), α-PDS5A (521, (Sumara et al., 2000)).

### 4.4 Immunofluorescence microscopy

see section 2.2.5.6

#### 4.5 Cloning

DNA was amplified in DH5 $\alpha$  *E. Coli* strains. For plasmid preparations the QIAGEN mini or maxi prep kits were used. Glycerol stock of strains carrying the final plasmids were generated using 0.5 ml of exponentially growing bacteria and 0.5 ml of 87% glycerol. PCR Primers were synthesized by MWG Biotech, Vienna, Austria (Table 2.3-1). PCR reactions were carried out using *Pfu* turbo Polymerase (Stratagene) according to manufacturers instructions with Tm adjusted according to primer length. Restriction enzymes as indicated were all from NEB and used according to manufacturers instructions. DNA fragments were ligated using the T4 ligase (Fermentas). Quickchange primers were designed according to manufacturers instructions (Stratagene) and PCR reactions performed with isopropanol precipitated mini prep DNA and *Pfu* Ultra II DNA polymerase (Stratagene). All final plasmids were sequenced with a set of sequencing primers designed either for PDS5A or PDS5B (Table 4.5-1).

Table 4.5-1: Primers used for amplification and Quickchange mutagenesis.

Name	#	Sequence 5'-addition/RE-sites/Kozak sequence/gly-linker	RE-site /note
pds5B_for_n-MYC	BJ35	GCGCTTGGCGCCGCTCATTCAAAGACTAGGACC	<i>NarI/KasI</i>
pds5B_rev_n-MYC	BJ36	CGGCTTGCGGCCGCTCATCGCCGTTCCCTTTTAG	<i>NotI</i>
pds5B_for_c-MYC	BJ39	GCGCTTGGCGCCGCCACCATGGCTCATTCAAAGACTAGG	<i>NarI/KasI</i>
pds5B_rev_c-MYC	BJ40	CGGCTTGCGGCCGCTCGCCGTTCCCTTTTAGCAC	<i>NotI</i>
pds5A_for_n-MYC	BJ37	GCGCTTGGCGCCGACTTCACCGCGCAGCCCAAG	<i>NarI/KasI</i>
pds5A_rev_n-MYC	BJ38	CGGCTTGCGGCCGCTTACCTTTGTAAGTCAATTTGTCTTTCTGC	<i>NotI</i>
pds5A_for_c-MYC	BJ41	GCGCTTGGCGCCGCCACCATGGACTTCACCGCGCAGCC	<i>NarI/KasI</i>
pds5A_rev_c-MYC	BJ42	CGGCTTGCGGCCGCTTACCTTTGTAAGTCAATTTGTCTTTCTGC	<i>NotI</i>
9xMYCN-term_for	BJ43	GCGCTTACGCGTGCCACCATGGCTAGTGGTGAACAAAAGTTG	<i>MluI</i>
9xMYCN-term_rev4	BJ71	GCGCTTGCTAGCGGCGCCACCACCACCTCTACTAGTGGATCCG TTCAAGTC	<i>NheI, NarI/KasI</i>
9xMYCC-term_for2	BJ63	GCGCTTACGCGTGGCGCCGCGGCCGCTGGTGGTGGTGGTCAA AAGTTGATTTCTGAAGAAGATTTG	<i>MluI, NarI/KasI</i> <i>NotI</i>
9xMYCC-term_rev	BJ46	GCGCTTGTCGACTCAGCTAGTGGATCCGTTT	<i>Sall</i>
pds5B_siRNA1-RES_6PM_for	BJ50	GCAATGAAATTTTCACG CAA TTG TAT CGA ACC TTATTTTCAGTTATAACAATGGCC	6 mismatches
pds5B_siRNA1-RES_6PM_rev	BJ51	GGCCATTGTTTATAACTGAAAATAAGGTTGATACAATTGCGTGAAA ATTCATTGC	6 mismatches
pds5A_siRNA1-RES_6PM_for	BJ57	CAATAAGAAGGTACAAA TG CAT ATG TTG GAC CTA ATGAGTTCTATCATCATGG	6 mismatches
pds5A_siRNA1-RES_6PM_rev	BJ58	CCATGATGATAGAACTCATTAGGTCCAACATATGCATTTGTACCTTC TTATTG	6 mismatches
pds5A_siRNA1-	BJ68	CAATAAGAAGGTACAAA TG CAC ATG TTA GAT TTG	1 mismatch

#### 4 Materials and Methods

RES_1-1PM_for		ATGAGTTCTATCATCATGG	
pds5A_siRNA1- RES_1-1PM_rev	BJ69	CCATGATGATAGAACTCATCAAATCTAACATGTGCATTTGTACCTTC TTATTG	1 mismatch
pds5A_TTdel_for	BJ75	GCATGCATTGCTAATTTTTTCAATCAAGTCCTGGTGCTGG	extra TT deletion
pds5A_TTdel_rev	BJ76	CCAGCACCAGGACTTGATTGAAAAAATTAGCAATGCATGC	extra TT deletion
pds5b_1	BJ08	GGATATGGACCAGGACTCTG	sequencing
pds5b_2	BJ09	CAAGCAAGCATATGATTTGGC	sequencing
pds5b_3	BJ10	GAGAGAGAACATTAGACAAAC	sequencing
pds5b_4	BJ11	CTTGTTAGTCCAACATGCTC	sequencing
pds5b_5	BJ12	CAAGCCAAATATGCCATTCATTG	sequencing
pds5b_6	BJ13	CAAGTGTTTGCCCAAGAAC	sequencing
pds5b_7	BJ14	CTCAACCTGACAAGAATTTTACG	sequencing
pds5b_8	BJ15	GAAGATGAACAGAATAGTC	sequencing
PDS5A	BJ72	CTTCCCATGATAAACTTAAGGAC	sequencing
PDS5A	BJ73	GCTGTTGTTTCGACTTCTAGC	sequencing
PDS5A	SEQ1	AGAACTCATCAAATCTAGCATGTGC	sequencing
PDS5A	SEQ2	TATCTTGTCCTCCCAACCTGG	sequencing
PDS5A	SEQ3	TGTTACAGTGCCTAAGAATGGAGG	sequencing
PDS5A	SEQ4	TGGTAGTGCCATAATGAAGC	sequencing
PDS5A	SEQ5	TGCAATGCAGATTCACCAAAGG	sequencing
PDS5A	SEQ6	AGGGAAAGAACACTGGATAAACG	sequencing
PDS5A	BJ74	GACAAGATCACACGGACG	sequencing

## 5 Appendix

### 5.1 Plasmids generated for studying PDS5A and PDS5B

**Table 5.1-1 Plasmids generated**

Name	db#
C-term 9x MYC-tag pTRE2hyg	1131
N-term 12x MYC-tag pTRE2hyg	1132
N-term 12x MYC -PDS5B pTRE2hyg	1133
PDS5B-9x MYC tag pTRE2hyg	1134
N-term 12x MYC -PDS5A pTRE2hyg	1135
PDS5A-9x MYC-tag pTRE2hyg	1136
124_6pm_siRNA#32	1137
KIAA0979	1138
KIAA0979_6pm_siRNA#34	1139

### 5.2 Sequence analysis of PDS5A and PDS5B

**Table 5.2-1: Detected conserved domains in PDS5A**

Protein	Domain	#	Start	End	Length	Remarks
PDSA	HEAT	1	69	107	38	
PDSA	HEAT/ARM	1	153	177	24	
PDSA	HEAT	3-5	169	285	116	boundaries undefined
PDSA	HEAT	6	285	319	34	
PDSA	HEAT	7	326	360	34	
PDSA	HEAT	8	363	397	34	
PDSA	HEAT	9	401	435	34	
PDSA	HEAT	10-15	435	668	233	boundaries undefined
PDSA	HEAT	16	673	711	38	
PDSA	HEAT	17	722	756	34	
PDSA	HEAT	18	756	793	37	
PDSA	ARM	1	829	870	41	HEAT also poss.
PDSA	ARM	2	995	1033	38	

**Table 5.2-2: Detected conserved domains in PDS5B**

Protein	Name	#	Start	End	Length	Remarks
PDSB	HEAT	1	58	93	35	
PDSB	HEAT/ARM	1	124	152	28	
PDSB	HEAT	3-5	155	271	116	boundaries undefined
PDSB	HEAT	6	271	305	34	
PDSB	HEAT	7	312	346	34	
PDSB	HEAT	8	349	383	34	
PDSB	HEAT	9	387	421	34	
PDSB	HEAT	10-15	421	659	238	boundaries undefined
PDSB	HEAT	16	659	697	38	
PDSB	HEAT	17	708	742	34	
PDSB	HEAT	18	745	779	34	
PDSB	Charged		1084	1447	363	KR, ED enriched
PDSB	AT-hook		1372	1384	12	

### 5.3 Interaction manuscript table S2 (all cleaned purifications)

Table summarising all 175 unique bait purifications plus all Cdc2 purifications after contaminant removal annotated with bait species (sp), bait human orthologue (HGNC symbol, bait), prey (human orthologue of bait is marked with [Mm] if bait was a mouse protein or [Hs] if bait was a human protein), additive Mascot score (aM-Sc. (Mascot score of all unique identified peptides added up)) and percent sequence coverage (%SC).

sp	bait	prey	aM-Sc.	%SC
Mm	ACTR1A	[Mm] ACTR1A	744	40.2
Mm	ACTR1A	DCTN2	1160	50.5
Mm	ACTR1A	DCTN1	1045	22.4
Mm	ACTR1A	ACTR1A	566	33.2
Mm	ACTR1A	DCTN3	303	44.3
Mm	AKAP12	[Mm] AKAP12	3295	51.5
Mm	AKAP12	LGALS7	352	55.1
Mm	AKAP12	PKM2	265	13
Mm	AKAP12	FABP5	222	61.4
Mm	AKAP12	ALDOA	144	9.1
Mm	AKAP12	PPIA	132	26.7
Mm	AKAP12	POF1B	128	6.8
Mm	AKAP12	PFN1	118	30
Mm	AKAP12	SBSN	96	11.3
Mm	AKAP12	TPI1	88	10
Mm	AKAP12	SPRR2E	79	36.1
Mm	AKAP12	TF	78	3.9
Mm	AKAP12	VCP	77	3.4
Mm	ANLN	[Mm] ANLN	2478	54.2
Mm	ARD1A	[Mm] ARD1A	657	53.6
Mm	ARD1A	NARG1	1555	35.8
Mm	ARD1A	NARG1L	1144	30.2
Mm	ARD1A	NAT13	312	69.5
Mm	ARD1A	SERF2	202	33.3
Mm	ARD1A	ARRB2	72	5.3
Mm	ARD1A	ARRB1	72	5.6
Mm	ATM	[Mm] ATM	2626	20
Mm	ATM	DDB1	966	20
Mm	ATM	CUL4A	634	21.7
Mm	ATM	WDR42A	302	14.9
Mm	ATM	LMNB1	143	11.6
Mm	ATM	IQWD1	108	3.5
Hs	ATM	[Hs] ATM	401	4.6
Hs	ATM	[Hs] ATM	1447	11.6
Hs	AURKA	[Hs] AURKA	1168	62.3
Hs	AURKA	AURKA	514	27.4
Hs	AURKA	CEP192	400	5.4
Hs	AURKA	TPX2	106	3.9
Hs	AURKA	CALU	89	6.7
Mm	AZI1	[Mm] AZI1	4869	74.9
Mm	AZI1	AZI1	3601	60.7
Mm	AZI1	RANBP5	1783	60.9
Mm	AZI1	MIB1	729	18.8
Mm	AZI1	PCM1	438	8.8
Mm	BACH1	[Mm] BACH1	1020	29.4
Mm	BACH1	HMMR	607	23
Mm	BACH1	MAFK	243	34
Mm	BACH1	ENSG00000215622	193	19.3
Mm	BACH1	DYNLL1	177	49.4

<i>Mm</i>	BACH1	FAM83D	115	5.9
<i>Mm</i>	BACH1	ARF1	104	13.8
<i>Mm</i>	BACH1	MAFF	83	15.2
<i>Mm</i>	BMPR1A	[Mm] BMPR1A	525	23.9
<i>Mm</i>	BUB1	[Mm] BUB1	3441	73.7
<i>Mm</i>	BUB1	CASC5	4310	46.9
<i>Mm</i>	BUB1	UBR5	3122	28.7
<i>Mm</i>	BUB1	BUB1B	1784	40.6
<i>Mm</i>	BUB1	NDC80	1336	42.1
<i>Mm</i>	BUB1	PMF1	762	77.6
<i>Mm</i>	BUB1	DSN1	713	48.6
<i>Mm</i>	BUB1	NUF2	489	29.7
<i>Mm</i>	BUB1	SPC25	486	37.1
<i>Mm</i>	BUB1	NSL1	479	35.9
<i>Mm</i>	BUB1	SPC24	419	50.3
<i>Mm</i>	BUB1	MIS12	337	31.7
<i>Mm</i>	BUB1	ZWINT	335	39.5
<i>Mm</i>	BUB1	PDE4D	163	4.8
<i>Mm</i>	BUB1	CDC20	78	5
<i>Hs</i>	BUB1	[Hs] BUB1	2781	49.4
<i>Hs</i>	BUB1	CASC5	3310	31.7
<i>Hs</i>	BUB1	UBR5	3133	24.8
<i>Hs</i>	BUB1	BUB1	2117	41.9
<i>Hs</i>	BUB1	BUB1B	1246	27
<i>Hs</i>	BUB1	NDC80	1112	34
<i>Hs</i>	BUB1	DSN1	680	43
<i>Hs</i>	BUB1	PMF1	547	55.6
<i>Hs</i>	BUB1	NSL1	504	51.2
<i>Hs</i>	BUB1	NUF2	467	19.4
<i>Hs</i>	BUB1	ZWINT	437	38.9
<i>Hs</i>	BUB1	MIS12	320	30.7
<i>Hs</i>	BUB1	SPC24	297	36
<i>Hs</i>	BUB1	SPC25	290	21.4
<i>Mm</i>	BUB1B	[Mm] BUB1B	3218	64.8
<i>Mm</i>	BUB1B	UBR5	4197	35.6
<i>Mm</i>	BUB1B	CASC5	4069	47
<i>Mm</i>	BUB1B	ANAPC1	1785	23.9
<i>Mm</i>	BUB1B	BUB1	1694	36.1
<i>Mm</i>	BUB1B	ANAPC5	1132	33.6
<i>Mm</i>	BUB1B	CDC23	1033	37.9
<i>Mm</i>	BUB1B	CDC20	1003	55.7
<i>Mm</i>	BUB1B	CDC27	928	33.3
<i>Mm</i>	BUB1B	NDC80	894	28
<i>Mm</i>	BUB1B	ASAH1	783	41.3
<i>Mm</i>	BUB1B	CDC16	746	27.6
<i>Mm</i>	BUB1B	DSN1	616	48.6
<i>Mm</i>	BUB1B	PMF1	545	42.4
<i>Mm</i>	BUB1B	NSL1	492	45.9
<i>Mm</i>	BUB1B	NUF2	422	18.5
<i>Mm</i>	BUB1B	SPC24	402	50.3
<i>Mm</i>	BUB1B	MIS12	320	34.1
<i>Mm</i>	BUB1B	ZWINT	312	24.9
<i>Mm</i>	BUB1B	MAD2L1	273	32.2
<i>Mm</i>	BUB1B	ANAPC10	215	32.4
<i>Mm</i>	BUB1B	SPC25	210	18.8
<i>Mm</i>	BUB1B	C10orf104	204	37.3
<i>Mm</i>	BUB1B	ANAPC2	184	5.7
<i>Mm</i>	BUB1B	CDC26	151	56.5
<i>Mm</i>	BUB1B	XPNPEP3	131	7.7
<i>Mm</i>	BUB1B	ANAPC13	92	37.8
<i>Hs</i>	BUB1B	[Hs] BUB1B	2017	50.5
<i>Hs</i>	BUB1B	BUB1B	1542	39.8
<i>Hs</i>	BUB1B	CDC20	227	14.4

## 5 Appendix

<i>Hs</i>	BUB1B	CDC27	191	5.9
<i>Mm</i>	C11orf68	[Mm] C11orf68	334	27.9
<i>Mm</i>	C11orf68	PKM2	328	16.2
<i>Mm</i>	C11orf68	PHGDH	320	11.6
<i>Mm</i>	C11orf68	ALDOA	258	17.6
<i>Mm</i>	C11orf68	HNRPK	256	14
<i>Mm</i>	C11orf68	PA2G4	230	15.5
<i>Mm</i>	C11orf68	TRAP1	221	7.4
<i>Mm</i>	C11orf68	HNRNPA2B1	220	13.6
<i>Mm</i>	C11orf68	DDX5	213	6.8
<i>Mm</i>	C11orf68	PPIB	199	20.8
<i>Mm</i>	C11orf68	GNB2L1	191	14.2
<i>Mm</i>	C11orf68	EIF4A1	186	8.1
<i>Mm</i>	C11orf68	P4HB	183	7.5
<i>Mm</i>	C11orf68	NRAS	180	4.3
<i>Mm</i>	C11orf68	HNRNPU	178	4.9
<i>Mm</i>	C11orf68	PHB2	176	11.7
<i>Mm</i>	C11orf68	NME2	171	35.1
<i>Mm</i>	C11orf68	FASN	169	1.8
<i>Mm</i>	C11orf68	CALR	159	8.4
<i>Mm</i>	C11orf68	PHB	150	11.4
<i>Mm</i>	C11orf68	XRCC6	141	4.3
<i>Mm</i>	C11orf68	GPI	139	6.1
<i>Mm</i>	C11orf68	NACA	136	12.6
<i>Mm</i>	C11orf68	NP_001005472.1	135	10.5
<i>Mm</i>	C11orf68	or: ENSG00000215576	135	10.5
<i>Mm</i>	C11orf68	SERBP1	135	10.3
<i>Mm</i>	C11orf68	RAN	134	14.8
<i>Mm</i>	C11orf68	CSTA	134	28.6
<i>Mm</i>	C11orf68	AHNAK	133	1.1
<i>Mm</i>	C11orf68	NONO	127	6.2
<i>Mm</i>	C11orf68	PABPC1	121	5.5
<i>Mm</i>	C11orf68	SFPQ	118	4.8
<i>Mm</i>	C11orf68	VDAC4	115	12
<i>Mm</i>	C11orf68	EIF4A3	115	8.5
<i>Mm</i>	C11orf68	SET	112	12.8
<i>Mm</i>	C11orf68	PDIA3	111	7.1
<i>Mm</i>	C11orf68	TPI1	109	10
<i>Mm</i>	C11orf68	RCN1	107	7.9
<i>Mm</i>	C11orf68	PPIA	107	15.2
<i>Mm</i>	C11orf68	PDIA6	104	7.3
<i>Mm</i>	C11orf68	HNRPAB	103	9.5
<i>Mm</i>	C11orf68	ARF1	101	13.8
<i>Mm</i>	C11orf68	STRAP	101	9.7
<i>Mm</i>	C11orf68	PFN1	100	18.6
<i>Mm</i>	C11orf68	GOT2	99	6
<i>Mm</i>	C11orf68	CAPRIN1	97	3.5
<i>Mm</i>	C11orf68	ENSG00000177219	91	5.3
<i>Mm</i>	C11orf68	or: ENSG00000188174	91	6.9
<i>Mm</i>	C11orf68	or: HNRPA3	91	5.5
<i>Mm</i>	C11orf68	VCP	90	3.1
<i>Mm</i>	C11orf68	PGK1	89	5.8
<i>Mm</i>	C11orf68	TFRC	88	3.3
<i>Mm</i>	C11orf68	HNRNPR	87	3.2
<i>Mm</i>	C11orf68	CANX	87	7.1
<i>Mm</i>	C11orf68	EIF4H	87	9.6
<i>Mm</i>	C11orf68	ANXA5	84	5.6
<i>Mm</i>	C11orf68	SFRS5	84	7.7
<i>Mm</i>	C11orf68	TAGLN2	82	11.6
<i>Mm</i>	C11orf68	PDIA4	82	3.3
<i>Mm</i>	C11orf68	TKT	81	4.2
<i>Mm</i>	C11orf68	BAT1	79	5.6
<i>Mm</i>	C11orf68	or: DDX39	79	5.6



<i>Mm</i>	C11orf68	or: UAP56_HUMAN	79	5.6
<i>Mm</i>	C11orf68	RBMX	78	6.6
<i>Mm</i>	C11orf68	SFRS6	76	5.2
<i>Mm</i>	C11orf68	DHX15	72	3
<i>Mm</i>	C11orf68	RUVBL2	70	4.3
<i>Mm</i>	C11orf68	ASS1	68	5
<i>Mm</i>	C13orf23	[Mm] C13orf23	30	5.6
<i>Mm</i>	C13orf23	ARF1	98	13.8
<i>Mm</i>	C9orf58	[Mm] C9orf58	243	32
<i>Mm</i>	C9orf58	THRAP3	75	2.6
<i>Mm</i>	C9orf58	PCBP1	74	8.7
<i>Mm</i>	C9orf58	or: PCBP3	74	9.9
<i>Mm</i>	CBX1	[Mm] CBX1	157	15.1
<i>Mm</i>	CBX1	GNAI3	633	43.5
<i>Mm</i>	CBX1	DSG2	619	17.4
<i>Mm</i>	CBX1	ALDH18A1	598	26.6
<i>Mm</i>	CBX1	GNAI1	537	40.7
<i>Mm</i>	CBX1	GNAI2	433	36.1
<i>Mm</i>	CBX1	GNB2	268	25.6
<i>Mm</i>	CBX1	RCN2	250	28.7
<i>Mm</i>	CBX1	ALPPL2	238	15.3
<i>Mm</i>	CBX1	RNH1	198	13.4
<i>Mm</i>	CBX1	FLOT1	182	14.3
<i>Mm</i>	CBX1	or: FLOT1	182	20
<i>Mm</i>	CBX1	FOLR1	181	21.4
<i>Mm</i>	CBX1	RPA2	180	18.5
<i>Mm</i>	CBX1	FLOT2	174	10.3
<i>Mm</i>	CBX1	RCN1	158	15.4
<i>Mm</i>	CBX1	CBX1	157	15.1
<i>Mm</i>	CBX1	GNAS	147	12.6
<i>Mm</i>	CBX1	FAM83B	144	3.7
<i>Mm</i>	CBX1	TMOD3	143	13.4
<i>Mm</i>	CBX1	STOM	122	10.8
<i>Mm</i>	CBX1	HNRPH1	119	7.6
<i>Mm</i>	CBX1	LGALS3BP	96	4.3
<i>Mm</i>	CBX1	FAM83H	88	3.8
<i>Mm</i>	CBX1	CSNK1A1L	82	6.5
<i>Mm</i>	CBX1	RBMX	81	6.6
<i>Mm</i>	CBX1	GNG12	75	41.7
<i>Mm</i>	CBX1	RTN4RL2	74	5.2
<i>Mm</i>	CCDC15	[Mm] CCDC15	118	3.2
<i>Mm</i>	CCDC15	HNRNPA2B1	228	19.7
<i>Mm</i>	CCDC15	NACA	208	26.5
<i>Mm</i>	CCDC15	FUS	173	24.5
<i>Mm</i>	CCDC15	TPM2	160	12.3
<i>Mm</i>	CCDC15	SERBP1	154	11.1
<i>Mm</i>	CCDC15	PYGM	145	4.1
<i>Mm</i>	CCDC15	C1QBP	135	19.1
<i>Mm</i>	CCDC15	PPIA	131	25.5
<i>Mm</i>	CCDC15	SET	130	13.2
<i>Mm</i>	CCDC15	HNRPK	115	12.4
<i>Mm</i>	CCDC15	SOD1	104	32.5
<i>Mm</i>	CCDC15	EIF4B	95	3.9
<i>Mm</i>	CCDC15	AHNAK	95	0.7
<i>Mm</i>	CCDC15	PTMS	81	22.5
<i>Mm</i>	CCDC15	Q9NYD7_HUMAN	77	18.4
<i>Mm</i>	CDC16	[Mm] CDC16	949	35.3
<i>Mm</i>	CDC16	ANAPC1	2650	38.1
<i>Mm</i>	CDC16	BUB1B	1791	46.2
<i>Mm</i>	CDC16	ANAPC5	1463	41.6
<i>Mm</i>	CDC16	CDC27	1208	43.3
<i>Mm</i>	CDC16	CDC23	1182	46.4
<i>Mm</i>	CDC16	ANAPC2	1062	28.3

## 5 Appendix

<i>Mm</i>	CDC16	CDC16	975	35.7
<i>Mm</i>	CDC16	CDC20	749	39.9
<i>Mm</i>	CDC16	HOMER3	412	34.5
<i>Mm</i>	CDC16	NEK2	310	20.9
<i>Mm</i>	CDC16	CDC26	304	54.1
<i>Mm</i>	CDC16	HOMER1	291	20.5
<i>Mm</i>	CDC16	ANAPC10	290	49.7
<i>Mm</i>	CDC16	C10orf104	244	51.8
<i>Mm</i>	CDC16	FBXO5	175	11
<i>Mm</i>	CDC16	ANAPC13	156	55.4
<i>Mm</i>	CDC16	FZR1	134	7.4
<i>Mm</i>	CDC16	ANAPC11	82	31
<i>Mm</i>	CDC16	MAD2L1	64	11.1
<i>Hs</i>	CDC16	[Hs] CDC16	50	3
<i>Hs</i>	CDC16	ANAPC1	198	3
<i>Hs</i>	CDC16	CDC20	134	7.4
<i>Mm</i>	CDC2	[Mm] CDC2	1158	69.7
<i>Mm</i>	CDC2	CCNB2	410	21.4
<i>Mm</i>	CDC2	CCNB1	300	17.3
<i>Mm</i>	CDC2	CCNA2	75	5.1
<i>Mm</i>	CDC2	[Mm] CDC2	648	34
<i>Mm</i>	CDC2	CCNB2	292	14.6
<i>Mm</i>	CDC2	CCNB1	263	13.9
<i>Mm</i>	CDC2	CKS2	74	24.1
<i>Mm</i>	CDC2	[Mm] CDC2	1438	78.8
<i>Mm</i>	CDC2	ESPL1	635	8.6
<i>Mm</i>	CDC2	CCNB2	564	34.4
<i>Mm</i>	CDC2	CCNB1	514	24.5
<i>Mm</i>	CDC2	SKP2	323	19.5
<i>Mm</i>	CDC2	CKS1B	162	38.8
<i>Mm</i>	CDC2	CCNA2	161	11.6
<i>Mm</i>	CDC2	SKP1A	160	20.9
<i>Mm</i>	CDC2	CKS2	88	24.1
<i>Mm</i>	CDC2	PKMYT1	80	4.4
<i>Mm</i>	CDC2	[Mm] CDC2	1561	83.5
<i>Mm</i>	CDC2	CCNB1	705	42.9
<i>Mm</i>	CDC2	CCNB2	703	49
<i>Mm</i>	CDC2	SKP2	477	22.9
<i>Mm</i>	CDC2	CCNA2	464	30.1
<i>Mm</i>	CDC2	ESPL1	335	4.6
<i>Mm</i>	CDC2	PKMYT1	264	11.2
<i>Mm</i>	CDC2	CKS1B	209	38.8
<i>Mm</i>	CDC2	SKP1A	196	25.8
<i>Mm</i>	CDC2	CCNO	163	10
<i>Mm</i>	CDC2	CKS2	161	44.3
<i>Mm</i>	CDC2	PHGDH	138	8.6
<i>Mm</i>	CDC2	CPS1	81	1.9
<i>Mm</i>	CDC2	AIFM1	81	4.6
<i>Mm</i>	CDC2	CDKN1C	72	8.4
<i>Mm</i>	CDC2	[Mm] CDC2	384	39.7
<i>Mm</i>	CDC2	[Mm] CDC2	1728	77.4
<i>Mm</i>	CDC2	CCNB2	929	50
<i>Mm</i>	CDC2	CCNB1	906	47.2
<i>Mm</i>	CDC2	CCNA2	341	21.5
<i>Mm</i>	CDC2	CKS1B	235	38.8
<i>Mm</i>	CDC2	CKS2	202	32.9
<i>Mm</i>	CDC2	NSUN2	155	8.3
<i>Mm</i>	CDC2	SKP2	137	6.3
<i>Mm</i>	CDC2	CDKN1B	104	7.1
<i>Mm</i>	CDC2	[Mm] CDC2	928	53.5
<i>Mm</i>	CDC2	CCNB1	310	18
<i>Mm</i>	CDC2	CCNB2	239	14.3
<i>Mm</i>	CDC2	CKS1B	105	28.4

Mm	CDC2	CKS2	85	24.1
Mm	CDC2	[Mm] CDC2	1102	68.4
Mm	CDC2	CCNB2	387	26.6
Mm	CDC2	CCNB1	359	25.6
Mm	CDC2	CKS1B	173	38.8
Mm	CDC2	[Mm] CDC2	1736	85.2
Mm	CDC2	CCNB2	806	48.5
Mm	CDC2	ASCC3L1	692	9
Mm	CDC2	CCNB1	602	31.1
Mm	CDC2	EFTUD2	413	11.1
Mm	CDC2	CCNA2	359	21.8
Mm	CDC2	C20orf4	220	21.1
Mm	CDC2	SKP2	176	11.5
Mm	CDC2	CKS2	171	34.2
Mm	CDC2	CKS1B	170	38.8
Mm	CDC2	CCNO	128	8.3
Mm	CDC2	WDR57	76	22
Mm	CDC2	[Mm] CDC2	937	40.1
Mm	CDC2	CCNB2	348	21.4
Mm	CDC2	CCNB1	269	12
Mm	CDC2	SKP2	141	7.6
Mm	CDC2	SSBP1	106	15.5
Mm	CDC2	ESPL1	101	1.1
Mm	CDC2	CKS2	95	24.1
Mm	CDC2	[Mm] CDC2	914	53.9
Mm	CDC2	CCNB2	382	25.1
Mm	CDC2	CCNB1	351	22.9
Mm	CDC2	ANAPC1	314	4
Mm	CDC2	CDC27	200	5.5
Mm	CDC2	CCNA2	186	10.9
Mm	CDC2	SKP2	148	9
Mm	CDC2	PKMYT1	130	7.8
Mm	CDC2	CDC23	128	7.3
Mm	CDC2	CDC25C	92	4.8
Mm	CDC2	SKP1A	90	8
Mm	CDC2	ANAPC2	82	2.7
Mm	CDC2	CORO1C	79	3.6
Mm	CDC2	CKS2	78	24.1
Mm	CDC2	[Mm] CDC2	1302	71.7
Mm	CDC2	CCNB2	578	34.2
Mm	CDC2	CCNB1	465	28.6
Mm	CDC2	CKS1B	121	38.8
Mm	CDC2	CKS2	105	25.3
Mm	CDC2	SKP2	100	4.9
Mm	CDC2	C19orf21	85	3.8
Mm	CDC2	[Mm] CDC2	1701	85.5
Mm	CDC2	CCNB2	1165	61.6
Mm	CDC2	CCNB1	1096	51.3
Mm	CDC2	CCNA2	349	19
Mm	CDC2	CKS1B	245	47.8
Mm	CDC2	CKS2	204	46.8
Mm	CDC2	ESPL1	170	2.7
Mm	CDC2	[Mm] CDC2	1444	69
Mm	CDC2	CCNB1	492	24.7
Mm	CDC2	CCNB2	482	31.2
Mm	CDC2	WEE1	461	15.3
Mm	CDC2	CCNA2	202	14.1
Mm	CDC2	SKP2	186	10
Mm	CDC2	CKS1B	144	38.8
Mm	CDC2	PKMYT1	71	4.2
Mm	CDC2	[Mm] CDC2	988	65.7
Mm	CDC2	CCNB1	328	19.4
Mm	CDC2	CCNB2	199	12.6

## 5 Appendix

Mm	CDC2	CKS1B	147	38.8
Mm	CDC2	MAD1L1	107	3.3
Mm	CDC2	PDLIM7	101	5.7
Mm	CDC2	CCNA2	100	8.1
Mm	CDC2	SKP2	99	5.1
Mm	CDC2	BSG	78	15.3
Mm	CDC2	CKS2	75	24.1
Mm	CDC2	[Mm] CDC2	1987	88.9
Mm	CDC2	CCNB2	923	45.7
Mm	CDC2	CCNB1	772	40.9
Mm	CDC2	CCNA2	689	38.9
Mm	CDC2	SKP2	671	39.2
Mm	CDC2	SKP1A	519	55.2
Mm	CDC2	CKS2	234	45.6
Mm	CDC2	ESPL1	208	2.2
Mm	CDC2	CCNO	197	10.9
Mm	CDC2	CKS1B	191	38.8
Mm	CDC2	PKMYT1	109	6.2
Mm	CDC2	[Mm] CDC2	1058	70.7
Mm	CDC2	CCNB2	432	32.2
Mm	CDC2	CCNB1	271	23.1
Mm	CDC2	CKS2	134	32.9
Mm	CDC2	CKS1B	124	38.8
Mm	CDC2	[Mm] CDC2	0	0
Mm	CDC20	[Mm] CDC20	982	47.7
Mm	CDC20	BUB1B	2744	51.1
Mm	CDC20	ANAPC1	2072	27.5
Mm	CDC20	ANAPC5	1638	45.7
Mm	CDC20	CDC27	1265	35.2
Mm	CDC20	CDC16	949	29.8
Mm	CDC20	ANAPC2	929	21.7
Mm	CDC20	CDC23	870	36.5
Mm	CDC20	CDC20	829	40.9
Mm	CDC20	CASC5	559	7.5
Mm	CDC20	BUB1	546	13
Mm	CDC20	NUDC	497	39
Mm	CDC20	MAD2L1	479	39.5
Mm	CDC20	RNH1	475	23.4
Mm	CDC20	ANAPC10	323	48.1
Mm	CDC20	CDC26	299	65.9
Mm	CDC20	C10orf104	274	51.8
Mm	CDC20	ANAPC13	164	55.4
Mm	CDC23	[Mm] CDC23	1574	50.6
Mm	CDC23	ANAPC1	1780	23.4
Mm	CDC23	BUB1B	1400	29
Mm	CDC23	CDC27	1209	34.2
Mm	CDC23	ANAPC5	1150	27.4
Mm	CDC23	CDC16	931	29.4
Mm	CDC23	ANAPC2	925	23
Mm	CDC23	CDC23	875	28.6
Mm	CDC23	CDC20	758	36.3
Mm	CDC23	CDC26	379	67.1
Mm	CDC23	ANAPC10	224	24.9
Mm	CDC23	C10orf104	188	37.3
Mm	CDC23	ANAPC13	146	55.4
Mm	CDC23	MAD2L1	111	13.2
Mm	CDC23	FZR1	77	6.4
Mm	CDC26	[Mm] CDC26	421	63.5
Mm	CDC26	ANAPC1	2215	27.8
Mm	CDC26	ANAPC5	1479	30.1
Mm	CDC26	BUB1B	1329	31
Mm	CDC26	CDC27	1188	32.6
Mm	CDC26	CDC16	1043	26.9

<i>Mm</i>	CDC26	CDC23	1039	37.7
<i>Mm</i>	CDC26	ANAPC2	985	23
<i>Mm</i>	CDC26	CDC20	721	34.9
<i>Mm</i>	CDC26	NEK2	422	24.7
<i>Mm</i>	CDC26	ANAPC10	255	40.5
<i>Mm</i>	CDC26	CDC26	234	65.9
<i>Mm</i>	CDC26	C10orf104	198	37.3
<i>Mm</i>	CDC26	ANAPC13	187	79.7
<i>Mm</i>	CDC26	FZR1	175	8.5
<i>Mm</i>	CDC26	FBXO5	146	9
<i>Mm</i>	CDC26	MAD2L1	136	13.2
<i>Mm</i>	CDC27	[Mm] CDC27	114	10.5
<i>Mm</i>	CDC27	CDC27	114	5.1
<i>Hs</i>	CDC27	[Hs] CDC27	0	0
<i>Mm</i>	CDC6	[Mm] CDC6	1071	35.2
<i>Mm</i>	CDC6	AIFM1	235	11.3
<i>Mm</i>	CDC6	THRAP3	219	6.7
<i>Mm</i>	CDC6	BCLAF1	74	2.2
<i>Mm</i>	CDCA5	[Mm] CDCA5	403	27.3
<i>Mm</i>	CDCA5	SMC1A	1143	32
<i>Mm</i>	CDCA5	SMC3	1006	20.4
<i>Mm</i>	CDCA5	RAD21	476	17.7
<i>Mm</i>	CDCA5	PDS5B	405	7.7
<i>Mm</i>	CDCA5	AURKB	97	9.3
<i>Mm</i>	CDCA5	LCN1	69	12.5
<i>Hs</i>	CDCA5	[Hs] CDCA5	331	35.7
<i>Mm</i>	CDCA8	[Mm] CDCA8	513	41.2
<i>Mm</i>	CDCA8	C1QBP	173	13.8
<i>Mm</i>	CDCA8	SIRT1	97	5
<i>Mm</i>	CDCA8	MRPS7	86	10.7
<i>Mm</i>	CDCA8	AURKB	84	6.4
<i>Mm</i>	CDCA8	CDCA8	79	10.7
<i>Mm</i>	CDCA8	EBNA1BP2	63	6.9
<i>Mm</i>	CENPE	[Mm] CENPE	7927	51.8
<i>Mm</i>	CENPE	CLASP1	787	15.2
<i>Mm</i>	CENPE	CLASP2	522	7.5
<i>Mm</i>	CEP110	[Mm] CEP110	6516	63.5
<i>Mm</i>	CEP110	SNAP29	238	18.2
<i>Mm</i>	CEP110	CEP110	227	10.3
<i>Mm</i>	CEP110	GOLGA3	158	2.2
<i>Mm</i>	CEP110	RAB14	133	14.9
<i>Mm</i>	CEP135	[Mm] CEP135	3824	59.6
<i>Mm</i>	CEP135	WDR8	670	33.6
<i>Mm</i>	CEP135	CEP135	139	2.1
<i>Mm</i>	CEP135	TTN	64	0
<i>Mm</i>	CEP152	[Mm] CEP152	3957	52.2
<i>Mm</i>	CEP152	CEP152	1823	29.3
<i>Mm</i>	CEP152	CEP63	387	17
<i>Mm</i>	CEP152	C15orf23	291	20.6
<i>Mm</i>	CEP152	DYNLL1	270	50.6
<i>Mm</i>	CEP152	SPAG5	259	8.6
<i>Mm</i>	CEP152	DYNLL2	250	50.6
<i>Mm</i>	CEP152	HNRPD	147	14.1
<i>Mm</i>	CEP152	CENPF	128	1.2
<i>Mm</i>	CEP152	SERBP1	93	7
<i>Mm</i>	CEP170	[Mm] CEP170	3332	46.3
<i>Mm</i>	CEP170	HERC2	2091	12.4
<i>Mm</i>	CEP170	KIFC3	1380	37.2
<i>Mm</i>	CEP170	CEP170	1298	21.6
<i>Mm</i>	CEP170	WDR62	625	10.1
<i>Mm</i>	CEP170	NP_115818.2	418	6.7
<i>Mm</i>	CEP170	KIAA1967	402	11.6
<i>Mm</i>	CEP170	SNAPAP	202	30.9

## 5 Appendix

Mm	CEP170	RALY	172	14.1
Mm	CEP170	SSBP1	169	23.6
Mm	CEP170	BEGAIN	149	8.8
Mm	CEP170	ZFP106	125	1.8
Mm	CEP170	PCM1	94	3
Mm	CEP170	PCYT1A	70	7.9
Mm	CEP192	[Mm] CEP192	1342	27.9
Mm	CEP192	LMO7	639	13.6
Mm	CEP192	AURKA	437	27.4
Mm	CEP192	C19orf21	227	10.2
Mm	CEP192	FOLR1	107	12.8
Mm	CEP27	[Mm] CEP27	258	32.2
Mm	CEP27	FAM29A	2211	47.6
Mm	CEP27	KIAA0841	1461	41.2
Mm	CEP27	C4orf15	1225	44.4
Mm	CEP27	CCDC5	871	57.9
Mm	CEP27	C14orf94	817	38.7
Mm	CEP27	UCHL5IP	682	50.4
Mm	CEP27	NP_219485.1	561	26.1
Mm	CEP290	[Mm] CEP290	1269	31.1
Mm	CEP290	TPM2	441	26.1
Mm	CEP290	TPM1	371	23.6
Mm	CEP290	RNH1	228	11.1
Mm	CEP290	CALD1	195	10
Mm	CEP290	NM_001014342.1	192	2.8
Mm	CEP290	PIP	169	29.5
Mm	CEP350	[Mm] CEP350	1578	20.3
Mm	CEP350	TLN2	3364	32.4
Mm	CEP350	TLN1	3226	36
Mm	CEP350	VCL	806	17.9
Mm	CEP350	C9orf140	605	39.3
Mm	CEP350	CTNNA1	566	16.3
Mm	CEP350	ENSG00000205476	288	19.6
Mm	CEP350	PPP2R1A	190	9
Mm	CEP350	PPP2R3C	98	5.7
Mm	CEP350	PAWR	95	8.5
Mm	CEP350	TES	93	8
Mm	CEP55	[Mm] CEP55	2013	65.7
Mm	CEP55	CEP55	1030	45.7
Mm	CEP55	TSG101	246	17.2
Mm	CEP55	PCBP1	238	18.8
Mm	CEP55	SPAG5	181	4
Mm	CEP55	PDCD6IP	147	4.1
Mm	CEP55	VPS37C	111	6.5
Mm	CEP55	C15orf23	108	7.3
Mm	CEP55	VPS28	104	11.8
Mm	CEP55	FBXO28	103	6.8
Mm	CEP55	NP_710154.1	97	5.8
Mm	CEP55	CEP170	88	1.5
Mm	CEP55	GNB2L1	79	7.3
Mm	CEP55	NP_001005472.1	77	7.1
Mm	CEP55	or: ENSG00000215576	77	7.1
Mm	CEP55	HNRNPA2B1	67	5.6
Mm	CEP55	SET	63	7.9
Mm	CEP72	[Mm] CEP72	457	18.6
Mm	CEP72	PPP1R12A	1748	31.1
Mm	CEP72	PPP1R12C	904	31.1
Mm	CEP72	SH2D4A	759	26.7
Mm	CEP72	PPP1CB	433	26.9
Mm	CEP72	PPP1R7	365	21.7
Mm	CEP72	PPP1R2	321	32.2
Mm	CEP72	PPP1R8	195	21.5
Mm	CEP72	YLPM1	191	3.4

<i>Mm</i>	CEP72	PPP1R12B	152	6.3
<i>Mm</i>	CEP72	PPP1R11	130	12.7
<i>Mm</i>	CEP72	PPP1R10	111	4.5
<i>Mm</i>	CEP76	[Mm] CEP76	1199	57.8
<i>Mm</i>	CEP76	DCTN2	593	40.1
<i>Mm</i>	CEP76	ACTR1A	397	31.4
<i>Mm</i>	CEP76	CORO1C	344	18.6
<i>Mm</i>	CEP76	GNAI2	318	23.3
<i>Mm</i>	CEP76	CEP76	303	22.6
<i>Mm</i>	CEP76	RAI14	290	6.9
<i>Mm</i>	CEP76	GNB2	253	18.5
<i>Mm</i>	CEP76	ANPEP	249	5.4
<i>Mm</i>	CEP76	CALD1	202	11.9
<i>Mm</i>	CEP76	C17orf84	188	5.9
<i>Mm</i>	CEP76	FOLR1	185	21.4
<i>Mm</i>	CEP76	CACNA2D1	181	6.8
<i>Mm</i>	CEP76	GNB1	179	14.1
<i>Mm</i>	CEP76	GNAI3	163	13
<i>Mm</i>	CEP76	ALPPL2	146	8.1
<i>Mm</i>	CEP76	DCTN1	134	3.3
<i>Mm</i>	CEP76	GNAI1	118	8.8
<i>Mm</i>	CEP78	[Mm] CEP78	2374	47.7
<i>Mm</i>	CEP78	CEP78	911	26.4
<i>Mm</i>	CEP78	UBR5	705	6.1
<i>Mm</i>	CEP78	SQSTM1	156	9.3
<i>Mm</i>	CEP78	NSUN2	137	5.5
<i>Mm</i>	CEP78	Q8TBD9_HUMAN	102	2.5
<i>Mm</i>	CEP78	NAP1L4	77	9.7
<i>Mm</i>	CETN2	[Mm] CETN2	427	65
<i>Mm</i>	CETN2	XPC	153	3.6
<i>Mm</i>	CETN2	CETN2	132	26.7
<i>Mm</i>	CETN2	CETN3	111	28.1
<i>Mm</i>	CETN2	RAD23B	101	7.8
<i>Mm</i>	CETN2	C5orf37	84	9
<i>Hs</i>	CHORDC1	[Hs] CHORDC1	1368	68.1
<i>Mm</i>	CKAP5	[Mm] CKAP5	1519	16.6
<i>Mm</i>	CKAP5	SET	71	9
<i>Mm</i>	CKAP5	[Mm] CKAP5	2804	31.3
<i>Mm</i>	CKAP5	TACC3	869	29.6
<i>Mm</i>	CKAP5	SLAIN2	292	11.1
<i>Mm</i>	CKAP5	APC	277	2.7
<i>Mm</i>	CKAP5	CKAP5	245	4.4
<i>Hs</i>	CKAP5	[Hs] CKAP5	4851	51.7
<i>Hs</i>	CKAP5	TACC3	1157	37
<i>Hs</i>	CKAP5	CKAP5	629	10
<i>Hs</i>	CKAP5	SLAIN2	232	12.3
<i>Hs</i>	CKAP5	TACC2	220	11.7
<i>Hs</i>	CKAP5	SNW1	70	4.3
<i>Mm</i>	CNOT3	[Mm] CNOT3	942	31
<i>Mm</i>	CNOT3	CNOT1	5472	53.2
<i>Mm</i>	CNOT3	TNKS1BP1	3852	63.8
<i>Mm</i>	CNOT3	CNOT10	1529	55.8
<i>Mm</i>	CNOT3	RAVER1	1444	65
<i>Mm</i>	CNOT3	CNOT2	1172	62.2
<i>Mm</i>	CNOT3	CNOT6L	1054	49.5
<i>Mm</i>	CNOT3	FHL2	882	64.2
<i>Mm</i>	CNOT3	RQCD1	752	50.5
<i>Mm</i>	CNOT3	CNOT8	619	55.1
<i>Mm</i>	CNOT3	CNOT6	593	28
<i>Mm</i>	CNOT3	C13orf7	549	17.6
<i>Mm</i>	CNOT3	CNOT7	498	50.9
<i>Mm</i>	CNOT3	C2orf29	463	24.1
<i>Mm</i>	CNOT3	TOB2	271	19.2

## 5 Appendix

<i>Mm</i>	CNOT3	BTG3	207	23.4
<i>Mm</i>	CNTROB	[Mm] CNTROB	0	0
<i>Mm</i>	CNTROB	DYNLL1	176	49.4
<i>Mm</i>	CNTROB	DYNLL2	159	49.4
<i>Mm</i>	CNTROB	DYNLT3	136	23.3
<i>Mm</i>	CNTROB	DYNLRB1	130	29.2
<i>Mm</i>	CNTROB	NSUN2	98	5.5
<i>Mm</i>	COPA	[Mm] COPA	3145	51.5
<i>Mm</i>	COPA	COPG	2468	57
<i>Mm</i>	COPA	COPB1	1987	40.5
<i>Mm</i>	COPA	COPB2	1731	45.5
<i>Mm</i>	COPA	ARCN1	1193	51.5
<i>Mm</i>	COPA	COPE	847	53.7
<i>Mm</i>	COPA	ENSG00000214133	481	41.9
<i>Mm</i>	COPA	BCAP31	351	26.4
<i>Mm</i>	COPA	COPZ1	316	36.2
<i>Mm</i>	COPA	ERGIC2	101	5.6
<i>Mm</i>	COPA	SIPA1L3	92	1.4
<i>Mm</i>	COPA	ARL6IP2	81	5.2
<i>Mm</i>	CSK	[Mm] CSK	1295	56.9
<i>Mm</i>	CSNK1E	[Mm] CSNK1E	974	50.2
<i>Mm</i>	CSNK1E	GAPVD1	2070	44.9
<i>Mm</i>	CSNK1E	PER1	1965	41.9
<i>Mm</i>	CSNK1E	VPS13B	986	8.8
<i>Mm</i>	CSNK1E	FAM83H	904	27.3
<i>Mm</i>	CSNK1E	STOX2	892	32.1
<i>Mm</i>	CSNK1E	PER3	878	26.5
<i>Mm</i>	CSNK1E	CRY2	763	38.1
<i>Mm</i>	CSNK1E	CRY1	654	37.9
<i>Mm</i>	CSNK1E	FAM110B	424	33
<i>Mm</i>	CSNK1E	RRP12	395	11.7
<i>Mm</i>	CSNK1E	AP2A1	382	13.6
<i>Mm</i>	CSNK1E	PER2	367	18.8
<i>Mm</i>	CSNK1E	TSR1	304	9.6
<i>Mm</i>	CSNK1E	PKM2	295	21.3
<i>Mm</i>	CSNK1E	PPIA	267	55.8
<i>Mm</i>	CSNK1E	AZI1	246	6.8
<i>Mm</i>	CSNK1E	HNRNPA2B1	241	22.3
<i>Mm</i>	CSNK1E	CPS1	234	4.9
<i>Mm</i>	CSNK1E	AP2M1	224	19.2
<i>Mm</i>	CSNK1E	SNX24	183	31.4
<i>Mm</i>	CSNK1E	TKT	173	10
<i>Mm</i>	CSNK1E	FAM110A	172	20
<i>Mm</i>	CSNK1E	MCC	161	4.1
<i>Mm</i>	CSNK1E	LTV1	157	8.6
<i>Mm</i>	CSNK1E	GPI	146	6.6
<i>Mm</i>	CSNK1E	TAGLN2	143	18.6
<i>Mm</i>	CSNK1E	RPSAP15	140	18.6
<i>Mm</i>	CSNK1E	ALDOA	139	9.1
<i>Mm</i>	CSNK1E	TPI1	123	19.3
<i>Mm</i>	CSNK1E	PFN1	115	21.4
<i>Mm</i>	CSNK1E	SFRS2	112	12.4
<i>Mm</i>	CSNK1E	NME2P1	107	19
<i>Mm</i>	CSNK1E	MIF	97	17.4
<i>Mm</i>	CSNK1E	EIF4A1	92	7.4
<i>Mm</i>	CSNK1E	C1QBP	92	12.1
<i>Mm</i>	CSNK1E	HNRPK	89	9.8
<i>Mm</i>	CSNK1E	RAN	87	11.1
<i>Mm</i>	CSNK1E	AHNAK	87	0.7
<i>Mm</i>	CSNK1E	PCBP1	86	9.3
<i>Mm</i>	CSNK1E	EIF5AP1	86	15.6
<i>Mm</i>	CSNK1E	PGK1	82	6.7
<i>Mm</i>	CSNK1E	NACA	82	13



<i>Mm</i>	CUL3	[Mm] CUL3	211	8.9
<i>Mm</i>	CUL3	GOLGA2	1421	29.3
<i>Mm</i>	CUL3	KLHDC5	83	5
<i>Mm</i>	CUL3	LGALS3BP	79	3.2
<i>Mm</i>	DCTN1	[Mm] DCTN1	3031	42.3
<i>Mm</i>	DCTN1	DCTN2	1091	71.9
<i>Mm</i>	DCTN1	DCTN1	959	18.5
<i>Mm</i>	DCTN1	ACTR1A	954	63.6
<i>Mm</i>	DCTN1	DCTN3	305	52.7
<i>Mm</i>	DCTN2	[Mm] DCTN2	709	35.1
<i>Mm</i>	DCTN2	DCTN2	1441	62.6
<i>Mm</i>	DCTN2	DCTN1	1072	22.5
<i>Mm</i>	DCTN2	ACTR1A	828	45.7
<i>Mm</i>	DCTN2	DCTN3	369	50
<i>Mm</i>	DCTN2	SHCBP1	339	15.6
<i>Mm</i>	DCTN2	KIF23	128	4.1
<i>Mm</i>	DCTN3	[Mm] DCTN3	34	4.8
<i>Mm</i>	DCTN3	DCTN2	1035	63.3
<i>Mm</i>	DCTN3	DCTN1	945	23.6
<i>Mm</i>	DCTN3	ACTR1A	891	66
<i>Mm</i>	DCTN3	SNAP29	279	27.9
<i>Mm</i>	DCTN3	DCTN3	274	40.3
<i>Mm</i>	DDX41	[Mm] DDX41	833	27
<i>Mm</i>	DDX41	NKAP	213	6.3
<i>Mm</i>	DDX41	CSTA	82	21.4
<i>Mm</i>	DDX41	APOD	78	9.5
<i>Mm</i>	DTL	[Mm] DTL	1072	39.9
<i>Mm</i>	DTL	DDB1	2349	45.3
<i>Mm</i>	DTL	CUL4A	1352	37.4
<i>Mm</i>	DTL	CUL4B	609	17.7
<i>Mm</i>	DTL	COPS4	135	8.4
<i>Mm</i>	DTL	COPS6	83	8
<i>Mm</i>	DTL	COPS2	71	5.6
<i>Mm</i>	DYNC1H1	[Mm] DYNC1H1	7533	32.6
<i>Mm</i>	DYNC1H1	FOLR1	133	12.8
<i>Mm</i>	DYNC1H1	DYNLRB1	125	29.2
<i>Mm</i>	DYNC1H1	NSUN2	124	8.3
<i>Mm</i>	DYNC1H1	DYNLT3	124	23.3
<i>Mm</i>	DYNC1I2	[Mm] DYNC1I2	1522	53.4
<i>Mm</i>	DYNLL1	[Mm] DYNLL1	484	69.7
<i>Mm</i>	DYNLL1	HMMR	2394	60.4
<i>Mm</i>	DYNLL1	ANKRD15	2297	42.4
<i>Mm</i>	DYNLL1	C20orf117	1859	31.8
<i>Mm</i>	DYNLL1	ZMYM4	1825	31.3
<i>Mm</i>	DYNLL1	KIAA0802	1772	26.2
<i>Mm</i>	DYNLL1	NP_001006948.1	1396	21.9
<i>Mm</i>	DYNLL1	EML3	1367	35.4
<i>Mm</i>	DYNLL1	CTTNBP2NL	1229	33.8
<i>Mm</i>	DYNLL1	FAM83D	1206	37.9
<i>Mm</i>	DYNLL1	TLK2	1194	33
<i>Mm</i>	DYNLL1	SPAG5	1110	21.5
<i>Mm</i>	DYNLL1	TLK1	1033	29
<i>Mm</i>	DYNLL1	ZMYM2	996	18.9
<i>Mm</i>	DYNLL1	ANKRD25	977	28.9
<i>Mm</i>	DYNLL1	MORC3	828	26.7
<i>Mm</i>	DYNLL1	STRN3	786	25.8
<i>Mm</i>	DYNLL1	TP53BP1	763	11.5
<i>Mm</i>	DYNLL1	ZNF609	737	13.9
<i>Mm</i>	DYNLL1	FBXO30	603	25.9
<i>Mm</i>	DYNLL1	STRN4	574	21.1
<i>Mm</i>	DYNLL1	C15orf23	563	40.8
<i>Mm</i>	DYNLL1	STRN	546	19.2
<i>Mm</i>	DYNLL1	DYNLL1	408	68.5

## 5 Appendix

Mm	DYNLL1	MOBKL3	376	35.8
Mm	DYNLL1	FBXO38	355	7.2
Mm	DYNLL1	AOF2	337	9.6
Mm	DYNLL1	C5orf21	335	22.8
Mm	DYNLL1	DYNLL2	330	55.1
Mm	DYNLL1	ZMYM3	307	6.6
Mm	DYNLL1	FAM40A	290	12.7
Mm	DYNLL1	SKP1A	290	52.1
Mm	DYNLL1	PAPD1	276	9.8
Mm	DYNLL1	RCOR1	270	16
Mm	DYNLL1	NEK9	265	7.2
Mm	DYNLL1	GLCCI1	247	9
Mm	DYNLL1	GPHN	239	6.9
Mm	DYNLL1	DYNLRB1	218	74
Mm	DYNLL1	TRPS1	214	4.5
Mm	DYNLL1	AGGF1	165	6
Mm	DYNLL1	PPP2R1A	158	6.8
Mm	DYNLL1	CREB3L2	145	7.7
Mm	DYNLL1	NP_057626.2	137	7.9
Mm	DYNLL1	RCOR3	137	9.6
Mm	DYNLL1	PPP2CA	128	11
Mm	DYNLL1	PRKAR2A	127	10.2
Mm	DYNLL1	Q9H7K0_HUMAN	126	11
Mm	DYNLL1	HDAC2	124	8.6
Mm	DYNLL1	PDCD10	117	16
Mm	DYNLL1	NP_060219.2	113	3.5
Mm	DYNLL1	CIZ1	102	6
Mm	DYNLL1	WDR60	77	2.5
Mm	DYNLL1	MASTL	67	1.8
Mm	ECT2	[Mm] ECT2	1984	58.7
Mm	ECT2	[Mm] ECT2	1622	45.4
Mm	EDA2R	[Mm] EDA2R	267	25.9
Mm	EDC4	[Mm] EDC4	3245	63.7
Mm	EDC4	HADHA	994	38.7
Mm	EDC4	EDC4	934	21.6
Mm	EDC4	HADHB	610	35.7
Mm	EDC4	CCDC101	442	37.2
Mm	EDC4	DCP2	273	14
Mm	EDC4	EDC3	164	8.5
Mm	EDC4	NP_689929.1	129	6
Mm	EDC4	AP2B1	127	7
Mm	EDC4	AP2A1	110	5
Mm	EDC4	AP2M1	108	5.8
Mm	EEA1	[Mm] EEA1	4364	59.9
Mm	EEA1	EEA1	1281	22.9
Mm	EIF4A3	[Mm] EIF4A3	1251	46.4
Mm	EIF4A3	EIF4A3	481	18.7
Mm	ERH	[Mm] ERH	194	34.6
Mm	ERH	THRAP3	1949	39.4
Mm	ERH	CLTC	1719	27.8
Mm	ERH	BCLAF1	1532	36.6
Mm	ERH	PRMT1	968	51.3
Mm	ERH	POLDIP3	967	54.6
Mm	ERH	SAMM50	471	20.9
Mm	ERH	TMOD3	424	28.1
Mm	ERH	C1QBP	386	40.8
Mm	ERH	SPECC1	342	9.6
Mm	ERH	CHCHD3	337	25.6
Mm	ERH	C19orf21	330	20
Mm	ERH	PPP1R12A	292	7.1
Mm	ERH	C1orf77	219	25.7
Mm	ERH	FANCE	134	4.5
Mm	ERH	C10orf18	130	1.4

<i>Mm</i>	ERH	CHCHD6	121	13.6
<i>Mm</i>	ERH	CXorf23	108	2.8
<i>Mm</i>	ERH	RBMX	96	5.4
<i>Mm</i>	ERH	C14orf173	93	8.2
<i>Mm</i>	ERH	ALPPL2	91	6.6
<i>Mm</i>	ERH	BAT1	88	5.6
<i>Mm</i>	ERH	or: DDX39	88	5.6
<i>Mm</i>	ERH	or: UAP56_HUMAN	88	5.6
<i>Mm</i>	ERH	THOC4	85	11.3
<i>Mm</i>	ERH	FLOT1	68	7
<i>Mm</i>	ERH	or: FLOT1	68	9.8
<i>Mm</i>	ESCO1	[Mm] ESCO1	859	23.5
<i>Mm</i>	ESPL1	[Mm] ESPL1	2773	31.1
<i>Mm</i>	ESPL1	C1QBP	195	14.9
<i>Mm</i>	ESPL1	ESPL1	133	1.4
<i>Mm</i>	ESPL1	CDC2	90	8.3
<i>Mm</i>	ESPL1	CCNB1	76	4.8
<i>Mm</i>	FAM107B	[Mm] FAM107B	516	58.8
<i>Mm</i>	FAM107B	PLOD1	485	25.4
<i>Mm</i>	FAM107B	RNH1	401	24.7
<i>Mm</i>	FAM107B	PLOD2	343	17
<i>Mm</i>	FAM107B	DYNLL1	202	49.4
<i>Mm</i>	FAM107B	CTSD	171	9
<i>Mm</i>	FAM107B	NM_001014342.1	89	1.3
<i>Mm</i>	FAM107B	RPA2	73	8.1
<i>Mm</i>	FAM29A	[Mm] FAM29A	1658	38.3
<i>Mm</i>	FAM29A	KIAA0841	1124	34.8
<i>Mm</i>	FAM29A	C4orf15	857	34.2
<i>Mm</i>	FAM29A	C14orf94	768	42.4
<i>Mm</i>	FAM29A	CCDC5	571	37.1
<i>Mm</i>	FAM29A	CEP27	486	35.3
<i>Mm</i>	FAM29A	NP_219485.1	483	25.6
<i>Mm</i>	FAM29A	UCHL5IP	470	42.5
<i>Mm</i>	FAM29A	PTMS	71	22.5
<i>Mm</i>	FANCC	[Mm] FANCC	479	25
<i>Mm</i>	FANCC	FANCE	885	40.3
<i>Mm</i>	FANCC	C17orf70	367	13.4
<i>Mm</i>	FANCC	FANCB	263	7.5
<i>Mm</i>	FANCC	LASP1	215	17.6
<i>Mm</i>	FBXO5	[Mm] FBXO5	281	16.9
<i>Mm</i>	FGFR1OP	[Mm] FGFR1OP	1127	51.5
<i>Mm</i>	FGFR1OP	PPP2R3C	260	12.8
<i>Mm</i>	FGFR1OP	SHCBP1	185	5.2
<i>Mm</i>	FGFR1OP	PPP2CA	93	6.1
<i>Hs</i>	FGFR1OP	[Hs] FGFR1OP	0	0
<i>Mm</i>	GORASP1	[Mm] GORASP1	209	13.9
<i>Mm</i>	GORASP1	GOLGA2	2875	55.4
<i>Mm</i>	GORASP1	KIF14	1094	19.1
<i>Mm</i>	GORASP1	LGALS3BP	374	13.5
<i>Mm</i>	GORASP1	SBSN	151	17
<i>Mm</i>	GORASP1	CLIP1	132	3.9
<i>Mm</i>	GORASP1	TMED7	129	13.8
<i>Mm</i>	GORASP1	LGALS7	109	16.9
<i>Mm</i>	GORASP1	FABP5	102	24.8
<i>Mm</i>	GORASP1	TMED2	89	10.4
<i>Mm</i>	GORASP1	LRRFIP2	85	14.1
<i>Mm</i>	GORASP1	CSTA	67	27.6
<i>Mm</i>	GORASP1	TMED4	66	8.8
<i>Mm</i>	GTF3C6	[Mm] GTF3C6	163	17.2
<i>Mm</i>	GTF3C6	GTF3C1	3352	38.3
<i>Mm</i>	GTF3C6	GTF3C3	1410	36.6
<i>Mm</i>	GTF3C6	GTF3C5	1207	59.8
<i>Mm</i>	GTF3C6	GTF3C2	1068	34.5

## 5 Appendix

Mm	GTF3C6	GTF3C4	945	53.7
Mm	GTF3C6	GTF2F1	214	11
Mm	HDAC6	[Mm] HDAC6	1097	24.5
Mm	HDAC6	PLAA	348	14.5
Mm	HDAC6	USP47	260	24.5
Mm	HDAC6	GARS	80	3.2
Mm	HSD17B7	[Mm] HSD17B7	251	15.6
Mm	HSD17B7	AHSG	98	3.5
Mm	HSP90AA1	[Mm] HSP90AA1	3549	73.5
Mm	ITSN2	[Mm] ITSN2	737	8.2
Mm	ITSN2	EIF4A3	132	3.4
Mm	KCTD5	[Mm] KCTD5	459	55.1
Mm	KCTD5	KCTD2	221	27
Mm	KCTD5	KCTD5	76	13.2
Mm	KIAA0892	[Mm] KIAA0892	42	1.5
Mm	KIAA0892	NIPBL	1435	13.9
Mm	KIAA0892	GNAI3	146	10.7
Mm	KIAA0892	RPA2	134	12.6
Mm	KIAA0892	LMO7	123	3.4
Mm	KIAA0892	GNG12	97	34.7
Mm	KIAA0892	SPECC1	79	2.7
Mm	KIAA0892	CHCHD3	77	11.5
Mm	KIAA0892	C19orf21	70	3.5
Mm	KIAA0892	GNB2	62	6.2
Mm	KIAA0892	or: GNB1	62	6.4
Mm	KIF1C	[Mm] KIF1C	1492	28.4
Mm	KIF1C	THRAP3	179	5.3
Mm	KIF1C	EIF4A3	167	9.2
Mm	KIF1C	SSBP1	138	20.9
Mm	KIF1C	C1orf77	135	20.8
Mm	KIF1C	THOC4	116	10.9
Mm	KIF1C	ARF1	115	13.8
Mm	KIF1C	CCDC9	114	5.3
Mm	KIF1C	HNRPD	82	7.8
Mm	KIF1C	SUB1	81	15.7
Mm	KIF20A	[Mm] KIF20A	2463	56.8
Mm	KIF20A	KIF20A	1692	43.7
Mm	KIF23	[Mm] KIF23	2276	56.2
Mm	KIF23	SHCBP1	1255	42.6
Mm	KIF23	CCAR1	1240	22.7
Mm	KIF23	RACGAP1	903	39.6
Mm	KIF23	KIF23	864	22.9
Mm	KIF23	MICAL3	492	24.2
Mm	KIF23	MICAL3	308	9.2
Mm	KIF23	PAWR	297	28.5
Mm	KIF23	CD2AP	276	13.1
Mm	KIF23	TRAF3IP1	192	9.4
Mm	KIF4A	[Mm] KIF4A	2844	41.8
Mm	KIF4A	KIF4A	1008	16.8
Mm	KIF4A	PRC1	210	9.7
Mm	KIF4A	CEP170	81	2.7
Mm	KIF4A	TUBGCP2	72	7.9
Mm	KIFC1	[Mm] KIFC1	1647	39.1
Mm	KIFC1	NUP153	1576	26.2
Mm	KIFC1	KIFC1	1411	41.5
Mm	KIFC1	NUP50	1065	49.3
Mm	KIFC1	KPNB1	914	25.6
Mm	KIFC1	IMA2_HUMAN	567	26.8
Mm	KIFC1	RANBP2	500	4.1
Mm	KIFC1	RANGAP1	392	16
Mm	KIFC1	TPR	144	8.7
Mm	LCK	[Mm] LCK	655	30.6
Mm	LCK	CSTA	96	30.6

<i>Mm</i>	MAD2L1	[Mm] MAD2L1	436	48.8
<i>Mm</i>	MAD2L1	MAD1L1	1127	34.4
<i>Mm</i>	MAD2L1	BUB1B	746	18.7
<i>Mm</i>	MAD2L1	KIF20A	731	21.3
<i>Mm</i>	MAD2L1	TPR	457	5.5
<i>Mm</i>	MAD2L1	CDC27	287	8.3
<i>Mm</i>	MAD2L1	NUDT5	276	24.2
<i>Mm</i>	MAD2L1	CDC20	239	13.4
<i>Mm</i>	MAD2L1	MAD2L1	237	25.9
<i>Mm</i>	MAD2L1	ANAPC1	235	3.1
<i>Mm</i>	MAD2L1	TOR1AIP1	219	12.2
<i>Mm</i>	MAD2L1	CDC16	191	7.2
<i>Mm</i>	MAD2L1	DNAJA1	149	9.3
<i>Mm</i>	MAD2L1	CDC23	135	4.4
<i>Mm</i>	MAD2L1	CDC26	129	14.1
<i>Mm</i>	MAD2L1	C1orf52	128	24
<i>Mm</i>	MAD2L1	THRAP3	123	4
<i>Mm</i>	MAD2L1	INSR	121	2.7
<i>Mm</i>	MAD2L1	TPX2	113	2.8
<i>Mm</i>	MAD2L1	C15orf23	101	7.3
<i>Mm</i>	MAD2L1	RCN1	97	7.9
<i>Mm</i>	MAD2L1	ANAPC5	95	5.5
<i>Mm</i>	MAD2L1	AHSG	87	3.5
<i>Mm</i>	MAD2L1	BCLAF1	74	3.2
<i>Mm</i>	MAD2L1	ANTXR1	73	6.6
<i>Mm</i>	MAD2L1	MAD2L1BP	65	7.7
<i>Hs</i>	MAD2L1	[Hs] MAD2L1	0	0
<i>Mm</i>	MAD2L1BP	[Mm] MAD2L1BP	306	21
<i>Mm</i>	MAD2L1BP	MAD1L1	1814	46
<i>Mm</i>	MAD2L1BP	LMO7	377	6.7
<i>Mm</i>	MAD2L1BP	MAD2L1	172	15.1
<i>Mm</i>	MAD2L1BP	PPIA	73	12.1
<i>Mm</i>	MAD2L2	[Mm] MAD2L2	248	40
<i>Mm</i>	MAD2L2	C13orf8	1716	43.3
<i>Mm</i>	MAD2L2	POGZ	974	18.8
<i>Mm</i>	MAD2L2	FAM35A	737	21.8
<i>Mm</i>	MAD2L2	GTF2I	613	16.4
<i>Mm</i>	MAD2L2	ZMYM4	462	10.3
<i>Mm</i>	MAD2L2	CBX3	421	36.6
<i>Mm</i>	MAD2L2	EHMT2	236	4.8
<i>Mm</i>	MAD2L2	or: BAT8_HUMAN	236	4.8
<i>Mm</i>	MAD2L2	EHMT1	218	6.8
<i>Mm</i>	MAD2L2	CALU	187	12.1
<i>Mm</i>	MAD2L2	RCN1	172	12.4
<i>Mm</i>	MAD2L2	ZNF644	159	21
<i>Mm</i>	MAD2L2	CBX1	120	15.1
<i>Mm</i>	MAD2L2	C20orf196	111	24.9
<i>Mm</i>	MAD2L2	SBSN	105	17
<i>Mm</i>	MAD2L2	ALDH3A2	90	5.2
<i>Mm</i>	MAD2L2	RCN2	73	9.8
<i>Mm</i>	MAD2L2	PGAM5	60	8.2
<i>Hs</i>	MARK2	[Hs] MARK2	1265	34.6
<i>Hs</i>	MARK2	KIAA0802	821	14.9
<i>Mm</i>	MIS12	[Mm] MIS12	799	69.9
<i>Mm</i>	MIS12	CASC5	5935	61.7
<i>Mm</i>	MIS12	NDC80	2164	63.2
<i>Mm</i>	MIS12	BUB1	1622	34.2
<i>Mm</i>	MIS12	BUB1B	1300	28.5
<i>Mm</i>	MIS12	PMF1	1286	84.4
<i>Mm</i>	MIS12	DSN1	1242	69.9
<i>Mm</i>	MIS12	SPC25	1022	63.8
<i>Mm</i>	MIS12	NUF2	953	46.3
<i>Mm</i>	MIS12	NSL1	834	60.5

## 5 Appendix

Mm	MIS12	ZWINT	814	62.4
Mm	MIS12	SPC24	583	74.6
Mm	MIS12	CNBP	269	34.7
Mm	MIS12	TRIM28	209	8.6
Mm	MIS12	CBX3	199	23
Mm	MIS12	AKAP8	159	9.8
Mm	MIS12	CYR61	113	7.1
Mm	MIS12	TRIM29	89	3.7
Mm	MIS12	CALU	77	7.6
Mm	MIS12	AKAP8L	67	3.7
Mm	MIS12	MYPN	67	2.4
Mm	MIS12	HNRPF	66	8
Hs	MIS12	[Hs] MIS12	511	43.9
Hs	MIS12	CASC5	4581	50.7
Hs	MIS12	NDC80	1823	55.6
Hs	MIS12	BUB1	1337	30.6
Hs	MIS12	DSN1	1200	68.5
Hs	MIS12	PMF1	1033	76.1
Hs	MIS12	NUF2	944	44.8
Hs	MIS12	SPC25	842	51.8
Hs	MIS12	ZWINT	754	70.7
Hs	MIS12	BUB1B	705	20
Hs	MIS12	NSL1	697	54.4
Hs	MIS12	SPC24	499	64
Hs	MIS12	MIS12	434	39.5
Hs	MIS12	CENPC1	199	6.8
Mm	MKI67	[Mm] MKI67	6608	47.3
Mm	MKI67	KPNB1	1958	49.5
Mm	MKI67	NUP153	1778	38.6
Mm	MKI67	IMA2_HUMAN	1401	68.8
Mm	MKI67	NUP50	782	49.1
Mm	MKI67	KPNA6	610	35.5
Mm	MKI67	KPNA3	525	33.6
Mm	MKI67	KPNA4	425	29.6
Mm	MKI67	PPP1CC	378	31.9
Mm	MKI67	KPNA1	375	18.2
Mm	MKI67	MKI67IP	310	23.5
Mm	MKI67	SFPQ	127	5.2
Mm	MKI67	MRTO4	114	12.1
Mm	MKI67	NONO	78	5.7
Mm	NARG1	[Mm] NARG1	2092	44
Mm	NARG1	NARG1	1307	25.9
Mm	NARG1	NAT13	551	74.4
Mm	NARG1	SERF2	326	50.4
Mm	NARG1	ARD1A	288	29.5
Mm	NAT13	[Mm] NAT13	340	61.2
Mm	NAT13	NAT13	263	56.1
Hs	NDC80	[Hs] NDC80	1033	35.2
Hs	NDC80	NDC80	951	32.4
Hs	NDC80	NUF2	321	20.5
Hs	NDC80	SPC24	311	57.4
Hs	NDC80	SPC25	262	25.4
Mm	NDC80	[Mm] NDC80	2044	53
Mm	NDC80	CASC5	2318	22.9
Mm	NDC80	HMMR	818	28.5
Mm	NDC80	NUF2	735	30
Mm	NDC80	DSN1	703	43.8
Mm	NDC80	SPC25	686	39.7
Mm	NDC80	C13orf24	597	18.1
Mm	NDC80	IQGAP3	463	6.3
Mm	NDC80	PCM1	462	6.2
Mm	NDC80	CCDC101	447	24.2
Mm	NDC80	ZWINT	444	31.8

<i>Mm</i>	NDC80	BUB1	440	11.2
<i>Mm</i>	NDC80	NDC80	403	12.1
<i>Mm</i>	NDC80	PMF1	395	36.6
<i>Mm</i>	NDC80	CALCOCO1	371	12.8
<i>Mm</i>	NDC80	EPS15L1	332	10.3
<i>Mm</i>	NDC80	RRBP1	307	7.6
<i>Mm</i>	NDC80	THRAP3	279	8.5
<i>Mm</i>	NDC80	MLF1IP	248	16.5
<i>Mm</i>	NDC80	NSL1	213	17.1
<i>Mm</i>	NDC80	SPC24	212	37.6
<i>Mm</i>	NDC80	BUB1B	196	3.3
<i>Mm</i>	NDC80	KIFC1	191	7.1
<i>Mm</i>	NDC80	BICD2	191	5.5
<i>Mm</i>	NDC80	MIS12	148	16.1
<i>Mm</i>	NDC80	ODF2L	147	4.4
<i>Mm</i>	NDC80	NPR1	145	4.3
<i>Mm</i>	NDC80	SNAP29	116	12.8
<i>Mm</i>	NDC80	PHKA2	112	3
<i>Mm</i>	NDC80	HNRNPU	96	2.7
<i>Mm</i>	NDC80	ASPM	91	1.3
<i>Mm</i>	NDC80	RCN1	83	7.9
<i>Mm</i>	NDC80	SNAPAP	74	17.6
<i>Mm</i>	NDC80	PHKB	68	1.9
<i>Mm</i>	NDC80	BEGAIN	62	4.7
<i>Mm</i>	NDE1	[Mm] NDE1	1532	79.9
<i>Mm</i>	NDE1	SYNE1	2032	14.4
<i>Mm</i>	NDE1	KIAA1128	857	30.5
<i>Mm</i>	NDE1	NDE1	659	47.4
<i>Mm</i>	NDE1	NDEL1	579	41.5
<i>Mm</i>	NDE1	DIXDC1	411	26.5
<i>Mm</i>	NDE1	RNH1	148	8.9
<i>Mm</i>	NDE1	LGALS7	121	18.4
<i>Mm</i>	NDE1	RPA2	81	9.6
<i>Mm</i>	NEDD1	[Mm] NEDD1	1284	44.4
<i>Mm</i>	NEDD1	NEDD1	1062	34.2
<i>Mm</i>	NEDD1	SET	69	8.6
<i>Mm</i>	NEK2	[Mm] NEK2	747	40.9
<i>Mm</i>	NEK2	NEK2	428	28.4
<i>Mm</i>	NEK2	ACAD8	83	6
<i>Mm</i>	NEK9	[Mm] NEK9	1973	37.6
<i>Mm</i>	NEK9	NEK9	455	12.3
<i>Mm</i>	NEK9	NP_060219.2	424	10.3
<i>Mm</i>	NEK9	COG7	400	10.1
<i>Mm</i>	NEK9	DYNLL1	292	64
<i>Mm</i>	NEK9	COG5	271	7.9
<i>Mm</i>	NEK9	DDB1	241	5.8
<i>Mm</i>	NEK9	DYNLL2	222	59.6
<i>Mm</i>	NEK9	TCEB1	97	23.2
<i>Mm</i>	NEK9	C19orf58	96	27.5
<i>Mm</i>	NEK9	RPA2	70	8.1
<i>Mm</i>	NEK9	AURKA	70	6.9
<i>Mm</i>	NHP2L1	[Mm] NHP2L1	479	78.1
<i>Mm</i>	NHP2L1	NOL5A	1701	64.8
<i>Mm</i>	NHP2L1	NOP5_HUMAN	1528	54.6
<i>Mm</i>	NHP2L1	TGS1	1338	43.6
<i>Mm</i>	NHP2L1	RRP9	1284	64.8
<i>Mm</i>	NHP2L1	KPNB1	989	29
<i>Mm</i>	NHP2L1	SSB	950	48.5
<i>Mm</i>	NHP2L1	IMA2_HUMAN	919	49.5
<i>Mm</i>	NHP2L1	FBL	871	59.2
<i>Mm</i>	NHP2L1	DHX15	760	20.6
<i>Mm</i>	NHP2L1	KPNA1	717	30.3
<i>Mm</i>	NHP2L1	KPNA6	649	31.2

## 5 Appendix

Mm	NHP2L1	DHX9	570	12.3
Mm	NHP2L1	RUVBL2	556	27.6
Mm	NHP2L1	COIL	524	20
Mm	NHP2L1	NOLC1	519	21.7
Mm	NHP2L1	DHX30	518	12.3
Mm	NHP2L1	DKC1	509	25.2
Mm	NHP2L1	NUFIP1	472	23.8
Mm	NHP2L1	RUVBL1	443	30
Mm	NHP2L1	HNRPUL1	413	11.6
Mm	NHP2L1	SART3	401	13.8
Mm	NHP2L1	MOV10	328	11
Mm	NHP2L1	PINX1_HUMAN	256	19
Mm	NHP2L1	C1QBP	251	26.2
Mm	NHP2L1	NOLA2	232	42.2
Mm	NHP2L1	HNRPCL1	219	17.1
Mm	NHP2L1	ZNHIT3	200	32.3
Mm	NHP2L1	TARDBP	187	10.1
Mm	NHP2L1	SNRPD3	170	40.5
Mm	NHP2L1	C1orf181	160	10.2
Mm	NHP2L1	RANBP5	158	3.9
Mm	NHP2L1	LARP7	146	13.6
Mm	NHP2L1	PABPC1	144	6
Mm	NHP2L1	SNRPB	133	16
Mm	NHP2L1	NOLA3	127	45.3
Mm	NHP2L1	SNRPD1	117	45.4
Mm	NHP2L1	WDR43	117	2.9
Mm	NHP2L1	NHP2L1	116	18.8
Mm	NHP2L1	URB1	110	1.4
Mm	NHP2L1	SNRPE	101	25
Mm	NHP2L1	WDR79	96	6.6
Mm	NHP2L1	HNRPF	92	8.2
Mm	NHP2L1	SNRPD2	82	16.1
Mm	NHP2L1	GPATCH4	64	8.5
Mm	NIPBL	[Mm] NIPBL	1599	13.8
Mm	NIPBL	NIPBL	631	5.9
Mm	NIPBL	KPNA6	88	3.5
Mm	NIPBL	KPNA1	85	3.7
Mm	NP_710154.1	[Mm] NP_710154.1	1041	45
Mm	NP_710154.1	LTF	971	35.1
Mm	NP_710154.1	NP_710154.1	643	30.8
Mm	NP_710154.1	AZGP1	206	15.7
Mm	NP_710154.1	WFDC2	147	43.8
Mm	NP_710154.1	TCN1	115	5.3
Mm	NP_710154.1	C20orf114	112	6.7
Mm	NP_710154.1	PLUNC	102	13.3
Mm	NRIP3	[Mm] NRIP3	31	5.4
Mm	NRIP3	SERPINB12	77	8.6
Mm	NUP107	[Mm] NUP107	1906	36.5
Mm	NUP107	NUP133	2165	40.9
Mm	NUP107	NUP160	1910	28.8
Mm	NUP107	NUP98	1457	18
Mm	NUP107	NUP85	1285	35.4
Mm	NUP107	SEH1L	822	41.9
Mm	NUP107	NUP107	574	13.3
Mm	NUP107	NUP37	473	33.7
Mm	NUP107	NUP43	447	27.6
Mm	NUP107	SEC13	442	34.4
Mm	NUP107	LGALS3BP	262	11.6
Mm	NUP155	[Mm] NUP155	4220	61.7
Mm	NUP188	[Mm] NUP188	1338	19
Mm	NUP188	NUP214	2059	26.5
Mm	NUP188	NUP93	2008	50.2
Mm	NUP188	NUP88	1012	31.2



Mm	NUP188	OGT	907	18.1
Mm	NUP188	RAE1	855	42.9
Mm	NUP188	NUP98	614	17.3
Mm	NUP188	NUP62	446	12.6
Mm	NUP188	XPO1	123	3.4
Mm	NUP188	PKM2	111	5.3
Mm	NUP188	RAN	74	10.2
Mm	NUP214	[Mm] NUP214	1704	23.8
Mm	NUP214	NUP93	745	19.8
Mm	NUP214	NUP88	683	24.3
Mm	NUP214	NUP188	382	6.9
Mm	NUP214	NUP62	360	12.5
Mm	NUP214	OGT	357	8.6
Mm	NUP214	NUP214	269	2.8
Mm	NUP214	RAE1	179	16.3
Mm	NUP88	[Mm] NUP88	1489	38.8
Mm	NUP88	NUP214	1918	25.2
Mm	NUP88	NUP62	440	12.6
Mm	NUP88	RAN	98	11.1
Mm	NUP88	XPO1	87	2.1
Mm	NUP98	[Mm] NUP98	1002	15.3
Mm	NUP98	NUP160	2686	34.1
Mm	NUP98	NUP133	2615	42.5
Mm	NUP98	NUP107	1915	42.6
Mm	NUP98	NUP85	1579	40.9
Mm	NUP98	AHCTF1	1370	15.6
Mm	NUP98	SEH1L	982	60
Mm	NUP98	NUP43	589	37.9
Mm	NUP98	SEC13	577	37.3
Mm	NUP98	NUP37	517	33.7
Mm	OGG1	[Mm] OGG1	582	47
Mm	OGG1	LAMB1	100	3.5
Mm	ORC1L	[Mm] ORC1L	548	13.3
Mm	ORC1L	ORC2L	287	10.1
Mm	ORC1L	ORC3L	181	3.9
Mm	ORC1L	ORC5L	166	7.8
Mm	ORC1L	NP_690852.1	129	4.9
Mm	PAFAH1B1	[Mm] PAFAH1B1	1516	66.8
Mm	PAFAH1B1	CALD1	977	39.8
Mm	PAFAH1B1	PLS3	646	23.6
Mm	PAFAH1B1	FSCN1	468	22.5
Mm	PAFAH1B1	PAFAH1B2	255	27.1
Mm	PAFAH1B1	PAFAH1B3	231	23.8
Mm	PAFAH1B1	NDEL1	182	11.9
Mm	PAFAH1B1	NDE1	167	11.9
Mm	PAFAH1B1	TMOD3	159	9.7
Mm	PAFAH1B1	TPM2	146	11.8
Mm	PAFAH1B1	PAFAH1B1	122	3.4
Mm	PAFAH1B1	KIAA1949	114	5.4
Mm	PAFAH1B1	or: KIAA1949	114	7.2
Mm	PAFAH1B1	PPP1CA	110	8.8
Mm	PAFAH1B1	EDIL3	78	6
Mm	PAFAH1B1	LMO7	72	1.5
Mm	PAPSS1	[Mm] PAPSS1	701	34.3
Mm	PAPSS1	PAPSS2	268	19.7
Mm	PCNA	[Mm] PCNA	293	35.2
Mm	PDS5A	[Mm] PDS5A	2242	39.6
Mm	PDS5A	PDS5A	1378	22.5
Mm	PDS5A	EDC4	307	7
Mm	PDS5A	LGALS7	304	39
Mm	PDS5A	FABP5	213	61.4
Mm	PDS5A	NACA	169	19.5
Mm	PDS5A	C1QBP	163	26.2

## 5 Appendix

<i>Mm</i>	PDS5A	SERPINB12	130	8.6
<i>Mm</i>	PDS5A	FUS	128	16.6
<i>Mm</i>	PDS5A	HNRPK	120	12.4
<i>Mm</i>	PDS5A	PTMS	109	22.5
<i>Mm</i>	PDS5A	SERBP1	103	7
<i>Mm</i>	PDS5A	SOD1	100	32.5
<i>Mm</i>	PDS5A	SET	99	9
<i>Mm</i>	PDS5A	HNRNPA2B1	96	7.3
<i>Mm</i>	PDS5A	ANXA5	94	7.8
<i>Mm</i>	PDS5A	EIF5AP1	90	15.6
<i>Mm</i>	PLK1	[Mm] PLK1	1369	43.6
<i>Mm</i>	PLK1	BICD2	540	13.7
<i>Mm</i>	PLK1	ERCC6L	287	8.4
<i>Mm</i>	PLK1	FABP5	137	33.7
<i>Mm</i>	PLK1	NSUN2	106	5.5
<i>Mm</i>	PLK1	RAI14	69	2.3
<i>Mm</i>	PLK2	[Mm] PLK2	547	16.4
<i>Mm</i>	PLK4	[Mm] PLK4	266	8.1
<i>Mm</i>	PLK4	SET	121	12.8
<i>Mm</i>	PLK4	NACA	113	12.6
<i>Mm</i>	PLK4	PTMS	84	22.5
<i>Mm</i>	PPP1R10	[Mm] PPP1R10	1405	36.3
<i>Mm</i>	PPP1R10	WDR82	338	21.1
<i>Mm</i>	PPP1R10	TOX4	329	12.9
<i>Mm</i>	PPP1R10	PPP1CA	327	21.8
<i>Mm</i>	PPP1R10	PPP1CC	327	21.4
<i>Mm</i>	PPP1R10	PPP1CB	298	20.2
<i>Mm</i>	PPP1R10	TERF2	208	11.6
<i>Mm</i>	PPP1R10	PPP1R2	138	17.6
<i>Mm</i>	PPP1R10	C19orf7	87	1.8
<i>Mm</i>	PPP2R1A	[Mm] PPP2R1A	1906	59.6
<i>Mm</i>	PPP2R1A	PPP2R5D	1519	53.2
<i>Mm</i>	PPP2R1A	PPP2R2A	1163	49.4
<i>Mm</i>	PPP2R1A	PPP2CA	1029	68
<i>Mm</i>	PPP2R1A	PPP2CB	984	65.4
<i>Mm</i>	PPP2R1A	PPME1	945	50.8
<i>Mm</i>	PPP2R1A	PPP2R2D	567	31.2
<i>Mm</i>	PPP2R1A	PPP2R5E	565	24
<i>Mm</i>	PPP2R1A	PPP2R5C	497	29.3
<i>Mm</i>	PPP2R1A	PPP2R1A	443	12.4
<i>Mm</i>	PPP2R1A	FECH	196	13
<i>Mm</i>	PPP2R1A	SGOL1	159	11
<i>Mm</i>	PPP2R1A	PPP2R5A	157	8.2
<i>Mm</i>	PREB	[Mm] PREB	354	25.4
<i>Mm</i>	PRPF8	[Mm] PRPF8	4068	39.2
<i>Mm</i>	PRPF8	ASCC3L1	4498	41.9
<i>Mm</i>	PRPF8	EFTUD2	2214	50.8
<i>Mm</i>	PRPF8	DDX23	2016	48.5
<i>Mm</i>	PRPF8	PRPF6	1924	40.3
<i>Mm</i>	PRPF8	SART1	1514	45.2
<i>Mm</i>	PRPF8	PRPF3	1056	32.4
<i>Mm</i>	PRPF8	AQR	861	11.2
<i>Mm</i>	PRPF8	CDC5L	840	25.9
<i>Mm</i>	PRPF8	PRPF4	806	35.9
<i>Mm</i>	PRPF8	TFIP11	742	23.1
<i>Mm</i>	PRPF8	XAB2	719	24.2
<i>Mm</i>	PRPF8	USP39	687	30.3
<i>Mm</i>	PRPF8	C21orf66	656	20.5
<i>Mm</i>	PRPF8	RUVBL2	639	32.4
<i>Mm</i>	PRPF8	ECD	606	20.8
<i>Mm</i>	PRPF8	WDR57	591	46.5
<i>Mm</i>	PRPF8	C20orf4	574	33.9
<i>Mm</i>	PRPF8	NCDN	558	19.3

<i>Mm</i>	PRPF8	SNW1	554	22.9
<i>Mm</i>	PRPF8	CRNKL1	521	12.8
<i>Mm</i>	PRPF8	PRPF31	515	24.6
<i>Mm</i>	PRPF8	PLRG1	494	30.7
<i>Mm</i>	PRPF8	SNRPB	470	31.2
<i>Mm</i>	PRPF8	CD2BP2	465	26.7
<i>Mm</i>	PRPF8	RUVBL1	448	19.7
<i>Mm</i>	PRPF8	DHX15	403	11.2
<i>Mm</i>	PRPF8	EAPP	383	19.3
<i>Mm</i>	PRPF8	TSSC4	339	41.7
<i>Mm</i>	PRPF8	SNRPD2	312	49.2
<i>Mm</i>	PRPF8	PRPF19	306	16.1
<i>Mm</i>	PRPF8	SNRPD3	290	47.6
<i>Mm</i>	PRPF8	NP_006848.1	243	23.9
<i>Mm</i>	PRPF8	RAB43	238	17.9
<i>Mm</i>	PRPF8	SYF2	210	23
<i>Mm</i>	PRPF8	SNRPD1	202	37.8
<i>Mm</i>	PRPF8	ZNHIT2	186	12.7
<i>Mm</i>	PRPF8	DHX38	182	3.3
<i>Mm</i>	PRPF8	RSRC1	166	14.9
<i>Mm</i>	PRPF8	C9orf78	164	12.8
<i>Mm</i>	PRPF8	BCAS2	143	21.8
<i>Mm</i>	PRPF8	TTC27	135	3.4
<i>Mm</i>	PRPF8	LSM4	133	25.2
<i>Mm</i>	PRPF8	SNRPE	132	30.8
<i>Mm</i>	PRPF8	PPIE	130	9.6
<i>Mm</i>	PRPF8	LSM8	123	27.1
<i>Mm</i>	PRPF8	CWC15	123	14
<i>Mm</i>	PRPF8	PPIH	123	17.2
<i>Mm</i>	PRPF8	NHP2L1	120	18.8
<i>Mm</i>	PRPF8	SNRPG	111	17.1
<i>Mm</i>	PRPF8	CCDC12	108	7.8
<i>Mm</i>	PRPF8	DHX35	104	3.1
<i>Mm</i>	PRPF8	PPIL1	81	16.9
<i>Hs</i>	PTTG1	[Hs] PTTG1	85	12.4
<i>Hs</i>	PTTG1	ESPL1	2778	32
<i>Hs</i>	PTTG1	DECR1	72	7.8
<i>Mm</i>	PTTG1	[Mm] PTTG1	56	9
<i>Mm</i>	PTTG1	CLTC	87	1.4
<i>Mm</i>	RAB4A	[Mm] RAB4A	0	0
<i>Mm</i>	RAB4A	EIF4A3	132	3.4
<i>Mm</i>	RAB5C	[Mm] RAB5C	1078	85.6
<i>Mm</i>	RAB5C	GDI2	987	50.2
<i>Mm</i>	RAB5C	APOD	285	28
<i>Mm</i>	RAB5C	FABP5	176	51.5
<i>Mm</i>	RAB5C	PIP	159	28.8
<i>Mm</i>	RAB5C	LGALS7	124	16.9
<i>Mm</i>	RAB5C	NM_001014342.1	96	0.8
<i>Mm</i>	RAB5C	CTSD	64	4.1
<i>Mm</i>	RAB8A	[Mm] RAB8A	159	15.9
<i>Mm</i>	RAB8A	MICAL2	245	9.2
<i>Mm</i>	RAB8A	SYTL4	148	6.3
<i>Mm</i>	RACGAP1	[Mm] RACGAP1	1304	55.4
<i>Mm</i>	RACGAP1	SHCBP1	1589	54.3
<i>Mm</i>	RACGAP1	KIF23	1233	33.3
<i>Mm</i>	RACGAP1	RACGAP1	1214	48.6
<i>Mm</i>	RACGAP1	CD2AP	589	26.3
<i>Mm</i>	RACGAP1	MICAL3	406	22.4
<i>Mm</i>	RACGAP1	MICAL3	359	9.7
<i>Mm</i>	RAD21	[Mm] RAD21	1239	37.3
<i>Mm</i>	RAD21	SMC1A	3724	52.1
<i>Mm</i>	RAD21	SMC3	3485	49.1
<i>Mm</i>	RAD21	PDS5B	1024	15.8

## 5 Appendix

Mm	RAD21	STAG1	1023	17.4
Mm	RAD21	RAD21	741	22.5
Mm	RAD21	WAPAL	563	13.2
Mm	RAD21	STAG2	338	4.8
Mm	RAD21	PDS5A	251	4.6
Mm	RAE1	[Mm] RAE1	0	0
Mm	RANBP2	[Mm] RANBP2	8731	57.6
Mm	RANBP2	RANBP2	2686	19
Mm	RANBP2	RANGAP1	2144	56.2
Mm	RANBP2	KPNB1	1328	33.1
Mm	RANBP2	RCC1	609	40.6
Mm	RANBP2	NUSAP1	527	29.5
Mm	RANBP2	NXF1	505	17.1
Mm	RANBP2	RAN	472	40.7
Mm	RANBP2	UBE2I	429	34.8
Mm	RANBP2	KIFC1	418	14.6
Mm	RANBP2	IMA2_HUMAN	296	15.7
Mm	RANBP2	KPNA4	198	8.8
Mm	RANBP2	RANBP1	197	44.3
Mm	RANBP2	SUMO1P3	179	29.7
Mm	RANBP2	BICD2	142	3.9
Mm	RANBP2	NUMA1	142	1.8
Mm	RANBP2	KPNA3	91	5.4
Mm	RANBP2	SUMO3	82	20.4
Mm	RANBP2	SUMO2	77	31
Mm	RASSF1	[Mm] RASSF1	633	41.5
Mm	RASSF1	STK4	1403	55
Mm	RASSF1	STK3	1149	53
Mm	RASSF1	VAPA	326	29.8
Mm	RASSF1	VAPB	171	26.3
Mm	RASSF1	TMEM109	128	12.8
Mm	RASSF1	MAP1S	85	2.5
Mm	RASSF1	KIAA1754	77	4.6
Mm	RECQL4	[Mm] RECQL4	918	19.5
Mm	RECQL4	GNAI2	162	12.7
Mm	RECQL4	or: GNAI3	162	12.7
Mm	RECQL4	STOM	159	10.8
Mm	RECQL4	ATAD3C	128	7.6
Mm	RECQL4	CHCHD3	108	11.5
Mm	RECQL4	HNRNPU	97	3.1
Mm	RECQL4	HNRNPA2B1	71	7.6
Mm	RHOA	[Mm] RHOA	367	35.2
Mm	RHOA	NM_001014342.1	86	0.9
Mm	SASS6	[Mm] SASS6	1284	52.6
Mm	SASS6	FSCN1	537	31
Mm	SASS6	TPM2	528	27.8
Mm	SASS6	TPM1	515	28.9
Mm	SASS6	PPP1R12A	495	10
Mm	SASS6	TMOD3	385	34.7
Mm	SASS6	CALD1	302	18
Mm	SASS6	CORO1C	212	13.5
Mm	SASS6	PPP1CC	171	21.1
Mm	SASS6	or: PPP1CB	171	20.8
Mm	SASS6	C17orf84	150	3.8
Mm	SASS6	C19orf21	84	4.6
Mm	SASS6	PLS3	79	6.4
Mm	SASS6	SASS6	74	5.6
Mm	SF3A1	[Mm] SF3A1	2092	57.3
Mm	SF3A1	SF3B1	3253	56.1
Mm	SF3A1	SF3B3	2550	47.2
Mm	SF3A1	DDX46	2494	45.1
Mm	SF3A1	SF3B2	1539	38.8
Mm	SF3A1	HTATSF1	1430	38.8

Mm	SF3A1	SF3A3	1319	51.5
Mm	SF3A1	DHX15	1148	32.8
Mm	SF3A1	O15042_HUMAN	645	16.3
Mm	SF3A1	DDX42	590	16.2
Mm	SF3A1	SNRPA1	575	89.7
Mm	SF3A1	SF3A2	509	21.1
Mm	SF3A1	CCDC97	416	41.1
Mm	SF3A1	SF3B4	374	25.7
Mm	SF3A1	SNRPD2	344	49.2
Mm	SF3A1	LEPRE1	337	10.5
Mm	SF3A1	CHERP	305	8.8
Mm	SF3A1	WDR61	286	29.5
Mm	SF3A1	RBM39	285	12.9
Mm	SF3A1	SNRPB	268	19.5
Mm	SF3A1	PM14_HUMAN	267	40.8
Mm	SF3A1	PHF5A	245	40.9
Mm	SF3A1	SNRPD3	241	47.6
Mm	SF3A1	SNRPB2	240	24.4
Mm	SF3A1	CRTAP	222	14
Mm	SF3A1	RBM17	203	14.5
Mm	SF3A1	SF3B5	201	55.8
Mm	SF3A1	SNRPD1	174	45.4
Mm	SF3A1	SNRPE	155	30.8
Mm	SF3A1	DNAJC8	136	17.4
Mm	SF3A1	TTC33	125	13
Mm	SF3A1	CCDC75	116	12.3
Mm	SF3A1	SNRPG	78	17.1
Mm	SF3A1	SNRPF	73	24.4
Mm	SGOL1	[Mm] SGOL1	372	19.1
Mm	SGOL1	LGALS7	177	27.2
Mm	SGOL2	[Mm] SGOL2	2471	47.3
Mm	SGOL2	SGOL2	1016	20.2
Mm	SGOL2	PPP2R5E	544	19.9
Mm	SGOL2	PPP2R5A	478	19.8
Mm	SGOL2	PPP2R1B	288	10.5
Mm	SGOL2	PPP2CA	215	16.2
Mm	SGOL2	SET	207	19.1
Mm	SGOL2	PPP2R1A	204	7.1
Mm	SGOL2	DHX30	85	1.7
Mm	SGOL2	GNL3	78	3.9
Mm	SGOL2	MYBBP1A	71	1.4
Mm	SHOC2	[Mm] SHOC2	858	25.9
Mm	SHOC2	SUGT1	457	29.4
Mm	SHOC2	SCRIB	206	2.6
Mm	SHOC2	NACA	198	19.5
Mm	SHOC2	RBMX	130	9.2
Mm	SHOC2	HNRNPA2B1	101	7.6
Mm	SHOC2	NP_001005472.1	100	7.8
Mm	SHOC2	or: ENSG00000215576	100	7.8
Mm	SHOC2	or: XP_371273.1	100	7.9
Mm	SHOC2	HNRPAB	97	8.4
Mm	SHOC2	SERBP1	84	7
Mm	SHOC2	FUS	81	16.6
Mm	SHOC2	HNRPD	81	7.8
Mm	SHOC2	SUB1	72	15.7
Mm	SHOC2	TMPO	71	9.3
Mm	SLC25A4	[Mm] SLC25A4	86	7
Mm	SLC25A4	BCLAF1	66	2
Mm	SMAD3	[Mm] SMAD3	643	41.5
Mm	SMAD3	LEMD3	544	18.3
Mm	SMAD3	AHSG	95	3.5
Mm	SMC6	[Mm] SMC6	976	16.2
Mm	SMC6	SMC5	2814	40.4

## 5 Appendix

Mm	SMC6	SMC6	1683	30
Mm	SMC6	NSMCE4A	552	22.1
Mm	SMC6	NSMCE2	536	36.4
Mm	SMC6	NDNL2	493	38.8
Mm	SMC6	TUFT1	460	25.4
Mm	SMC6	NSMCE1	367	21.4
Mm	SMC6	RAD18	150	8.5
Mm	SNW1	[Mm] SNW1	1146	50.4
Mm	SNW1	ASCC3L1	1213	18.1
Mm	SNW1	EFTUD2	1078	24.3
Mm	SNW1	CDC5L	905	32.4
Mm	SNW1	SAAL1	778	33.1
Mm	SNW1	PRPF19	469	37.5
Mm	SNW1	XAB2	422	12.9
Mm	SNW1	SNW1	422	20.3
Mm	SNW1	AQR	405	6.8
Mm	SNW1	HOMER3	402	33.8
Mm	SNW1	SYF2	375	23
Mm	SNW1	PLRG1	356	26.1
Mm	SNW1	WDR57	334	38.6
Mm	SNW1	HOMER1	263	21.2
Mm	SNW1	CCDC12	219	33.1
Mm	SNW1	CRNKL1	214	6
Mm	SNW1	RAB43	206	17.5
Mm	SNW1	PPIL1	205	26.5
Mm	SNW1	PPIE	200	15.6
Mm	SNW1	C20orf4	198	18.2
Mm	SNW1	RSRC1	179	18.8
Mm	SNW1	CDC40	178	8.2
Mm	SNW1	DHX15	132	4.2
Mm	SNW1	SNRPD3	124	24.6
Mm	SNW1	C21orf66	115	5.5
Mm	SNW1	CWC15	106	15.4
Mm	SNW1	SNRPD2	72	16.1
Mm	SNW1	SNRPD1	72	20.2
Mm	SNW1	SNRPE	71	25
Mm	SPAG5	[Mm] SPAG5	2328	45.9
Mm	SPAG5	SPAG5	2118	45.5
Mm	SPAG5	C15orf23	973	52.5
Mm	SPAG5	CDK5RAP2	682	15.1
Mm	SPAG5	SNAP29	613	62
Mm	SPAG5	DYNLL1	284	64
Mm	SPAG5	DYNLL2	193	50.6
Mm	SPAG5	ATAD3B	178	16.4
Mm	SPAG5	or: ENSG00000215733	178	8.7
Mm	SPAG5	WDR68	124	8.2
Mm	SPAG5	TROAP	122	6.6
Mm	SPC24	[Mm] SPC24	145	18.1
Mm	SPC24	LMO7	195	3.7
Mm	STAG2	[Mm] STAG2	2361	40.8
Mm	STAG2	SMC1A	4143	56.5
Mm	STAG2	SMC3	3948	54.3
Mm	STAG2	PDS5B	1843	29.4
Mm	STAG2	RAD21	1444	44.2
Mm	STAG2	WAPAL	1259	28.2
Mm	STAG2	RNH1	472	22.8
Mm	STAG2	ALDH3A2	468	20.4
Mm	STAG2	PDS5A	371	7.2
Mm	TACC3	[Mm] TACC3	1264	28.3
Mm	TACC3	CKAP5	453	8
Mm	TACC3	TACC3	217	15.9
Mm	TIMELESS	[Mm] TIMELESS	1307	26.9
Mm	TIMELESS	TIPIN	368	25.6

Mm	TIMELESS	CRY1	289	17.1
Mm	TIMELESS	RPA2	83	7.4
Mm	TIPIN	[Mm] TIPIN	272	21.9
Mm	TIPIN	TIMELESS	2071	35.9
Mm	TIPIN	THRAP3	403	11.9
Mm	TIPIN	RPA2	212	26.7
Mm	TIPIN	TIPIN	155	11.3
Mm	TIPIN	RPA3	138	38.8
Mm	TIPIN	BCLAF1	120	4.3
Mm	TIPIN	PCMTD1	84	6.7
Mm	TMEM48	[Mm] TMEM48	1164	41.9
Mm	TOP2B	[Mm] TOP2B	3423	36.7
Mm	TOP2B	Q71UN1_HUMAN	1609	20.5
Mm	TOP2B	ZNF451	1092	23.5
Mm	TOP2B	TOP2B	463	4.9
Mm	TOP2B	LMO7	349	7.2
Mm	TOP2B	ITPR1	112	0.6
Mm	TOR1AIP1	[Mm] TOR1AIP1	1311	53.7
Mm	TOR1AIP1	CANX	78	3.5
Mm	TPR	[Mm] TPR	7351	52.4
Mm	TPR	TPR	1090	11
Mm	TPR	LGALS7	383	46.3
Mm	TPR	PPIA	166	23
Mm	TPR	FABP5	130	24.8
Mm	TPR	POF1B	114	4.9
Mm	TPR	AHNAK	98	0.9
Mm	TPR	TRIM29	86	3.7
Mm	TPR	PKM2	85	4.5
Mm	TRIM69	[Mm] TRIM69	129	7.4
Mm	TRIM69	DSG2	1355	40
Mm	TRIM69	FLOT1	1122	60.7
Mm	TRIM69	GNAI2	782	49.9
Mm	TRIM69	GNAI3	766	44.4
Mm	TRIM69	ALPPL2	765	37.8
Mm	TRIM69	LMO7	729	15.9
Mm	TRIM69	FLOT2	659	41.7
Mm	TRIM69	GNB2	646	41.2
Mm	TRIM69	GNAI1	635	39.3
Mm	TRIM69	GNB4	593	44.7
Mm	TRIM69	GNB1	591	46.8
Mm	TRIM69	C19orf21	574	23.6
Mm	TRIM69	GNAS	551	40
Mm	TRIM69	SPECC1	516	16.4
Mm	TRIM69	C17orf84	468	12.8
Mm	TRIM69	YES1	447	25.2
Mm	TRIM69	STOM	433	48.8
Mm	TRIM69	FYN	395	24.3
Mm	TRIM69	LYN	379	25.8
Mm	TRIM69	CPM	350	21.7
Mm	TRIM69	PACSLN3	304	19.1
Mm	TRIM69	PPP1R12A	304	7.6
Mm	TRIM69	FABP5	208	62.4
Mm	TRIM69	FOLR1	206	21.4
Mm	TRIM69	LYPD3	200	20.4
Mm	TRIM69	HNRPCL1	199	17.7
Mm	TRIM69	LGALS1	185	31.9
Mm	TRIM69	TMOD3	182	12.5
Mm	TRIM69	RRAS2	171	19.1
Mm	TRIM69	ABCG2	168	4.9
Mm	TRIM69	RTN4RL2	161	10
Mm	TRIM69	GPRC5A	160	18.8
Mm	TRIM69	HNRNPU	159	5.3
Mm	TRIM69	GNG12	150	56.9

## 5 Appendix

<i>Mm</i>	TRIM69	SVIL	138	2.6
<i>Mm</i>	TRIM69	PKM2	129	9.8
<i>Mm</i>	TRIM69	ALDH18A1	125	4.7
<i>Mm</i>	TRIM69	NEXN	79	4.6
<i>Mm</i>	TRIM69	RBMX	67	6.6
<i>Mm</i>	TTK	[Mm] TTK	1101	36.6
<i>Mm</i>	TTK	NM_001014342.1	112	1.3
<i>Mm</i>	TTK	CTSD	88	4.6
<i>Mm</i>	TTK	TGM1	77	3.4
<i>Hs</i>	TTK	[Hs] TTK	1822	49.6
<i>Mm</i>	TUBA1B	[Mm] TUBA1B	1200	58.1
<i>Mm</i>	TUBA1B	DNAJA1	126	6.3
<i>Mm</i>	TUBA3D	[Mm] TUBA3D	714	45.3
<i>Mm</i>	TUBA3D	ACTR1A	325	27.7
<i>Mm</i>	TUBA3D	DCTN1	308	7.4
<i>Mm</i>	TUBA3D	PFDN2	177	29.9
<i>Mm</i>	TUBA3D	PFDN4	114	20.1
<i>Mm</i>	TUBA3D	VBP1	107	11.7
<i>Mm</i>	TUBA3D	DCTN2	105	11.6
<i>Mm</i>	TUBA3D	AIFM1	100	6.4
<i>Mm</i>	TUBB	[Mm] TUBB	1912	73.2
<i>Mm</i>	TUBB	TBCD	866	22.9
<i>Mm</i>	TUBB	DNAJA1	721	46.7
<i>Mm</i>	TUBB	TCP11L1	363	13
<i>Mm</i>	TUBB	AIFM1	346	12.8
<i>Mm</i>	TUBB	DNAJA2	179	11.7
<i>Mm</i>	TUBB	PNKD	148	30.3
<i>Mm</i>	TUBB	THBS1	120	3.5
<i>Mm</i>	TUBB	NME2	100	33.8
<i>Mm</i>	TUBB	CDKN2A	72	15.6
<i>Mm</i>	TUBB	DNAJA4	61	5
<i>Mm</i>	TUBB2C	[Mm] TUBB2C	2102	75.7
<i>Mm</i>	TUBB2C	TBCD	1338	28
<i>Mm</i>	TUBB2C	AIFM1	909	42.6
<i>Mm</i>	TUBB2C	MAP7D1	689	18.9
<i>Mm</i>	TUBB2C	DNAJA1	570	38.8
<i>Mm</i>	TUBB2C	DNAJA2	370	17.2
<i>Mm</i>	TUBB2C	VBP1	242	25.4
<i>Mm</i>	TUBB2C	RRAS2	235	23
<i>Mm</i>	TUBB2C	MGST3	224	18.4
<i>Mm</i>	TUBB2C	PFDN2	207	30.5
<i>Mm</i>	TUBB2C	CYC1	178	14.8
<i>Mm</i>	TUBB2C	PFDN6	156	28.7
<i>Mm</i>	TUBB2C	ICAM1	147	7.3
<i>Mm</i>	TUBB2C	CHCHD4	146	33.1
<i>Mm</i>	TUBB2C	PFDN5	138	19.5
<i>Mm</i>	TUBB2C	PFDN1	111	21.3
<i>Mm</i>	TUBB2C	PHGDH	105	3.8
<i>Mm</i>	TUBB2C	FBLN1	99	3.5
<i>Mm</i>	TUBB2C	BSG	97	14.2
<i>Mm</i>	TUBB2C	TIMM50	86	4.8
<i>Mm</i>	TUBB2C	C2orf47	76	6.5
<i>Mm</i>	TUBB2C	NME2P1	64	13.9
<i>Mm</i>	TUBG1	[Mm] TUBG1	1012	41
<i>Mm</i>	TUBG1	TUBGCP2	931	23.1
<i>Mm</i>	TUBG1	TUBGCP4	819	33.8
<i>Mm</i>	TUBG1	TUBGCP3	794	20.1
<i>Mm</i>	TUBG1	TUBGCP5	405	8.9
<i>Mm</i>	TUBG1	TUBGCP6	281	5.1
<i>Mm</i>	TUBG1	TUBG1	177	8.4
<i>Mm</i>	TUBG1	AIFM1	172	12
<i>Mm</i>	TUBG1	FAM128B	168	31
<i>Mm</i>	TUBG1	NSUN2	99	5.5



<i>Mm</i>	TUBGCP2	[Mm] TUBGCP2	460	11.3
<i>Mm</i>	TUBGCP2	TUBGCP3	168	5.9
<i>Mm</i>	TUBGCP2	TUBGCP2	138	3.4
<i>Mm</i>	TUBGCP2	FAM128B	118	22.8
<i>Mm</i>	TUBGCP2	TUBG2	99	6.7
<i>Mm</i>	TUBGCP3	[Mm] TUBGCP3	2672	55.4
<i>Mm</i>	TUBGCP3	TUBGCP2	2614	56.9
<i>Mm</i>	TUBGCP3	TUBGCP3	976	21.6
<i>Mm</i>	TUBGCP3	TUBGCP5	955	20.8
<i>Mm</i>	TUBGCP3	NEDD1	916	32.9
<i>Mm</i>	TUBGCP3	TUBGCP4	901	31.1
<i>Mm</i>	TUBGCP3	TUBG1	849	57.6
<i>Mm</i>	TUBGCP3	TUBGCP6	482	7
<i>Mm</i>	TUBGCP3	FAM128B	348	51.9
<i>Mm</i>	TUBGCP3	NEXN	345	14
<i>Mm</i>	TUBGCP3	TMOD3	304	21.9
<i>Mm</i>	TUBGCP3	C19orf21	202	8.7
<i>Mm</i>	TUBGCP3	Q5VXS7_HUMAN	193	52.4
<i>Mm</i>	UBE1	[Mm] UBE1	3994	73.9
<i>Mm</i>	UBE1	NM_001014342.1	173	2
<i>Mm</i>	UBE1	PIP	130	19.2
<i>Mm</i>	UBE2C	[Mm] UBE2C	514	46.9
<i>Mm</i>	WAPAL	[Mm] WAPAL	0	0
<i>Hs</i>	WAPAL	[Hs] WAPAL	4724	71.7
<i>Hs</i>	WAPAL	SMC1A	3879	59.6
<i>Hs</i>	WAPAL	SMC3	3138	48.9
<i>Hs</i>	WAPAL	PDS5A	3025	43.8
<i>Hs</i>	WAPAL	PDS5B	2367	31.9
<i>Hs</i>	WAPAL	RAD21	1487	44.7
<i>Hs</i>	WAPAL	WAPAL	1419	26.7
<i>Hs</i>	WAPAL	STAG1	767	12.9
<i>Hs</i>	WAPAL	STAG2	346	6.2
<i>Mm</i>	WDR38	[Mm] WDR38	0	0
<i>Mm</i>	WDR51B	[Mm] WDR51B	641	32.8
<i>Mm</i>	WDR51B	CALD1	659	33.6
<i>Mm</i>	WDR51B	WDR51A	319	25.6
<i>Mm</i>	WDR51B	TPM1	316	19
<i>Mm</i>	WDR51B	EXOC4	311	9.4
<i>Mm</i>	WDR51B	C17orf84	310	9.7
<i>Mm</i>	WDR51B	CORO1C	284	14.3
<i>Mm</i>	WDR51B	TMOD3	249	24.1
<i>Mm</i>	WDR51B	EXOC3	248	7.5
<i>Mm</i>	WDR51B	TPM2	223	15.8
<i>Mm</i>	WDR51B	RAI14	212	6.7
<i>Mm</i>	WDR51B	PKM2	180	7.5
<i>Mm</i>	WDR51B	LMO7	173	4.2
<i>Mm</i>	WDR51B	GNAI2	173	13.3
<i>Mm</i>	WDR51B	WDR51B	161	13
<i>Mm</i>	WDR51B	C19orf21	158	7.7
<i>Mm</i>	WDR51B	PPP1R12A	153	4.9
<i>Mm</i>	WDR51B	EIF4A1	151	11.1
<i>Mm</i>	WDR51B	FOLR1	134	21.4
<i>Mm</i>	WDR51B	STOM	123	19.5
<i>Mm</i>	WDR51B	HNRPK	121	11.9
<i>Mm</i>	WDR51B	SQSTM1	109	7
<i>Mm</i>	WDR51B	HSBP1	94	39
<i>Mm</i>	WDR51B	SPECC1	80	3.1
<i>Mm</i>	WDR51B	COG7	77	5.5
<i>Mm</i>	WDR51B	GNG12	76	37.5
<i>Mm</i>	WDR51B	COG5	64	6.2
<i>Mm</i>	ZW10	[Mm] ZW10	714	17.3
<i>Mm</i>	ZW10	KNTC1	2710	29.7
<i>Mm</i>	ZW10	RINT1	851	28.2

## 5 Appendix

<i>Mm</i>	ZW10	ZWILCH	836	35
<i>Mm</i>	ZW10	ZW10	744	27.7
<i>Mm</i>	ZW10	APOD	253	23.3
<i>Mm</i>	ZW10	C19orf25	207	41.6
<i>Mm</i>	ZW10	SCFD2	186	7.3
<i>Mm</i>	ZW10	NP_056993.2	66	0.9
<i>Mm</i>	ZWINT	[Mm] ZWINT	666	58.7
<i>Mm</i>	ZWINT	TACC3	936	28.9
<i>Mm</i>	ZWINT	OGT	716	14.8
<i>Mm</i>	ZWINT	EPS15	656	17.9
<i>Mm</i>	ZWINT	NUP62	506	19.2
<i>Mm</i>	ZWINT	CASC5	358	3.7
<i>Mm</i>	ZWINT	EPS15L1	232	8.3
<i>Mm</i>	ZWINT	HSF1	197	8.1
<i>Mm</i>	ZWINT	KIFC3	156	5.4
<i>Mm</i>	ZWINT	TPM2	143	10.6
<i>Mm</i>	ZWINT	NDC80	139	5
<i>Mm</i>	ZWINT	PRKCSH	132	6.8
<i>Mm</i>	ZWINT	DSN1	126	10.4
<i>Mm</i>	ZWINT	PMF1	112	17.1
<i>Mm</i>	ZWINT	GOLGA2	97	2.3
<i>Mm</i>	ZWINT	HSF2	89	3.7
<i>Mm</i>	ZWINT	NUP62CL	81	15.8
<i>Mm</i>	ZWINT	SPC24	81	9.1
<i>Mm</i>	ZWINT	EDEM3	78	2.5
<i>Mm</i>	ZWINT	THAP11	72	5.4
<i>Mm</i>	ZWINT	GANAB	69	2
<i>Mm</i>	ZWINT	NUF2	64	4.1
<i>Hs</i>	ZWINT	[Hs] ZWINT	874	62.6
<i>Hs</i>	ZWINT	CASC5	5882	58.8
<i>Hs</i>	ZWINT	RRBP1	2893	53.2
<i>Hs</i>	ZWINT	NDC80	2045	62
<i>Hs</i>	ZWINT	BUB1	1383	34.1
<i>Hs</i>	ZWINT	DSN1	1269	72.8
<i>Hs</i>	ZWINT	NUF2	1093	52.4
<i>Hs</i>	ZWINT	BUB1B	936	21.4
<i>Hs</i>	ZWINT	PMF1	846	72.2
<i>Hs</i>	ZWINT	ZWINT	795	62.4
<i>Hs</i>	ZWINT	SPC25	739	60.7
<i>Hs</i>	ZWINT	NSL1	662	57.3
<i>Hs</i>	ZWINT	MIS12	523	44.9
<i>Hs</i>	ZWINT	SPC24	520	74.6
<i>Hs</i>	ZWINT	LMNB1	256	17.6
<i>Hs</i>	ZWINT	DDX5	254	8.6
<i>Hs</i>	ZWINT	CNBP	178	20.6
<i>Hs</i>	ZWINT	DDX17	172	6.6
<i>Hs</i>	ZWINT	SMTN	157	4.8
<i>Hs</i>	ZWINT	HNRPF	157	12
<i>Hs</i>	ZWINT	CENPC1	156	5.1
<i>Hs</i>	ZWINT	HNRPH1	133	10.5
<i>Hs</i>	ZWINT	RCN1	125	8.5
<i>Hs</i>	ZWINT	TRIM28	114	4.2
<i>Hs</i>	ZWINT	CYR61	87	7.1
<i>Hs</i>	ZWINT	SNAP29	74	7.8
<i>Hs</i>	ZWINT	TRIM5	70	6.6

#### 5.4 Interaction manuscript table S3 (all annotated complexes)

Table summarising all identified clusters, annotated with complex number, baits within these clusters, known interactions of the bait within the cluster, total known interactions within the cluster, probability of observing the given number of interactions with each cluster at random, summary of mitotic screen hits per cluster, screen hits (fly: Goshima et al., 2007; human esiRNA: Kittler et al., 2007; human siRNA: Neumann et al., in preparation; worm: Sonnichsen et al., 2005).

Complex	Bait	Gene	Known interactions/bait within complex	Known interactions/complex	probability of known interactions/complex	RNAi hits/complex	Mitochek hit	Kittler et al. 2007 hit	Goshima et al. 2007 hit	Sonnichsen et al. 2005
0	X	TTK	0			1				
0		TGM1	0			1				
1		THBS1	0	1	6.47E-02	4				
1		PNKD	0	1	6.47E-02	4		X		
1		NME2	0	1	6.47E-02	4				
1		TUBB	0	1	6.47E-02	4		X		
1		TBCD	1	1	6.47E-02	4				X
1		DNAJA2	0	1	6.47E-02	4				
1		TCP11L1	0	1	6.47E-02	4				
1		CDKN2A	0	1	6.47E-02	4	X			
1		DNAJA4	0	1	6.47E-02	4				
2		TPM1	1	1	5.40E-03					
2		TPM2	1	1	5.40E-03					
2		CALD1	0	1	5.40E-03					
3		LTF	0							
3		WFDC2	0							
3		C20orf114	0							
3		TCN1	0							
3		PLUNC	0							
3		AZGP1	0							
4		NXF1	0	4	4.60E-06	6		X		
4		SUMO2	2	4	4.60E-06	6				
4		NUSAP1	0	4	4.60E-06	6	X			
4		SUMO3	1	4	4.60E-06	6			X	
4		SUMO1P3	1	4	4.60E-06	6	X			
4		RANBP1	1	4	4.60E-06	6				
4		NUMA1	0	4	4.60E-06	6				
4		UBE2I	4	4	4.60E-06	6				
4		RCC1	1	4	4.60E-06	6	X			X
5		FANCE	0	3	3.62E-03	2	X			
5		CXorf23	0	3	3.62E-03	2				
5		CHCHD6	0	3	3.62E-03	2				
5		BAT1/UAP56_HUMAN/DDX39	4	3	3.62E-03	2				
5		C1orf77	1	3	3.62E-03	2				
5		C14orf173	0	3	3.62E-03	2				

## 5 Appendix

5		SAMM50	0	3	3.62E-03	2				
5		POLDIP3	0	3	3.62E-03	2				
5		PRMT1	0	3	3.62E-03	2	X			
5		C10orf18	0	3	3.62E-03	2				
5		THOC4/ENSG00000215640	1	3	3.62E-03	2				
5	X	ERH	0	3	3.62E-03	2		X		
6		SIRT1	0			5		X		
6		MRPS7	0			5		X		
6	X	CDCA8	0			5	X	X	X	
6		EBNA1BP2	0			5				
7		FANCB	1	1	1.08E-02	2				
7		LASP1	0	1	1.08E-02	2				
7	X	FANCC	0	1	1.08E-02	2	X	X		
7		C17orf70	1	1	1.08E-02	2				
8	X	DDX41	0			4	X	X		
8		NKAP	0			4	X	X		
9		PFN1	0			1				
9		ALDOA	0			1	X			
9		TPI1	0			1				
10	X	RAB5C	0			1				
10		GDI2	0			1		X		
10		APOD	0			1				
11	X	ZW10	3	4	4.83E-07	4	X			
11		NP_056993.2	0	4	4.83E-07	4				X
11		ZWILCH	2	4	4.83E-07	4	X			
11		SCFD2	0	4	4.83E-07	4				
11		RINT1	1	4	4.83E-07	4		X		
11		KNTC1	2	4	4.83E-07	4				
11		C19orf25	0	4	4.83E-07	4				
12	X	MARK2	0			1				
12		KIAA0802	0			1				
13		Q8TBD9_HUMAN	0							
13	X	CEP78	0							
13		NAP1L4	0							
14		CBX3	0			2		X		
14		AKAP8	0			2		X		
14		TRIM29	0			2				
14		AKAP8L	0			2				
14		CALU	0			2				
14		MYPN	0			2				
15	X	FAM107B	0			1		X		
15		PLOD2	0			1				
15		PLOD1	0			1				
16		VPS13B	0	14	1.39E-13	2				
16		NME2P1/NME2	0	14	1.39E-13	2				
16		LTV1	0	14	1.39E-13	2		X		
16		SNX24	0	14	1.39E-13	2				
16		PER3	5	14	1.39E-13	2				
16		TSR1	0	14	1.39E-13	2				
16	X	CSNK1E	0	14	1.39E-13	2				
16		RPSAP15	0	14	1.39E-13	2				
16		MIF	0	14	1.39E-13	2				
16		FAM110B	0	14	1.39E-13	2				
16		CRY2	3	14	1.39E-13	2	X			
16		PER2	5	14	1.39E-13	2				
16		RRP12	0	14	1.39E-13	2				

16		MCC	1	14	1.39E-13	2				
16		SFRS2	0	14	1.39E-13	2				
16		STOX2	0	14	1.39E-13	2				
16		FAM110A	0	14	1.39E-13	2				
16		FAM83H	0	14	1.39E-13	2				
16		PER1	5	14	1.39E-13	2				
16		GAPVD1	0	14	1.39E-13	2				
16		CRY1	4	14	1.39E-13	2				
17		DNAJA1	0			3				
17	X	TUBA1B	0			3	X	X		X
18		HNRPD	0			2				
18	X	CEP152	0			2				
18		CEP63	0			2		X		
18		CENPF	0			2	X			
19	X	ESPL1	0			4	X	X		X
19		CLTC	0			4				X
19	X	PTTG1	0			4				
19		DECR1	0			4				
20		CCNO	0	26	9.71E-31	13				
20		BSG	2	26	9.71E-31	13				
20		SKP2	9	26	9.71E-31	13				
20		CPS1	0	26	9.71E-31	13				
20		CCNB1	5	26	9.71E-31	13	X			X
20		CDKN1B	5	26	9.71E-31	13				
20		PHGDH	0	26	9.71E-31	13				
20		WDR57	2	26	9.71E-31	13				
20	X	CDC2	11	26	9.71E-31	13	X	X		
20		CCNA2	6	26	9.71E-31	13	X	X		
20		PKMYT1	2	26	9.71E-31	13				
20		CKS1B	5	26	9.71E-31	13				X
20		CCNB2	2	26	9.71E-31	13				
20		EFTUD2	2	26	9.71E-31	13	X	X		
20		PDLIM7	2	26	9.71E-31	13				
20		CDC25C	4	26	9.71E-31	13				
20		ASCC3L1	2	26	9.71E-31	13	X			
20		WEE1	2	26	9.71E-31	13	X	X		
20		CKS2	2	26	9.71E-31	13				
20		CDKN1C	1	26	9.71E-31	13				
20		SKP1A	4	26	9.71E-31	13				
20		C20orf4	0	26	9.71E-31	13		X		
21	X	CBX1	0			1	X			
21		RCN2	0			1				
22		GNAI1/GNAI3/GNAI2	0			1				
22	X	RECQL4	0			1				
22		STOM	0			1				
22		ATAD3C	0			1				
22		HNRNPU	0			1		X		
23	X	SMAD3	0			1	X			
23		LEMD3	0			1				
24		DYNLL2	1	1	1.80E-03	2				
24	X	DYNLL1	1	1	1.80E-03	2		X		X
25		MAFF	0	1	3.78E-02	1				
25		FAM83D	0	1	3.78E-02	1				
25	X	BACH1	1	1	3.78E-02	1				
25		HMMR	0	1	3.78E-02	1	X			
25		MAFK	1	1	3.78E-02	1				

# 5 Appendix

25		MAFG/ENSG00000215622	0	1	3.78E-02	1				
26	X	CDC16	6	32	6.85E-55	14	X			
26		ANAPC7	9	32	6.85E-55	14				
26		ANAPC10	9	32	6.85E-55	14	X	X		
26	X	CDC27	8	32	6.85E-55	14	X	X		
26	X	CDC20	3	32	6.85E-55	14	X	X		X
26	X	MAD2L1	3	32	6.85E-55	14	X			
26	X	CDC23	4	32	6.85E-55	14	X			
26		ANAPC1	3	32	6.85E-55	14				X
26		ANAPC13	0	32	6.85E-55	14				
26		C10orf104	0	32	6.85E-55	14				
26		ANAPC4	9	32	6.85E-55	14	X			
26		CDC26	0	32	6.85E-55	14				
26		ANAPC2	4	32	6.85E-55	14	X			
26		ANAPC5	3	32	6.85E-55	14	X			
27		MRT04	0	2	3.91E-03					
27	X	MKI67	1	2	3.91E-03					
27		SFPQ	1	2	3.91E-03					
27		KPNA4	0	2	3.91E-03					
27		KPNA1	0	2	3.91E-03					
27		KPNA6	0	2	3.91E-03					
27		MKI67IP	1	2	3.91E-03					
27		NONO	1	2	3.91E-03					
27		KPNA3	0	2	3.91E-03					
28		NP_689929.1	0	5	2.79E-08					
28		HADHB	1	5	2.79E-08					
28		AP2B1	3	5	2.79E-08					
28		AP2M1	3	5	2.79E-08					
28		EDC3	1	5	2.79E-08					
28		HADHA	1	5	2.79E-08					
28		AP2A1	2	5	2.79E-08					
28		DCP2	1	5	2.79E-08					
29		TTC33	0	41	3.87E-48	23				
29		CRTAP	0	41	3.87E-48	23	X			
29		PM14_HUMAN	6	41	3.87E-48	23		X	X	
29		SF3B4	6	41	3.87E-48	23		X	X	
29		SF3A2	18	41	3.87E-48	23			X	
29		CCDC75	0	41	3.87E-48	23				
29		O15042_HUMAN	0	41	3.87E-48	23				
29	X	SF3A1	2	41	3.87E-48	23	X	X	X	
29		DDX42	1	41	3.87E-48	23				
29		LEPRE1	0	41	3.87E-48	23				
29		SF3B3	5	41	3.87E-48	23		X	X	
29		HTATSF1	2	41	3.87E-48	23				
29		SNRPF	1	41	3.87E-48	23	X	X	X	
29		SF3A3	2	41	3.87E-48	23		X	X	
29		SNRPA1	5	41	3.87E-48	23		X		
29		PHF5A	5	41	3.87E-48	23				
29		CHERP	0	41	3.87E-48	23				
29		SNRPB2	6	41	3.87E-48	23		X		
29		CCDC97	0	41	3.87E-48	23				
29		DNAJC8	1	41	3.87E-48	23				
29		RBM17	1	41	3.87E-48	23				
29		SF3B5	9	41	3.87E-48	23	X		X	
29		DDX46	1	41	3.87E-48	23				
29		SF3B2	6	41	3.87E-48	23				

29		WDR61	0	41	3.87E-48	23	X			
29		SF3B1	6	41	3.87E-48	23	X	X		
29		RBM39	1	41	3.87E-48	23				
30	X	LCK	0			1	X			
30		CSTA	0							
31		Q71UN1_HUMAN	0			4			X	X
31		ZNF451	0			4				
31	X	TOP2B	0			4				X
31		ITPR1	0			4	X			
32		FABP5	0			4				
32		PKM2	0			4				
32		TF	0			4		X		
32		PPIA	0			4				
32		VCP	0			4				X
32		POF1B	0			4	X			
32		LGALS7	0			4				
32	X	AKAP12	0			4		X		
32		SPRR2E	0			4				
32		SBSN	0			4				
33		ZMYM4	0			1				
33		PGAM5	0			1				
33	X	MAD2L2	0			1				
33		GTF2I	0			1	X			
33		ALDH3A2	0			1				
33		C13orf8	0			1				
33		POGZ	0			1				
33		BAT8_HUMAN/EHMT2	0			1				
33		ZNF644	0			1				
33		FAM35A	0			1				
33		EHMT1	0			1				
33		C20orf196	0			1				
34	X	ATM	0							
34		WDR42A	0							
34		LMNB1	0							
34		IQWD1	0							
34		CUL4A	0							
35		BICD2	0			3				
35	X	PLK1	0			3	X	X	X	
35		ERCC6L	0			3				
36	X	TOR1AIP1	0			6	X			
36		INSR	0			6				
36	X	KIF20A	0			6	X	X		
36	X	MAD2L1BP	0			6				
36		NUDT5	0			6				
36		TPX2	0			6	X	X		
36		ANTXR1	0			6				
36		MAD1L1	0			6	X			
36		C1orf52	0			6				
37		TLN2	0	3	1.57E-04					
37		C9orf140	0	3	1.57E-04					
37		VCL	2	3	1.57E-04					
37		TLN1	2	3	1.57E-04					
37		ENSG00000205476	0	3	1.57E-04					
37		CTNNA1	1	3	1.57E-04					
37	X	CEP350	0	3	1.57E-04					
37		TES	1	3	1.57E-04					

## 5 Appendix

37		PAWR	0	3	1.57E-04					
38		PTMS	0							
38		NACA	0							
39		TUBGCP6	0	1	2.70E-02	7	X		X	
39	X	TUBG1	1	1	2.70E-02	7			X	X
39		TUBGCP4	1	1	2.70E-02	7			X	
39		Q5VXS7_HUMAN	0	1	2.70E-02	7				
39	X	NEDD1	0	1	2.70E-02	7		X	X	
39		TUBGCP5	0	1	2.70E-02	7				
40	X	BUB1B	0			4	X	X	X	
40		XPINPEP3	0			4	X			
40		PDE4D	0			4				
40		UBR5	0			4				
40		ASAH1	0			4				
41		SMC1A	7	27	1.15E-65	5	X			
41		STAG1	7	27	1.15E-65	5		X		X
41		PDS5B	6	27	1.15E-65	5				
41		SMC3	7	27	1.15E-65	5	X			
41	X	WAPAL	7	27	1.15E-65	5				
41	X	PDS5A	6	27	1.15E-65	5				
41	X	RAD21	7	27	1.15E-65	5	X			
41	X	STAG2	7	27	1.15E-65	5				
42	X	SGOL2	3	8	3.88E-13	3	X			
42		PPP2R5A	4	8	3.88E-13	3				
42	X	PPP2R1A	1	8	3.88E-13	3	X			X
42		MYBBP1A	1	8	3.88E-13	3				
42		XP_496190.1	0	8	3.88E-13	3				
42		DHX30	1	8	3.88E-13	3				
42		PPP2R1B	3	8	3.88E-13	3				
42		GNL3	1	8	3.88E-13	3				
42		PPP2R5E	2	8	3.88E-13	3				
43		SNRPB/SNURF	4	11	2.11E-07	4				
43		GPATCH4	0	11	2.11E-07	4				
43		DKC1	0	11	2.11E-07	4				
43		NOLC1	1	11	2.11E-07	4				
43		LARP7	0	11	2.11E-07	4				
43		RRP9	0	11	2.11E-07	4				
43		ZNHIT3	0	11	2.11E-07	4				
43		NOLA2	0	11	2.11E-07	4		X		
43		URB1	0	11	2.11E-07	4				
43		WDR43	0	11	2.11E-07	4		X		
43		NUFIP1	0	11	2.11E-07	4				
43		PINX1_HUMAN	3	11	2.11E-07	4				
43		NOP5_HUMAN	0	11	2.11E-07	4				
43		TGS1	1	11	2.11E-07	4				
43		PABPC4/PABPC1	2	11	2.11E-07	4				
43		COIL	4	11	2.11E-07	4				
43		NOL5A	0	11	2.11E-07	4				
43		HNRPUL1	1	11	2.11E-07	4				
43		WDR79	0	11	2.11E-07	4				
43		C1orf181	0	11	2.11E-07	4				
43		NOLA3	0	11	2.11E-07	4				
43		SSB	0	11	2.11E-07	4				
43		DHX9	3	11	2.11E-07	4				
43		FBL	1	11	2.11E-07	4	X			
43		TARDBP	0	11	2.11E-07	4				



43		SART3	2	11	2.11E-07	4	X			
43		MOV10	0	11	2.11E-07	4				
44		KIAA1967	0	1	5.03E-02	2				
44		ZFP106	0	1	5.03E-02	2				
44		HERC2	0	1	5.03E-02	2				
44		PCYT1A	0	1	5.03E-02	2		X		
44		NP_115818.2	0	1	5.03E-02	2				
44		RALY	1	1	5.03E-02	2				
44		KIFC3	0	1	5.03E-02	2	X			
44		WDR62	1	1	5.03E-02	2				
45		GPRC5A	0			2				
45	X	TRIM69	0			2				
45		LYN	0			2				
45		LYPD3	0			2				
45		YES1	0			2				
45		PACSIN3	0			2				
45		CPM	0			2	X			
45		FYN	0			2				
45		RRAS2	0			2				
45		LGALS1	0			2				
45		SVIL	0			2				
45		NEXN	0			2				
45		ABCG2	0			2				
45		HNRPCL1	0			2				
45		GNB4	0			2	X			
46	X	WDR51B	0			2				
46		EXOC3	0			2	X			
46		HSBP1	0			2	X			
46		EXOC4	0			2				
46		WDR51A	0			2				
47		CSNK1A1L/CSNK1A1	0			2				X
47		FAM83B	0			2		X		
48	X	CKAP5	0			7	X	X	X	X
48		SLAIN2	0			7				
48	X	SNW1	0			7	X	X		
48	X	TACC3	0			7	X			
48		TACC2	0			7				
48		APC	0			7				
49		PFDN4	1	2	9.67E-05	1				
49		PFDN2	2	2	9.67E-05	1				
49		VBP1	1	2	9.67E-05	1				X
49	X	TUBA3D	0	2	9.67E-05	1				
50		PCM1	0							
50		MIB1	0							
50		RANBP5	0							
50	X	AZI1	0							
51		SEC13	1	16	2.16E-28	4				
51	X	NUP107	4	16	2.16E-28	4		X		
51	X	NUP98	5	16	2.16E-28	4				
51		NUP37	3	16	2.16E-28	4				
51		NUP160	4	16	2.16E-28	4				
51		SEH1L	2	16	2.16E-28	4				
51		NUP133	6	16	2.16E-28	4	X	X		
51		AHCTF1	4	16	2.16E-28	4				
51		NUP43	3	16	2.16E-28	4				
51		NUP85	2	16	2.16E-28	4				X

# 5 Appendix

52		AIFM1	0			3				
52	X	CDC6	0			3	X	X		X
53		RAB14	0							
53		GOLGA3	0							
53	X	CEP110	0							
54	X	AURKA	0			4	X	X		
54	X	CEP192	0			4	X	X		
55		PRPF31	0	15	8.78E-12	15				
55		LSM8	1	15	8.78E-12	15				
55		C9orf78	0	15	8.78E-12	15				
55		SART1	0	15	8.78E-12	15	X			
55		BCAS2	0	15	8.78E-12	15	X			
55		TSSC4	0	15	8.78E-12	15				
55		DHX35	0	15	8.78E-12	15				
55		PRPF3	0	15	8.78E-12	15				
55		PRPF6	4	15	8.78E-12	15	X			
55		SNRPB	4	15	8.78E-12	15			X	X
55		NP_006848.1	0	15	8.78E-12	15				
55		TFIP11	0	15	8.78E-12	15				
55		RUVBL1	0	15	8.78E-12	15				
55		PRPF4	2	15	8.78E-12	15				X
55		DHX38	1	15	8.78E-12	15				
55		EAPP	0	15	8.78E-12	15				
55	X	PRPF8	1	15	8.78E-12	15	X	X		
55	X	NHP2L1	3	15	8.78E-12	15	X	X		
55		CD2BP2	8	15	8.78E-12	15				
55		ZNHIT2	0	15	8.78E-12	15				
55		DDX23	3	15	8.78E-12	15				
55		NCDN	0	15	8.78E-12	15				
55		ECD	0	15	8.78E-12	15				
55		PPIH	1	15	8.78E-12	15		X		
55		LSM4	1	15	8.78E-12	15				
55		SNRPG	2	15	8.78E-12	15	X	X	X	X
55		TTC27	0	15	8.78E-12	15				
55		USP39	1	15	8.78E-12	15				
56	X	KIF4A	0			6	X	X	X	X
56		PRC1	0			6	X	X		
56	X	CEP170	0			6				
57		DCTN6	0			3		X		
57		CAPZA2	0			3				
57		DCTN4	0			3				X
57		DCTN5	0			3				X
57	X	DCTN3	0			3				
58		RPA2	0			1		X		
58		KIAA1128	0			1				
58		RNH1	0			1				
58		SYNE1	0			1				
58		DIXDC1	0			1				
59		RANGAP1	1	1	1.80E-03					
59	X	RANBP2	1	1	1.80E-03					
60		SHCBP1	0			3				
60		PPP2R3C	0			3				X
60	X	FGFR1OP	0			3				
60		PPP2CB/PPP2CA	0			3	X			X
61		NDEL1	0			2	X			
61	X	NDE1	0			2		X		

62	X	CDCA5	0			5	X	X		
62		LCN1L1/LCN1	0			5				
62		AURKB	0			5	X	X		X
63		PPP1CB	0			2	X	X		
63		PPP1R2	0			2				
63		PPP1R10	0			2				
64		NUP153	2	5	7.48E-11	3				
64		IMA2_HUMAN/KPNA2	2	5	7.48E-11	3				X
64		NUP50	3	5	7.48E-11	3				
64		KPNB1	3	5	7.48E-11	3		X		X
65		C13orf24	0	1	1.61E-01	2				
65		RRBP1	0	1	1.61E-01	2				
65		SNAPAP	0	1	1.61E-01	2				
65		EPS15L1	0	1	1.61E-01	2				
65		IQGAP3	0	1	1.61E-01	2				
65		MLF1IP	0	1	1.61E-01	2				
65		BEGAIN	0	1	1.61E-01	2				
65		PHKB	1	1	1.61E-01	2				
65		NPR1	0	1	1.61E-01	2				
65		PHKA2	1	1	1.61E-01	2				
65		ODF2L	0	1	1.61E-01	2				
65		CCDC101	0	1	1.61E-01	2				
65		CALCOCO1	0	1	1.61E-01	2				
65		ASPM	0	1	1.61E-01	2	X		X	
66		BTG3	2	12	3.26E-13	7		X		
66		NUDC	0	12	3.26E-13	7	X			X
66		CNOT10	0	12	3.26E-13	7				
66	X	CNOT3	3	12	3.26E-13	7		X		X
66		RAVER1	0	12	3.26E-13	7				
66		CNOT6L	0	12	3.26E-13	7				
66		FHL2	0	12	3.26E-13	7				
66		CNOT6	2	12	3.26E-13	7				
66		CNOT1	5	12	3.26E-13	7				X
66		CNOT8	7	12	3.26E-13	7				
66		CNOT2	4	12	3.26E-13	7				
66		C13orf7	0	12	3.26E-13	7				
66		RQCD1	0	12	3.26E-13	7				
66		C2orf29	0	12	3.26E-13	7				
66		CNOT7	3	12	3.26E-13	7				X
66		TOB2	2	12	3.26E-13	7				
66		TNKS1BP1	0	12	3.26E-13	7				
66		KLHL2	0	12	3.26E-13	7				
67	X	ZWINT	6	18	5.95E-31	12	X			
67		CASC5	3	18	5.95E-31	12		X		
67	X	BUB1	0	18	5.95E-31	12	X			
67		DSN1	5	18	5.95E-31	12		X		
67		PMF1	3	18	5.95E-31	12				
67		SPC25	2	18	5.95E-31	12		X		
67		NUF2	1	18	5.95E-31	12	X	X	X	
67	X	NDC80	5	18	5.95E-31	12		X	X	
67	X	SPC24	3	18	5.95E-31	12	X			
67		NSL1	2	18	5.95E-31	12				
67	X	MIS12	6	18	5.95E-31	12			X	
68		SNAP29	0			2				X
68		CDK5RAP2	0			2	X			
68		WDR68	0			2				

# 5 Appendix

68		TROAP	0			2				
68		ENSG00000215733/ATAD3B/ATAD3C	0			2				
69	X	TIPIN	1	1	1.08E-02	2		X		
69		PCMTD1	0	1	1.08E-02	2				
69	X	TIMELESS	1	1	1.08E-02	2		X		
69		RPA3	0	1	1.08E-02	2				
70		EML3	0	4	2.05E-01	7	X			
70		C5orf21	0	4	2.05E-01	7				
70		TLK2	1	4	2.05E-01	7				
70		FBXO30	0	4	2.05E-01	7				
70		CIZ1	0	4	2.05E-01	7				
70		ANKRD15	0	4	2.05E-01	7				
70		STRN3	0	4	2.05E-01	7				
70		WDR60	0	4	2.05E-01	7				
70		GPHN	0	4	2.05E-01	7				
70		RCOR1	2	4	2.05E-01	7				
70		FBXO38	0	4	2.05E-01	7				
70		TP53BP1	0	4	2.05E-01	7				
70		FAM40A	0	4	2.05E-01	7				
70		PRKAR2A	0	4	2.05E-01	7		X		
70		PAPD1	0	4	2.05E-01	7				
70		ZMYM2	0	4	2.05E-01	7				
70		TRPS1	0	4	2.05E-01	7				
70		CREB3L2	0	4	2.05E-01	7				
70		ANKRD25	0	4	2.05E-01	7				
70		STK25/NP_057626.2	1	4	2.05E-01	7	X			
70		Q9H7K0_HUMAN	0	4	2.05E-01	7				
70		TLK1	1	4	2.05E-01	7			X	
70		AOF2	1	4	2.05E-01	7				
70		ZMYM3	0	4	2.05E-01	7				
70		CTTNBP2NL	0	4	2.05E-01	7				
70		NP_001006948.1	0	4	2.05E-01	7				
70		MOBK13	0	4	2.05E-01	7				
70		STRN	0	4	2.05E-01	7	X			
70		AGGF1	0	4	2.05E-01	7				
70		GLCCI1	0	4	2.05E-01	7				
70		PDCD10	1	4	2.05E-01	7				
70		RCOR3	0	4	2.05E-01	7		X		
70		MASTL	0	4	2.05E-01	7	X			
70		ZNF609	0	4	2.05E-01	7				
70		HDAC2	1	4	2.05E-01	7				
70		MORC3	0	4	2.05E-01	7				
70		C20orf117	0	4	2.05E-01	7		X		
70		STRN4	0	4	2.05E-01	7				
71		FAM128B	0	2	2.89E-04	3				
71		TUBG1/TUBG2	2	2	2.89E-04	3	X			
71	X	TUBGCP3	2	2	2.89E-04	3			X	
71	X	TUBGCP2	0	2	2.89E-04	3			X	
72		LGALS3BP	0			2				
72	X	CUL3	0			2	X			X
72		GOLGA2	0			2				
72		KLHDC5	0			2				
73		RPSAP15/NP_001005472.1/ENSG00000215576	0	5	2.32E-06	4				
73		PDCD6IP	2	5	2.32E-06	4				
73	X	NP_710154.1	0	5	2.32E-06	4		X		

73		TSG101	5	5	2.32E-06	4		X		
73	X	CEP55	1	5	2.32E-06	4	X			
73		FBXO28	0	5	2.32E-06	4				
73		GNB2L1	0	5	2.32E-06	4				X
73		VPS37C	1	5	2.32E-06	4				
73		PCBP1	0	5	2.32E-06	4				
73		VPS28	3	5	2.32E-06	4				
74	X	DCTN2	0	2	2.89E-04	6			X	X
74	X	ACTR1A	1	2	2.89E-04	6				X
74		ACTR10	0	2	2.89E-04	6				X
74		ACTR1B	1	2	2.89E-04	6				
74	X	DCTN1	2	2	2.89E-04	6			X	X
75	X	HSD17B7	0			1	X			
75		AHSG	0			1				
76		CCDC9	0			1	X			
76	X	KIF1C	0			1				
76		THOC4	0			1				
76		AHCY	0			1				
76		SSBP1	0			1				
77	X	DTL	1	4	1.73E-08	5	X	X		
77		COPS6	2	4	1.73E-08	5				X
77		COPS4	2	4	1.73E-08	5				X
77		COPS2	2	4	1.73E-08	5				X
77		CUL4B	1	4	1.73E-08	5				
78	X	KIAA0892	0	3	7.29E-05	1				
78		LMO7	0	3	7.29E-05	1				
78	X	NIPBL	0	3	7.29E-05	1				
78		GNB1/GNB2/GNB4	3	3	7.29E-05	1	X			
78		SPECC1	0	3	7.29E-05	1				
78		GNG12	3	3	7.29E-05	1				
79		NP_219485.1	0			7				
79	X	FAM29A	0			7			X	
79		UCHL5IP	0			7				
79		C14orf94	0			7	X			
79		CCDC5	0			7	X			
79	X	CEP27	0			7		X		
79		C4orf15	0			7	X		X	
79		KIAA0841	0			7		X		
80		SET/ENSG00000203911	0							
80		SERPINB12	0							
81		CENPC1	0	4	1.33E-03	2				X
81		HNRPH1	1	4	1.33E-03	2		X		
81		DDX5	1	4	1.33E-03	2				
81		GANAB	1	4	1.33E-03	2				
81		EDEM3	0	4	1.33E-03	2				
81		HSF1	1	4	1.33E-03	2				
81		EPS15	0	4	1.33E-03	2				
81		THAP11	0	4	1.33E-03	2				
81		CNBP	0	4	1.33E-03	2				
81		TRIM5	0	4	1.33E-03	2				
81		CYR61	0	4	1.33E-03	2				
81		PRKCSH	1	4	1.33E-03	2				
81		HSF2	1	4	1.33E-03	2				
81		DDX17	1	4	1.33E-03	2				
81		SMTN	0	4	1.33E-03	2				
81		HNRPF	1	4	1.33E-03	2				

# 5 Appendix

81		TRIM28	0	4	1.33E-03	2				
81		NUP62CL	0	4	1.33E-03	2				
82	X	FBXO5	2	1	1.08E-02	3		X	X	
82		ANAPC11/ENSG00000215639	0	1	1.08E-02	3				X
82		FZR1	2	1	1.08E-02	3				
83		ARF1/ARF3	0			1				
83	X	C13orf23	0			1	X			
84		THRAP3	0	1	1.80E-02	1				
84	X	C9orf58	0	1	1.80E-02	1		X		
84		PCBP3/PCBP1/PCBP2	2	1	1.80E-02	1				
85		KIF14	0	1	3.78E-02	3	X	X		
85		LRRFIP2	0	1	3.78E-02	3				
85		TMED2	1	1	3.78E-02	3				
85		TMED4	0	1	3.78E-02	3				
85		CLIP1	0	1	3.78E-02	3				
85	X	GORASP1	1	1	3.78E-02	3	X			
85		TMED7	0	1	3.78E-02	3				
86	X	SASS6	0			3	X		X	
86		PPP1CB/PPP1CC/PPP1CA	0			3			X	
86		FSCN1	0			3				
86		PLS3	0			3				
87		PPP2R5D	1	4	4.60E-06	4				
87		PPP2CB	0	4	4.60E-06	4				
87		FECH	0	4	4.60E-06	4				
87	X	SGOL1	2	4	4.60E-06	4	X	X		
87		PPP2CA	3	4	4.60E-06	4	X			X
87		PPP2R2D	0	4	4.60E-06	4				
87		PPME1	0	4	4.60E-06	4				
87		PPP2R5C	1	4	4.60E-06	4				
87		PPP2R2A	0	4	4.60E-06	4				
88		SERPINB12	0			1				
88	X	NRIP3	0			1		X		
89	X	DYNC1H1	0			3	X		X	X
89		FOLR1	0			3				
90		NUP93	2	6	3.84E-10	2				
90	X	NUP88	3	6	3.84E-10	2				
90	X	NUP188	0	6	3.84E-10	2				
90	X	NUP214	2	6	3.84E-10	2	X			
90		XPO1	2	6	3.84E-10	2		X		
90	X	RAE1	2	6	3.84E-10	2				
90		NUP62	0	6	3.84E-10	2				
90		OGT	0	6	3.84E-10	2				
91	X	SLC25A4	0							
92		PFDN5	1	1	1.18E-01	5				X
92		MGST3	0	1	1.18E-01	5				
92		PFDN6	1	1	1.18E-01	5				
92		PFDN1	0	1	1.18E-01	5				X
92	X	TUBB2C	0	1	1.18E-01	5	X	X		
92		TIMM50	0	1	1.18E-01	5				
92		C2orf47	0	1	1.18E-01	5				
92		ICAM1	0	1	1.18E-01	5				
92		CYC1	0	1	1.18E-01	5	X			
92		FBLN1	0	1	1.18E-01	5				
92		MAP7D1	0	1	1.18E-01	5				
92		CHCHD4	0	1	1.18E-01	5				
93		CCAR1	0	1	2.70E-02	9	X			

93	X	RACGAP1	1	1	2.70E-02	9	X	X	X	X
93		CD2AP	0	1	2.70E-02	9				
93		MICAL3	0	1	2.70E-02	9	X			
93	X	KIF23	1	1	2.70E-02	9	X	X	X	
93		TRAF3IP1	0	1	2.70E-02	9				
94	X	CEP76	0							
94		ANPEP	0							
94		CACNA2D1	0							
95		EDIL3	0	3	1.04E-05	3				
95		PAFAH1B3	2	3	1.04E-05	3				
95	X	PAFAH1B1	2	3	1.04E-05	3	X	X		X
95		PAFAH1B2	2	3	1.04E-05	3				
95		XP_941179.1/KIAA1949	0	3	1.04E-05	3				
96		TMOD3	0			1				
96		PPP1R12A	0			1		X		
96		C19orf21	0			1				
97		C15orf23	0			1	X			
97	X	SPAG5	0			1				
98		FLOT2	0			1				
98		DSG2	0			1				
98		ALDH18A1	0			1				
98		GNAS	0			1	X			
98		RTN4RL2	0			1				
99	X	CEP72	0			4				
99		PPP1R12B	0			4				
99		SH2D4A	0			4	X			
99		PPP1R7	0			4		X		X
99		PPP1R8	0			4		X		
99		PPP1R11	0			4				
99		PPP1R12C	0			4				
99		YLPM1	0			4				
100		RAN	0			3		X		X
100		GPI	0			3				
100		TAGLN2	0			3	X			
100		PGK1	0			3				
100		TKT	0			3				
101	X	NEK2	0			2	X	X		
101		ACAD8	0			2				
102		SNRPD3	3	6	5.27E-12	8		X	X	X
102		SNRPD2	3	6	5.27E-12	8		X	X	X
102		SNRPD1	3	6	5.27E-12	8		X		
102		DHX15	0	6	5.27E-12	8				
102		SNRPE/SNRPEL1	0	6	5.27E-12	8				X
103		PPIE	3	5	1.38E-04	10	X			
103		RSRC1	0	5	1.38E-04	10				
103		SAAL1	0	5	1.38E-04	10				
103		CDC5L	2	5	1.38E-04	10	X	X		
103		PLRG1	2	5	1.38E-04	10	X	X		
103		CDC40	0	5	1.38E-04	10	X			
103		HOMER1	1	5	1.38E-04	10				
103		PRPF19	1	5	1.38E-04	10	X			
103		AQR	0	5	1.38E-04	10				
103		PPIL1	0	5	1.38E-04	10				
103		CCDC12	0	5	1.38E-04	10				
103		SYF2	0	5	1.38E-04	10				
103		HOMER3	1	5	1.38E-04	10				

## 5 Appendix

103		RAB43	0	5	1.38E-04	10		X		
103		C21orf66	0	5	1.38E-04	10				
103		CRNKL1	1	5	1.38E-04	10				
103		CWC15	0	5	1.38E-04	10		X	X	
103		XAB2	3	5	1.38E-04	10				
104	X	HSD17B7	0			9	X			
104	X	EIF4A3	0			9		X		
104	X	CEP192	0			9	X	X		
104		NUDC	0			9	X			X
104	X	CEP290	0			9				
104	X	RAB4A	0			9		X		
104	X	NRIP3	0			9		X		
104	X	ITSN2	0			9		X		
104	X	UBE1	0			9				
104		KLHL2	0			9				
105	X	CCDC15	0	1	6.47E-02	3				
105		SOD1	0	1	6.47E-02	3	X	X		
105		HMGB1/Q9NYD7_HUMAN	1	1	6.47E-02	3				
105		EIF4B	0	1	6.47E-02	3				
105		C1QBP	0	1	6.47E-02	3				
105		HNRPK	1	1	6.47E-02	3		X		
105		PYGM	0	1	6.47E-02	3				
105		AHNAK	0	1	6.47E-02	3				
106		SET	0			2				
106	X	PLK4	0			2	X		X	
107		TERF2	0			1				
107		TOX4	0			1				
107		C19orf7	0			1	X			
107		PPP1CC	0			1				
107		WDR82	0			1				
108		GNB2	0							
108		ALPPL2	0							
108		GNAI2	0							
108		GNAI3	0							
108		GNAI1	0							
109		RPA2	0	1	5.03E-02	5		X		
109		DDB1	0	1	5.03E-02	5		X		
109		NP_060219.2	0	1	5.03E-02	5				
109		C19orf58	0	1	5.03E-02	5				
109		COG7	2	1	5.03E-02	5	X			
109		COG5	2	1	5.03E-02	5				
109		TCEB1	0	1	5.03E-02	5				X
109	X	NEK9	0	1	5.03E-02	5	X			
110		DDX5	0	14	3.27E-08	7				
110		CAPRIN1	0	14	3.27E-08	7				
110		EIF4H	3	14	3.27E-08	7				
110		SFRS5	3	14	3.27E-08	7				
110		NRAS	2	14	3.27E-08	7				
110		SFRS6	3	14	3.27E-08	7				
110		ASS1	0	14	3.27E-08	7				
110		PHGDH	0	14	3.27E-08	7				
110		GOT2	0	14	3.27E-08	7				
110		P4HB	1	14	3.27E-08	7		X		
110		CANX	1	14	3.27E-08	7		X		
110		VDAC1/VDAC4	0	14	3.27E-08	7				
110		PA2G4	0	14	3.27E-08	7				



110		PHB	0	14	3.27E-08	7		X		
110		PDIA3	3	14	3.27E-08	7				
110	X	C11orf68	2	14	3.27E-08	7		X		
110		PDIA6	0	14	3.27E-08	7	X			
110		CALR	1	14	3.27E-08	7				
110		TFRC	0	14	3.27E-08	7				
110		RUVBL2	0	14	3.27E-08	7				
110		PDIA4	0	14	3.27E-08	7				
110		SYNCRIP/HNRNPR	5	14	3.27E-08	7				
110		PPIB	0	14	3.27E-08	7		X		
110		STRAP	0	14	3.27E-08	7				
110		PHB2	0	14	3.27E-08	7				
110		FASN	0	14	3.27E-08	7				
110		TRAP1	0	14	3.27E-08	7		X		
110		XRCC6	0	14	3.27E-08	7				
110		HNRPA3/ENSG00000176825/ENSG00000177219/ENSG00000188174	3	14	3.27E-08	7				
110		PABPC1	3	14	3.27E-08	7				
111		CORO1C	0							
111		C17orf84	0							
112		DYNLT3	0			1				
112	X	CNTROB	0			1				
112		NSUN2	0			1				
112		DYNLRB1	0			1				X
113	X	RHOA	0			8				
113	X	HSD17B7	0			8	X			
113	X	CEP192	0			8	X	X		
113		NUDC	0			8	X			X
113	X	CEP290	0			8				
113	X	RAB4A	0			8		X		
113	X	NRIP3	0			8		X		
113	X	ITSN2	0			8		X		
113	X	UBE1	0			8				
113		KLHL2	0			8				
114		SUGT1	0			1				
114		TMPO	0			1				
114		SCRIB	0			1				
114		SUB1	0			1				
114	X	SHOC2	0			1	X			
114		RPSAP15/XP_371273.1/NP_001005472.1/ENSG00000215576	0			1				
114		HNRPAB	0			1				
114		RBMX	0			1				
115		THRAP3	0							
115		BCLAF1	0							
116		PAPSS2	0			1				
116	X	PAPSS1	0			1	X			
117	X	KCTD5	0			1		X		
117		KCTD2	0			1				
118		CLASP2	0			5	X	X		
118	X	CENPE	0			5	X			
118		CLASP1	0			5	X		X	X
119	X	TMEM48	0							
120	X	UBE2C	0							
121		NARG1L	0	1	3.78E-02	1				
121	X	NAT13	0	1	3.78E-02	1				

## 5 Appendix

121	X	NARG1	0	1	3.78E-02	1		X		
121		SERF2	0	1	3.78E-02	1				
121		ARRB2	1	1	3.78E-02	1				
121	X	ARD1A	0	1	3.78E-02	1				
121		ARRB1	1	1	3.78E-02	1				
122		SYTL4	1	1	5.40E-03	2				
122		MICALL2	0	1	5.40E-03	2	X			
122	X	RAB8A	1	1	5.40E-03	2	X			
123		ARL6IP2	0	18	2.73E-29	7				
123		ENSG00000214133	0	18	2.73E-29	7				
123		ERGIC2	0	18	2.73E-29	7		X		
123		COPE	7	18	2.73E-29	7				
123		COPB1	5	18	2.73E-29	7		X		
123		SIPA1L3	0	18	2.73E-29	7				
123		ARCN1	6	18	2.73E-29	7		X		
123		BCAP31	0	18	2.73E-29	7				
123		COPZ1	5	18	2.73E-29	7		X		
123		COPB2	6	18	2.73E-29	7		X		
123		COPG	5	18	2.73E-29	7		X		
123	X	COPA	4	18	2.73E-29	7		X		
124		GTF2F1	0	10	6.06E-20	1				
124	X	GTF3C6	0	10	6.06E-20	1		X		
124		GTF3C2	4	10	6.06E-20	1				
124		GTF3C5	4	10	6.06E-20	1				
124		GTF3C3	4	10	6.06E-20	1				
124		GTF3C1	5	10	6.06E-20	1				
124		GTF3C4	5	10	6.06E-20	1				
125	X	HSP90AA1	0							
126	X	CSK	0			1		X		
127		XPC	2	2	2.89E-04	1		X		
127		C5orf37	0	2	2.89E-04	1				
127	X	CETN2	1	2	2.89E-04	1				
127		RAD23B	1	2	2.89E-04	1				
127		CETN3	0	2	2.89E-04	1				
128	X	OGG1	0			1	X			
128		LAMB1	0			1				
129	X	EEA1	0			1		X		
130	X	WDR38	0							
131	X	EDA2R	0			1		X		
132	X	HDAC6	1	1	1.08E-02	1		X		
132		USP47	0	1	1.08E-02	1				
132		GARS	0	1	1.08E-02	1				
132		PLAA	1	1	1.08E-02	1				
133	X	DYNC1I2	0							
134	X	NUP155	0							
135	X	CEP135	1	1	5.40E-03	1	X			
135		TTN	0	1	5.40E-03	1				
135		WDR8	1	1	5.40E-03	1				
136	X	BMPR1A	0			2	X	X		
137		STK4	1	1	5.03E-02	1				
137	X	RASSF1	1	1	5.03E-02	1				
137		TMEM109	0	1	5.03E-02	1				
137		KIAA1754	0	1	5.03E-02	1				
137		STK3	0	1	5.03E-02	1		X		
137		VAPB	0	1	5.03E-02	1				
137		MAP1S	0	1	5.03E-02	1				

137		VAPA	0	1	5.03E-02	1				
138	X	ANLN	0			3	X	X		X
139	X	PREB	0							
140	X	ORC1L	3	6	2.24E-13	1		X		
140		NP_690852.1	0	6	2.24E-13	1				
140		ORC5L	4	6	2.24E-13	1				
140		ORC3L	5	6	2.24E-13	1				
140		ORC2L	4	6	2.24E-13	1				
141	X	CHORDC1	0							
142	X	PCNA	0			2		X		X
143	X	ESCO1	0			1			X	
144	X	PLK2	0			2	X	X		
145	X	ECT2	0			2	X	X		
146		NSMCE4A	0							
146		TUFT1	0							
146		NSMCE1	0							
146		NDNL2	0							
146	X	SMC6	0							
146		NSMCE2	0							
146		SMC5	0							
146		RAD18	0							

### 5.5 Phosphorylation manuscript table S2 (all phospho-peptides)

List of all determined phospho-peptides annotated with bait species (sp), bait, purification method used (Pur., either LAP or immunoaffinity purification using polyclonal antibodies (IP), the protein, the phospho-peptide (# indicates phosphorylation-site, % indicates ambiguous phosphorylation sites), the phosphorylated residue, the cell cycle phase specificity (phase, see material and methods of phospho-site manuscript for details (2.2.5.3)) and the inhibitor sensitivity (Inh sens).

sp	Bait	Pur.	Protein	peptide	site	phase	Inh sens
mm	Aurkb	LAP	AURKB	TSQSGNLTL#QR	S25	M	BI+Hes-sens
mm	Aurkb	LAP	AURKB	NKSQGSTASQGS#QNKQPFTIDNFE	S71	M	BI+Hes-sens
mm	Aurkb	LAP	AURKB	IADFGWSVHAPS#LR	S232	I	Hes-sens
mm	Aurkb	LAP	AURKB	RKT#MCGTLDYLPPEMIEGR	T237	M	Hes-sens
mm	Aurkb	LAP	AURKB	FPS#SVPSGAQDLISK	S299	M	
mm	Aurkb	LAP	Borealin	LTAETIQT#PLK	T106	M	BI+Hes-sens
mm	Aurkb	LAP	Borealin	LEVSMVKPT#PGLTPR	T185	M	BI+Hes-sens
mm	Aurkb	LAP	Borealin	IYNISGNNGS#PLADSK	S219	M	
mm	Aurkb	LAP	CBX5	RKS#NFSNSADDIK	S92	M?	BI+Hes-sens
mm	Aurkb	LAP	Cdc37	TGDEKDVS#V	S377	M	BI-sens
mm	Aurkb	LAP	HSP90 alpha	ESEDKPEIEDVGS#DEEEKK	S263	I/M	
mm	Aurkb	LAP	INCENP	RIS#YVQDENRDPIR	S72	I/M	Hes-sens
mm	Aurkb	LAP	INCENP	ALAAPSS#PTPESPTML	S143	M?	
mm	Aurkb	LAP	INCENP	ALAAPSSPT#PESPTML	T145	M?	
mm	Aurkb	LAP	INCENP	ALAAPSSPTPES#PTML	S148	M?	
mm	Aurkb	LAP	INCENP	T#LSPTPASATAPTSQGIPTSDDEESTPKK	T195	M?	

## 5 Appendix

mm	Aurkb	LAP	INCENP	TLSPTPASATAPTS#QGIPTSDEES TPKK	S208	M?	Hes-sens
mm	Aurkb	LAP	INCENP	TLSPTPASATAPTSQGIPT#SDEES TPKK	T213	M?	Hes-sens
mm	Aurkb	LAP	INCENP	TLSPTPASATAPTSQGIPTS#DEES TPKK	S214	M?	
mm	Aurkb	LAP	INCENP	TLSPTPASATAPTSQGIPTSDEES# TPKK	S218	M?	
mm	Aurkb	LAP	INCENP	TLSPTPASATAPTSQGIPTSDEEST #PKK	T219	M?	
mm	Aurkb	LAP	INCENP	ILESITVSSLMAT#PQDPK	T239	M	
mm	Aurkb	LAP	INCENP	MATPQDPKGQGVGTGRSAS#KL	S255	M?	
mm	Aurkb	LAP	INCENP	IAQVS#PGPRDSPAFPDSPWRER	S263	I/M	
mm	Aurkb	LAP	INCENP	IAQVSPGPRDS#PAFPDSPWRER	S269	M?	
mm	Aurkb	LAP	INCENP	IAQVSPGPRDSPAFPDS#PWRER	S275	M?	
mm	Aurkb	LAP	INCENP	T#DSQSVRHSPIAPSSPSPQVLAQ K	T298	M	
mm	Aurkb	LAP	INCENP	TDS#QSVRHSPIAPSSPSPQVLAQ K	S300	M	
mm	Aurkb	LAP	INCENP	TDSQSVRHS#PIAPSSPSPQVLAQ K	S306	I/M	
mm	Aurkb	LAP	INCENP	TDSQSVRHSPIAPSS#PSPQVLAQ K	S312	M	
mm	Aurkb	LAP	INCENP	TDSQSVRHSPIAPSSPS#PQVLAQ K	S314	M	
mm	Aurkb	LAP	INCENP	NNGNNS#WPHNDTE	S400	M?	
mm	Aurkb	LAP	INCENP	IANSTPNPKPAASS#PETPSAGQQ E	S421	M	
mm	Aurkb	LAP	INCENP	IANSTPNPKPAASSPET#PSAGQQ E	T424	M	
mm	Aurkb	LAP	INCENP	TDQADGPREPPQS#AR	S446	M	Hes-sens
mm	Aurkb	LAP	INCENP	SKTPSS#PCPASK	S481	M	
mm	Aurkb	LAP	INCENP	NQMLMT#PTSAPR	T507	M	BI+Hes- sens
mm	Aurkb	LAP	INCENP	INPDNYGMDLNS#DDSTDDEAHP R	S828	M	BI-sens
mm	Aurkb	LAP	INCENP	INPDNYGMDLNSDDS#TDDEAHP R	S831	M	BI-sens
mm	Aurkb	LAP	INCENP	INPDNYGMDLNSDDST#DDEAHP R	T832	M	BI-sens
mm	Aurkb	LAP	INCENP	RTS#SAVWNSPPLQGAR	S893	M	BI+Hes- sens
mm	Aurkb	LAP	INCENP	RTSS#AVWNSPPLQGAR	S894	M	BI+Hes- sens
mm	Aurkb	LAP	INCENP	RTSSAVWNS#PPLQGAR	S899	M	
mm	Aurkb	LAP	INCENP	VPSSLAYS#LK	S914	M	BI+Hes- sens
mm	Aurkb	LAP	INCENP	VLAPILPDNFS%T%PTGSR	S291 or T292	M	
mm	Aurkb	LAP	INCENP	RT%S%S%AVWNSPPLQGAR	T892 or S893 or S894	M	BI+Hes- sens
mm	Bub1	LAP	Bub1	QVMMTNSS#PEK	S177	M?	
mm	Bub1	LAP	Bub1	DLPASENRPDVS#LVCVGQ	S320	M	BI-sens
mm	Bub1	LAP	Bub1	SESSGEKPQEES#VPLMVN	S359	BI-ind	
mm	Bub1	LAP	Bub1	ANLPALVPVS#GQSLTDSR	S386	M	BI+Hes- sens
mm	Bub1	LAP	Bub1	CVNQS#VHEFMPQCGPETK	S399	M	BI-sens
mm	Bub1	LAP	Bub1	DFHTT#PNTSL	T429	M	
mm	Bub1	LAP	Bub1	VASINDFHTTPNTS#LGMVQG	S433	M	
mm	Bub1	LAP	Bub1	VASINDFHTTPNTSLGMVQGT#PC K	T440	I/M	
mm	Bub1	LAP	Bub1	KVQPS#PTVHTK	S447	I/M	

mm	Bub1	LAP	Bub1	QAPTLPDIS#DDKDE	S472	M	BI-sens
mm	Bub1	LAP	Bub1	AVSS#GDWGVK	S499	I/M	
mm	Bub1	LAP	Bub1	APS#PKSIGDF	S579	M	
mm	Bub1	LAP	Bub1	TGKCETS#GFQCPEML	S942	I/M	
mm	Bub1	LAP	Bub1	TGIHLPAQAT%T%S%EPLHSAQI L	T157/58/ S159	M	BI+Hes- sens
mm	Bub1	LAP	Bub1	S%QGS%ECSGVASSTCDEK	S188/92	I/M	BI-sens
mm	Bub1	LAP	Bub3	VAVEYLDPS#PEVQK	S211	M	BI-sens
mm	Bub1	LAP	Bub3	IRQVTDKETPKS%PCT%	S325/T3 28	M	
mm	Bub1	LAP	BubR1	KNKS#PPADPPRVL	S543	M	
mm	Bub1	LAP	BubR1	KLS#PIEDSR	S670	M	
mm	Bub1	LAP	BubR1	LT%S%PGALLFQ	T1042/S 1043	M	Bi-sens?
mm	Bub1	LAP	CASC5	HSSILKPPRS#PLQDL	S32	M?	Hes-sens?
mm	Bub1	LAP	CASC5	TIYSGEENMDIT#K	T487	M	Hes-sens
mm	Bub1	LAP	CASC5	SHT#VAIDNQIFK	T491	M	BI+Hes- sens
mm	Bub1	LAP	CASC5	AAPT#PEKEMMLQ	T513	M	
mm	Bub1	LAP	CASC5	TVS#PDEITTRPMDK	S930	M	
mm	Bub1	LAP	CASC5	NIKDVQS#PGFLNEPLSSK	S1050	I/M	
mm	Bub1	LAP	CASC5	S%LS%NPTPDYCHDK	S739/41	M	BI+Hes- sens
mm	Bub1	LAP	Cdc20	VQTT#PSKPGGDR	T70	BI-ind	
mm	Bub1	LAP	NSL1	KPDAKPENFITQIET%T%PTETAS R	T241/42	M	BI-sens?
mm	Bub1	LAP	Nuf2	IVDS#PEKLK	S247	I/M	
mm	Bub1	LAP	PMF1	THDHQLESS#L	S28	M?	
mm	Bub1	LAP	PMF1	LS#PVEVFAK	S30	M?	
mm	Bub1	LAP	PMF1	SLHLS#PQEQSASYQDR	S81	M?	
mm	Bub1	LAP	PMF1	SMQQLDPS#PAR	S331	M	
mm	Bub1	LAP	UBR5	RIS#QSQPVR	S1549	I/M	
mm	Bub1	LAP	UBR5	RISQS#QPVR	S1551	I/M	
mm	Bub1	LAP	UBR5	GQHDEHDEDS#DMELDLL	S1610	I?	
mm	Bub1b	LAP	ANANAPC7	VRPSTGNSAST#PQSQCLPSEIEV K	T92	M?	
mm	Bub1b	LAP	ANANAPC7	VRPSTGNSAST#PQSQCLPSEIEV K	T126	M?	
mm	Bub1b	LAP	ANANAPC8	QLRNQGET#PTTEVPAPF	T556	Hes-ind	
mm	Bub1b	LAP	ANANAPC8	RVS#PLNLSSVT#P	S582+T5 90	M?	Hes-sens?
mm	Bub1b	LAP	ANAPC1	KFSEQGGT#PQNVATSSSL	T291	BI+Hes- ind?	
mm	Bub1b	LAP	ANAPC1	AHS#PALGVHFSFGVQR	S355	M?	
mm	Bub1b	LAP	ANAPC1	NFDFEGSL#PVIAPK	S688	M?	
mm	Bub1b	LAP	ANAPC1	S%PS%ISNMAALSR	S341/34 3	M	Hes-sens?
mm	Bub1b	LAP	ANAPC1	AHS#PALGVHFS%FS%GVQR	S355+S3 62/364	M?	
mm	Bub1b	LAP	ANAPC1	SNTMPRPST#PLDGVST#PKPL	T530+T5 37	M?	
mm	Bub1b	LAP	ANAPC2	LLQS#PLCAGCSSDK	S218	M?	
mm	Bub1b	LAP	ANAPC2	LQDGPAPAS#PEAGNTL	S314	M	
mm	Bub1b	LAP	BUB1	VANTSSFHTTNPNTSLGMVQAT#PS K	T452	M?	Hes-sens
mm	Bub1b	LAP	BUB1	TAKCETS#GFQCVEML	S969	I/M	
mm	Bub1b	LAP	BUB1	GIRCNKTLAPS#PKS#PGDFTSAA QL	S593+S5 96	M?	Hes-sens?
mm	Bub1b	LAP	Bub1b	AEAS#EAMCLEGAEWELSK	S5	M?	
	Bub1b	LAP	Bub1b	STLQGALAKQESAGHT#AL	T47	M	BI-sens

## 5 Appendix

mm	Bub1b	LAP	Bub1b	AKENELQPGPWS#TDRPAGR	S307	Bi+Hes-ind	
mm	Bub1b	LAP	Bub1b	VEESAQQTVM#PCKIEPSINH	T347	M	
mm	Bub1b	LAP	Bub1b	IEPSINHVLS#TR	S360	M	
mm	Bub1b	LAP	Bub1b	LQIASGPQEMSGVPLSCSICPLSS#NPR	S496	Hes-ind	
mm	Bub1b	LAP	Bub1b	SSNPRES#PAENILQEQPDSKGS SMPF	S502	I/M	
mm	Bub1b	LAP	Bub1b	KDKS#PATGGPQVLNAQR	S535	I/M	
hs	BUB1B	LAP	BUB1B	FLLS#EK	S537	M	
mm	Bub1b	LAP	Bub1b	NVTLCNPEDT#CDFAR	T601	M	
mm	Bub1b	LAP	Bub1b	LAST#PFHEILSSK	T613	Bi-ind	
mm	Bub1b	LAP	Bub1b	SRSSSSAPSTSS#IKGF	S686	I	
mm	Bub1b	LAP	Bub1b	LELT#NDGAENAIQSPWCSQYR	T699	M	
mm	Bub1b	LAP	Bub1b	TIS#PEALLTQQDK	1033	M	
mm	Bub1b	LAP	Bub1b	VMS%T%LQGALAK	S33/T34	M	
mm	Bub1b	LAP	Bub1b	GS%S%MPFSIFDESLSKD	S517/S518	Bi-ind	
mm	Bub1b	LAP	Bub1b	GSSMPFSIFDES%LS%DKK	S527/S529	I/M	
mm	Bub1b	LAP	Bub1b	LASTPFHEILS%S%K	S620/S621	I/M	
mm	Bub1b	LAP	BUB3	IRQVTDATKPKS#PCT	S325	M	BI-sens
mm	Bub1b	LAP	CASC5	SHT#VAIDNQIFK	T517	BI-ind	
mm	Bub1b	LAP	CASC5	TVS#PDEITTRPMDK	S956	Hes-ind?	
mm	Bub1b	LAP	CASC5	DVQS#PGFLNEPLSSK	S1076	M?	
mm	Bub1b	LAP	CDC16	LKDES#GFKDPSSDW	S111	M	BI+Hes-sens
mm	Bub1b	LAP	CDC16	NIIS#PPWDFR	S559	M	
mm	Bub1b	LAP	CDC16	QTAEETGLT#PLETSR	T580	BI-ind?	
mm	Bub1b	LAP	CDC20	QRKAKEAAGPAPS#PMRAAN	S41	Hes-Ind?	
mm	Bub1b	LAP	CDC20	LLSKENQPENSQT#PTKKEHQKAW	T106	M?	
mm	Bub1b	LAP	CDC26	QKEDVEVVGGSDGEGAIGLSS#D PK	S52	M?	
mm	Bub1b	LAP	CDC26	SSQFGS#LEF	S82	M?	
mm	Bub1b	LAP	CDC26	QKEDVEVVGGSDGEGAIGLSS#DPK	S42+S52	M?	Hes-sens
mm	Bub1b	LAP	CDC27	QPETVLTET#PQDTIELNR	T205	M?	
mm	Bub1b	LAP	CDC27	GGITQPNINDS#LEITK	S432	M	
mm	Bub1b	LAP	CDC27	ISTIT#PQIQAFNLQK	T452	M	
mm	Bub1b	LAP	CDC27	IDSAVIS%PDT%VPLGTGTSIL	S241/T244	M?	Bi-sens?
mm	Bub1b	LAP	DSN1	S%LHLS%PQEQSASYQDR	S77/S81	BI-ind?	
mm	Bub1b	LAP	EDD	AMNQQTTLDT#PQLER	T1969	BI-ind?	
mm	Bub1b	LAP	EDD	RRQLS#IDTRPF	S2369	I?	
mm	Bub1b	LAP	UBR5	TSDS#PWFLSGSETLGR	S110	M	Hes-sens
mm	Bub1b	LAP	UBR5	WLDGAS#FDNER	S327	M	BI-Hes-sens
mm	Bub1b	LAP	UBR5	FRRSDS#MTFL	S2028	I/M	Bi+Hes-sens?
hs	CDC27	IP	ANAPC1	VGS#LQEV	S60	Hes-ind	
hs	CDC27	IP	ANAPC1	VPPGS#PREPLPTMF	S202	I/M	
hs	CDC27	IP	ANAPC1	KFS#EQGG	S286	BI-ind	
hs	CDC27	IP	ANAPC1	KFSEQGGT#PQNVA	T291	I/M	
hs	CDC27	IP	ANAPC1	SLSKGDS#PV	S313	BI-ind	
hs	CDC27	IP	ANAPC1	PVTS#PFQNY	S317	BI+Hes-ind	

hs	CDC27	IP	ANAPC1	STSSPSLHS#R	S339	I	Bi-sens
hs	CDC27	IP	ANAPC1	SPS#ISNMAALSR	S343	I/M	
hs	CDC27	IP	ANAPC1	AALS#RAH	S351	M	
hs	CDC27	IP	ANAPC1	AHS#PALGVHSFSGVQR	S355	I/M	
hs	CDC27	IP	ANAPC1	FNISSHNQS#PK	S377	I/M	
hs	CDC27	IP	ANAPC1	HSISHS#PNSNSNGSFL	S386	I/M?	
hs	CDC27	IP	ANAPC1	KVFIPGLPAPS#LTMS	S518	Hes-ind	
hs	CDC27	IP	ANAPC1	PSLTMS#NTMPRPSTPL	S522	I/M?	
hs	CDC27	IP	ANAPC1	PSLTMSNT#MPRPS	T524	I?	
hs	CDC27	IP	ANAPC1	TMPRPS#TPLDG	S529	I?	
hs	CDC27	IP	ANAPC1	NTMPRPST#PLDGV	T530	I/M?	
hs	CDC27	IP	ANAPC1	DGV#TPKPL	S536	M	
hs	CDC27	IP	ANAPC1	DGVST#PKPL	T537	M	
hs	CDC27	IP	ANAPC1	LLGS#LDEVV	S547	I/M	
hs	CDC27	IP	ANAPC1	LLGSLDEVVLLS#PVPELR	S555	I/M	
hs	CDC27	IP	ANAPC1	LHDS#LYNEDCTF	S569	I/M	
hs	CDC27	IP	ANAPC1	NDFEFGS#LS	S686	I/M	
hs	CDC27	IP	ANAPC1	NDFEFGSLS#PVIAPK	S688	I/M	
hs	CDC27	IP	ANAPC1	SLCLS#PSEASQMK	S731	I	
hs	CDC27	IP	ANAPC1	LQVEQEENRFS#FR	S916	M	
hs	CDC27	IP	ANAPC1	KHKS#PSYQIK	S1347	Hes-ind	
hs	CDC27	IP	ANAPC1	STS%S%PSLHSR	S333/34	M	BI+Hes-sens
hs	CDC27	IP	ANAPC1	SELWS%S%DGAA	S50/51	I/M	
hs	CDC27	IP	ANAPC1	VVLLSPVPELRDS%S%K	S563/64	I/M	
hs	CDC27	IP	ANAPC1	ARPS%ET%GS%DDDWE	S699/T701/S703	I/M	
hs	CDC27	IP	ANAPC2	RLLQS#PL	S218	I/M	
hs	CDC27	IP	ANAPC2	RPAS#PEAGNTL	S314	I/M	
hs	CDC27	IP	ANAPC2	GQDS#EDDSGEP	S470	I/M	
hs	CDC27	IP	ANAPC2	DNMVLIDS#DDES	S732	Hes-ind?	
hs	CDC27	IP	ANAPC2	DDES#DSGMASQ	S736	Hes-ind?	
hs	CDC27	IP	ANAPC2	LLHQFSFS#PER	S532/34	I/M	
hs	CDC27	IP	ANAPC4	IKEEVLS#ESEAEEN	S777	I/M	BI+Hes-sens
hs	CDC27	IP	ANAPC4	ES#EAENQQA	S779	I/M	
hs	CDC27	IP	ANAPC5	TVEDADMELT#SR	T178	M	
hs	CDC27	IP	ANAPC5	S#RDEGER	S179	M	
hs	CDC27	IP	ANAPC5	KMEKEELDVS#VR	S195	M	
hs	CDC27	IP	ANAPC5	QAEFFLSQQAS#LLK	S221	M	
hs	CDC27	IP	ANAPC5	KNDETKALT#PASL	T232	I/M	
hs	CDC27	IP	ANAPC6	YLKDES#GFKDPSS	S112	M	
hs	CDC27	IP	ANAPC6	KNIIS#PPWDFREF	S560	I/M	
hs	CDC27	IP	ANAPC6	QTAEETGLT#PLETSR	T581	I/M	
hs	CDC27	IP	ANAPC6	RKT#PDSRPSLEETFEIE	T589	Hes-ind?	Bi-sens
hs	CDC27	IP	ANAPC6	MNES#DMMLET	S607	Hes-ind?	
hs	CDC27	IP	ANAPC6	MNESDMMLETS#MSDHST	S614	Hes-ind?	
hs	CDC27	IP	ANAPC7	GNSAST#PQSQ	T126	I/M	
hs	CDC27	IP	ANAPC8	RNQGET#PTTEVPAPF	T556	I/M	Bi-sens
hs	CDC27	IP	ANAPC8	EVPAPFFLPAS#LS	S570	I/M	

## 5 Appendix

hs	CDC27	IP	ANAPC8	LS#ANNTPTRR	S572	I/M	
hs	CDC27	IP	ANAPC8	PASLSANNT#PT	T576	I/M	
hs	CDC27	IP	ANAPC8	NNTPT#RR	T578	M	
hs	CDC27	IP	ANAPC8	PTRRVS#PL	S582	I/M	
hs	CDC27	IP	ANAPC8	PLNLS#SVT	S587	M	
hs	CDC27	IP	ANAPC8	PLNLSS#VT	S588	I/M	
hs	CDC27	IP	ANAPC8	VSPLNLSSVT#P	T590	I/M	
hs	CDC27	IP	BUB1B	IEPSINHILS#TR	S367	M?	
hs	CDC27	IP	BUB1B	KNKS#PPADPPR	S543	M?	
hs	CDC27	IP	BUB1B	KLS#PIEDSR	S670	M	
hs	CDC27	IP	BUB1B	LT%S%PGALLFQ	T1042/S1043	M	
hs	CDC27	IP	C10orf104	FLCES#VFSYQVASTLK	S57	Hes-ind	
hs	CDC27	IP	CDC20	EAAGPAPS#PMR	S41	I/M	
hs	CDC27	IP	CDC20	VQTT#PSKPGGDR	T70	I, Hes-ind	
hs	CDC27	IP	CDC20	VQTTPS#KPGGDR	S72	BI-ind	
hs	CDC27	IP	CDC20	PENSQT#PTKKEHQKAW	T106	I/M	
hs	CDC27	IP	CDC26	VVGGS#DGEGAIGLSSDPK	S42	M	
hs	CDC27	IP	CDC26	KPQPKPNRSS#QFG	S78	I/M	
hs	CDC27	IP	CDC26	SSQFGS#LEF	S82	I/M	
hs	CDC27	IP	CDC26	VVGGSDEGAIGLS%S%DPK	S52/53	M	Bi-sens
hs	CDC27	IP	CDC27	FSNCLPNS#CTTQVPNH	S183	BI-ind	
hs	CDC27	IP	CDC27	QPETVLTET#PQDTIELNR	T205	M	
hs	CDC27	IP	CDC27	NRLNLESS#NSKY	S220	M	
hs	CDC27	IP	CDC27	NLESSNS#KY	S222	I/M	
hs	CDC27	IP	CDC27	IDSAVIS#PDTVPL	S241	M	
hs	CDC27	IP	CDC27	GTGTS#ILSK	S252	Hes-ind?	
hs	CDC27	IP	CDC27	GGPAALS#PLTPSF	S276	BI+Hes-ind	
hs	CDC27	IP	CDC27	PLT#PSFGILPL	T279	BI+Hes-ind	
hs	CDC27	IP	CDC27	TNT#PPVIDV	T304	Hes-ind?	
hs	CDC27	IP	CDC27	TNTPPVIDVPS#TGAPSKK	S312	Hes-ind?	
hs	CDC27	IP	CDC27	VPST#GAPSKK	T313	Hes-ind?	
hs	CDC27	IP	CDC27	SVFSQSGNS#R	S345	M	
hs	CDC27	IP	CDC27	SSGQTSTT#PQVL	T365	BI-ind	
hs	CDC27	IP	CDC27	TTPQVLS#PTIT	S370	M	
hs	CDC27	IP	CDC27	TSTTPQVLSPT#IT	T372	M	Bi-sens
hs	CDC27	IP	CDC27	IT#SPPNALPR	T374	M	
hs	CDC27	IP	CDC27	PQTSTTPQVLSPTITS#PPNALPR	S375	I/M	
hs	CDC27	IP	CDC27	LFTSDS#STTK	S392	M	
hs	CDC27	IP	CDC27	LFTSDSS#TTK	S393	M	
hs	CDC27	IP	CDC27	T#TKENSK	T394	M	
hs	CDC27	IP	CDC27	LFTSDSSTT#KENSK	T395	M	
hs	CDC27	IP	CDC27	TSDSSTTKENS#KKL	S399	I/M	
hs	CDC27	IP	CDC27	GGITQPNINDS#LEITK	S432	I/M	
hs	CDC27	IP	CDC27	IIS#EGKIS	S444	M	
hs	CDC27	IP	CDC27	ISTIT#PQIQAFNLQK	T452	M?	
hs	CDC27	IP	CDC27	KLDS%S%IISEGK	S440/41	M	
hs	CDC27	IP	FZR1	INENEKS#PSQNRK	S70	I/M	
hs	CDC27	IP	FZR1	SLSTKRS%S%PDDGNDVSPY	S137/138	I?	



hs	CDC27	IP	NEK2	TFVGTPYYMS#PEQMNR	S184	Hes-ind?	
hs	CDC27	IP	NEK2	KFLSLASNPELLNLPS%S%VIK	S378/79	Hes-ind?	
mm	Dctn1	LAP	DCTN1	VLTS#PGA	S203	I/M	
mm	Dctn1	LAP	DCTN1	QEAS#VER	S541	Hes-ind	
mm	Dctn1	LAP	DCTN1	SPET#PDS	T105/108	I/M	
mm	Dctn1	LAP	DCTN1	PLPS%PSK	S212/214	I/M	
mm	Kif23	LAP	Kif23	S%VS%PSPLPLSSNIAQISNGQ QLMSQPQLHR	S683/S685	M	BI-sens
mm	Kif23	LAP	RACGAP1	PVKKTRS#IGSAVDQGNESIVAK	S203	M	BI-sens
mm	Mad2L1	LAP	BUB1B	VEETAQQPVMT#PC	T354	M	Hes-sens
mm	Mad2L1	LAP	BUB1B	REAELLTS#AEKR	S435	M?	
mm	Mad2L1	LAP	BUB1B	SIFDEFLS#EK	S537	M	
mm	Mad2L1	LAP	BUB1B	SEKKNKs#PPADPPRVL	S543	M?	
mm	Mad2L1	LAP	BUB1B	EDVS#PDVCDEFTGIEPL	S574	M	
mm	Mad2L1	LAP	BUB1B	KLS#PIEDSR	S670	M	
mm	Mad2L1	LAP	BUB1B	LELTNETSENPTQS#PWCSQYR	S720	M?	
mm	Mad2L1	LAP	BUB1B	WCSQYRRQLLKS#LPELSASAELC IED	S733	M?	BI+Hes-sens
mm	Mad2L1	LAP	BUB1B	GKLTS#PGAL	S1043	M?	
mm	Mad2L1	LAP	CDC20	EAAGPAPS#PMR	S41	I/M	
mm	Mad2L1	LAP	CDC20	SKVQTT#PSKPGGD	T70	I/M	
mm	Mad2L1	LAP	CDC20	LSKENQPENSQT#PTKK	T106	I/M	
mm	Mad2L1	LAP	MAD1L1	MQMELS#HKR	S77	M	
mm	Mad2L1	LAP	MAD1L1	AILGSYDSELTPAEYS#PQLTR	S428	I/M	
mm	Mad2L1	LAP	MAD1L1	SQSSSAEQS#FLFSR	S490	M	BI-sens
mm	Mad2L1	LAP	MAD1L1	SSSAEQS#FLFSR	S490	M	
mm	Mad2L1	LAP	MAD1L1	LNPTS#VARQR	S547	M	Hes-sens
mm	Mad2L1	LAP	MAD1L1	LNPTS#VARQR	S551	M	
mm	Mad2L1	LAP	MAD1L1	QPLRQGRIMS%T%LQGALAQES ACN	S12/T13	M?	
mm	Mad2L1	LAP	MAD1L1	ERAAS%T%S%ARNY	S91/92/93	M?	
mm	Mad2L1	LAP	Mad2l1	VQTTPS#KPGGDRIYPH	S72	M	BI-sens
mm	Mad2L1	LAP	Mad2l1	AIQDEIRS#VIR	S130	I	
mm	Mad2L1	LAP	Mad2l1	LRS#FTTTIHK	S185	BI-ind	
mm	Mad2L1	LAP	Mad2l1	VNS#MVAYK	S195	I/M	
mm	Mad2L1	LAP	Mad2l1	LEVS%CS%FDLL	S148 OR S150	M	BI-sens
mm	Mad2L1	LAP	MAD2L1BP	STQEPLNAS#EAFPCR	S78	M	BI-sens
mm	Mad2L1	LAP	MAD2L1BP	KPS#PQAEEMLK	S134	I/M	
mm	Mad2L1	LAP	MAD2L1BP	IELLET%S%S%T%QEPLN	T68/S69 /S70/T71	I/M	
mm	Mis12	LAP	BUB1	S#PGDFTSAAQLASTPFHK	S596	Hes-ind?	
mm	Mis12	LAP	BUB1B	nd			
mm	Mis12	LAP	BUB3	nd			
mm	Mis12	LAP	CASC5	RVS#FADTIK	S60	I, BI-ind	
mm	Mis12	LAP	CASC5	TVS#PDEITTRPMDK	S930	BI+Hes-ind?	
mm	Mis12	LAP	CASC5	LVANDSQLT#PLEEWSNNR	T1016	BI+Hes-ind	
mm	Mis12	LAP	CASC5	DVQS#PGFLNEPLSSK	S1050	I/M	
mm	Mis12	LAP	CASC5	RCS#LGIFLPR	S1675	M?	

# 5 Appendix

mm	Mis12	LAP	CASC5	TPS#SCSSSLDSIK	S1819	I?	
mm	Mis12	LAP	CASC5	NCS%VT%GIDDLEQIPADTTDIN HLETQPVSSK	S1664/T 1666	I	
mm	Mis12	LAP	CASC5	T%VNT%PPT%PEDLMLSQY	T1922/2 5/28	Hes-ind	
mm	Mis12	LAP	CASC5	nd			
mm	Mis12	LAP	CBX5	SLSDS#ESDDSKSKKRDAADKP RGF	S97	I?	
mm	Mis12	LAP	CBX5	LT%WHS%CPEDAEQ	T173/S1 76	I, BI-ind	
mm	Mis12	LAP	CBX5	nd			
mm	Mis12	LAP	DSN1	SKTHDQHLESSLS#PVEVF	S14	I, Hes- ind	
mm	Mis12	LAP	DSN1	THDQHLESSLS#PVEVF	S30	I/M	
mm	Mis12	LAP	DSN1	LS#PVEVF	S30	I/M	
mm	Mis12	LAP	DSN1	TSASLEMNQGV#EER	S49	Hes-ind	
mm	Mis12	LAP	DSN1	S#LHL	S71	I/M	
mm	Mis12	LAP	DSN1	SLHLS#PQEQSASY	S81	I/M	
mm	Mis12	LAP	DSN1	RKS#LHPIHQGITELSR	S109	BI-ind	
mm	Mis12	LAP	DSN1	SIS#VDLAESK	S125	I/M	
mm	Mis12	LAP	DSN1	SRSISVDLAES#KRL	S131	I, Hes- ind	
mm	Mis12	LAP	DSN1	MQQLDPS#PARKL	S331	I/M	
mm	Mis12	LAP	DSN1	THDQHLES%S%L	S27/28	I/M	
mm	Mis12	LAP	DSN1	THDQHLES%S%LSPVEVF	S27/28	I/M	
mm	Mis12	LAP	DSN1	KLQLQNPPAIHGS%GS%GSCQ	S350/52 /54	BI+Hes- ind	
mm	Mis12	LAP	DSN1	T%S%AS%LEMNQGVSEER	T38/S39 /S41	I/M	Hes-sens
mm	Mis12	LAP	DSN1	RIHLGS%S%PKKG	S57/58	I/M	
mm	Mis12	LAP	HEC1	nd			
mm	Mis12	LAP	Mis12	nd			
mm	Mis12	LAP	NSL1	KPDAKPENFITQIET%T%PTETAS R	T241/42/ 44	I/bi+hes- ind	
mm	Mis12	LAP	NSL1	nd			
mm	Mis12	LAP	NUF2	IVDS#PEKLKNY	S247	I/M	
mm	Mis12	LAP	NUF2	DLY#PNPKPEVL	Y37	Hes-ind	
mm	Mis12	LAP	PMF1	nd			
mm	Mis12	LAP	SPBC24	DIEEVS#QGLLSLLGANR	S11	I	
mm	Mis12	LAP	SPBC25	nd			
mm	Mis12	LAP	ZWINT	nd			
mm	Nup107	LAP	Nup107	S#GFGGM	S4	M	BI+Hes- sens
mm	Nup107	LAP	Nup107	KHS#AHKR	S27	M	Hes-sens
mm	Nup107	LAP	Nup107	VLIQANQEDNFGTAT#PR	T46	M	
mm	Nup107	LAP	Nup107	SQIIPRT#PSSF	T55	M	
mm	Nup107	LAP	Nup107	LGLYTNTTEHHS#MTEDVNLSTVML R	S130	I/M	
mm	Nup107	LAP	Nup107	MTEDVNLS#TVMLR	S138	M	BI+Hes- sens
mm	Nup107	LAP	Nup107	TSVMTQDDS#EELPR	S476	M	
mm	Nup107	LAP	Nup107	DNGEFS#HHDLAPSLDTGTTEED RLK	S653	M	BI+Hes- sens
mm	Nup107	LAP	Nup107	HMNSAPQKPTLLSQATFT#EK	T784	M	BI+Hes- sens
mm	Nup107	LAP	Nup107	SGFGGMS%S%PVIR	S10/11	I/M	
mm	Nup107	LAP	Nup107	SQIIPRTPS%S%FRQPFVTPS	S57/58	M?	
mm	Nup107	LAP	Nup107	QPFVT%PS%SR	T65/S67	M	
mm	Nup107	LAP	Nup107	HPDIS%YILGTEGRS%PR	S78/87	M?	

mm	Nup107	LAP	Nup107	HT%QS%S%GY%LGNLS%MVT NLDDSNWAAAFSSQR	T91/S93 /S94/Y96 /S101	M	Hes-sens
mm	Nup107	LAP	NUP133	APSPRT#PGTGSRR	S10	Hes-ind	
mm	Nup107	LAP	NUP133	GPLAGLPGS#	S27	M	
mm	Nup107	LAP	NUP133	RGPLAGLPGST#PR	T28	M	
mm	Nup107	LAP	NUP133	RT#ASR	T31	M	
mm	Nup107	LAP	NUP133	GLPLGS#AVS	S41	M	
mm	Nup107	LAP	NUP133	AVSS#PVLF	S45	I/M?	
mm	Nup107	LAP	NUP133	PVLFS#PVGR	S50	I/M?	
mm	Nup107	LAP	NUP133	GT#PTRMFPH	T63	M?	Hes-sens
mm	Nup107	LAP	NUP133	MFPHHS#ITESVNYDVK	S72	I/M	
mm	Nup107	LAP	NUP133	GILS#PSSDLTSL	S267	M	
mm	Nup107	LAP	NUP133	ENVSILAEDLEGSLASSVAGPNS# ESMIFETTTK	S499	BI-ind	
mm	Nup107	LAP	NUP133	DLGHAQMVDELFSHSDLDSD#D SELDL	S553	BI-ind	
mm	Nup107	LAP	NUP133	KGLPLGSAVSS%PVLF%PVGR	S45/50	I/M	
mm	Nup107	LAP	NUP160	LIRPEYAWIVQPVSGAVYDRPGAS #PK	S1157	I/M	
mm	Nup107	LAP	NUP37	nd			
mm	Nup107	LAP	NUP43	SIGDFGNLDS#DGGFEGDHQLL	S57	BI-ind	
mm	Nup107	LAP	NUP43	S%S%T%FLSHSISNQANVHQSV ISSWLSTDPKDR	S369/S3 70/T371	I	
mm	Nup107	LAP	NUP85	IDEELT#GK	T91	M	Hes-sens
mm	Nup107	LAP	NUP85	EADAS#PASAGICR	S224	M	BI-sens
mm	Nup107	LAP	NUP98	YGLQDS#DEEEEEHPSK	S871	I/M	
mm	Nup107	LAP	NUP98	KLKTAPLPPASQTT#PLQM	T899	M	
mm	Nup107	LAP	NUP98	GKPAPPPQSQS#PEVEQL	S917	I/M	
mm	Nup107	LAP	NUP98	LEES#MPEDQEPVSAS	S949	M	BI-sens
mm	Nup107	LAP	NUP98	ASLLT#DEEDVDMALDQR	T983	M	BI-sens
mm	Nup107	LAP	NUP98	LPS#KADTSQEICSPR	S1001	I/M	Hes-sens
mm	Nup107	LAP	NUP98	LPIS#ASHSSK	S1017	M	
mm	Nup107	LAP	NUP98	TRS#LVGGLLQSK	S1026	M	
mm	Nup107	LAP	NUP98	FTSGAFLS#PSVSVQECR	S1043	I/M	
mm	Nup107	LAP	NUP98	VSVQECRT#PR	T1053	M?	
mm	Nup107	LAP	NUP98	VFTMPS#PAPEVPLKTV	S1082	I/M	
mm	Nup107	LAP	NUP98	QIADS#MEFGFLPNPVAVKPL	S1157	BI-ind	
mm	Nup107	LAP	NUP98	YACS#PLPSYLEGSGCVIAEEQNS QTPLR	S1448	M	Hes-sens
mm	Nup107	LAP	NUP98	LMPEDYAMDELRSLTQSYLR	S1786	BI-ind	
mm	Nup107	LAP	NUP98	LPSKADT%S%QEICS	T1005/S 1006	M	
mm	Nup107	LAP	NUP98	FT%S%GAFLSPS	T1037/S 1038	M?	BI+Hes- sens
mm	Nup107	LAP	NUP98	VVLSLHHPPDRT%S%DSTPDPQR	T1751/S 1752	M	
mm	Nup107	LAP	NUP98	EEEEEHPSKT%S%T%K	T882/S8 83/T884	M	
mm	Nup107	LAP	SEH1L	nd			
hs	PDS5A	IP	PDS5A	LKMVVKT#FMDMDQDSEDEK	T55	M	
hs	PDS5A	IP	PDS5A	KDLTEYLKVRSL#	S373	M	
hs	PDS5A	IP	PDS5A	NENNS#HAFMKK	S1051	M	
hs	PDS5A	IP	PDS5A	SALCNADS#PKDPVLPKM	S1057	M	
hs	PDS5A	IP	PDS5A	NSKS#ALCN	S1098	M	BI-sens?
hs	PDS5A	IP	PDS5A	SREQSSEAAETGVS#ENEENPVR	S1155	M	

## 5 Appendix

hs	PDS5A	IP	PDS5A	IISVT#PVK	T1212	M	
hs	PDS5A	IP	PDS5A	AAVGQES#PGGL	S1309	I/M	
hs	PDS5A	IP	PDS5A	SYIS%EET%R	S1127/T 1130	M	
hs	PDS5A	IP	PDS5A	EINSDQATQGNIS#SDR	S1236/S 1237	M	
hs	PDS5A	IP	RAD21	nd			
hs	PDS5A	IP	SMC1	nd			
hs	PDS5A	IP	SMC3	nd			
hs	PDS5A	IP	STAG2	nd			
hs	PDS5A	IP	WAPAL	nd			
hs	PDS5B	IP	PDS5B	KFT#QVLEDDEK	550	M?	
hs	PDS5B	IP	PDS5B	SFFT#PGKPK	S1121	Hes-ind?	
hs	PDS5B	IP	PDS5B	SNPSS#PGRIK	S1166	M	
hs	PDS5B	IP	PDS5B	LDS#SEMDHSENYDTMS	S1176	I/M	
hs	PDS5B	IP	PDS5B	LDSSEMDHS#ENEDYTMS	S1182	I/M	
hs	PDS5B	IP	PDS5B	DHSENYDT#MSSPLPG	T1188	M?	
hs	PDS5B	IP	PDS5B	KKT#PVTEQEEKLGMDLTKL	S1220	I/M	Hes-sens
hs	PDS5B	IP	PDS5B	GHTAS#ESDEQQWPEEK	S1257	I/M	
hs	PDS5B	IP	PDS5B	EDILENEDEQNS#PPK	S1283	I/M	
hs	PDS5B	IP	PDS5B	GGGT#PKEEPTMK	T1301	M	Bi-sens
hs	PDS5B	IP	PDS5B	AES#PESSAIESTQSTPQK	S1358	I/M	
hs	PDS5B	IP	PDS5B	AESPESAIESTQST#PQK	T1370	M	
hs	PDS5B	IP	PDS5B	GRPSKT#P	T1381	I/M	
hs	PDS5B	IP	PDS5B	GRPSKT#P	T1382	I/M	
hs	PDS5B	IP	PDS5B	TPS#PSQPKK	S1384	I/M	
hs	PDS5B	IP	PDS5B	TTNVLGAVNKPLS%S%AGK	1139/40	bi-ind?	
hs	PDS5B	IP	PDS5B	SGPPAPEEEEEERQS%GNT%EQ K	S1334/T 1337	S	
hs	PDS5B	IP	PDS5B	ENDS%S%EEVDVF	S1406/0 7	I/M	
hs	PDS5B	IP	PDS5B	QGS%S%PVDDIPQEETEEEEVST V	S1416/1 7	I/M	Hes-sens
mm	Plk1	LAP	CDC25C	YLGS#PITTV	S168	BI-ind	
mm	Plk1	LAP	NCAPG2	KEITGS%S%LIQ	S935/36	I/BI-ind?	
mm	Plk1	LAP	Plk1	PSS#LDP	S331	M	BI-sens
mm	Plk1	LAP	Plk1	KKT%LCGT%PNY	T210/21 4	I/M	
mm	Plk1	LAP	TP53BP1	VPSS#PTE	S380	BI-ind	
mm	Plk1	LAP	TP53BP1	GKLS#PR	S1362	BI-ind	
mm	Smc6	LAP	NDNL2	RGPQGSQGSQGPS#PQGA	S64	I/M	
mm	Smc6	LAP	NDNL2	CEALADEENRARPQSGPAPSS#	S304	I/M	
mm	Smc6	LAP	NSMCE4A	REAPERPSLEDT#EP	T58	I/M	Bi-sens
mm	Smc6	LAP	NSMCE4A	EPS#DS	S61	I/M	
mm	Smc6	LAP	NSMCE4A	DS#GDEMMDPA	S63	I/M	
hs	SMC6	LAP	NSMCE4A	LPVIEPVINEENEGFEHNT#QVR	T345	I?	
hs	SMC6	LAP	NSMCE4A	TFEISEPVIT#PSQR	T375	M	
hs	SMC6	LAP	NSMCE4A	EISEPVITPS#QRQKPSA	S377	I?	
hs	SMC6	LAP	NSMCE4A	EISEPVITPSQRQKPS#A	S384	BI-ind?	
hs	SMC6	LAP	SMC5	TSTPS#PQPSKR	S12	M	Hes-sens
hs	SMC6	LAP	SMC5	ALPRDPS#SEVPSK	S25	I/M	
hs	SMC6	LAP	SMC5	KNS#APQLPLLQSSGPFVEGSIVR	S35	I/M	
hs	SMC6	LAP	SMC5	NKLESDYMAASS#QLR	S793	I/M	
hs	SMC6	LAP	SMC5	LHELT#PHHQSGGER	T987	BI+hes- ind	

hs	SMC6	LAP	SMC5	FRS%S%TQLHEL	S979/80	M	Hes-sens
hs	SMC6	LAP	SMC6	FQSIAGLS#TMK	S265	Bi-ind	
hs	SMC6	LAP	SMC6	DVDSEIS#DLENEVENK	S669	I	
hs	SMC6	LAP	SMC6	RMS#DPERGQTTLPRPV	S1068	M	BI+Hes-sens
hs	SMC6	LAP	TUFT1	ISKPPS#PKPMPVIR	S378	BI+hes-ind?	
hs	STAG1	IP	RAD21	SLNQSRVEEITMREEVGNIS#ILQ ENDFGDF	S153	M	
hs	STAG1	IP	RAD21	EGS#AFEDDDMLVSTTTSNLLLES EQSTSNLNEK	S175	M	
hs	STAG1	IP	RAD21	S%LNQS%RVEEIT%MREEV	S134/38 /T144+S 153	M	
hs	STAG1	IP	SMC1	nd			
hs	STAG1	IP	SMC3	nd			
hs	STAG1	IP	STAG1	SFVMDHVFIDQDEENQS#MEGDE EDEANKIEAL	S847	I/M	
hs	STAG1	IP	STAG1	ARRFALT#FGLDQIK	T963	M	
hs	STAG1	IP	STAG1	STNET%T%AHS%DAGSELEETE	T16/T17/ S20	M	
hs	STAG1	IP	STAG1	LVKIT%DGS%PS%KEDLLVLRK	T753/S7 56/58	M	
hs	STAG2	IP	PDS5A	NEENPVRIISVT#PVKNIDPVKNKE	T1168	M	
hs	STAG2	IP	PDS5A	AAVGQES#PGGLEAGNAK	S1265	M	
hs	STAG2	IP	PDS5A	INSDQATQGNIS%S%DRGKKR	S1192/9 3	M	
hs	STAG2	IP	PDS5B	GRPPKPLGGGT#PKEEPTMK	S1301	M	
hs	STAG2	IP	RAD21	AHVFEKNLESSVESIIS#PK	S46	M	
hs	STAG2	IP	RAD21	EEVGNIS#ILQENDFGDFGMDDR	S153	M	
hs	STAG2	IP	RAD21	GMDDREIMREGS#AFEDDDMLVS TTTSLN	S175	M	BI-sens
hs	STAG2	IP	RAD21	DDMDEDDNVS#MGGPDS	S271	M	
hs	STAG2	IP	RAD21	EDAS#GGD	S545	M	BI-sens
hs	STAG2	IP	RAD21	TQEEPYSIIAT#PGPR	T623	M	
hs	STAG2	IP	RAD21	QQFS%LNQS%R	S134/S1 38	M	BI-sens
hs	STAG2	IP	RAD21	GGPDS%PDS%VDPVEPMPT	S277/28 0	M?	
hs	STAG2	IP	SMC1	EQT#VKKDENEIEKL	T841	I/M	
hs	STAG2	IP	SMC1	SKGTMDDISQEEGS%S%QGEDS VSGSQRISSIY	S956/57	M	
hs	STAG2	IP	SMC3	KGDVEGS%QS%QDEGEGSGESE R	S1065/6 7	I/M	
hs	STAG2	IP	STAG2	ILDHVFIEQDDDNNS#ADGQQED	912	I/M	
hs	STAG2	IP	STAG2	GMQLS#LTEE	S1091	M	BI-sens
hs	STAG2	IP	STAG2	LRPEDSFMSVYPMQTEHHQT#PL DYNR	1151	M	
hs	STAG2	IP	STAG2	EQT%LHT%PVMMQTPQLTSTIMR	1109/12	M	
hs	STAG2	IP	STAG2	RGT%S%LMEDDEEPIVEDVMMS SEGR	1160/61	M	
hs	STAG2	IP	STAG2	GTSLMEDDEEPIVEDVMMS%S% EGR	1177/78	M	
hs	STAG2	IP	STAG2	SIMDES#VLGVS	S1224	M	BI-sens
hs	STAG2	IP	STAG2	VYPMQTEHHQT#PLDYNR		M	
hs	STAG2	IP	WAPAL	VEEESTGDPFGFDS#DDESLPVSS K	S162	M	
hs	STAG2	IP	WAPAL	RPES#PSEI	S306	M	

# 5 Appendix

hs	STAG2	IP	WAPAL	PSEIS#PIK	S311	M	
hs	STAG2	IP	WAPAL	S#MDEFTASTPADLGEAGR	S465	M	BI-sens
hs	STAG2	IP	WAPAL	LEFFGFEDHETGGDEGGS#GSSN YK	S528	M	BI-sens
hs	STAG2	IP	WAPAL	AEDS#ICLADSKPLPHQNVTNHVG K	S989	M	
hs	STAG2	IP	WAPAL	DAPTTQHDKS#GEWQETSGEIQ WVSTEK	S1154	M	BI-sens
hs	STAG2	IP	WAPAL	KNSHHIHKNAADS%T%KKPNAE	S275/T2 76	M	
hs	STAG2	IP	WAPAL	S%GPKRS%PTKAVY	S581/86	M	
mm	Tubg1	LAP	Tubg1	CAEHGIS#PEGIVEEF	S32	M	BI+Hes- sens
mm	Tubg1	LAP	Tubg1	SQGEKIHEDIFDIIDREADGSDS# LEGF	S131	I/M	BI-sens
mm	Tubg1	LAP	Tubg1	TTDQSVAS#VR	S284	M?	Hes-sens
mm	Tubg1	LAP	Tubg1	KS#PYLPSAHR	S364	BI+Hes- ind	
mm	Tubg1	LAP	Tubg1	NFDEMDT%S%REIVQQL	T423/S4 24	Hes-ind	
mm	Tubg1	LAP	Tubg1	ILNS%S%YAKLY	S80/81	Hes-ind	
mm	Tubg1	LAP	TUBGCP3	S%AES%PQDAADLFTDLENAFQG K	S512/S5 15	I/M	
mm	Tubg1	LAP	TUBGCP4	REGPSRETS#PREAPASGW	S441	M	
mm	Tubg1	LAP	TUBGCP5	MSDNASASS%GS%DQGPSSR	S535/S5 37	I/M	
mm	Tubg1	LAP	TUBGCP5	HGEDS%T%PQVLTEQQATK	S610/T6 11	M	Hes-sens
mm	Tubg1	LAP	TUBGCP6	LGLPPVPDNADLS#GLAIK	S242	M	BI-sens
mm	Tubg1	LAP	TUBGCP6	VHPQVTS#PGPEHPEGQGC	S831	I/M	
mm	Tubg1	LAP	TUBGCP6	QHS#PAWDGW	S852	I/M	
mm	Tubg1	LAP	TUBGCP6	NRPGLLT#PQPLKPL	T865	M	
mm	Tubg1	LAP	TUBGCP6	GALS#PEAEPN	S1283	BI+Hes- ind?	
mm	Tubg1	LAP	TUBGCP6	TPRPQQS#PPGHTSQ	S1296	I/M	
mm	Tubg1	LAP	TUBGCP6	WNIHGHVS%NAS%IR	S1111/S 1114	BI-ind	
mm	Tubg1	LAP	TUBGCP6	EDT%AAQS%S%PGRGEEAEAS	T1392/S 1396/S1 397	BI-ind?	
mm	Tubg1	LAP	TUBGCP6	RHSS%VS%KEEKELRME	S655/S5 7	M	Hes-sens
mm	Tubg1	LAP	TUBGCP6	RPAVAT%S%PAPGPL	T963/T9 64	M	BI-sens
hs	WAPAL	IP	PDS5A	IISVT#PVKNIDPVK	T1211	I/M	
hs	WAPAL	IP	PDS5A	AAVGQES#PGGLEAGNAK	S1305	M	Hes-sens
hs	WAPAL	IP	RAD21	AHVFECLNESSVESIIS#PK	S46	M	Hes-sens
hs	WAPAL	IP	RAD21	SLNQS#RVEEITMR	S142	M?	Bi-sens?
hs	WAPAL	IP	RAD21	EEVGNIS#ILQENDFGDFGMDDR	S153	I/M	BI-sens
hs	WAPAL	IP	RAD21	GMDDREIMREGS#AFEDDDMLVS	S175	I/M	BI-sens?
hs	WAPAL	IP	SMC1	nd			
hs	WAPAL	IP	SMC3	nd			
hs	WAPAL	IP	STAG1	nd			
hs	WAPAL	IP	STAG2	nd			
hs	WAPAL	IP	WAPAL	VEEESTGDPFGFDS#DDESLPVSS K	S162	I/M	
hs	WAPAL	IP	WAPAL	CSSYS#ESSEAAQLEEVTSVLEAN SK	S183	I/M	
hs	WAPAL	IP	WAPAL	NADDS#TKKPNAETTVASEIK	S275	M	
hs	WAPAL	IP	WAPAL	FGKRPE#PSEI	S306	I/M?	
hs	WAPAL	IP	WAPAL	PSEIS#PIKGS	S311	I/M	

hs	WAPAL	IP	WAPAL	SEDCILS#LDSDPLLEMK	S339	M	BI-sens
hs	WAPAL	IP	WAPAL	SEDCILSLDS#DPLLEMK	S342	M?	
hs	WAPAL	IP	WAPAL	NEAIEEDIVQS#VLRPT	S371	M	BI+Hes-sens
hs	WAPAL	IP	WAPAL	GGVSCGTS#FR	S432	I/M	
hs	WAPAL	IP	WAPAL	S#MDEFTASTPADLGEAGR	S465	M	BI-sens
hs	WAPAL	IP	WAPAL	TAST#PADLGEAGRL	T473	M	BI-sens
hs	WAPAL	IP	WAPAL	TKTAPSPS#LQPPESNDNSQDS QSGTN	S487	bi-ind?	
hs	WAPAL	IP	WAPAL	GFEDHETGGDEGGS#GSSNY	S528	M	BI-sens
hs	WAPAL	IP	WAPAL	YFGFDDLS#E	S544	I/M	
hs	WAPAL	IP	WAPAL	ES#EDDEDDDCQVERK	S546	I/M	
hs	WAPAL	IP	WAPAL	KIFSGPKRS#PTKA	S586	I/M	
hs	WAPAL	IP	WAPAL	DFTEDLPGVPES#VKKPINKQ	S608	M	
hs	WAPAL	IP	WAPAL	AEDS#ICLADSKPLPHQNVTHVG K	S989	M	BI-sens
hs	WAPAL	IP	WAPAL	HDKS#GEWQET	S1154	M	BI-sens
hs	WAPAL	IP	WAPAL	GEWQETS#GEIQ	S1161	M	BI-sens

## 6 Abbreviations

Human gene symbols from HGNC ([www.genenames.org](http://www.genenames.org)) were used for genes and their respective gene products within the text and in all tables and figures. The following table lists symbols frequently used in the text:

HGNC symbol	Name	Ensembl ID
AURKB	Aurora kinase B	ENSG00000178999
BIRC5	Baculoviral IAP repeat-containing protein 5, Survivin	ENSG00000089685
BUB1	Mitotic checkpoint serine/threonine-protein kinase BUB1	ENSG00000169679
BUB1B	Mitotic checkpoint S/T-protein kinase BUB1 beta (BubR1)	ENSG00000156970
BUB3	Mitotic checkpoint protein BUB3	ENSG00000154473
C10orf104	Uncharacterized protein C10orf104	ENSG00000166295
C14orf94	Uncharacterized protein C14orf94	ENSG00000092036
C4orf15	Uncharacterized protein C4orf15	ENSG00000214367
CASC5	Protein CASC5, Blinkin	ENSG00000137812
CCDC5	Coiled-coil domain-containing protein 5	ENSG00000152240
CCNA1	Cyclin-A1	ENSG00000133101
CCNB1	G2/mitotic-specific cyclin-B1	ENSG00000134057
CCND1	G1/S-specific cyclin-D1	ENSG00000110092
CCNE1	G1/S-specific cyclin-E1	ENSG00000105173
CDC20	Cell division cycle protein 20 homolog	ENSG00000117399
CDC25A	M-phase inducer phosphatase 1	ENSG00000164045
CDC25B	M-phase inducer phosphatase 2	ENSG00000101224
CDC25C	M-phase inducer phosphatase 3	ENSG00000158402
CDC27	Cell division cycle protein 27 homolog	ENSG00000004897
CDCA8	Borealin	ENSG00000134690
CDK1	Cyclin-dependent kinase 1	ENSG00000170312
CDK2	Cyclin-dependent kinase 2	ENSG00000123374
CDK4	Cyclin-dependent kinase 4	ENSG00000135446
CDK6	Cyclin-dependent kinase 6	ENSG00000105810
CDKN1B	Cyclin-dependent kinase inhibitor 1B	ENSG00000111276
CEP27	Centrosomal protein of 27 kDa	ENSG00000137814
CHEK1	CHK1	ENSG00000149554
CHEK2	CHK2	ENSG00000183765
FAM128B	Family with sequence similarity 128, member B	ENSG00000152082
FAM29A	Protein FAM29A	ENSG00000147874
FZR1	hCDH1, Fizzy-related protein homolog	ENSG00000105325
KIF23	Kinesin-like protein KIF23	ENSG00000137807
MAD2L1	Mitotic spindle assembly checkpoint protein MAD2A	ENSG00000164109
MIS12	Protein MIS12 homolog	ENSG00000167842
NCAPD2	Condensin complex subunit 1	ENSG00000010292
NCAPH	Condensin complex subunit 2	ENSG00000121152
NDC80	Kinetochore protein Hec1	ENSG00000080986
NEDD1	Protein NEDD1	ENSG00000139350
PDS5A	PDS5, homolog A isoform 1	ENSG00000121892
PDS5B	Androgen-induced proliferation inhibitor	ENSG00000083642
PLK1	Serine/threonine-protein kinase PLK1	ENSG00000166851
RACGAP1	Rac GTPase-activating protein 1	ENSG00000161800



RAD21	Double-strand-break repair protein rad21 homolog	ENSG00000164754
SGOL1	Shugoshin-like 1	ENSG00000129810
SMC1A	Structural maintenance of chromosomes protein 1A	ENSG00000072501
SMC3	Structural maintenance of chromosomes 3	ENSG00000108055
SMC6	Structural maintenance of chromosomes protein 6	ENSG00000163029
STAG1	Cohesin subunit SA-1	ENSG00000118007
STAG2	Cohesin subunit SA-2	ENSG00000101972
TUBG1	Tubulin gamma-1 chain	ENSG00000131462
TUBGCP2	Gamma-tubulin complex component 2	ENSG00000130640
TUBGCP3	Gamma-tubulin complex component 3	ENSG00000126216
TUBGCP4	Gamma-tubulin complex component 4	ENSG00000137822
TUBGCP5	Gamma-tubulin complex component 5	ENSG00000153575
TUBGCP6	Gamma-tubulin complex component 6	ENSG00000128159
UBR5	E3 ubiquitin-protein ligase EDD1	ENSG00000104517
UCHL5IP	UCHL5-interacting protein	ENSG00000213397
WAPAL	Wings apart-like protein homolog	ENSG00000062650

Other abbreviations used in this work:

Abbreviation	Explanation
Å	Ångstrom
aa	amino acid
AGC	automatic gain control
APC/C	anaphase-promoting complex
AP-MS	affinity purification followed by MS
as-kinase	analogue-sensitive kinase
BAC	bacterial artificial chromosomes
BI-ind	induced after BI4834 treatment
BI-sens	sensitive to BI4834 treatment
CAD	collision activated dissociation
ChT	chymotrypsin protease
CPC	chromosomal passenger complex
<i>D. melanogaster/Dm</i>	<i>Drosophila. melanogaster</i>
DAPI	4',6-Diamidino-2-phenylindol
DMEM	Dulbecco's Modified Eagle Medium
dox	doxycyclin
<i>E. Coli</i>	<i>Escherichia coli</i>
ESI	electrospray ionisation
FCS	fetal calf serum
FT-ICR	fourier transform – ion cyclotron resonance
G1	gap-phase 1
G2	gap-phase 2
G418	geneticin
<i>H. sapiens/Hs</i>	<i>Homo sapiens</i>
Hes-ind	induced after Hesperadin treatment
Hes-sens	sensitive to Hesperadin treatment
HGNC	humane genome project genome nomenclature committee
HMM	hidden Markov model
HPLC	high pressure liquid chromatography
hyg	hygromycin
I	interphase-specific
I/M	interphase- and mitosis-specific
IF	immunofluorescence microscopy
L	log-phase cells
LAP	localisation and affinity purification tag
LC	liquid chromatography
M	mitosis-specific

MCC	mitotic checkpoint complex
MGI	mouse genome informatics
M-phase	mitosis
MS	mass spectrometry
N	noc arrest 18 h
NB	noc18 h, incl 2 h BI4834 treatment
NHM	noc 18 h, incl 2 h Hesperadin and MG132 treatment
OT	orbital trap
PBD	polo box domain
PIM	protease inhibitor mix
preRC	prereplication complex
RNAi	RNA interference
S	serine
<i>S. cerevisiae/Sc</i>	<i>Saccharomyces cerevisiae</i>
<i>S. pombe/Sp</i>	<i>Schizosaccharomyces pombe</i>
SAC	spindle assembly checkpoint
SCF	Skip1, Cullin, F-box ubiquitin ligase
SDS-PAGE	Sodium dodecyl sulfate polyacrylamid electrophoresis
SFCM	spectral fuzzy c-means
siRNA	small interfering RNA
sN	synchronised cells, 3 h noc treatment
sNB	synchronised cells, 3 h noc treatment incl 2 h BI4834 treatment
sNHM	synchronised cells, 3 h noc treatment incl 2 h Hesperadin and MG132 treatment
SO	mitotic shake off
S-phase	synthesis-phase
Sub	subtilisin protease
T	threonine
Try	trypsin protease
WB	western blot
<i>X. laevis/Xl</i>	<i>Xenopus laevis</i>
Y	tyrosine
Y2H	yeast two hybrid assay
γ-TuRC	γ-tubulin ring complex

## 7 References

- Adams, R. R., Wheatley, S. P., Gouldsworthy, A. M., Kandels-Lewis, S. E., Carmena, M., Smythe, C., Gerloff, D. L., and Earnshaw, W. C. (2000). INCENP binds the Aurora-related kinase AIRK2 and is required to target it to chromosomes, the central spindle and cleavage furrow. *Curr Biol* *10*, 1075-1078.
- Ahonen, L. J., Kallio, M. J., Daum, J. R., Bolton, M., Manke, I. A., Yaffe, M. B., Stukenberg, P. T., and Gorbsky, G. J. (2005). Polo-like kinase 1 creates the tension-sensing 3F3/2 phosphoepitope and modulates the association of spindle-checkpoint proteins at kinetochores. *Curr Biol* *15*, 1078-1089.
- Alberts, B. (1998). The cell as a collection of protein machines: preparing the next generation of molecular biologists. *Cell* *92*, 291-294.
- Allen, J. J., Lazerwith, S. E., and Shokat, K. M. (2005). Bio-orthogonal affinity purification of direct kinase substrates. *J Am Chem Soc* *127*, 5288-5289.
- Andersen, J. S., Wilkinson, C. J., Mayor, T., Mortensen, P., Nigg, E. A., and Mann, M. (2003). Proteomic characterization of the human centrosome by protein correlation profiling. *Nature* *426*, 570-574.
- Andrade, M. A., Petosa, C., O'Donoghue, S. I., Muller, C. W., and Bork, P. (2001). Comparison of ARM and HEAT protein repeats. *J Mol Biol* *309*, 1-18.
- Andrade, M. A., Ponting, C. P., Gibson, T. J., and Bork, P. (2000). Homology-based method for identification of protein repeats using statistical significance estimates. *J Mol Biol* *298*, 521-537.
- Andrews, P. D., Knatko, E., Moore, W. J., and Swedlow, J. R. (2003). Mitotic mechanics: the auroras come into view. *Curr Opin Cell Biol* *15*, 672-683.
- Arnaud, L., Pines, J., and Nigg, E. A. (1998). GFP tagging reveals human Polo-like kinase 1 at the kinetochore/centromere region of mitotic chromosomes. *Chromosoma* *107*, 424-429.
- Asano, S., Park, J. E., Sakchaisri, K., Yu, L. R., Song, S., Supavilai, P., Veenstra, T. D., and Lee, K. S. (2005). Concerted mechanism of Swe1/Wee1 regulation by multiple kinases in budding yeast. *Embo J* *24*, 2194-2204.
- Ashburner, M., Ball, C. A., Blake, J. A., Botstein, D., Butler, H., Cherry, J. M., Davis, A. P., Dolinski, K., Dwight, S. S., Eppig, J. T., *et al.* (2000). Gene ontology: tool for the unification of biology. The Gene Ontology Consortium. *Nat Genet* *25*, 25-29.
- Bantscheff, M., Schirle, M., Sweetman, G., Rick, J., and Kuster, B. (2007). Quantitative mass spectrometry in proteomics: a critical review. *Anal Bioanal Chem* *389*, 1017-1031.
- Barr, F. A., Sillje, H. H., and Nigg, E. A. (2004). Polo-like kinases and the orchestration of cell division. *Nat Rev Mol Cell Biol* *5*, 429-440.
- Baumann, C., Korner, R., Hofmann, K., and Nigg, E. A. (2007). PICH, a centromere-associated SNF2 family ATPase, is regulated by Plk1 and required for the spindle checkpoint. *Cell* *128*, 101-114.
- Beausoleil, S. A., Jedrychowski, M., Schwartz, D., Elias, J. E., Villen, J., Li, J., Cohn, M. A., Cantley, L. C., and Gygi, S. P. (2004). Large-scale characterization of HeLa cell nuclear phosphoproteins. *Proc Natl Acad Sci U S A* *101*, 12130-12135.
- Belgareh, N., Rabut, G., Bai, S. W., van Overbeek, M., Beaudouin, J., Daigle, N., Zatsepina, O. V., Pasteau, F., Labas, V., Fromont-Racine, M., *et al.* (2001). An evolutionarily conserved

## 7 References

- NPC subcomplex, which redistributes in part to kinetochores in mammalian cells. *J Cell Biol* **154**, 1147-1160.
- Bishop, J. D., and Schumacher, J. M. (2002). Phosphorylation of the carboxyl terminus of inner centromere protein (INCENP) by the Aurora B Kinase stimulates Aurora B kinase activity. *J Biol Chem* **277**, 27577-27580.
- Blethrow, J. D., Glavy, J. S., Morgan, D. O., and Shokat, K. M. (2008). Covalent capture of kinase-specific phosphopeptides reveals Cdk1-cyclin B substrates. *Proc Natl Acad Sci U S A* **105**, 1442-1447.
- Brohee, S., and van Helden, J. (2006). Evaluation of clustering algorithms for protein-protein interaction networks. *BMC Bioinformatics* **7**, 488.
- Burkard, M. E., Randall, C. L., Larochelle, S., Zhang, C., Shokat, K. M., Fisher, R. P., and Jallepalli, P. V. (2007). Chemical genetics reveals the requirement for Polo-like kinase 1 activity in positioning RhoA and triggering cytokinesis in human cells. *Proc Natl Acad Sci U S A* **104**, 4383-4388.
- Casenghi, M., Barr, F. A., and Nigg, E. A. (2005). Phosphorylation of Nlp by Plk1 negatively regulates its dynein-dynactin-dependent targeting to the centrosome. *J Cell Sci* **118**, 5101-5108.
- Casenghi, M., Meraldi, P., Weinhart, U., Duncan, P. I., Korner, R., and Nigg, E. A. (2003). Polo-like kinase 1 regulates Nlp, a centrosome protein involved in microtubule nucleation. *Dev Cell* **5**, 113-125.
- Chan, C. S., and Botstein, D. (1993). Isolation and characterization of chromosome-gain and increase-in-ploidy mutants in yeast. *Genetics* **135**, 677-691.
- Chan, G. K., Jablonski, S. A., Sudakin, V., Hittle, J. C., and Yen, T. J. (1999). Human BUBR1 is a mitotic checkpoint kinase that monitors CENP-E functions at kinetochores and binds the cyclosome/APC. *J Cell Biol* **146**, 941-954.
- Chatr-aryamontri, A., Ceol, A., Palazzi, L. M., Nardelli, G., Schneider, M. V., Castagnoli, L., and Cesareni, G. (2007). MINT: the Molecular INTERaction database. *Nucleic Acids Res* **35**, D572-574.
- Cheeseman, I. M., Anderson, S., Jwa, M., Green, E. M., Kang, J., Yates, J. R., 3rd, Chan, C. S., Drubin, D. G., and Barnes, G. (2002). Phospho-regulation of kinetochore-microtubule attachments by the Aurora kinase Ipl1p. *Cell* **111**, 163-172.
- Cheeseman, I. M., Chappie, J. S., Wilson-Kubalek, E. M., and Desai, A. (2006). The conserved KMN network constitutes the core microtubule-binding site of the kinetochore. *Cell* **127**, 983-997.
- Cheeseman, I. M., and Desai, A. (2005). A combined approach for the localization and tandem affinity purification of protein complexes from metazoans. *Sci STKE* **2005**, pl1.
- Cheeseman, I. M., and Desai, A. (2008). Molecular architecture of the kinetochore-microtubule interface. *Nat Rev Mol Cell Biol* **9**, 33-46.
- Cheeseman, I. M., Hori, T., Fukagawa, T., and Desai, A. (2008). KNL1 and the CENP-H/I/K Complex Coordinately Direct Kinetochore Assembly in Vertebrates. *Mol Biol Cell* **19**, 587-594.
- Cheeseman, I. M., Niessen, S., Anderson, S., Hyndman, F., Yates, J. R., 3rd, Oegema, K., and Desai, A. (2004). A conserved protein network controls assembly of the outer kinetochore and its ability to sustain tension. *Genes Dev* **18**, 2255-2268.
- Choe, L., D'Ascenzo, M., Relkin, N. R., Pappin, D., Ross, P., Williamson, B., Guertin, S., Pribil, P., and Lee, K. H. (2007). 8-plex quantitation of changes in cerebrospinal fluid protein expression in subjects undergoing intravenous immunoglobulin treatment for Alzheimer's disease. *Proteomics* **7**, 3651-3660.

- Collins, S. R., Kemmeren, P., Zhao, X. C., Greenblatt, J. F., Spencer, F., Holstege, F. C., Weissman, J. S., and Krogan, N. J. (2007). Toward a comprehensive atlas of the physical interactome of *Saccharomyces cerevisiae*. *Mol Cell Proteomics* 6, 439-450.
- Crosio, C., Fimia, G. M., Loury, R., Kimura, M., Okano, Y., Zhou, H., Sen, S., Allis, C. D., and Sassone-Corsi, P. (2002). Mitotic phosphorylation of histone H3: spatio-temporal regulation by mammalian Aurora kinases. *Mol Cell Biol* 22, 874-885.
- Dai, J., Sullivan, B. A., and Higgins, J. M. (2006). Regulation of mitotic chromosome cohesion by Haspin and Aurora B. *Dev Cell* 11, 741-750.
- D'Avino, P. P., Savoian, M. S., and Glover, D. M. (2005). Cleavage furrow formation and ingression during animal cytokinesis: a microtubule legacy. *J Cell Sci* 118, 1549-1558.
- DeLuca, J. G., Gall, W. E., Ciferri, C., Cimini, D., Musacchio, A., and Salmon, E. D. (2006). Kinetochore microtubule dynamics and attachment stability are regulated by Hec1. *Cell* 127, 969-982.
- Di Fiore, B., and Pines, J. (2007). Emi1 is needed to couple DNA replication with mitosis but does not regulate activation of the mitotic APC/C. *J Cell Biol* 177, 425-437.
- Ditchfield, C., Johnson, V. L., Tighe, A., Ellston, R., Haworth, C., Johnson, T., Mortlock, A., Keen, N., and Taylor, S. S. (2003). Aurora B couples chromosome alignment with anaphase by targeting BubR1, Mad2, and Cenp-E to kinetochores. *J Cell Biol* 161, 267-280.
- Einarson, M. B., Cukierman, E., Compton, D. A., and Golemis, E. A. (2004). Human enhancer of invasion-cluster, a coiled-coil protein required for passage through mitosis. *Mol Cell Biol* 24, 3957-3971.
- Elia, A. E., Cantley, L. C., and Yaffe, M. B. (2003a). Proteomic screen finds pSer/pThr-binding domain localizing Plk1 to mitotic substrates. *Science* 299, 1228-1231.
- Elia, A. E., Rellos, P., Haire, L. F., Chao, J. W., Ivins, F. J., Hoepker, K., Mohammad, D., Cantley, L. C., Smerdon, S. J., and Yaffe, M. B. (2003b). The molecular basis for phosphodependent substrate targeting and regulation of Plks by the Polo-box domain. *Cell* 115, 83-95.
- Elowe, S., Hummer, S., Uldschmid, A., Li, X., and Nigg, E. A. (2007). Tension-sensitive Plk1 phosphorylation on BubR1 regulates the stability of kinetochore microtubule interactions. *Genes Dev* 21, 2205-2219.
- Ewing, R. M., Chu, P., Elisma, F., Li, H., Taylor, P., Climie, S., McBroom-Cerajewski, L., Robinson, M. D., O'Connor, L., Li, M., *et al.* (2007). Large-scale mapping of human protein-protein interactions by mass spectrometry. *Mol Syst Biol* 3, 89.
- Felix, M. A., Pines, J., Hunt, T., and Karsenti, E. (1989). A post-ribosomal supernatant from activated *Xenopus* eggs that displays post-translationally regulated oscillation of its cdc2+ mitotic kinase activity. *Embo J* 8, 3059-3069.
- Fischle, W., Tseng, B. S., Dormann, H. L., Ueberheide, B. M., Garcia, B. A., Shabanowitz, J., Hunt, D. F., Funabiki, H., and Allis, C. D. (2005). Regulation of HP1-chromatin binding by histone H3 methylation and phosphorylation. *Nature* 438, 1116-1122.
- Francisco, L., and Chan, C. S. (1994). Regulation of yeast chromosome segregation by Ipl1 protein kinase and type 1 protein phosphatase. *Cell Mol Biol Res* 40, 207-213.
- Fukunaga, R., and Hunter, T. (1997). MNK1, a new MAP kinase-activated protein kinase, isolated by a novel expression screening method for identifying protein kinase substrates. *Embo J* 16, 1921-1933.
- Gandhi, R., Gillespie, P. J., and Hirano, T. (2006). Human Wapl is a cohesin-binding protein that promotes sister-chromatid resolution in mitotic prophase. *Curr Biol* 16, 2406-2417.

## 7 References

- Gavin, A. C., Aloy, P., Grandi, P., Krause, R., Boesche, M., Marzioch, M., Rau, C., Jensen, L. J., Bastuck, S., Dumpelfeld, B., *et al.* (2006). Proteome survey reveals modularity of the yeast cell machinery. *Nature* **440**, 631-636.
- Gieffers, C., Peters, B. H., Kramer, E. R., Dotti, C. G., and Peters, J. M. (1999). Expression of the CDH1-associated form of the anaphase-promoting complex in postmitotic neurons. *Proc Natl Acad Sci U S A* **96**, 11317-11322.
- Gingras, A. C., Gstaiger, M., Raught, B., and Aebersold, R. (2007). Analysis of protein complexes using mass spectrometry. *Nat Rev Mol Cell Biol* **8**, 645-654.
- Glavy, J. S., Krutchinsky, A. N., Cristea, I. M., Berke, I. C., Boehmer, T., Blobel, G., and Chait, B. T. (2007). Cell-cycle-dependent phosphorylation of the nuclear pore Nup107-160 subcomplex. *Proc Natl Acad Sci U S A* **104**, 3811-3816.
- Glotzer, M., Murray, A. W., and Kirschner, M. W. (1991). Cyclin is degraded by the ubiquitin pathway. *Nature* **349**, 132-138.
- Glover, D. M., Leibowitz, M. H., McLean, D. A., and Parry, H. (1995). Mutations in aurora prevent centrosome separation leading to the formation of monopolar spindles. *Cell* **81**, 95-105.
- Golsteyn, R. M., Schultz, S. J., Bartek, J., Ziemiecki, A., Ried, T., and Nigg, E. A. (1994). Cell cycle analysis and chromosomal localization of human Plk1, a putative homologue of the mitotic kinases *Drosophila* polo and *Saccharomyces cerevisiae* Cdc5. *J Cell Sci* **107** ( Pt 6), 1509-1517.
- Goshima, G., Wollman, R., Goodwin, S. S., Zhang, N., Scholey, J. M., Vale, R. D., and Stuurman, N. (2007). Genes required for mitotic spindle assembly in *Drosophila* S2 cells. *Science* **316**, 417-421.
- Guse, A., Mishima, M., and Glotzer, M. (2005). Phosphorylation of ZEN-4/MKLP1 by aurora B regulates completion of cytokinesis. *Curr Biol* **15**, 778-786.
- Hanisch, A., Wehner, A., Nigg, E. A., and Sillje, H. H. (2006). Different Plk1 functions show distinct dependencies on Polo-Box domain-mediated targeting. *Mol Biol Cell* **17**, 448-459.
- Harlow, E., and Lane, D. (1988). *Antibodies: A Laboratory Manual*, 1st edn. edn (Cold Spring Harbor, Cold Spring Harbor Laboratory).
- Hartman, T., Stead, K., Koshland, D., and Guacci, V. (2000). Pds5p is an essential chromosomal protein required for both sister chromatid cohesion and condensation in *Saccharomyces cerevisiae*. *J Cell Biol* **151**, 613-626.
- Hauf, S., Cole, R. W., LaTerra, S., Zimmer, C., Schnapp, G., Walter, R., Heckel, A., van Meel, J., Rieder, C. L., and Peters, J. M. (2003). The small molecule Hesperadin reveals a role for Aurora B in correcting kinetochore-microtubule attachment and in maintaining the spindle assembly checkpoint. *J Cell Biol* **161**, 281-294.
- Hauf, S., Roitinger, E., Koch, B., Dittrich, C. M., Mechtler, K., and Peters, J. M. (2005). Dissociation of cohesin from chromosome arms and loss of arm cohesion during early mitosis depends on phosphorylation of SA2. *PLoS Biol* **3**, e69.
- Hauf, S., Waizenegger, I. C., and Peters, J. M. (2001). Cohesin cleavage by separase required for anaphase and cytokinesis in human cells. *Science* **293**, 1320-1323.
- Heald, R., and McKeon, F. (1990). Mutations of phosphorylation sites in lamin A that prevent nuclear lamina disassembly in mitosis. *Cell* **61**, 579-589.
- Henderson, M. J., Munoz, M. A., Saunders, D. N., Clancy, J. L., Russell, A. J., Williams, B., Pappin, D., Khanna, K. K., Jackson, S. P., Sutherland, R. L., and Watts, C. K. (2006). EDD mediates DNA damage-induced activation of CHK2. *J Biol Chem* **281**, 39990-40000.

- Herzog, F., Dube, P., Primorac, I., Stark, H., and Peters, J. M. (in preparation).
- Hirano, T. (2005). SMC proteins and chromosome mechanics: from bacteria to humans. *Philos Trans R Soc Lond B Biol Sci* *360*, 507-514.
- Hirano, T. (2006). At the heart of the chromosome: SMC proteins in action. *Nat Rev Mol Cell Biol* *7*, 311-322.
- Hirota, T., Gerlich, D., Koch, B., Ellenberg, J., and Peters, J. M. (2004). Distinct functions of condensin I and II in mitotic chromosome assembly. *J Cell Sci* *117*, 6435-6445.
- Hirota, T., Lipp, J. J., Toh, B. H., and Peters, J. M. (2005). Histone H3 serine 10 phosphorylation by Aurora B causes HP1 dissociation from heterochromatin. *Nature* *438*, 1176-1180.
- Honda, R., Korner, R., and Nigg, E. A. (2003). Exploring the functional interactions between Aurora B, INCENP, and survivin in mitosis. *Mol Biol Cell* *14*, 3325-3341.
- Jablonski, S. A., Chan, G. K., Cooke, C. A., Earnshaw, W. C., and Yen, T. J. (1998). The hBUB1 and hBUBR1 kinases sequentially assemble onto kinetochores during prophase with hBUBR1 concentrating at the kinetochore plates in mitosis. *Chromosoma* *107*, 386-396.
- Jackman, M., Lindon, C., Nigg, E. A., and Pines, J. (2003). Active cyclin B1-Cdk1 first appears on centrosomes in prophase. *Nat Cell Biol* *5*, 143-148.
- Janssens, V., Goris, J., and Van Hoof, C. (2005). PP2A: the expected tumor suppressor. *Curr Opin Genet Dev* *15*, 34-41.
- Jeyaprakash, A. A., Klein, U. R., Lindner, D., Ebert, J., Nigg, E. A., and Conti, E. (2007). Structure of a Survivin-Borealin-INCENP core complex reveals how chromosomal passengers travel together. *Cell* *131*, 271-285.
- Kang, Y. H., Park, J. E., Yu, L. R., Soung, N. K., Yun, S. M., Bang, J. K., Seong, Y. S., Yu, H., Garfield, S., Veenstra, T. D., and Lee, K. S. (2006). Self-regulated Plk1 recruitment to kinetochores by the Plk1-PBIP1 interaction is critical for proper chromosome segregation. *Mol Cell* *24*, 409-422.
- Karsenti, E., Bravo, R., and Kirschner, M. (1987). Phosphorylation changes associated with the early cell cycle in *Xenopus* eggs. *Dev Biol* *119*, 442-453.
- Kelm, O., Wind, M., Lehmann, W. D., and Nigg, E. A. (2002). Cell cycle-regulated phosphorylation of the *Xenopus* polo-like kinase Plx1. *J Biol Chem* *277*, 25247-25256.
- Kerrien, S., Alam-Faruque, Y., Aranda, B., Bancarz, I., Bridge, A., Derow, C., Dimmer, E., Feuermann, M., Friedrichsen, A., Huntley, R., *et al.* (2007). IntAct--open source resource for molecular interaction data. *Nucleic Acids Res* *35*, D561-565.
- King, E. M., Rachidi, N., Morrice, N., Hardwick, K. G., and Stark, M. J. (2007). Ipl1p-dependent phosphorylation of Mad3p is required for the spindle checkpoint response to lack of tension at kinetochores. *Genes Dev* *21*, 1163-1168.
- Kitajima, T. S., Hauf, S., Ohsugi, M., Yamamoto, T., and Watanabe, Y. (2005). Human Bub1 defines the persistent cohesion site along the mitotic chromosome by affecting Shugoshin localization. *Curr Biol* *15*, 353-359.
- Kittler, R., Heninger, A. K., Franke, K., Habermann, B., and Buchholz, F. (2005a). Production of endoribonuclease-prepared short interfering RNAs for gene silencing in mammalian cells. *Nat Methods* *2*, 779-784.
- Kittler, R., Pelletier, L., Heninger, A. K., Slabicki, M., Theis, M., Miroslaw, L., Poser, I., Lawo, S., Grabner, H., Kozak, K., *et al.* (2007). Genome-scale RNAi profiling of cell division in human tissue culture cells. *Nat Cell Biol* *9*, 1401-1412.

## 7 References

- Kittler, R., Pelletier, L., Ma, C., Poser, I., Fischer, S., Hyman, A. A., and Buchholz, F. (2005b). RNA interference rescue by bacterial artificial chromosome transgenesis in mammalian tissue culture cells. *Proc Natl Acad Sci U S A* *102*, 2396-2401.
- Kiyomitsu, T., Obuse, C., and Yanagida, M. (2007). Human Blinkin/AF15q14 is required for chromosome alignment and the mitotic checkpoint through direct interaction with Bub1 and BubR1. *Dev Cell* *13*, 663-676.
- Koch, C. A., Anderson, D., Moran, M. F., Ellis, C., and Pawson, T. (1991). SH2 and SH3 domains: elements that control interactions of cytoplasmic signaling proteins. *Science* *252*, 668-674.
- Kocher, T., and Superti-Furga, G. (2007). Mass spectrometry-based functional proteomics: from molecular machines to protein networks. *Nat Methods* *4*, 807-815.
- Kraft, C., Herzog, F., Gieffers, C., Mechtler, K., Hagting, A., Pines, J., and Peters, J. M. (2003). Mitotic regulation of the human anaphase-promoting complex by phosphorylation. *Embo J* *22*, 6598-6609.
- Krogan, N. J., Cagney, G., Yu, H., Zhong, G., Guo, X., Ignatchenko, A., Li, J., Pu, S., Datta, N., Tikuisis, A. P., *et al.* (2006). Global landscape of protein complexes in the yeast *Saccharomyces cerevisiae*. *Nature* *440*, 637-643.
- Kueng, S., Hegemann, B., Peters, B. H., Lipp, J. J., Schleiffer, A., Mechtler, K., and Peters, J. M. (2006). Wapl controls the dynamic association of cohesin with chromatin. *Cell* *127*, 955-967.
- Labbe, J. C., Capony, J. P., Caput, D., Cavadore, J. C., Derancourt, J., Kaghad, M., Lelias, J. M., Picard, A., and Doree, M. (1989). MPF from starfish oocytes at first meiotic metaphase is a heterodimer containing one molecule of cdc2 and one molecule of cyclin B. *Embo J* *8*, 3053-3058.
- Lane, H. A., and Nigg, E. A. (1996). Antibody microinjection reveals an essential role for human polo-like kinase 1 (Plk1) in the functional maturation of mitotic centrosomes. *J Cell Biol* *135*, 1701-1713.
- Lenart, P., Petronczki, M., Steegmaier, M., Di Fiore, B., Lipp, J. J., Hoffmann, M., Rettig, W. J., Kraut, N., and Peters, J. M. (2007). The small-molecule inhibitor BI 2536 reveals novel insights into mitotic roles of polo-like kinase 1. *Curr Biol* *17*, 304-315.
- Li, H., Coghlan, A., Ruan, J., Coin, L. J., Heriche, J. K., Osmotherly, L., Li, R., Liu, T., Zhang, Z., Bolund, L., *et al.* (2006). TreeFam: a curated database of phylogenetic trees of animal gene families. *Nucleic Acids Res* *34*, D572-580.
- Lindon, C., and Pines, J. (2004). Ordered proteolysis in anaphase inactivates Plk1 to contribute to proper mitotic exit in human cells. *J Cell Biol* *164*, 233-241.
- Lipp, J. J., Hirota, T., Poser, I., and Peters, J. M. (2007). Aurora B controls the association of condensin I but not condensin II with mitotic chromosomes. *J Cell Sci* *120*, 1245-1255.
- Liu, X., Zhou, T., Kuriyama, R., and Erikson, R. L. (2004). Molecular interactions of Polo-like-kinase 1 with the mitotic kinesin-like protein CHO1/MKLP-1. *J Cell Sci* *117*, 3233-3246.
- Llamazares, S., Moreira, A., Tavares, A., Girdham, C., Spruce, B. A., Gonzalez, C., Karess, R. E., Glover, D. M., and Sunkel, C. E. (1991). polo encodes a protein kinase homolog required for mitosis in *Drosophila*. *Genes Dev* *5*, 2153-2165.
- Liodice, I., Alves, A., Rabut, G., Van Overbeek, M., Ellenberg, J., Sibarita, J. B., and Doye, V. (2004). The entire Nup107-160 complex, including three new members, is targeted as one entity to kinetochores in mitosis. *Mol Biol Cell* *15*, 3333-3344.



- Losada, A., Hirano, M., and Hirano, T. (2002). Cohesin release is required for sister chromatid resolution, but not for condensin-mediated compaction, at the onset of mitosis. *Genes Dev* 16, 3004-3016.
- Losada, A., Yokochi, T., and Hirano, T. (2005). Functional contribution of Pds5 to cohesin-mediated cohesion in human cells and *Xenopus* egg extracts. *J Cell Sci* 118, 2133-2141.
- Losada, A., Yokochi, T., Kobayashi, R., and Hirano, T. (2000). Identification and characterization of SA/Scs3p subunits in the *Xenopus* and human cohesin complexes. *J Cell Biol* 150, 405-416.
- Lowery, D. M., Clauser, K. R., Hjerrild, M., Lim, D., Alexander, J., Kishi, K., Ong, S. E., Gammeltoft, S., Carr, S. A., and Yaffe, M. B. (2007). Proteomic screen defines the Polo-box domain interactome and identifies Rock2 as a Plk1 substrate. *Embo J* 26, 2262-2273.
- Luders, J., Patel, U. K., and Stearns, T. (2006). GCP-WD is a gamma-tubulin targeting factor required for centrosomal and chromatin-mediated microtubule nucleation. *Nat Cell Biol* 8, 137-147.
- Mailand, N., Podtelejnikov, A. V., Groth, A., Mann, M., Bartek, J., and Lukas, J. (2002). Regulation of G(2)/M events by Cdc25A through phosphorylation-dependent modulation of its stability. *Embo J* 21, 5911-5920.
- Maller, J., Wu, M., and Gerhart, J. C. (1977). Changes in protein phosphorylation accompanying maturation of *Xenopus laevis* oocytes. *Dev Biol* 58, 295-312.
- Matsumura, S., Toyoshima, F., and Nishida, E. (2007). Polo-like kinase 1 facilitates chromosome alignment during prometaphase through BubR1. *J Biol Chem* 282, 15217-15227.
- Meila, M., and Shi, J. (2001). A Random Walks View of Spectral Segmentation. Paper presented at: International Conference on AI and Statistics (AISTAT).
- Mewes, H. W., Frishman, D., Guldener, U., Mannhaupt, G., Mayer, K., Mokrejs, M., Morgenstern, B., Munsterkotter, M., Rudd, S., and Weil, B. (2002). MIPS: a database for genomes and protein sequences. *Nucleic Acids Res* 30, 31-34.
- Morgan, D. O. (1997). Cyclin-dependent kinases: engines, clocks, and microprocessors. *Annu Rev Cell Dev Biol* 13, 261-291.
- Morgan, D. O. (2007). *The Cell Cycle - Principles of Control*, 1 edn (London, New Science Press).
- Morgan, D. O., Kaplan, J. M., Bishop, J. M., and Varmus, H. E. (1989). Mitosis-specific phosphorylation of p60c-src by p34cdc2-associated protein kinase. *Cell* 57, 775-786.
- Morla, A. O., Draetta, G., Beach, D., and Wang, J. Y. (1989). Reversible tyrosine phosphorylation of cdc2: dephosphorylation accompanies activation during entry into mitosis. *Cell* 58, 193-203.
- Morrow, C. J., Tighe, A., Johnson, V. L., Scott, M. I., Ditchfield, C., and Taylor, S. S. (2005). Bub1 and aurora B cooperate to maintain BubR1-mediated inhibition of APC/CCdc20. *J Cell Sci* 118, 3639-3652.
- Mueller, L. N., Rinner, O., Schmidt, A., Letarte, S., Bodenmiller, B., Brusniak, M. Y., Vitek, O., Aebersold, R., and Muller, M. (2007). SuperHirn - a novel tool for high resolution LC-MS-based peptide/protein profiling. *Proteomics* 7, 3470-3480.
- Mueller, P. R., Coleman, T. R., Kumagai, A., and Dunphy, W. G. (1995). Myt1: a membrane-associated inhibitory kinase that phosphorylates Cdc2 on both threonine-14 and tyrosine-15. *Science* 270, 86-90.

## 7 References

- Munoz, M. A., Saunders, D. N., Henderson, M. J., Clancy, J. L., Russell, A. J., Lehrbach, G., Musgrove, E. A., Watts, C. K., and Sutherland, R. L. (2007). The E3 ubiquitin ligase EDD regulates S-phase and G(2)/M DNA damage checkpoints. *Cell Cycle* 6, 3070-3077.
- Musacchio, A., and Salmon, E. D. (2007). The spindle-assembly checkpoint in space and time. *Nat Rev Mol Cell Biol* 8, 379-393.
- Nagase, T., Ishikawa, K., Suyama, M., Kikuno, R., Hirose, M., Miyajima, N., Tanaka, A., Kotani, H., Nomura, N., and Ohara, O. (1999). Prediction of the coding sequences of unidentified human genes. XIII. The complete sequences of 100 new cDNA clones from brain which code for large proteins in vitro. *DNA Res* 6, 63-70.
- Nakajima, H., Toyoshima-Morimoto, F., Taniguchi, E., and Nishida, E. (2003). Identification of a consensus motif for Plk (Polo-like kinase) phosphorylation reveals Myt1 as a Plk1 substrate. *J Biol Chem* 278, 25277-25280.
- Nasmyth, K., and Haering, C. H. (2005). The structure and function of smc and kleisin complexes. *Annu Rev Biochem* 74, 595-648.
- Neef, R., Gruneberg, U., Kopajtich, R., Li, X., Nigg, E. A., Sillje, H., and Barr, F. A. (2007). Choice of Plk1 docking partners during mitosis and cytokinesis is controlled by the activation state of Cdk1. *Nat Cell Biol* 9, 436-444.
- Nesvizhskii, A. I., and Aebersold, R. (2005). Interpretation of shotgun proteomic data: the protein inference problem. *Mol Cell Proteomics* 4, 1419-1440.
- Neumann, B., Erfle, H., Heriche, J. K., others, a., and Ellenberg, J. (in preparation).
- Ohshima, R., Ohta, T., Wu, W., Koike, A., Iwatani, T., Henderson, M., Watts, C. K., and Otsubo, T. (2007). Putative tumor suppressor EDD interacts with and up-regulates APC. *Genes Cells* 12, 1339-1345.
- Olsen, J. V., Blagoev, B., Gnäd, F., Macek, B., Kumar, C., Mortensen, P., and Mann, M. (2006). Global, in vivo, and site-specific phosphorylation dynamics in signaling networks. *Cell* 127, 635-648.
- Ong, S. E., Blagoev, B., Kratchmarova, I., Kristensen, D. B., Steen, H., Pandey, A., and Mann, M. (2002). Stable isotope labeling by amino acids in cell culture, SILAC, as a simple and accurate approach to expression proteomics. *Mol Cell Proteomics* 1, 376-386.
- Orjalo, A. V., Arnaoutov, A., Shen, Z., Boyarchuk, Y., Zeitlin, S. G., Fontoura, B., Briggs, S., Dasso, M., and Forbes, D. J. (2006). The Nup107-160 nucleoporin complex is required for correct bipolar spindle assembly. *Mol Biol Cell* 17, 3806-3818.
- Osmani, A. H., O'Donnell, K., Pu, R. T., and Osmani, S. A. (1991). Activation of the nimA protein kinase plays a unique role during mitosis that cannot be bypassed by absence of the bimE checkpoint. *Embo J* 10, 2669-2679.
- Panizza, S., Tanaka, T., Hochwagen, A., Eisenhaber, F., and Nasmyth, K. (2000). Pds5 cooperates with cohesin in maintaining sister chromatid cohesion. *Curr Biol* 10, 1557-1564.
- Parrish, J. R., Gulyas, K. D., and Finley, R. L., Jr. (2006). Yeast two-hybrid contributions to interactome mapping. *Curr Opin Biotechnol* 17, 387-393.
- Peri, S., Navarro, J. D., Amanchy, R., Kristiansen, T. Z., Jonnalagadda, C. K., Surendranath, V., Niranjana, V., Muthusamy, B., Gandhi, T. K., Gronborg, M., *et al.* (2003). Development of human protein reference database as an initial platform for approaching systems biology in humans. *Genome Res* 13, 2363-2371.
- Peter, M., Heitlinger, E., Haner, M., Aebi, U., and Nigg, E. A. (1991). Disassembly of in vitro formed lamin head-to-tail polymers by CDC2 kinase. *Embo J* 10, 1535-1544.

- Peter, M., Nakagawa, J., Doree, M., Labbe, J. C., and Nigg, E. A. (1990). In vitro disassembly of the nuclear lamina and M phase-specific phosphorylation of lamins by cdc2 kinase. *Cell* 61, 591-602.
- Peters, J. M. (2006). The anaphase promoting complex/cyclosome: a machine designed to destroy. *Nat Rev Mol Cell Biol* 7, 644-656.
- Peters, J. M., King, R. W., Hoog, C., and Kirschner, M. W. (1996). Identification of BIME as a subunit of the anaphase-promoting complex. *Science* 274, 1199-1201.
- Petretti, C., Savoian, M., Montembault, E., Glover, D. M., Prigent, C., and Giet, R. (2006). The PITSLRE/CDK11p58 protein kinase promotes centrosome maturation and bipolar spindle formation. *EMBO Rep* 7, 418-424.
- Petronczki, M., Glotzer, M., Kraut, N., and Peters, J. M. (2007). Polo-like kinase 1 triggers the initiation of cytokinesis in human cells by promoting recruitment of the RhoGEF Ect2 to the central spindle. *Dev Cell* 12, 713-725.
- Piwnica-Worms, H., Atherton-Fessler, S., Lee, M. S., Ogg, S., Swenson, K. I., and Parker, L. L. (1991). p107wee1 is a serine/threonine and tyrosine kinase that promotes the tyrosine phosphorylation of the cyclin/p34cdc2 complex. *Cold Spring Harb Symp Quant Biol* 56, 567-576.
- Poser, I., Sarov, M., Hutchins, J. R., Heriche, J. K., Toyoda, Y., Pozniakovsky, A., Weigl, D., Nitzsche, A., Hegemann, B., Bird, A. W., *et al.* (2008). BAC TransgeneOmics: a high-throughput method for exploration of protein function in mammals. *Nat Methods* 5, 409-415.
- Potapova, T. A., Daum, J. R., Pittman, B. D., Hudson, J. R., Jones, T. N., Satinover, D. L., Stukenberg, P. T., and Gorbsky, G. J. (2006). The reversibility of mitotic exit in vertebrate cells. *Nature* 440, 954-958.
- Qi, W., Tang, Z., and Yu, H. (2006). Phosphorylation- and polo-box-dependent binding of Plk1 to Bub1 is required for the kinetochore localization of Plk1. *Mol Biol Cell* 17, 3705-3716.
- Raynaud-Messina, B., and Merdes, A. (2007). Gamma-tubulin complexes and microtubule organization. *Curr Opin Cell Biol* 19, 24-30.
- Reeves, R. (2001). Molecular biology of HMGA proteins: hubs of nuclear function. *Gene* 277, 63-81.
- Rigaut, G., Shevchenko, A., Rutz, B., Wilm, M., Mann, M., and Seraphin, B. (1999). A generic protein purification method for protein complex characterization and proteome exploration. *Nat Biotechnol* 17, 1030-1032.
- Rines, D. R., Gomez-Ferreria, M. A., Zhou, Y., Dejesus, P., Grob, S., Batalov, S., Labow, M., Huesken, D., Mickanin, C., Hall, J., *et al.* (2008). Whole genome functional analysis identifies novel components required for mitotic spindle integrity in human cells. *Genome Biol* 9, R44.
- Rinner, O., Mueller, L. N., Hubalek, M., Muller, M., Gstaiger, M., and Aebersold, R. (2007). An integrated mass spectrometric and computational framework for the analysis of protein interaction networks. *Nat Biotechnol* 25, 345-352.
- Roessner-Tunali, U., Hegemann, B., Lytovchenko, A., Carrari, F., Bruedigam, C., Granot, D., and Fernie, A. R. (2003). Metabolic profiling of transgenic tomato plants overexpressing hexokinase reveals that the influence of hexose phosphorylation diminishes during fruit development. *Plant Physiol* 133, 84-99.
- Rosasco-Nitcher, S. E., Lan, W., Khorasanizadeh, S., and Stukenberg, P. T. (2008). Centromeric Aurora-B activation requires TD-60, microtubules, and substrate priming phosphorylation. *Science* 319, 469-472.
- Ross, P. L., Huang, Y. N., Marchese, J. N., Williamson, B., Parker, K., Hattan, S., Khainovski, N., Pillai, S., Dey, S., Daniels, S., *et al.* (2004). Multiplexed protein quantitation in

## 7 References

- Saccharomyces cerevisiae* using amine-reactive isobaric tagging reagents. *Mol Cell Proteomics* **3**, 1154-1169.
- Ruchaud, S., Carmena, M., and Earnshaw, W. C. (2007). Chromosomal passengers: conducting cell division. *Nat Rev Mol Cell Biol* **8**, 798-812.
- Sandall, S., Severin, F., McLeod, I. X., Yates, J. R., 3rd, Oegema, K., Hyman, A., and Desai, A. (2006). A Bir1-Sli15 complex connects centromeres to microtubules and is required to sense kinetochore tension. *Cell* **127**, 1179-1191.
- Santamaria, A., Neef, R., Eberspacher, U., Eis, K., Husemann, M., Mumberg, D., Prechtel, S., Schulze, V., Siemeister, G., Wortmann, L., *et al.* (2007). Use of the novel Plk1 inhibitor ZK-thiazolidinone to elucidate functions of Plk1 in early and late stages of mitosis. *Mol Biol Cell* **18**, 4024-4036.
- Schleiffer, A., Kaitna, S., Maurer-Stroh, S., Glotzer, M., Nasmyth, K., and Eisenhaber, F. (2003). Kleisins: a superfamily of bacterial and eukaryotic SMC protein partners. *Mol Cell* **11**, 571-575.
- Sessa, F., Mapelli, M., Ciferri, C., Tarricone, C., Areces, L. B., Schneider, T. R., Stukenberg, P. T., and Musacchio, A. (2005). Mechanism of Aurora B activation by INCENP and inhibition by hesperadin. *Mol Cell* **18**, 379-391.
- Shah, K., and Shokat, K. M. (2002). A chemical genetic screen for direct v-Src substrates reveals ordered assembly of a retrograde signaling pathway. *Chem Biol* **9**, 35-47.
- Shenoy, S., Choi, J. K., Bagrodia, S., Copeland, T. D., Maller, J. L., and Shalloway, D. (1989). Purified maturation promoting factor phosphorylates pp60c-src at the sites phosphorylated during fibroblast mitosis. *Cell* **57**, 763-774.
- Shi, J., and Malik, J. (2000). Normalized Cuts and Image Segmentation. *IEEE Transactions on Pattern Analysis and Machine Intelligence* **22**, 888-905.
- Simanis, V., and Nurse, P. (1986). The cell cycle control gene *cdc2+* of fission yeast encodes a protein kinase potentially regulated by phosphorylation. *Cell* **45**, 261-268.
- Skibbens, R. V. (2005). Unzipped and loaded: the role of DNA helicases and RFC clamp-loading complexes in sister chromatid cohesion. *J Cell Biol* **169**, 841-846.
- Skoufias, D. A., Indorato, R. L., Lacroix, F., Panopoulos, A., and Margolis, R. L. (2007). Mitosis persists in the absence of Cdk1 activity when proteolysis or protein phosphatase activity is suppressed. *J Cell Biol* **179**, 671-685.
- Snead, J. L., Sullivan, M., Lowery, D. M., Cohen, M. S., Zhang, C., Randle, D. H., Taunton, J., Yaffe, M. B., Morgan, D. O., and Shokat, K. M. (2007). A coupled chemical-genetic and bioinformatic approach to Polo-like kinase pathway exploration. *Chem Biol* **14**, 1261-1272.
- Sonnichsen, B., Koski, L. B., Walsh, A., Marschall, P., Neumann, B., Brehm, M., Alleaume, A. M., Artelt, J., Bettencourt, P., Cassin, E., *et al.* (2005). Full-genome RNAi profiling of early embryogenesis in *Caenorhabditis elegans*. *Nature* **434**, 462-469.
- Steegmaier, M., Hoffmann, M., Baum, A., Lenart, P., Petronczki, M., Krssak, M., Gurtler, U., Garin-Chesa, P., Lieb, S., Quant, J., *et al.* (2007). BI 2536, a potent and selective inhibitor of polo-like kinase 1, inhibits tumor growth in vivo. *Curr Biol* **17**, 316-322.
- Steen, H., and Mann, M. (2004). The ABC's (and XYZ's) of peptide sequencing. *Nat Rev Mol Cell Biol* **5**, 699-711.
- Stelzl, U., Worm, U., Lalowski, M., Haenig, C., Brembeck, F. H., Goehler, H., Stroedicke, M., Zenkner, M., Schoenherr, A., Koeppen, S., *et al.* (2005). A human protein-protein interaction network: a resource for annotating the proteome. *Cell* **122**, 957-968.

- Strom, L., and Sjogren, C. (2007). Chromosome segregation and double-strand break repair - a complex connection. *Curr Opin Cell Biol* 19, 344-349.
- Sudakin, V., Chan, G. K., and Yen, T. J. (2001). Checkpoint inhibition of the APC/C in HeLa cells is mediated by a complex of BUBR1, BUB3, CDC20, and MAD2. *J Cell Biol* 154, 925-936.
- Sumara, I., Gimenez-Abian, J. F., Gerlich, D., Hirota, T., Kraft, C., de la Torre, C., Ellenberg, J., and Peters, J. M. (2004). Roles of polo-like kinase 1 in the assembly of functional mitotic spindles. *Curr Biol* 14, 1712-1722.
- Sumara, I., Vorlaufer, E., Gieffers, C., Peters, B. H., and Peters, J. M. (2000). Characterization of vertebrate cohesin complexes and their regulation in prophase. *J Cell Biol* 151, 749-762.
- Sumara, I., Vorlaufer, E., Stukenberg, P. T., Kelm, O., Redemann, N., Nigg, E. A., and Peters, J. M. (2002). The dissociation of cohesin from chromosomes in prophase is regulated by Polo-like kinase. *Mol Cell* 9, 515-525.
- Takemoto, A., Murayama, A., Katano, M., Urano, T., Furukawa, K., Yokoyama, S., Yanagisawa, J., Hanaoka, F., and Kimura, K. (2007). Analysis of the role of Aurora B on the chromosomal targeting of condensin I. *Nucleic Acids Res* 35, 2403-2412.
- Tanaka, T. U., Rachidi, N., Janke, C., Pereira, G., Galova, M., Schiebel, E., Stark, M. J., and Nasmyth, K. (2002). Evidence that the Ipl1-Sli15 (Aurora kinase-INCENP) complex promotes chromosome bi-orientation by altering kinetochore-spindle pole connections. *Cell* 108, 317-329.
- Taylor, S., and Peters, J. M. (2008). Polo and Aurora kinases: lessons derived from chemical biology. *Curr Opin Cell Biol* 20, 77-84.
- Terada, Y., Tatsuka, M., Suzuki, F., Yasuda, Y., Fujita, S., and Otsu, M. (1998). AIM-1: a mammalian midbody-associated protein required for cytokinesis. *Embo J* 17, 667-676.
- Toyoda, Y., and Hyman, A. (in preparation).
- Toyoshima-Morimoto, F., Taniguchi, E., Shinya, N., Iwamatsu, A., and Nishida, E. (2001). Polo-like kinase 1 phosphorylates cyclin B1 and targets it to the nucleus during prophase. *Nature* 410, 215-220.
- Ubersax, J. A., Woodbury, E. L., Quang, P. N., Paraz, M., Blethrow, J. D., Shah, K., Shokat, K. M., and Morgan, D. O. (2003). Targets of the cyclin-dependent kinase Cdk1. *Nature* 425, 859-864.
- Vagnarelli, P. B., and Earnshaw, W. C. (2001). INCENP loss from an inactive centromere correlates with the loss of sister chromatid cohesion. *Chromosoma* 110, 393-401.
- van Vugt, M. A., van de Weerd, B. C., Vader, G., Janssen, H., Calafat, J., Klomp, R., Wolthuis, R. M., and Medema, R. H. (2004). Polo-like kinase-1 is required for bipolar spindle formation but is dispensable for anaphase promoting complex/Cdc20 activation and initiation of cytokinesis. *J Biol Chem* 279, 36841-36854.
- Waizenegger, I. C., Hauf, S., Meinke, A., and Peters, J. M. (2000). Two distinct pathways remove mammalian cohesin from chromosome arms in prophase and from centromeres in anaphase. *Cell* 103, 399-410.
- Ward, G. E., and Kirschner, M. W. (1990). Identification of cell cycle-regulated phosphorylation sites on nuclear lamin C. *Cell* 61, 561-577.
- Wasserman, W. J., and Masui, Y. (1975). Effects of cyclohexamide on a cytoplasmic factor initiating meiotic maturation in *Xenopus* oocytes. *Exp Cell Res* 91, 381-388.

## 7 References

- Watanabe, N., Arai, H., Iwasaki, J., Shiina, M., Ogata, K., Hunter, T., and Osada, H. (2005). Cyclin-dependent kinase (CDK) phosphorylation destabilizes somatic Wee1 via multiple pathways. *Proc Natl Acad Sci U S A* *102*, 11663-11668.
- Watanabe, N., Arai, H., Nishihara, Y., Taniguchi, M., Hunter, T., and Osada, H. (2004). M-phase kinases induce phospho-dependent ubiquitination of somatic Wee1 by SCFbeta-TrCP. *Proc Natl Acad Sci U S A* *101*, 4419-4424.
- Watrin, E., Schleiffer, A., Tanaka, K., Eisenhaber, F., Nasmyth, K., and Peters, J. M. (2006). Human Scc4 is required for cohesin binding to chromatin, sister-chromatid cohesion, and mitotic progression. *Curr Biol* *16*, 863-874.
- Wiese, C., and Zheng, Y. (2006). Microtubule nucleation: gamma-tubulin and beyond. *J Cell Sci* *119*, 4143-4153.
- Wirth, K. G., Ricci, R., Gimenez-Abian, J. F., Taghybeeglu, S., Kudo, N. R., Jochum, W., Vasseur-Cognet, M., and Nasmyth, K. (2004). Loss of the anaphase-promoting complex in quiescent cells causes unscheduled hepatocyte proliferation. *Genes Dev* *18*, 88-98.
- Witucki, L. A., Huang, X., Shah, K., Liu, Y., Kyin, S., Eck, M. J., and Shokat, K. M. (2002). Mutant tyrosine kinases with unnatural nucleotide specificity retain the structure and phospho-acceptor specificity of the wild-type enzyme. *Chem Biol* *9*, 25-33.
- Wong, J., Nakajima, Y., Westermann, S., Shang, C., Kang, J. S., Goodner, C., Houshmand, P., Fields, S., Chan, C. S., Drubin, D., *et al.* (2007). A protein interaction map of the mitotic spindle. *Mol Biol Cell* *18*, 3800-3809.
- Wong, O. K., and Fang, G. (2005). Plx1 is the 3F3/2 kinase responsible for targeting spindle checkpoint proteins to kinetochores. *J Cell Biol* *170*, 709-719.
- Yang, D., Buchholz, F., Huang, Z., Goga, A., Chen, C. Y., Brodsky, F. M., and Bishop, J. M. (2002). Short RNA duplexes produced by hydrolysis with *Escherichia coli* RNase III mediate effective RNA interference in mammalian cells. *Proc Natl Acad Sci U S A* *99*, 9942-9947.
- Yasui, Y., Urano, T., Kawajiri, A., Nagata, K., Tatsuka, M., Saya, H., Furukawa, K., Takahashi, T., Izawa, I., and Inagaki, M. (2004). Autophosphorylation of a newly identified site of Aurora-B is indispensable for cytokinesis. *J Biol Chem* *279*, 12997-13003.
- Yeong, F. M., Hombauer, H., Wendt, K. S., Hirota, T., Mudrak, I., Mechtler, K., Loregger, T., Marchler-Bauer, A., Tanaka, K., Peters, J. M., and Ogris, E. (2003). Identification of a subunit of a novel Kleisin-beta/SMC complex as a potential substrate of protein phosphatase 2A. *Curr Biol* *13*, 2058-2064.
- Yu, T. S., Zeeman, S. C., Thorneycroft, D., Fulton, D. C., Dunstan, H., Lue, W. L., Hegemann, B., Tung, S. Y., Umemoto, T., Chapple, A., *et al.* (2005). alpha-Amylase is not required for breakdown of transitory starch in *Arabidopsis* leaves. *J Biol Chem* *280*, 9773-9779.

## 8 Acknowledgements

I would like to thank Jan for giving me the chance to work in his lab and for his support during my PhD project.

Further I would like to thank the past and present members of my PhD committee Kim Nasmyth, Gustav Ammerer and Franz Klein for helpful discussions of the diverse problems associated with carrying out a PhD project within a large research consortium. I am especially grateful to Franz Klein and Anthony Hyman for reviewing this thesis.

I very much enjoyed the great collaborations within the MitoCheck project. I would like to especially thank Ina Poser, Laurence Pelletier and Anthony Hyman at the Max-Planck-Institute for Molecular Cell Biology in Dresden, Germany and Jose Luis Jimenez and Jean-Karim Hériché at the Sanger Institute, Hinxton, UK. I am very grateful to Jean-Karim for critical reading of the interaction mapping manuscript and endless attempts to explain graph theory and clustering algorithms to me. Within the IMP I am indebted to the great expertise, patience and helpfulness of the IMP/IMBA protein chemistry facility, especially Karl, Lisi, Otto, Michi S, Michi M, Mathias, Gabi, Christoph and Ines.

Life at the IMP was only fun because of all the nice members of the Peters lab, past and present. I would like to especially thank Jim, Martina and Kristina for lots of fun in the second floor lab. All the time outside of the lab and inside the fourth floor office was especially joyful thanks to Jim, Julia, Peter, Erwan and Kerstin who proved to me that total crazyness and serious science are not mutually exclusive. For more serious science I want to thank Stephie (but also for great skiing and concerts), Antonio and Bettina. Apart from science, Bettina deserves exceptional thanks for pretty much everything.

Finally, for always supporting me I sincerely thank my parents, my sister and my grandparents; and for sharing my life I am grateful to Michèle.

## 9 Curriculum Vitae

### Personal Details:

Name: Björn Hegemann  
Date of birth: 08.12.1978  
Place of birth: Giessen, Germany  
Nationality: German  
Gender: Male

### Education:

Since 2004/05 PhD thesis work with Jan-Michael Peters, Research Institute of Molecular Pathology, Vienna, Austria  
2004/03 Diploma degree in biochemistry, University of Potsdam, Germany  
2003/05 - 12 Diploma thesis work with Jan Hofsteenge, Friedrich Miescher Institute, Basel, Switzerland  
1999/10 - 2004/03 Programme in biochemistry, University of Potsdam, Germany

### Research experience:

Since 2004/05 Ph D student in the group of Jan-Michael Peters at the Research Institute of Molecular Pathology, Vienna, Austria  
Thesis project title: Understanding human mitotic protein complex organisation and phospho-regulation using a combined proteomics and chemical biology approach  
2003/05 - 2003/12 Diploma student in the group of Jan Hofsteenge at the Friedrich Miescher Institute, Basel, Switzerland  
Thesis title: Structural determinants of C-mannosylation of the fourth thrombospondin type 1 repeat of F-Spondin  
2002/10 - 2003/04 Student worker in the group of Regina Brigelius-Flohé at the German Institute for Nutrition, Potsdam, Germany  
Contribution to a project for identifying downstream targets of Toll like receptors  
2002/07 - 09 Internship in the group of Alison Smith at the John Innes Centre in Norwich, UK  
Contribution to a study on the role of alpha amylase in starch metabolism in arabidopsis thaliana (Yu et al., 2005)  
2000/10 - 2002/06 Student worker at the Max-Planck-Institute for Molecular Plant Physiology in Golm, Germany, Group of Lothar Willmitzer/Alisdair Fernie



Contribution to a metabolomic profiling study on tomato plants overexpressing hexokinase (Roessner-Tunali et al., 2003)

2000/08 - 09: Internship at the Max-Planck-Institute for Molecular Plant Physiology in Golm, Group of Lothar Willmitzer/Alisdair Fernie

#### **Publications:**

Poser, I., Sarov, M., Hutchins, J. R., Heriche, J. K., Toyoda, Y., Pozniakovsky, A., Weigl, D., Nitzsche, A., **Hegemann, B.**, Bird, A. W., *et al.* (2008). BAC TransgeneOmics: a high-throughput method for exploration of protein function in mammals. *Nat Methods* 5, 409-415.

Jiménez, J.L., **Hegemann, B.**, Hutchins, J.R.A., Peters, J.M., Durbin, R. (2007). A systematic comparative and structural analysis of protein phosphorylation sites based on the mtcPTM database. *Genome Biol* 8, R90.

Kozma, K., Keusch, J.J., **Hegemann, B.**, Luther, K.B., Klein, D., Hess, D., Haltiwanger, R.S., Hofsteenge, J. (2008). Identification and characterization of abeta1,3-glucosyltransferase that synthesizes the Glc-beta1,3-Fuc disaccharide on thrombospondin type 1 repeats. *J Biol Chem* 281, 36742-36751.

Kueng, S., **Hegemann, B.**, Peters, B. H., Lipp, J. J., Schleiffer, A., Mechtler, K., and Peters, J. M. (2006). Wapl controls the dynamic association of cohesin with chromatin. *Cell* 127, 955-967.

Yu, T.S., Zeeman, S.C., Thorneycroft, D., Fulton, D.C., Dunstan, H., Lue W.L., **Hegemann, B.**, Tung, S.Y., Umemoto, T., Chapple, A., Tsai, D.L., Wang, S.M., Smith, A.M., Chen, J., Smith, S.M. (2005). alpha-Amylase is not required for breakdown of transitory starch in Arabidopsis leaves. *J Biol Chem* 280, 9773-9779.

Roessner-Tunali, U., **Hegemann, B.**, Lytovchenko, A., Carrari, F., Bruedigam, C., Granot, D., Fernie, A.R. (2003). Metabolic profiling of transgenic tomato plants overexpressing hexokinase reveals that the influence of hexose phosphorylation diminishes during fruit development. *Plant Physiol* 133, 84-99.